A design and performance prediction method for axial piston pumps with integral controls

Thesis

A DESIGN AND PERFORMANCE PREDICTION METHOD FOR AXIAL PISTON PUMPS WITH INTEGRAL CONTROLS

by

William John Beswarick
C.Eng., M.I.Mech.E., F.I.Plant E

A Thesis for the Award of the Degree of

Doctor of Philosophy

of the

Council for National Academic Awards

The Hatfield Polytechnic
Hatfield, Hertfordshire

September 1978

ACKNOWLEDGMENTS

The author wishes to acknowledge with sincere thanks the considerable advice, encouragement and assistance he received from :-

F S BHINDER, Ph.D., B.Sc., D.I.C., C.Eng., F.I.Mech.E., Mem.A.S.M.E., M.R.Ae.S.
Reader in Mechanical Engineering

H M el GAMMAL, Ph.D., B.Sc., M.Sc., C.Eng., M.I.Mech.E.,
Senior Lecturer in Control

at The Hatfield Polytechnic.

and

C M EDGHILL, B.Sc., A.F.I.P.
Technical Director

N F APLIN, Chief Designer

A RUBERY, Chief Development Engineer

at Lucas Industrial Equipment Limited, Liverpool.

Special thanks are also due to Mrs. May Wilkins and Miss Ann Roddy for their assistance in the presentation of this thesis.

DECLARATION

No material contained in this thesis and which is claimed to be the author's own contribution has been used before except as the basis of internal reports of The Hatfield Polytechnic and during the specified period of research.

PERMISSION TO COPY

Power of discretion to reproduce this thesis in part or in full is given to The Hatfield Polytechnic Library without further reference to the author.

This permission covers only single copies made for study or research purposes and is subject to normal conditions of acknowledgment.

ABSTRACT

The thesis presents the findings of a programme of research into the design and performance of variable displacement axial piston pumps of the swashplate type with integral controls. The work is principally concerned with developing a systematic design and performance prediction method for use at the design stage.

The method developed outlines stage by stage the problems which arise and give guidance on the decisions which have to be made during the design process. Existing theory and technological data is integrated in the method and is augmented by the author's own contributions in the area of force analysis and contact stresses in the cylinder bores. Graphical optimisation methods are employed and the effects of manufacturing tolerances and pump working ranges are investigated. The effectiveness of the method is demonstrated by designing a pump to the same specification as that of an existing industrial pump and by making a critical comparison of the two designs.

Various regions of power loss are identified and equations derived for estimating these losses. The equations are developed and integrated into a performance prediction method which is novel in that unlike any known method, pump performance can be predicted without the need to test a similar pump. Using data readily available at the design stage the method is used to compare the performance of the existing pump with predicted values. Close agreement is claimed as an indication of the reliability of the method.

The thesis gives an account of the historical development of the axial piston pump, a survey of published work on design and performance and a description of axial piston pumps and hydrostatic transmissions. Also included is an analytical treatment for the frequency response of servo controlled pumps by manual and electro-hydraulic control.

NOTATION

Symbols and abbreviations used in the frequency response analysis are defined within the text.

Symbol		Meaning
A	=	Cross sectional area of a flow path
A^1	=	Cross sectional area of a 'vena contracta'
A_o	=	Cross sectional area of an orifice
B	=	Bulk modulus for an hydraulic fluid
B_{FSB}	=	Slipper bearing balance factor
B_{FVP}	=	Valve plate balance factor
C	=	Fluid compressibility
C_d	=	Piston diametral clearance
C_h	=	Coefficient for hydrodynamic torque loss
C_{hB}	=	Coefficient for hydrodynamic torque loss in bearings
C_{hFP}	=	Coefficient for hydrodynamic torque loss in flow path
C_f	=	Coefficient for dry friction torque loss
C_{fP}	=	Coefficient for dry friction torque loss at the piston
C_{fSB}	=	Coefficient for dry friction torque loss at the slipper bearings
C_{fVP}	=	Coefficient for dry friction torque loss at the valve plate
C_V	=	Coefficient for viscous torque loss
C_{VP}	=	Coefficient for viscous torque loss at the piston
C_{VSB}	=	Coefficient for viscous torque loss at the slipper bearings
C_{VVP}	=	Coefficient for viscous torque loss at the valve plate

Symbol		Meaning
C_S	=	Coefficient for slip leakage
C_{SP}	=	Coefficient for slip leakage at the piston
C_{SSB}	=	Coefficient for slip leakage at the slipper bearings
C_{SVP}	=	Coefficient for slip leakage at the valve plate
C_{SB}	=	Couple acting on slipper bearing
D	=	Pitch circle diameter at cylinder bores
D_S	=	Pitch circle diameter of shaft splines
D_c	=	Diameter of cylinder bore
D_{L1}	=	Inside diameter of valve plate inner land
D_{L2}	=	Outside diameter of valve plate inner land
D_{L3}	=	Inside diameter of valve plate outer land
D_{L4}	=	Outside diameter of valve plate outer land
D_P	=	Plunger diameter
D_1	=	Outside diameter of slipper bearing working face
D_e	=	Diameter of slipper bearing recess
E	=	Young's modulus of elasticity
E_P	=	Percentage loss of efficiency at piston
E_{SB}	=	Percentage loss of efficiency at slipper bearing
E_{VP}	=	Percentage loss of efficiency at valve plate
F_B	=	Load on bearing
F_e	=	Factor for piston eccentricity
F_P	=	Normal force on a surface
F_T	=	Tangential force on a surface
F_{CS}	=	Static control force on a swashplate
F_{CD}	=	Dynamic control force on a swashplate

Symbol		Meaning
F_{pp}	=	Pressure force on a piston
F_{paC}	=	Centrifugal force on a piston
F_{pal}	=	Linear acceleration force on a piston
F_{pf}	=	Coulomb friction force on a piston
F_{pv}	=	Viscous drag on a piston
F_{SBaC}	=	Centrifugal force on a slipper bearing
J	=	Mechanical equivalent of heat
I	=	Second moment of area
K_e	=	Eccentricity of an ellipse
K_D	=	Pitch circle correction factor
K_c	=	Stress concentration factor
K_P	=	Pressure coefficient of viscosity
K_R	=	Control regulation factor
K_T	=	Temperature coefficient of viscosity
L_B	=	Length between pump bearings
L_{SP}	=	Distance from swashplate to first bearing
L_S	=	Length of shaft splines
M_{cy}	=	Mass of cylinder block
M	=	Torque
M_e	=	Effective torque
M_c	=	Frictional torque which is independent of pressure and speed
M_h	=	Torque loss due to hydrodynamic effects
M_f	=	Torque loss due to coulomb friction
M_v	=	Torque loss due to viscous drag
M_M	=	Hydraulic motor torque
M_S	=	Torque in splines or shaft
M_{SB}	=	Couple on slipper bearing
M_{yy}	=	Bending Moment on YY axis of swashplate

Symbol		Meaning
P	=	Power
P_L	=	Power loss
P_{me}	=	Effective mechanical power
P_{he}	=	Effective hydraulic power
Q	=	Volume flow rate
Q_e	=	Effective volume flow rate
Q_h	=	Leakage volume flow rate due to fluid inertia
Q_S	=	Slip flow rate
Q_{SP}	=	Slip flow rate at piston
Q_{SSB}	=	Slip flow rate at slipper bearing
Q_{SVP}	=	Slip flow rate at valve plate
Q_r	=	Volume flow rate loss at pump inlet due to cavitation
Q_{L1}	=	Leakage at valve plate inlet port
Q_{L2}	=	Leakage at piston
Q_{L3}	=	Leakage at valve plate outlet port
Q_{SSB}	=	Leakage from slipper bearing
Q_{INST}	=	Instantaneous volume flow rate
Q_c	=	Volume flow rate to pump controls
R_A	=	Reaction between piston and cylinder bore at A
R_B	=	Reaction between piston and cylinder bore at B
R_c	=	Reaction between slipper bearing and piston
R_{cB}	=	Reaction between cylinder block and valve plate
R_e	=	Reynold's Number
R_P	=	Reaction of slipper bearing and piston along axis of cylinder bore
R_{SP}	=	Reaction between slipper bearing and swashplate

Symbol		Meaning
S	=	Piston stroke
S_{SB}	=	Axial stiffness of slipper bearing
$\overline{S}_{SB}$	=	Axial stiffness coefficient for slipper bearing
T_o	=	Temperature of fluid at pump inlet
V_c	=	Volume of a cylinder bore
V_1 ETC	=	Volume of fluid in an enclosed space
V_o	=	Velocity of a surface
$\overline{V}$	=	Mean velocity
X	=	Distance from cylinder face to centre of swashplate axis
Y_c	=	Distance that the control force act from the centre line of the swashplate
Y_1 ETC	=	Distance from the centre line of a swashplate to the centre line of a particular slipper bearing in the Y direction
a	=	Half length of major axis of ellipse
a_p	=	Piston acceleration
b	=	Half length of minor axis of ellipse
d	=	Diameter of a flow path
d_h	=	Hydraulic diameter
dp	=	Piston diameter
e	=	Eccentricity
f_B	=	Coefficient of friction with mixed lubrication
f	=	Fluid flow friction factor

Symbol		Meaning
h	=	Length of shorter side of rectagonal flow path
h	=	Gap height
h_s	=	Height of pump centre line above centre of pump inlet port
ℓ	=	Length of flow path
ℓ_i	=	Length of immersion of piston in cylinder bore
ℓ_p	=	Length of piston
m_p	=	Mass of piston
m_{SB}	=	Mass of slipper bearing
n	=	Pump speed in revolutions per second
n_s	=	Slip frequency
P	=	Pressure
P_L	=	Pressure loss
P_c	=	Constant pressure loss
P_v	=	Viscous friction pressure loss
P_h	=	Hydromechanical pressure loss
P_f	=	Coulomb friction pressure loss
P_V	=	Vapour pressure
r	=	Radius
r_c	=	Pitch circle radius of cylinder bores
q	=	Volumetric displacement per revolution
q_o	=	Full stroke volumetric displacement per revolution
r_e	=	Effective radius for slipper bearings
t	=	Thickness
V_p	=	Piston velocity

Symbol		Meaning
w	=	Length of sides of square section flow path
w	=	Length of longer side of rectangular flow path
w_A	=	Intensity of distributed loading at A
w_B	=	Intensity of distributed loading at B
$\bar{X}_p$	=	Distance of centre of mass of piston from centre of ball joint
$\bar{X}_{SB}$	=	Distance of centre of mass of slipper bearing from bearing face
α	=	Coefficient of expansion for a flow path
α	=	Displacement setting
β	=	Coefficient of contraction for a flow path
β	=	Angle from top dead centre of the pump in the plane of rotation
δ	=	Gradient of gap height
η	=	Overall efficiency
η_m	=	Mechanical efficiency
η_v	=	Volumetric efficiency
λ_p	=	Piston parameter
λ_{SB}	=	Slipper bearing parameter
μ	=	Absolute viscosity
ν	=	Kinematic viscosity
ξ	=	Flow path loss coefficient
ρ	=	Mass density
σ	=	Normal stress
τ	=	Shear stress
ϕ	=	Swashplate angle
ω	=	Angular velocity

Symbol		Meaning
N.P.S.E.	=	Net positive suction energy
B.W.S.	=	Beginning of working stroke
E.W.S.	=	End of working stroke

CONTENTS

CHAPTER 1. INTRODUCTION

1.1 Initiation of Research Programme

Transmission of power from a prime mover to a load; particularly if the load is remote; may be accomplished electrically, pneumatically or hydraulically as shown diagrammatically in the following sketches.

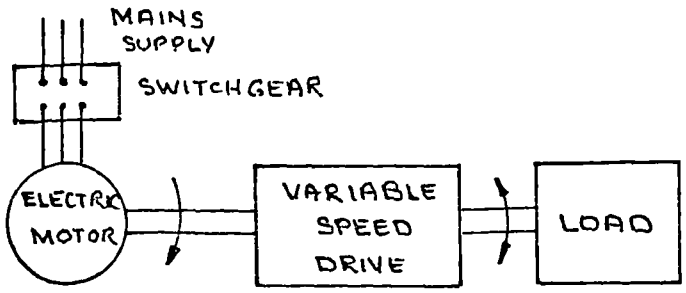

Electrical Transmission

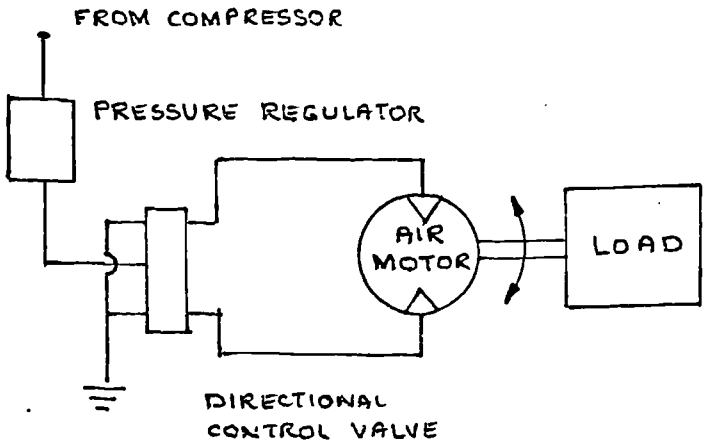

Pneumatic Transmission

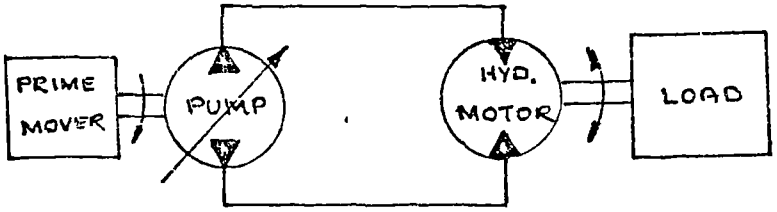

Hydraulic Transmission

The hydraulic transmissions are of two types:

i) hydrostatic;

ii) hydrokinetic.

The former transmits power by virtue of the pressure developed in the hydraulic fluid whereas hydrokinetic drives make use of the effects of change of momentum in the fluid. Hydrokinetic systems are not normally used where the load is remote from the prime mover because of the losses associated with high fluid velocity.

Hydrostatic transmissions are ideal for applications requiring high torque capacity and ease of speed control. Operational considerations are:

i) matching the prime mover characteristics with the load requirements;

ii) control system and response;

iii) noise.

The essential components of the hydrostatic transmission are shown in the sketch. The pump and hydraulic motor may be of gear, vane or piston design. In the case of piston type machines the cylinders may be arranged either radially or axially. This study deals with the design, performance and control of axial piston pumps only.

This research arose from a notion that as in so many other areas of engineering design, relatively few aids exist for the design of axial piston pumps and in particular for predicting the performance of a new design prior to the manufacture and testing of a prototype pump. It was generally known that the axial piston pump presents several areas of conflicting physical and economic considerations and that at the design stage it was not easy to obtain guidance towards the satisfactory solution of these problems. However a systematic study of the design methodology and the important criteria should help to reduce the uncertainties at the design stage. It was felt that such a study would be relevant to industrial needs and was also timely because of the growing interest in hydrostatic transmissions.

As a result of an approach to the Lucas organisation, who are in the forefront of the design and manufacture of axial piston pumps, it was decided to initiate a programme

of research into the design and performance of this type of pump. An excellent personal relationship was quickly established with senior personnel in the company and it was agreed that the work would be of considerable interest to Lucas. Since the project would involve active design and supporting experimental work, it was also agreed that the necessary advice and facilities would be provided by the company. The project was initiated in January 1972.

1.2 Aims and Objectives

The aims of the research project were to study the problems of design associated with the successful manufacture of variable displacement axial piston pumps of the swash plate type and having integral controls for use in hydrostatic transmission systems. This would involve the study of the basic concepts of axial piston pumps and their configuration, together with a background study of fluid mechanics, mechanical design and control engineering. It would also include such design and experimental work as would be required to test any recommendations or procedures developed. Furthermore it was intended to present the findings of the research in a manner suitable for use by pump designers and researchers in the field of fluid power.

At the commencement of the work it was clear that a considerable amount of design information was available, mainly based on research into specific areas of design. The value of this information varied from being of considerable practical use to that of being of academic interest only and this realisation served to reinforce the aim that the results of this project should be of significance in the process of pump design. The aims of the project therefore included an appraisal of the design information already available with the view of integrating these for practical use and for further study.

An additional aim was to study the theory of pump performance and of presenting these in a form usable at the design stage. Here again it was recognised that considerable work has already been done but that the application of the

theories was not always as straightforward as the time demands of pump design allow.

The aims of the project can therefore be summarised as being to provide for use at the design stage, aids to the successful design and performance prediction of axial piston pumps of the swash plate type and with integral controls.

The objectives followed naturally from the aims of the project. To present the design and performance prediction information suggested the development of a design and performance prediction method whereby a systematic procedure could be followed quickly and conveniently at the design stage. Early study showed that the design and performance prediction of axial piston pumps is mainly based on an empirical approach backed up by past experience. To provide a systematic method for the design and performance prediction would meet the aims of the project.

The design method would outline a logical procedure for selecting the principal dimensions of a pump for a given specification and would include graphical techniques for obtaining conditions within the pump leading to minimum working losses. The reiterative nature of design would be catered for in the design method. The method would give guidance on the total design of the pump and consider such aspects as material selection, manufacturing considerations, cost and the factors affecting reliability.

The performance prediction method would give an analytical approach to estimating the performance of an axial piston pump at the design stage. It was found that considerable work had been done in a number of countries and the findings presented as mathematical models. It was also found that the use of these models required the determination of various coefficients by testing pumps of similar design. This restricts the use of the mathematical models to aiding the design of pumps which are extensions to an existing range of pumps. The objective therefore would be to select the most reliable of these mathematical models and to extend their application by developing a method of analytically estimating the coefficients used in the models.

The objectives of the project can be summarised as:

1. To develop a systematic method of designing axial piston pumps from a given design specification.

2. To develop a performance prediction method for axial piston pumps for use at the design stage.

Supporting work would be necessary to test the efficacy of the design method and the reliability of the performance prediction method. This would be done by the additional objectives:

3. To test the design method by designing an axial piston pump to the specification of an existing highly successful pump and to make a critical comparison of the two designs.

4. To test the performance prediction method by comparing the estimated performance of the existing pump with its measured performance.

5. To compare the frequency response of the existing pump and its controls, obtained experimentally with those derived from theory.

1.3 Implementation of the Research Programme

The research programme was implemented by an extensive period of study of published work and supporting theory related to positive displacement pumps and motors, hydrostatic transmissions, power requirements in machines and vehicles and the control of hydraulic systems.

The design work was carried out in the Engineering Design Centre of The Hatfield Polytechnic with visits to and direct communication with the Design Department of Lucas Industrial Equipment Limited, at Fazakerley in Liverpool.

The experimental work was carried out in the Development Department of Lucas Industrial Equipment Limited, and the computation in the School of Engineering at The Hatfield Polytechnic.

CHAPTER 2. HISTORICAL DEVELOPMENT OF THE AXIAL PISTON PUMP

The historical development of the axial piston pump can be traced from the pioneering work at the beginning of the 20th century. Already a change from the use of water as a hydraulic fluid for power transmission to oil had resulted in the development of vane and radial piston pumps and motors but it was the designs of Williams and Janney in 1905 that resulted in the first successful application of the axial piston pump and motor to form a fluid power transmission.

The general construction of the Williams and Janney transmission is shown in Fig.2.1, as a back to back assembly. An early application was to manoeuvre the heavy marine guns of those days. Many of the principal design features such as the rolling bearing swashplate, the ball ended connecting rods and the face type valve plate were major innovations of design which were to be incorporated in other pump designs for many years.

It is remarkable how little published work on axial piston pump design can be cited up until the end of the First World War. This can to some extent be attributed to the keen sense of competition and industrial confidentiality that existed in Britain, Germany and the United States, in the field of power transmission. This had been stimulated by the demands for infinitely variable transmissions for the ever increasing range of motor vehicles and by the needs of naval and merchantile marine. Hence it is particularly difficult to obtain reliable information on the detailed design and performance of the early units. What is known however is that the quality of the design in the light of the theoretical knowledge then available was often of a very high order. Although the improvements in mechanical and subsequent hydrokinetic transmissions for motor vehicles soon displaced these early hydrostatic transmissions, the axial piston pump and motor had by then been firmly established as units with promising potential.

Between the two world wars there was a steady development in oil hydraulics for marine and industrial applications

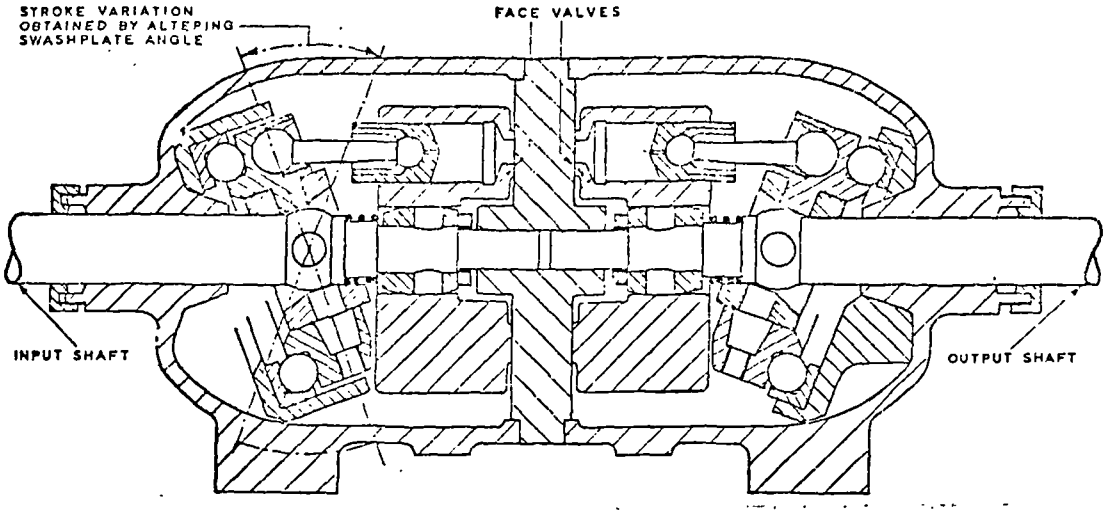

FIGURE 2.1. WILLIAMS AND JANNEY TRANSMISSION.

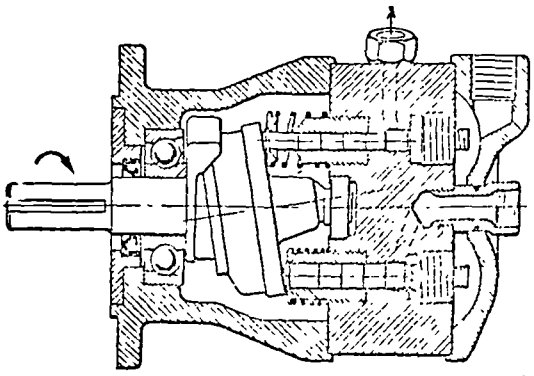

FIGURE 2.2. CONSTANT DELIVERY FIXED ANGLE SWASHPLATE PUMP.

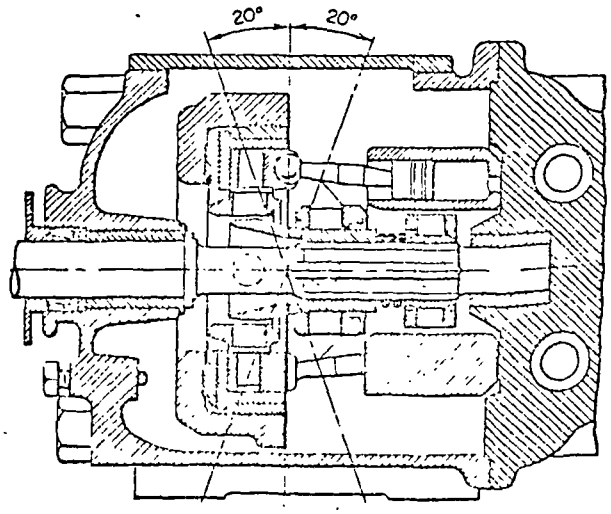

FIGURE 2.3.VARIABLE DELIVERY AXIAL PISTON PUMP(V.S.C)

and this was augmented by the expansion of the machine tool industry. The outstanding features of oil hydraulics as a means of power transmission were fully appreciated and the ease of flow control and the compact design of the axial piston pump gave new incentive for design improvement. Notable contributions were made by Hans Thoma in Germany in 1930 with the introduction of the swashplate pump shown in Fig.2.2, and by the Towler brothers in Britain.

The Thoma design eliminated the main weakness of earlier designs in which the mechanical power to the pump was transmitted through the connecting rods, by introducing a substantial universal joint. The design also eliminated the need of a large rolling bearing in the swashplate. Because the cylinder block was held in a cradle supported by trunnion bearings, the reaction forces from the connecting rods were supported by the shaft thrust bearing.

The Towlers incorporated seated valves which gave higher volumetric efficiencies than those obtainable at that time from face valves. As a result they raised the level of operating pressures to the 300 bar range, pump speeds to 1500 rev/min and powers up to 120 kW. These were major developments which gave the growing fluid power industry the fillip it needed and established the axial piston pump as a linchpin in its development.

There is little evidence of major developments in axial piston pump design during the Second World War. The use of fluid power was greatly advanced by the needs of fighting aircraft and other military equipment but it would seem that these were mainly met by single and two stage gear and vane pumps. However, the progress that was made in component design, for example, rolling bearings and elastomer seals together with improvements in material technology and manufacturing methods were to contribute appreciably to the post war development of axial piston pumps.

Major developments since the war have been in reducing internal pump losses such as leakage and friction in the regions of the pistons, swashplate and the valve plate. Research in all the leading industrialised countries has led to a greater understanding of these problems and it is satis-

fying to realise the considerable contribution that British research has made. This period has seen the introduction of hydrostatically balanced slipper bearings and valve plates whereby only a small proportion of the pump forces result in metal to metal contact and wear. This has led to improved mechanical efficiency and pump life and reliability although the advantages have to some extent been offset by small reductions in pump volumetric efficiency.

Examples of pumps of modern design are shown in Figs.2.3 to 2.8. Improvements in design and performance have resulted in the axial piston pump being most versatile for high pressure applications since its compactness and high power to weight ratios are not surpassed by other types of pump and these are important considerations in present day power transmission systems.

The search for par excellence has led to a most recent advancement of combining hydrostatic and elasto-hydrodynamic lubrication of slipper bearings. Vickers have introduced this concept in their pumps and make strong claims as to the advantages to be realised. This is but another reminder that even in a well developed area of technology, improvements can result from a continuing programme of research and development.

Side by side with the pump, developments have also been made in its control. Until about 1935 pump controls consisted of mechanical means of altering the swashplate angle to vary the pump displacement. Electrical methods had also been used, with the necessary thrust and movement being provided by electric geared motors. It was realised that a very convenient device would be the hydraulic cylinder with control by means of a directional control valve.

During the Second World War the development of electro-hydraulic servo valves stimulated interest in controlling pump flow by this means and it was found that if mechanical feedback was incorporated, close control could be maintained. Since the war this interest has been further developed and as a result many pump manufacturers offer pumps with a most comprehensive range of manual, servo-assisted and integral electro-hydraulic controls. In addition to these controls, because of

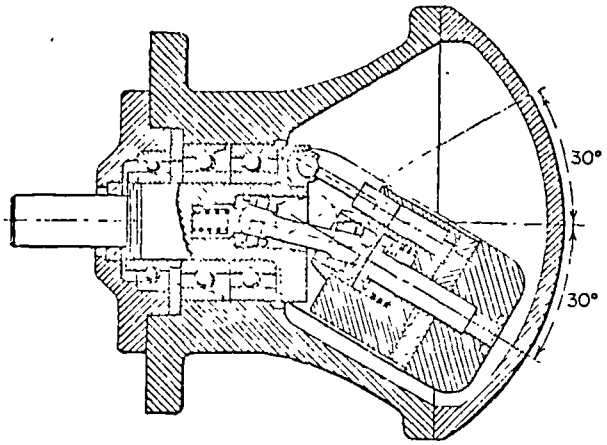

FIGURE 2.4 TILTING HEAD VARIABLE DELIVERY AXIAL PISTON PUMP (THOMA)

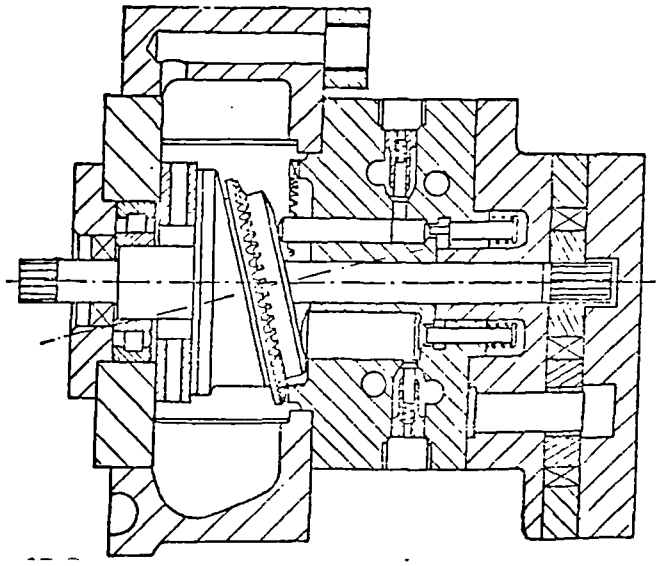

FIGURE 2.5. HIGH PRESSURE PUMP

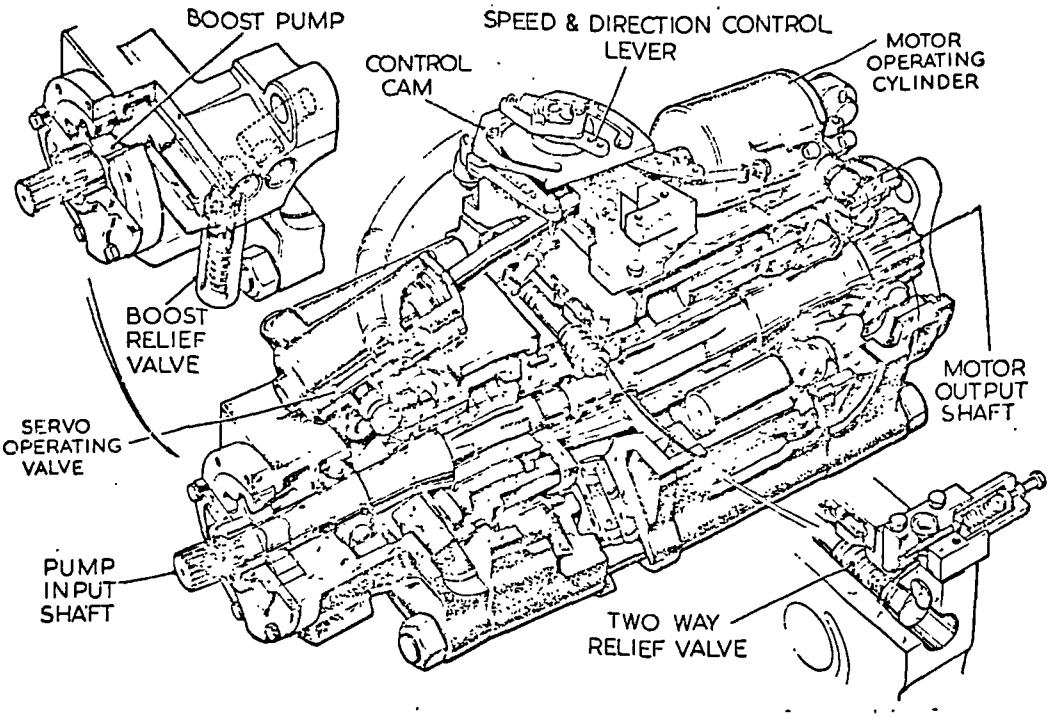

FIGURE 2.6. LUCAS HYDROSTATIC TRANSMISSION.

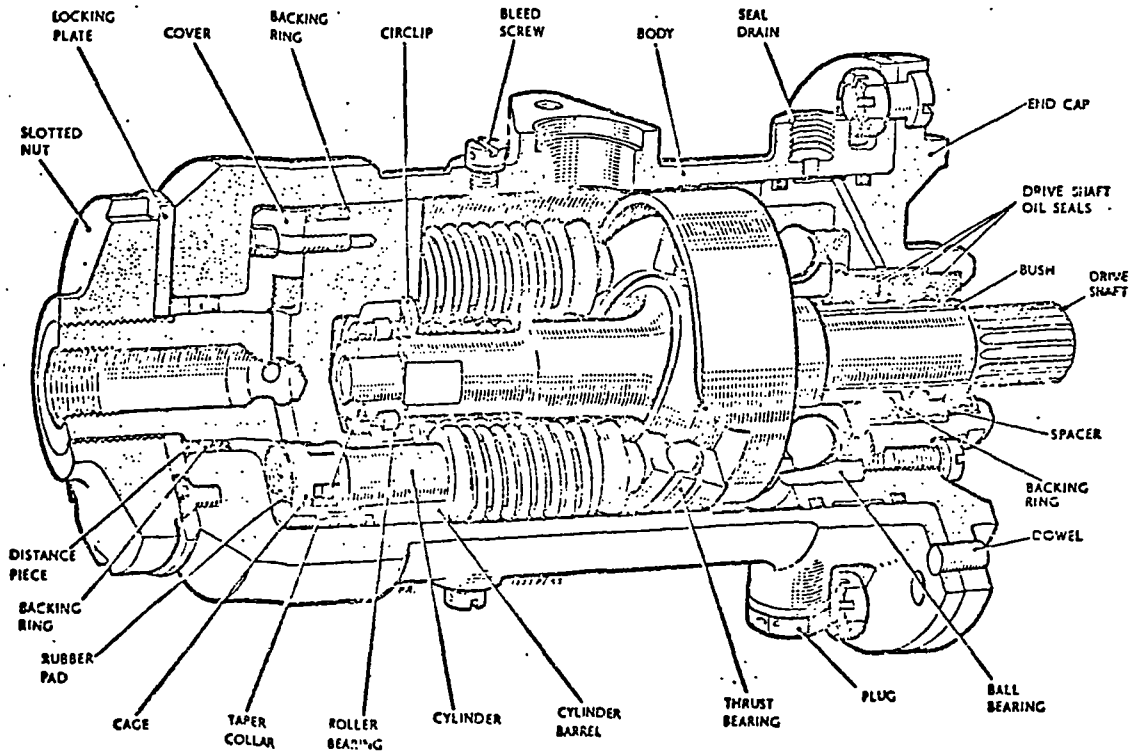

FIGURE 2.7. ASSEMBLY OF DOWTY AXIAL PISTON PUMP.

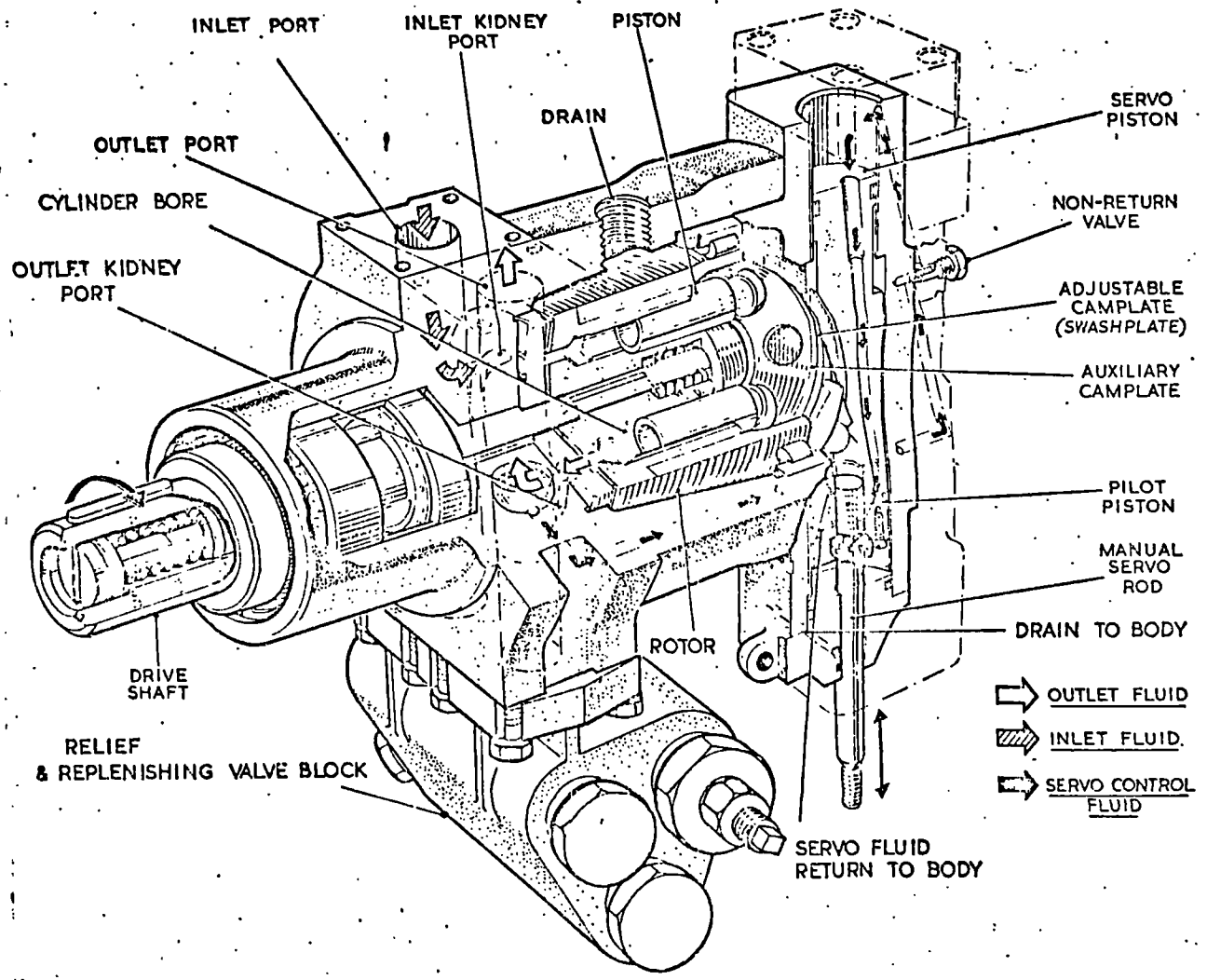

FIGURE 2.8. CROSS SECTIONAL VIEW OF LUCAS TYPE PM AXIAL PISTON PUMP

the wide use of hydrostatic transmissions, controls have been developed as integral pressure relief, replenishing, power and torque limiting and cross line protection controls within the pump assembly.

It is certain that the axial piston pump will become increasingly important in fluid power systems. Its potential as a low weight high pressure pump will ensure this and development work to reduce weight, bulk and manufacturing costs together with improvements in performance and reliability will increase the commercial value of this type of pump.

Other areas for development are in the reduction of noise and the increase of pump speeds. Considerable research has already taken place in noise reduction with some success but the distribution of recent research grants to British institutions would suggest that there is scope for further improvements. It is also recognised that advantages would be gained if pump speeds could be increased from the general level of 3000 rev/min. Obvious advantages would be the direct coupling to high speed diesel engines, eliminating the costly power take off units and reduction drives. Increased pump speeds would also facilitate drives from industrial turbines.

The quality of control is already to a high order and probably meets the needs of most industrial and transport requirements. However, even in this specialised area, development work is likely to be substantial.

The historical development of the axial piston pump is therefore one of sustained development from the initial concepts to that of a high level of attainment. The brilliance of Janney, Thoma, the Towler brothers and others has been matched, (though less acknowledged), by the many pump engineers who have furthered the design of this particularly interesting engineering machine.

CHAPTER 3. LITERATURE SURVEY

In all probability the published work in the field of hydrostatic transmissions exceeds that which has been published about any other branch of fluid power technology. This has been particularly the case during the past ten years or so during which time numerous conferences of international interest have been held and the learned institutions in this country, in Europe and in the United States, have received many papers on this form of power transmission. At a lower academic level but nonetheless of considerable importance, have been the numerous articles and reports which have been published by the engineering journals. These have been intended to acquaint and inform the practising engineer of the basic concepts, applications, unit design and availability of hydrostatic transmissions.

To attempt to present an adequate survey of these works would be a formidable task, although its value to the fluid power industry, colleges, universities, research establishments and other institutions with an active interest in this field would be appreciable, particularly if the existence of the survey was well publicised. However as the main aims of this research work are concerned with axial piston pumps and their associated controls, only literature related to these topics are surveyed here.

3.1 Pump Design

Wilson (1) has written a standard textbook on the basic theory of pump design and performance. Although the first edition was published in 1950, the clear and logical presentation used makes the book a most useful work for primary study. The book is very much concerned with gear and vane pumps but Wilson indicates how the basic concepts of torque generation and leakage flow could be applied to axial piston pumps. Wilson has also contributed to detail pump design in the areas of working clearances. His papers (2) and (3) are representative of these and present ways of determining clearances for minimum losses of power due to

pressure flow and viscous drag. His treatise on viscous flow between parallel plates is deep but he assists the designer by introducing non-dimensional parameters and related charts which reduce the computation appreciably.

A more comprehensive treatment of pump design is that of Thoma (4). Thoma deals in detail with various aspects of pump design and relates basic fluid mechanics theory to the design. The work is refreshing since it shows a most satisfactory balance between theory and technology and observations and recommendations based on the author's own experience and that of other engineers, makes this book of more than usual value to the pump designer. Additional sections on pump design are to be found in an earlier book by Thoma (5). Thoma uses the electrical analogy of dipoles to develop equations for fluid flow in gaps and other restrictions and he has made a useful contribution to this aspect of pump design in a paper (6). He suggests that the temperature effect on viscosity for fluid flow in a gap be expressed as the 'thermal pressure' which is a constant value across the leakage path and augments the static pressure. Thoma (7) has also published a paper on the systematic design of axial piston hydraulic machines but apart from identifying some of the design aspects, this work falls far short of what its title would suggest.

Mention must be made of Ernst (8) whose textbook is very well known and which has held a unique position amongst the publications on fluid power for many years. His treatment of axial piston pumps is however only a minor part of the work, but it does contain some interesting and informative data.

A book of recent publication is that by Turnbull (9) and sets out the problems of axial piston pump design in a very informative manner. Having been associated with several of the research reports quoted in his text, Turnbull has made a valuable reference book for the theoretical aspects of axial piston pump design. However as already implied, the book does not introduce new concepts or theories.

As is to be expected, detailed contributions to axial piston pump design are mainly contained in technical papers.

The balancing of forces at the valve plate is dealt with by Franco (10) and he goes to some trouble to derive theory for the variation of leakage flow across the bearing surfaces due to centrifugal force on the fluid in the gap. Saitchenko (11) has proposed a simple but effective method of determining the forces at the valve plate face and also the swashplate reactions, the pump bearing forces and the torque on the pump shaft.

The hydrostatic balancing of valve plates has been dealt with by Palmer, Stott, Shute and Turnbull (12). Pressure fed recesses in the lands of the valve plate with matching chokes are proposed and analysed and theory is presented for estimating the axial and rotational stiffness of the design. Extensions to this work are due to Shute, et al (13).

Published reports on conditions at the pistons are aimed at obtaining minimum power losses. Shute and Turnbull (14) give a classical approach to the problems and have been able to develop power loss equations expressed in terms of percentage loss of efficiency. By using non-dimensional parameters, curves are presented for constant percentage losses and include optimisation curves to enable the selection of working conditions. These concepts which the authors use again for slipper bearing design are very useful at the design stage and have been incorporated in a modified form in the design method used in this present work.(15).

Slipper bearings are subjected to a tilting moment due to centrifugal force and this aspect has been dealt with by Fisher (16) and Shute and Turnbull (17). The authors show that the axial and tilting stiffness can be of a very high order and present means of designing to achieve adequate stiffnesses.

Richmond (18) has researched into the many problems of returning pistons with compression springs and this is very relevant to axial piston pump design. He shows that a spring may be compressed some 2×10^9 times during its working life and that careful attention must be given at the design stage if spring failure resulting in expensive maintenance and lost production costs are to be avoided.

Gerber (19) deals specifically with the forces that are present in an axial piston pump, particularly in the region of the cylinder bore, piston and slipper bearing. The work is rudimentary and as such makes no attempt to include the dynamic forces and resulting stresses which are of considerable concern in the design of high speed pumps.

McCallum (20) has written an informative paper containing a theoretical analysis of the valve plate bearing whilst Nau (21) was able to indicate typical film thicknesses, flow losses and noise and temperature levels in a series of tests on valve plates. As indicated in Chapter 8, Nau's findings on working clearances are particularly useful in estimating losses in this region of the pump.

Of equal importance to the theoretical aspects of axial piston pump design are those dealing with pump reliability. Edghill and Rubery (22) have presented a most useful indication of the sources and causes of failure in axial piston pumps and the possible changes to design to alleviate these problems.

3.2 Pump Controls

Literature on pump controls can be grouped into that which in general describes the types and applications of pump controls and that which in the main is concerned with functional analysis.

Beasley (23) is an example of the first group and in the main he describes types of controls associated with axial piston pumps. Specific information is given by Price (24) on the control of axial piston pumps of the types manufactured by Lucas Industrial Equipment whilst Edghill (25) discusses the various features which influence the choice of control for hydrostatic transmission systems. These papers set the scene for an informed approach to the choice, application and design of axial piston pump controls.

Thoma (4) includes useful chapters on pump control and bridges the gap between concept and practical considerations such as flow rates, control leakage and pressure drops across control elements. Merritt (26) develops in a very clear

manner the basic theory for load servo systems of the types used for swash plate control and once again as a practising engineer this author passes on valuable observations and data. His treatment of non-linearities is also most helpful. Augmenting works are those of Watson (27), Walters (28) and Guillon (29) who each makes contributions to pump control theory.

All these authors deal with system response but since in the case of swashplate control the signals are frequently of large magnitude, an extension to the theory of small perturbations is required. The work of Nikoforuk and Westlund (30) is particularly helpful for the analysis of the large stroking of axial piston pumps.

The increased use of electro-hydraulic controllers for axial piston pumps makes the work of Thayer (31) in which he sets out the possible derivation of suitable transfer functions, an important contribution to the formulation of functions to describe the response of a complete pumping system.

3.3 Pump Performance

Specific pump performance is dealt with by Wilson (32), Schlösser (33) and Thoma (34). As discussed in Chapter 5, these researchers present mathematical models which are helpful in the understanding of axial piston pump performance but because the models require the determination of several coefficients to enable performance predictions to be made, the methods have limited use at the design stage. Dozortsev (35) has proposed the definition of pump delivery and volumetric efficiency by the use of coefficients and although the treatment of the topic is deep, it again provides little help in the important task of performance prediction.

Testing methods for positive displacement pumps are described by Schlösser (36). In his methods great care was taken to measure accurately such values as the input torque by suspending the pump drive motor in low friction bearing mountings, stream temperatures by immersed thermometers and continuous measurement of fluid viscosity. Such detailed measurements are not usually taken during commercial testing.

Smith and Williamson (37) describe a method of steady state performance testing of pumps and motors which is generally in agreement with BS4617:1970 'Method of Testing Hydraulic Pumps and Motors for Hydrostatic Transmissions'.

Elloy (38) has described time sharing techniques for the quick and accurate plotting of the results of pump testing by computers. These methods are particularly suitable for the carpet plots favoured by pump manufacturers.

Three researchers Helgestad, Foster and Bannister (39) have made significant contributions to the understanding of noise in axial piston pumps and have extended this work (40) by deriving methods for calculating pressure transients in these pumps. Their findings on silencing grooves for the kidney ports in the valve plate are major advances in noise reduction and will increase in importance as pump speeds and pressures increase.

A general understanding of noise in hydraulic systems is given by Wilson (41) and Currie and Kane (42) have made some useful observations on the same problem. Willekens (43) has analysed the modes of noise generation using analogies between hydraulic and electrical systems. His noise analysis chart gives a vivid impression of the complexity of the topic.

3.4 Discussion

The literature surveyed above represents leading published works on pump design, control and performance. It will be seen that in the main the topics are well covered but it would also seem that in the case of pump design there is scope for the integration of design information already to hand in the form of a logical design method. Again, although considerable information is on record on pump performance and testing, no method of performance prediction to an acceptable level of accuracy for design appraisal appears to be available. These deficiencies in the aids available to pump designers are considerable and identify the main objectives of this present work.

CHAPTER 4. HYDROSTATIC TRANSMISSIONS AND AXIAL PISTON PUMPS

4.1 Description of Hydrostatic Transmissions

A hydrostatic transmission can be defined as a system which is capable of transmitting power from a prime mover by means of a non-compressible fluid and by using positive displacement pumps and motors. The system is essentially an assemblage of hydraulic equipment such that the power received from a prime mover is transmitted and delivered as rotary power at the output shaft. Mechanical energy from the prime mover rotates the pump and for each revolution of the pump, a fixed quantity of hydraulic fluid is pumped from the suction to the delivery side of the pump. The pump is connected by pipes or hoses to a hydraulic motor and the output speed of the system will depend upon the relative displacements of the pump and the motor.

Frequently the prime mover is a governed I.C. engine or an A.C. induction electric motor and has near constant speed for the range of working torques required for the system. Thus to vary the output speed requires some form of speed control. It is also probable that the prime mover is to be run unidirectionally and the need to be able to reverse the rotation of the system output shaft requires special features in the system. In addition all hydrostatic transmissions must include controls for limiting the system output and for overall safety.

Since the pump outlet is connected by a pipe or a hose to the inlet to the hydraulic motor, the full fluid flow passes through the motor causing it to rotate at a speed directly related to the speed of the prime mover and to the relative displacements of the pump and motor. The hydraulic fluid is piped back to the pump or to an intermediate reservoir for subsequent recirculation. It will be apparent that the system described has the capability of converting mechanical energy into fluid energy at the pump and of reconverting the fluid energy into mechanical energy at the hydraulic motor. The pump operates as a flow generating unit and the flow rate is to a large degree dependent only on the displacement of

the pump and the speed at which it is rotated. Similarly because of the positive displacement nature of the motor, the speed of the output shaft is dependent only on the flow rate of the fluid it receives, and the displacement of the motor.

In practice small leakages occur in the system, particularly in the pump and motor and these losses are dependent on the speed of rotation of the units, the system pressure and the effective viscosity of the fluid. However, a simple basic relationship will hold for the speed of rotation of the pump and motor, viz:

$$n_p q_p = n_m q_m \tag{4.1}$$

The pressure generated in the system is dependent upon the resistance to the flow of the fluid and if the motor shaft is connected to a rotating load, the fluid has to exert a pressure on the working parts of the motor to generate the torque to overcome the load. Additional pressure has to be developed in the system to overcome mechanical and fluid friction where these occur. As a result, a pressure differential is developed across the pump which is the sum of all the pressure differentials in the system.

The input torque to the pump and the output torque from the motor are directly related to the pressure differential across each unit. In an idealised case, where the pressure rise across the pump is equal to the pressure drop across the motor, that is where all system losses are ignored, a simple relationship exists between the power conversion, the system pressure, the speed of rotation and the displacement of the units.

$$P = QP = nqP \tag{4.2}$$

$$P = 2\pi n M$$

$$M_m = \frac{q_m P}{2\pi} \tag{4.3}$$

Whilst discussing the relationship between torque and pressure, it will be seen that in such a simple hydrostatic system as this, and in the absence of a pressure limiting device, if the reactive torque on the motor shaft is increasing, the system pressure will also increase and eventually a condition of failure of the hydraulic system or of failure or stalling of the prime mover could result. Fortunately, the provision of a pressure relief valve of suitable characteristics can prevent the pressure rising above a safe level and in this event the hydraulic motor will stall with no damage to any part of the system. Immediately the reactive torque is reduced to any acceptable value, the hydraulic motor will recommence the rotation of the load.

The system described is analogous to a mechanical drive of fixed ratio and if the pump and motor have equal displacements, a similarity exists with that of a simple shaft drive. A system incorporating units of unequal displacement can be likened to a fixed ratio gear, belt or chain drive. It will be apparent that for many applications a need arises for the facility to vary the speed of the motor without necessarily altering the speed of the prime mover. This can be achieved in three ways:

1. <u>By varying the flow rate to the motor by using a flow control valve</u>

   This is essentially the inclusion in the system of an adjustable orifice through which some of the pump flow is bypassed to tank. The greater the flow rate to tank the slower the rotation of the hydraulic motor and vice versa. Since the pressure drop across the flow control valve is equal to the system pressure, this method of control will result in heating of the hydraulic fluid and has the disadvantage that the power input to the hydraulic system is maintained at a level dictated by the system pressure and the full flow rate, irrespective of the motor speed. Such a means of control is therefore restricted to low power, low capital cost applications.

2. By varying the displacement of either the pump or the motor

Some positive displacement pumps and motors can be designed so that by altering the relative positions of the working parts, the amount of fluid pumped or received per revolution can be varied. Axial piston pumps, radial piston pumps and vane pumps are common examples of pumps with this capability and variable displacement motors are also available. Varying the displacement of a unit does not affect the system pressure and the power input is therefore reduced if the displacement of either unit is reduced. Frequently the pump or motor has full flow regulation in both a positive and a negative direction and this feature eliminates the need for directional control valves for output shaft reversal.

3. By varying the displacement of both the pump and the motor

Such a system has operational advantages but with an inevitable prime cost penalty which may be excessive for many power transmission systems. Care must be taken when the motor is of variable displacement to ensure that a very low displacement cannot be selected. Failure to ensure this could result in excessive output speeds with possible damage to machinery and injury to personnel.

Fig.4.1, shows the basic characteristics of the methods described.

Advantages and Disadvantages of Hydrostatic Transmissions.

So far it has been seen that a hydrostatic transmission may have the following features which are often required in a power transmission system:

(a) infinitely variable speed regulation;
(b) easy reversal of direction of rotation of output shaft;
(c) positive overload protection of complete system.

1. FIXED DISPLACEMENT PUMP AND MOTOR

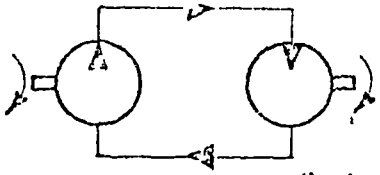

Speed ratio= $\frac{\text{pump displacement}}{\text{motor displacement}}$

Torque ratio= $\frac{\text{motor displacement}}{\text{pump displacement}}$

Power & Torque

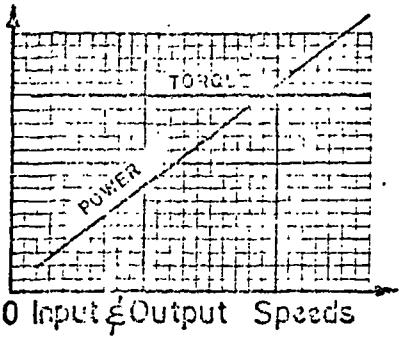

2. VARIABLE DISPLACEMENT PUMP, FIXED DISPLACEMENT MOTOR.

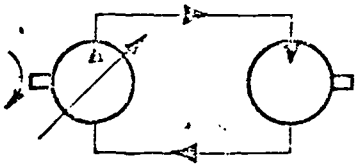

Speed ratio ∝ pump/ motor displacement ratio.
Torque ratio ∝ motor / pump displacement ratio.

Power & Torque

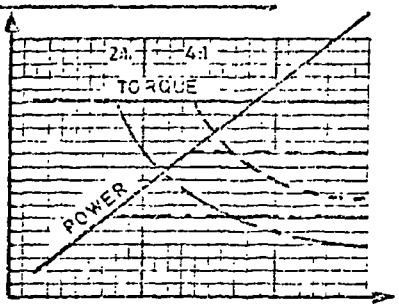

3. FIXED DISPLACEMENT PUMP, VARIABLE DISPLACEMENT MOTOR.

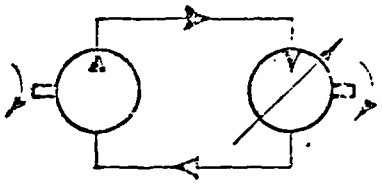

Power & Torque

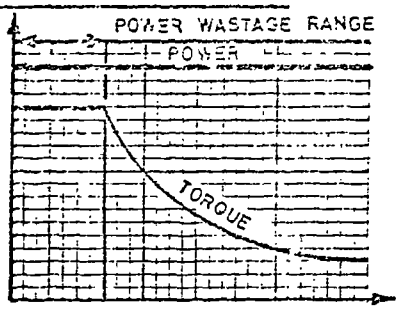

4. VARIABLE DISPLACEMENT PUMP AND MOTOR.

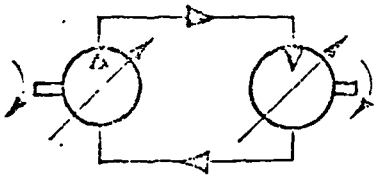

a) Motor fixed at max. displacement. Pump displacement increased.
b) Pump fixed at max. displacement. Motor displacement reduced.

Power
Torque
Pressure
Flow

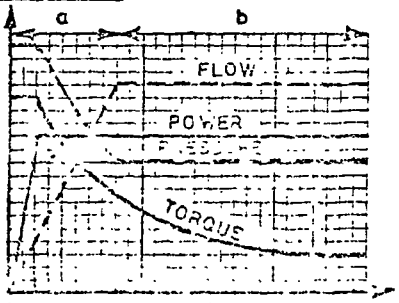

FIGURE 4.1 BASIC CHARACTERISTICS OF HYDROSTATIC TRANSMISSIONS

Additional features are:

(d) High power to weight ratios.

Modern pumps and motors are generally compact and correspondingly low in weight. Power to weight ratios vary considerably at the dictates of the application and environment for which the unit must be suitable, but ratios of the order of 3kW/kg are possible. This compares very favourably with any competitive electrical or mechanical units.

(e) Flexibility of installation.

Because of the compactness of the units, the absence of 'rigid' connections between the pump and the motor and the ability of the units to work in any positional orientation and (within reason) at any distance from one another, a hydrostatic transmission has a minimum of installation constraints. In the field of transport engineering this is clearly shown by the common practice of mounting the hydraulic motors within the wheel axles. The outstanding success which has been achieved in flexible hose and coupling manufacture has contributed to this advantage.

(f) Reliability.

Since all parts liable to wear are immersed in hydraulic fluid having good lubricity, the wear rate of well designed and well manufactured units is generally low resulting in low maintenance costs and long service life. It is also possible by design to achieve hydrodynamic and hydrostatic lubrication of heavily loaded components and thus an improvement in reliability and a reduction in wear and frictional losses. System reliability is further improved by the close control of pressure testing after manufacture and by the provision of pressure relief valves in the system. In addition, all systems include filtration units to give protection from abrasive wear and the silting of controls and working surfaces by contaminants in the hydraulic fluid.

(g) Low system inertia.

Hydrostatic transmission pumps and motors are generally compact with low rotational inertias and because the quantity

of fluid in the units and the pipes is relatively small, hydrostatic transmission systems generally possess low system inertia. This results in lower torque demands on the prime mover or possible braking system and an increase in the rate of acceleration possible and improved speed control.

The main disadvantages are twofold:

(i) relatively high prime cost of units;

(ii) rather low overall system efficiency.

In common with other power transmission systems, the prime cost of the equipment is directly related to the levels of power to be transmitted, the standards of control required and the degrees of utilisation, life and reliability expected from the equipment. To achieve these requirements the quality of design, development and manufacture called for is generally very high.

Complex design, high quality materials and close manufacturing tolerances lead to high unit costs. Furthermore, since the specifications tend to vary from one application to another, product rationalisation is not easy. Hence it is usually necessary to tailor make the system to suit a particular application. The cost is also high because of low batch production levels. However, the picture is generally encouraging. Widespread publicity and sales campaigns are stimulating usage and this together with improvements in manufacturing techniques are tending to reduce the adverse prime costs.

The losses which affect system efficiency are:

1) mechanical losses)
2) volumetric losses) in pump and motor
3) hydrodynamic losses)
4) flow losses in pipes and ancillary units.

An appreciation of this disadvantage can be obtained by considering the losses in a purely mechanical transmission such as a change gearbox. The losses are due to friction at the gear contacts, in the seals, in the bearings and due to shearing and displacing the lubricant. The

friction losses at the gear contacts can be very low and generally of the order of 2% for spur gears whilst the seals are seldom under fluid pressure and require low contact pressure, low frictional losses can be expected using modern improved elastomers. Extensive use is made of rolling element bearings having coefficients of friction of say 0.001 to 0.002 and so very little power loss occurs in the bearings. Again by the correct selection of the lubricant and the mode of lubricating the gears and bearings, low frictional losses result from shearing and displacing the lubricant.

On the other hand, the losses in a hydrostatic transmission are not so easily minimised and can in the aggregate be appreciable. Despite the fact that the working parts of the pumps and motors are operating under most favourable conditions of lubrication, mechanical losses do occur. Such losses are in the bearings, rubbing surfaces, seals, etc., and unlike the gearbox application, a proportion of the moving surfaces slide, e.g., pistons in cylinder bores. In addition, losses occur due to internal leakage, i.e., volumetric losses and these occur whenever a pressure differential exists across a sealing gap, e.g., pistons and cylinders, valve faces, etc. Some degree of leakage is of course necessary for lubrication purposes but volumetric losses significantly reduce unit efficiency.

Within the pump and motor, hydrodynamic losses occur due to fluid flow through the various flow paths. In many instances this is turbulent in nature and results in pressure losses proportional to the mass density of the fluid and to the square of the fluid velocity. Flow losses due to change of flow path dimensions and direction are difficult to avoid in practical design and these contribute to the losses in the pump and motor.

Further losses occur in pipes and ancillary equipment and although these depend very much on the system layout and pipeline sizing, they are significant when compared with the low losses in the mechanical equivalent of say a prop-shaft. Considerable losses can take place in directional and flow

control valves and this gives added cause for considering variable displacement and reversible flow pumps in a hydrostatic transmission.

The sum total of these losses often results in a system efficiency which is appreciably lower than that of a competitive mechanical system, although this may be offset by the considerable advantages already discussed. It is thus apparent that the more widespread acceptance of hydrostatic power transmissions will result only if progress is made in:

(a) design engineering to reduce manufacturing costs and to improve unit and system performance;

(b) manufacturing technology to give lower costs.

Another disadvantage which is receiving considerable attention both by designers and researchers is that of noise. By good design, the noise generated in pumps, motors and valves can be reduced to acceptable levels. In a complete hydrostatic transmission noise is produced by three basic causes:

i) by the rapid change of component impedance;

ii) by the instability of control valves;

iii) by the periodic pressure variations within the pumps and motors.

The rapid change of component impedance is typified by the fast closing of a flow valve and results in shock waves being generated which cause the emission of high amplitude noise. These effects can be reduced by the slower closing of such valves and if this is not entirely satisfactory, by the inclusion of hydraulic accumulators at the point of maximum pressure shock.

Instability of control valves is very complex but is often due to the use of springs of low spring rate. However the problem is sometimes due to disturbing forces resulting from varying flow patterns within the valves.

The noise emitted by pumps and motors is less easily reduced and invariably some loss of efficiency is incurred. The periodic pressure variations occur during the switch of the displacement chamber between the inlet and outlet ports, that is, between the low pressure suction condition to the high pressure delivery condition. An instantaneous switching would result in very high pressure gradients and the generation of shock waves with the frequency of the switching. A more gradual switching would reduce the noise levels but this also increases internal leakage losses in the unit. The detrimental effects of noise may be reduced by careful attention in design and installation of the complete transmission system.

4.2 The Control of Hydrostatic Transmissions

The basic controls of hydrostatic transmissions are designed to regulate the operating variables, i.e., flow rate and pressure, and to control the direction of flow in the system. By regulating the operating variables it is possible to control the dependent variables, i.e., speed and torque respectively. Since both the products of flow rate and pressure and of speed and torque are measures of input and output power, effective control can be achieved of the power levels in the overall drive system. Again by controlling the fluid pressure it is possible to limit to safe values the applied stresses on the system components.

The controls can therefore be grouped as:

a) speed / power b) torque / safety c) directional

Speed control can be effected by using either:

a) a spill system;
b) a throttle system; or
c) a variable displacement system.

With a spill system, the flow rate to the hydraulic motor can be varied by bypassing part of the pump output directly back to tank. Depending upon the flow characteristics of the spill valve, the motor speed can be varied between wide limits -

with a maximum of -

$$n_{m(MAX)} = \frac{n_p q_p}{q_m}$$ with the spill valve closed

and a minimum of -

$$n_{m(MIN)} = 0$$

if the spill valve is able to pass the full pump flow to tank at a pressure differential less than that required to rotate the hydraulic motor and the coupled load.

From Mass Continuity

$$Q_m = Q_p - Q_s = Q_p(1 - K_R) \tag{4.4}$$

where K_R is the regulation factor $= \frac{Q_s}{Q_p}$

$$n_m q_m = n_p q_p (1 - K_R)$$

from which -

$$n_m = \frac{n_p q_p (1 - K_R)}{q_m} \tag{4.5}$$

Assuming no power losses in the system -

$$P_{IN} = n_p q_p P$$

then $$P_{OUT} = n_p q_p P (1 - K_R) \tag{4.6}$$

Such a system is power wasteful since when the spill valve is open to any degree, hydraulic fluid is being passed to tank at full system pressure. Fig.4.2, shows the characteristics for this type of control given by equation (4.6). It will be noted that at low motor speeds the power losses are very high indeed. These power losses cause

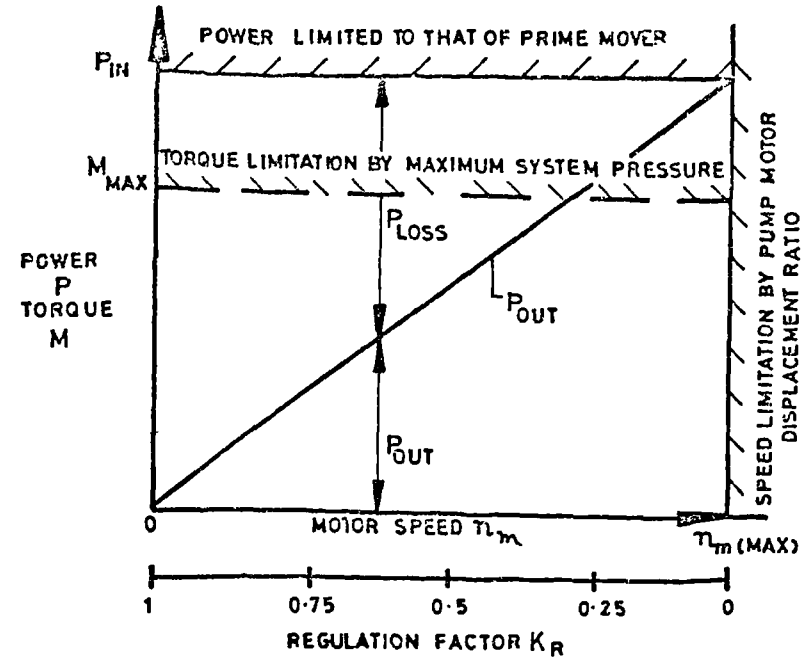

FIGURE 4.2. CHARACTERISTICS OF SPILL CONTROL SYSTEM WHEN USED WITH CONSTANT SPEED PRIME MOVER.

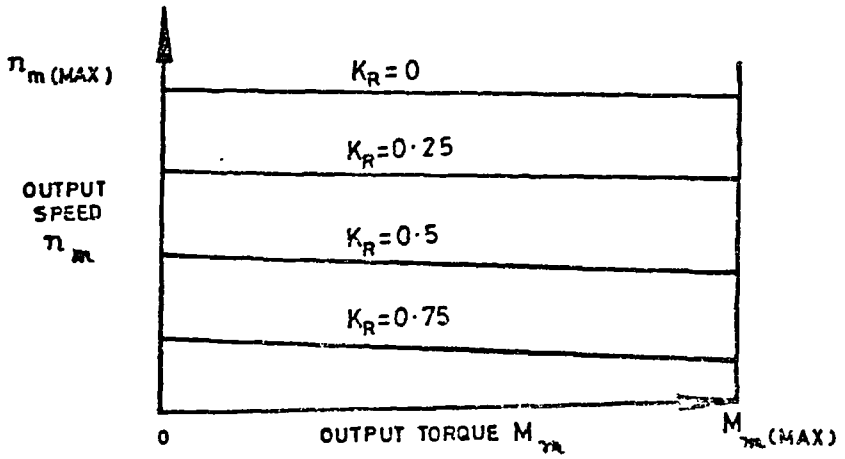

FIGURE 4. 3. VARIATIONS IN OUTPUT SPEED WITH OUTPUT TORQUE FOR THROTTLE CONTROL SYSTEM.

temperature rises in the fluid and in the units and this leads to changes in the system performance, because the fluid viscosity is decreased and there is a reduction in the volumetric efficiency of the pump and motor. Thermal expansion can adversely affect the working of the pump, motor and controls. For these reasons the spill control system is mainly used for lower power transmissions in which the system efficiency takes second place to low prime cost and where the quality of the control required is of a low order.

A throttle system of control incorporates in some form a flow control valve whereby the flow rate to the motor is regulated by a variable flow passage. In effect the controlling feature is an orifice or tube which, by varying its cross-sectional area or its length, is capable of regulating the flow of fluid. The flow control valve acts as a variable restrictor and the flow rate is a function of the pressure differential across the valve.

Since the system uses a positive displacement pump, the flow rate in excess of that required to rotate the motor at the required speed, must be returned to tank and this is achieved by setting a pressure relief valve at a suitable pressure level. The system has similar uses and much the same disadvantages as the spill system except that it is necessary for the pump in a throttle system to develop an additional pressure to compensate for the pressure drop across the throttle valve.

In its simplest form a flow control valve is a fixed throttle with an inlet pressure equal to that of the pressure relief valve setting. Since variations of load on the hydraulic motor will create pressure changes to the output of the control valve, the flow rate through the valve will vary resulting in characteristics as shown in Fig.4.3. Also a change of fluid viscosity due to temperature changes will affect the flow rate. These disadvantages are overcome in practice by incorporating pressure and temperature compensating devices in the control valve.

However a further complication still exists in the form of the 'rate effect' of the pressure relief valve. Invariably

the controlling element in such a valve is a fixed rate compression spring and this results in the relief pressure increasing as the flow rate through the relief valve increases. As a consequence the pressure on the inlet to the flow control valve will vary with the flow requirements of the hydraulic motor.

A Variable Displacement System is one in which the pump or motor (and in some instances both) has provision for varying the displacement. A description of variable displacement axial piston pumps is made later in this Chapter and similar methods can be applied to vane type units and also radial piston units. This method of speed control is by far the best of the three methods being considered. With the most common control of a variable displacement pump, only sufficient fluid to rotate the hydraulic motor at the required speed, is pumped, with no excess fluid under pressure being passed to tank. Thus the system has infinitely variable control, often with provision for reversing the rotation of the output shaft, and with a minimum of power wastage.

Power controls are frequently used with hydrostatic transmissions. By the inclusion of suitable controls, virtually all the available power from a prime mover can be fully utilised. This is best illustrated by means of Fig.4.4, which shows a typical output torque and power curve for a hydrostatic transmission fitted with power controls and driven by an I.C. engine. It will be seen from the power curve that the hydrostatic transmission is able to transmit the maximum power of the prime mover for most of the range of output speeds. This means that the prime mover can be run at a speed which gives maximum power and the drive system has the capability of transmitting this power over a wide range of speeds. By superimposing the torque and power output curves which would be possible using a four speed gearbox instead of the hydrostatic transmission, the shaded areas indicate levels of torque and power not available at specific speeds when using the gearbox but available with the hydraulic drive.

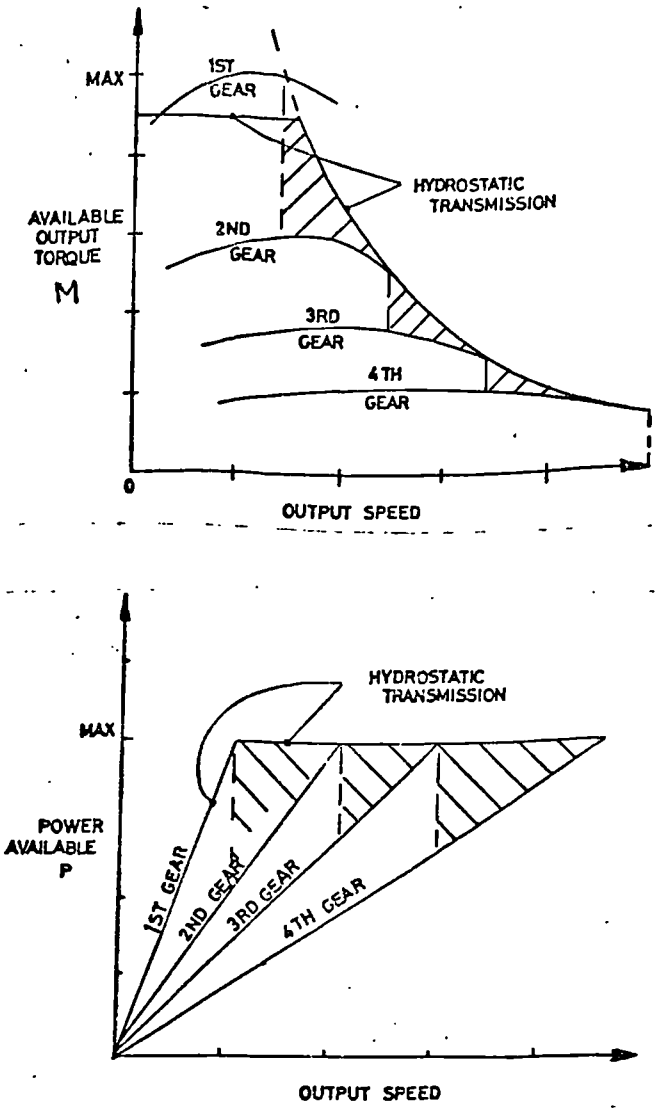

FIGURE 4.4. COMPARISON OF AVAILABLE OUTPUT TORQUE FOR A FOUR SPEED GEARBOX AND FOR A HYDROSTATIC DRIVE USING THE SAME PRIME MOVER.

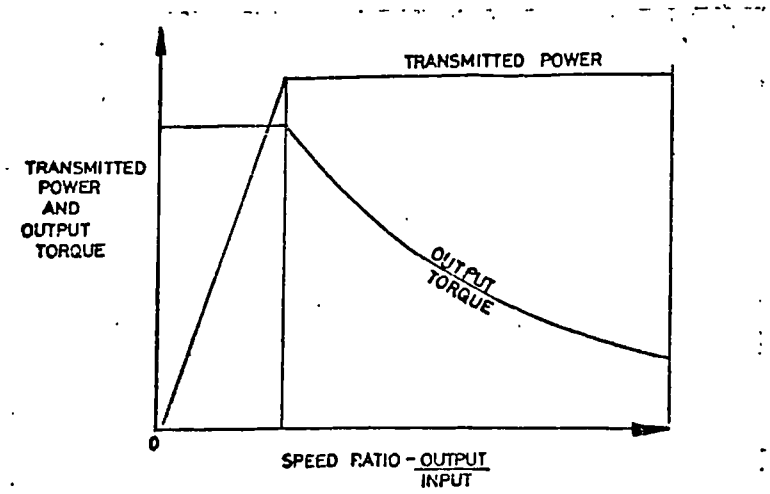

FIGURE 4.5. TYPICAL PERFORMANCE OF A HYDROSTATIC TRANSMISSION WITH CONSTANT POWER CONTROLS ON THE PUMP.

The control of the power input to the pump is effected by varying the flow rate with respect to the system pressure. The system pressure can be sensed and compared with the load/deflection characteristics of a spring (or springs) assembly and the required change of pump displacement made by giving a signal to a servo assisted flow control similar to that already described. Thus for a system using a constant speed input, as the output speed varies from zero to a maximum, the flow rate from the pump is regulated so that the pressure in the system and hence the output torque, is also regulated and the power remains near constant. Fig.4.13, shows a typical constant power control for use with an axial piston pump and Fig.4.5, shows the performance curves for a hydrostatic transmission with power control.

Torque control is often desirable in a hydrostatic transmission to control the output torque. This necessitates regulating the pump pressure since the torque developed by the hydraulic motor is directly proportional to the pressure across the motor. The pump pressure is controlled by regulating the flow rate from the pump and a servo system described later will achieve this if the force resulting from the pump pressure acting on a piston is compared with a suitable preloaded compression spring force. A relatively simple control is shown in Fig.4.14, with typical characteristics in Fig.4.6. At low pump flow rates it is not possible to control the pressure level and the pressure can rise to the setting of the system pressure relief valve.

Safety controls in hydrostatic transmissions are essentially valves which prevent the flow of fluid at pressures below a predetermined level but which allow high flow rates at and above that pressure. In their simplest form these units are direct acting spring loaded relief valves but more frequently pilot operated relief valves are used.

In many drives, the facility to reverse the rotation of the motor and its coupled load, induces high pressure build up in the system and safety controls in the form of double acting relief valves are used to cater for the bi-directional nature of the problem. An additional safety control is the inclusion

of a low pressure replenishing valve which ensures that the system is completely full of fluid and so safeguards against cavitation effects with motor overrun.

Directional control is a facility to vary the direction of rotation of the hydraulic motor without changing the rotation of the prime mover. This can be achieved in two ways.

a) by a directional control valve in the circuit, or

b) by using a variable displacement pump with full variable displacement in both directions.

A typical circuit using a unidirectional flow pump and a directional control valve is shown in Fig.4.7. It will be seen that unless the pump output is reduced prior to reversing the flow to the motor, a sudden change in motor rotation is to be expected. On the other hand the use of a pump with full variable displacement in both directions has the advantage that the action of reversing the direction of flow causes the pump flow to decrease to zero before rising again to the required reversed flow rate. Although the prime cost of method (b) may be expected to be higher, the smoothness of reversing the rotation of the load will often outweigh this disadvantage.

The modern practice in hydrostatic transmissions is to incorporate as many of the system controls as is convenient within the pump and/or the hydraulic motor units. Taking the common system of a variable displacement pump with a fixed displacement motor as an example, it is of considerable advantage to integrate the speed, torque, power, safety and directional controls within the pump assembly. The benefits to be derived from this concept are considerable since in addition to the close matching of the pump and the controls, pipe runs and connections are reduced to a minimum and installation difficulties are made easier.

Some pump manufacturers make provision for directly coupling a boost pump to an extension of the main pump shaft and this is of considerable benefit for closed circuit systems as shown in Fig.4.8.

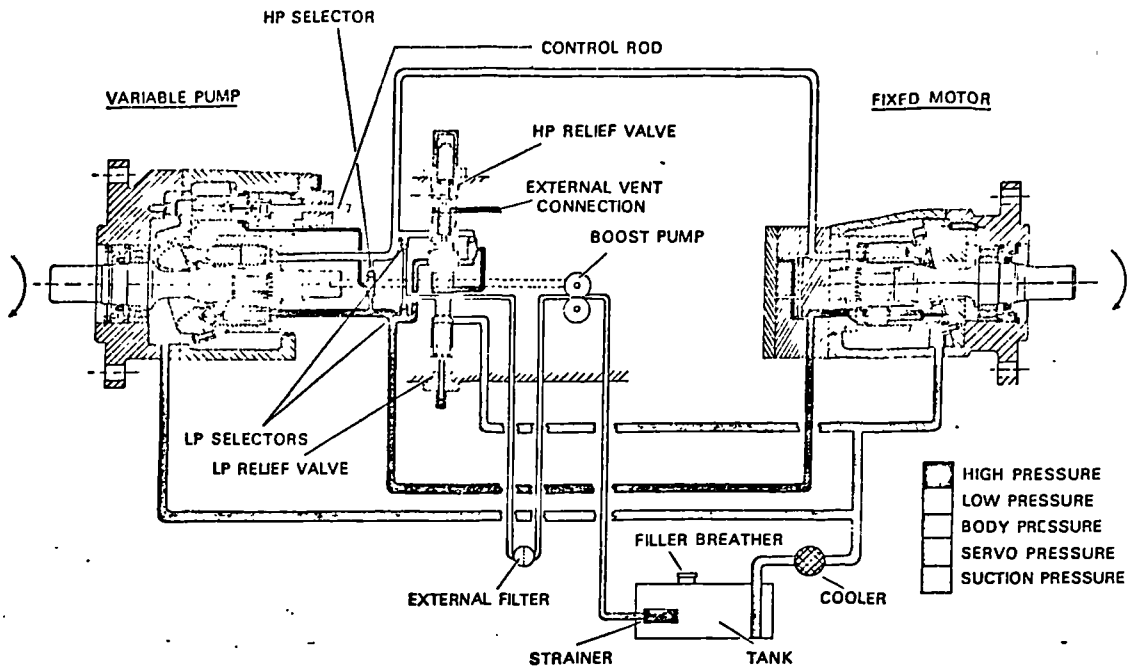

FIGURE 4.7. A TYPICAL CIRCUIT USING A VARIABLE DISPLACEMENT PUMP WITH A DIRECTIONAL CONTROL VALVE.

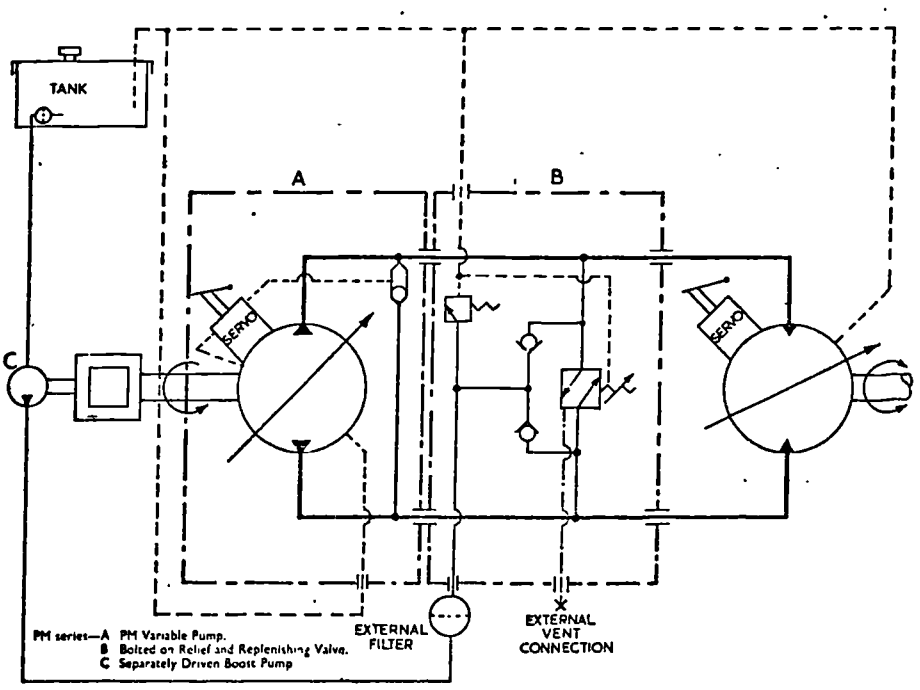

FIGURE 4.8. A CIRCUIT DIAGRAM FOR A CLOSED CIRCUIT HYDROSTATIC TRANSMISSION SYSTEM.

4.3 Applications of Hydrostatic Transmissions

Hydrostatic transmissions are widely used in industry and transport where the advantages of control and installation flexibility outweigh the disadvantages already discussed. In many instances the use of a hydraulic system can combine both primary and secondary drives, e.g., movement of the machine to the place of operating and powering the operation itself. This often results in simplifying the design of the machine and leads to compact installations.

In the machine tool industry, hydrostatic transmissions are used to drive tool spindles and rotating work tables. The full potential of smooth infinitely variable speed control, fast reversal and high torque/low speed characteristics can be fully utilised and are easily integrated with numerical controls. The flexibility of installation is particularly advantageous since a centralised hydraulic power pack can supply several working areas of the machine tool, each having the necessary hydraulic motor or linear actuator. The size and weight benefits of hydraulic motors result in compact workheads and a minimum of interference with workpieces.

In addition to normal and special machine tools, hydrostatic transmissions are extensively used in production transfer lines. Once again centralised hydraulics is common and the distinct advantages of easy installation, low maintenance, ease of control, system safety, and the 'uncluttered' arrangements compared with a mechanical drive system, can far outweigh a prime cost disadvantage.

Manufacturing process industries frequently use hydrostatic transmissions and a typical example is that in which continuous film, strip, or the like, is produced and the requirements are for constant tension in the product with infinitely variable speed control. Sensitive control of these conditions is possible by using the positive flow, variable pressure characteristics of the system. This is further facilitated by the positive control of the system and its low inertia benefits.

In the heavy process industries, hydrostatic transmissions are in direct competition with mechanical/hydrokinetic trans-

missions. For high working speed the hydrostatic systems are at some disadvantage, but for low speed high torque conditions, the successful design of low speed motors has put hydrostatic transmissions in a highly competitive position. This is particularly so where high starting torques are experienced and in such cases, hydraulic motors can be used which develop 95% full load starting torque, at high levels of efficiency. Whilst on the subject of low speed high torque hydraulic motors, it is worth discussing the choice a designer has to make. Speed reduction and torque amplification is possible using a reduction gearbox driven by an electric motor but only modest reductions are possible without resort to compound gear trains, epicyclics, worm or spiroid gearing. Each of these can be power consuming but the high ratio worm gearing is the least favourable. In addition the inertia effects in such mechanical drives can greatly reduce the starting torque available at the output shaft. The use of a fluid coupling or torque convertor will assist start up but will not alleviate the speed change problem. On the other hand the hydrostatic transmission benefits from relatively low system inertia and has the provision for start up with the prime mover running at speed.

In transport, hydrostatic transmissions are used for vehicle drives, ship propulsion and control and handling functions in aircraft. Vehicle drives for heavy crawlers, harvesters and off-road vehicles often utilise hydrostatic transmissions as either straight drives or associated as shunt drives in which, by the use of differential units, the main power transfer is through a high efficiency mechanical drive involving gears, connecting shafts and couplings, whilst the hydrostatic drive enables variable speed and direction reversal to be obtained. Off-road vehicles frequently use low speed high torque motors built into the wheel hubs. The positive nature of the drive sometimes eliminates the need for power brakes since the hydrostatic system admirably meets this requirement. Often only low cost, low power brakes need to be provided for parking the vehicle. The high strength construction of the hydrostatic units, together with the

pressure relief valve protection makes this form of drive very suitable for the heavy stress reversals encountered in these vehicles.

Considerable effort is being made to gain acceptance of hydrostatic transmissions for on-road vehicles. Here the levels of overall efficiency and prime costs are dominant factors. The successful development of automatic gear transmissions has had adverse influence on the prospects of hydrostatic transmissions for vehicles.

In marine transport, hydrostatic transmissions are widely used for deck machinery and high efficiency systems are sometimes used for the main ship propulsion. These enable the ship's engines to operate at constant speed for optimum efficiency and both propeller speed and direction of rotation are controlled by the hydrostatic transmission. Additional applications include the driving of small propellers located in the bow of the ship, at right angles to the ship's length for in-port manoeuvering.

Modern aircraft are hydraulic power extensively for flight controls, landing gear, etc. In general, linear hydraulic actuators are used and as such the system is not a hydrostatic transmission in the accepted sense, but frequently parts of the plane's hydraulic system employs hydraulic motors to change flight configuration, transfer fuel, open and close loading bays and power cargo hoists.

The main applications in rail transport are for shunting engine drives and powering winches for movement of rolling stock. In the example of shunting engines the variable speed high torque characteristics can be fully utilised and the ease of applying the principles of dynamic braking make the use of hydrostatic transmissions particularly advantageous.

Hydraulic equipment (incorporating hydrostatic transmissions) is used extensively in mining, quarrying and power drives for the long heavy duty conveyor systems. Also many of the specialised cutting and clearing plant to be found in a modern mine are equipped with hydrostatic drives.

4.4. Description of Axial Piston Pumps

The 'heart' of a hydraulic system is the pump and as in the human body the physical performance is to a large degree dependent on the quality of the heart as a pumping unit, so too in the hydraulic system, the overall performance will only be as efficient as the quality of the pump will allow. It is therefore of prime importance that the pump which is chosen for a hydraulic system, has the performance characteristics necessary for the system as a whole and is of a quality of design and manufacture such that the important aspects of reliability and design life are fully satisfied. An additional consideration, which does not apply to the human heart analogy, is that the capital cost of the pump is acceptable in the light of the total system cost.

Many hydraulic systems require flow control and this can be adequately achieved in some instances by the use of flow control valves. In hydrostatic transmission however the facility to have infinitely variable flow control from zero to a maximum value, without the adverse losses of power associated with flow control valves, makes the use of variable displacement pumps a common feature of such transmissions. It is therefore apposite to consider axial piston pumps against the background of hydrostatic transmissions.

Figs.4.9. and 4.10, show outside and sectional views of a typical pump. The pump consists basically of a cylinder block which rotates with a shaft between bearings and which has a number of cylinder bores equally spaced on a pitch circle and with the axes of the bores parallel to the axis of rotation of the shaft and cylinder block. Each bore has a piston that is reciprocated by the reactions from a swash plate assembly, which is basically a stationary flat plate set at an angle to the axis of rotation. A slipper bearing at one end of each piston transfers the forces across the interface with the swash plate and during half of the rotation, the piston is partially withdrawn from the cylinder bore and this causes fluid to flow into the pump. During the second half rotation, the piston is forced into the cylinder bore and in so doing pumps hydraulic fluid out of the pump.

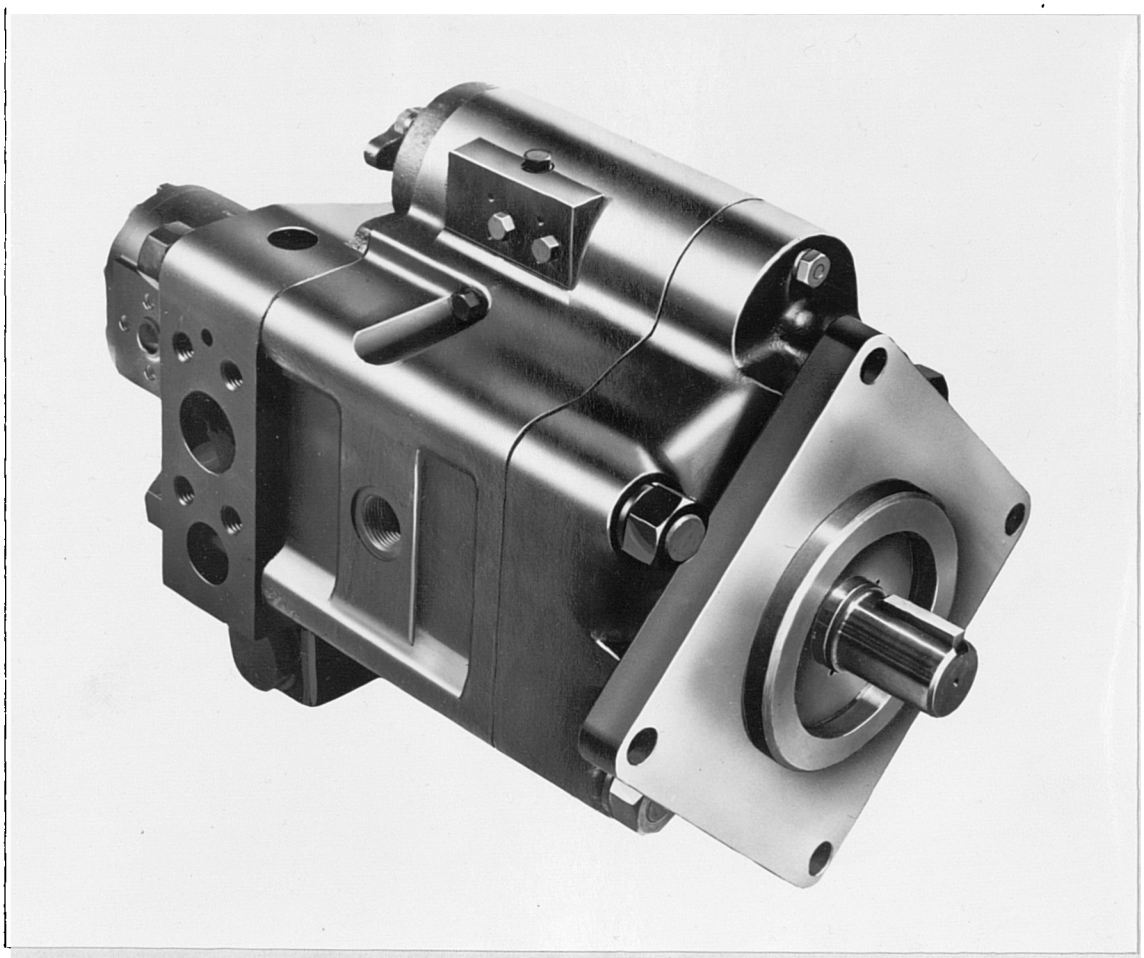

FIGURE 4.9. OUTSIDE VIEW OF THE LUCAS TYPE HD 900 VARIABLE DISPLACEMENT AXIAL PISTON PUMP.

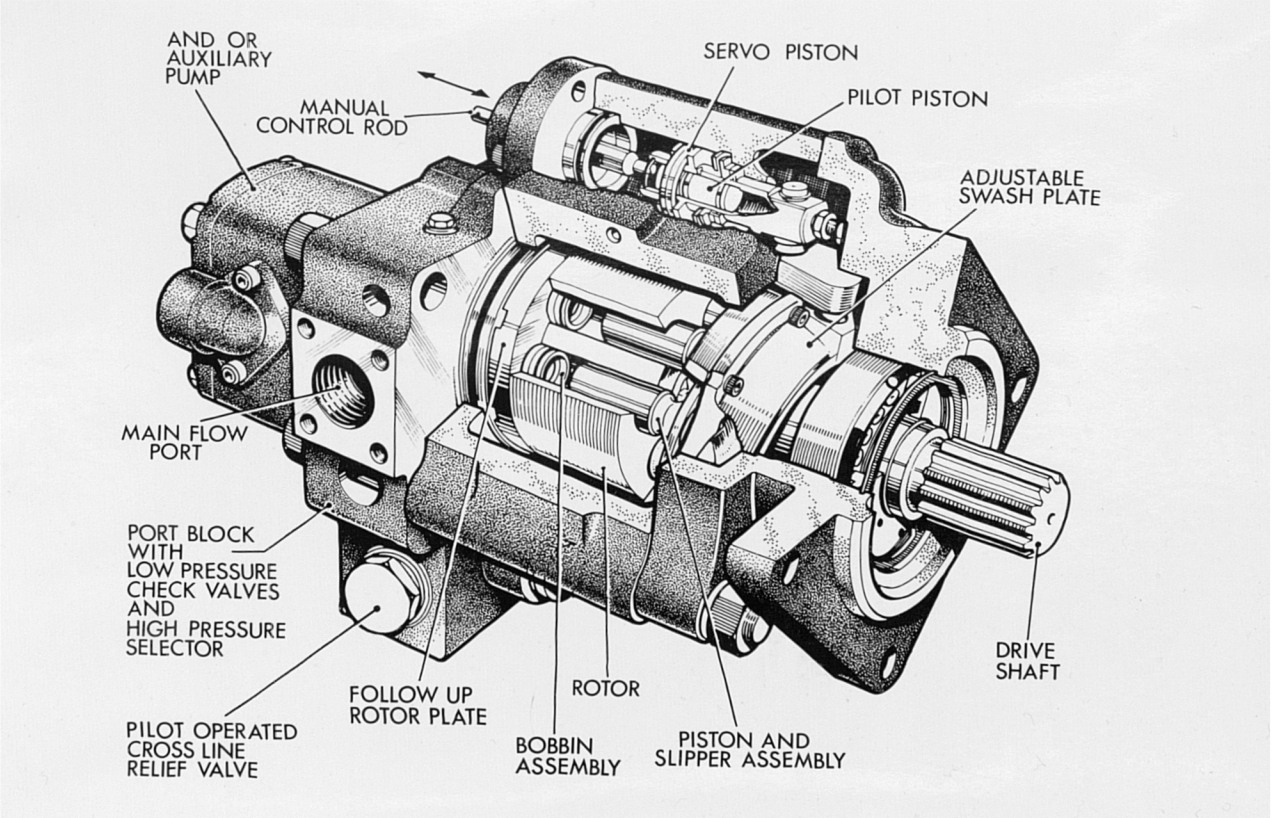

FIGURE 4.10. SECTIONAL VIEW OF THE LUCAS TYPE HD900 VARIABLE DISPLACEMENT AXIAL PISTON PUMP.

Between the inlet and outlet ports of the pump is a flat plate which is generally known as the valve plate and this is the means of directing the flow of hydraulic fluid from the inlet port to the cylinder bore and eventually from the cylinder bore to the outlet port of the pump. This is achieved by having two kidney shaped slots about a pitch circle of much the same size as that for the piston cylinder bores and with each slot extending for near 160^{o} of the pitch circle. With the slots either side of the top dead centre to bottom dead centre axis of the pump, suction flow will occur through one slot and delivery flow through the other slot.

The swash plate is frequently adjustable for angle of tilt and a change in the angle will result in a change in the length of stroke of the piston. Since the volume of fluid drawn into the cylinder bore and subsequently pumped out is approximately equal to the product of the area of the piston and the piston stroke, a change in the swash plate angle will alter the pump displacement. A pump having a fixed angle of tilt of the swash plate is a fixed displacement pump whilst a pump having the provision for varying the swash plate angle is a variable displacement pump.

Axial piston pumps of the swash plate variety are particularly suitable for use as variable displacement pumps. No design or constructional difficulties are encountered in varying the angle of tilt from zero to a maximum value in both a positive and in a negative direction. This means that such a pump has a full range of displacement from a maximum in one direction to a maximum in the opposite direction with the advantages of zero displacement at the zero tilt angle position. The operational advantages of the pump are apparent, with the provision for adjusting the flow rate to match the output requirements of the hydraulic system, to obtain the condition of zero flow rate when no motion is required from the system and to reverse the direction of movement of the hydraulic actuators without the use of expensive and power consuming directional control valves.

Axial piston pumps are frequently coupled directly to prime movers such as I.C. engines and electric motors and the facility of varying the displacement of the pump allows the

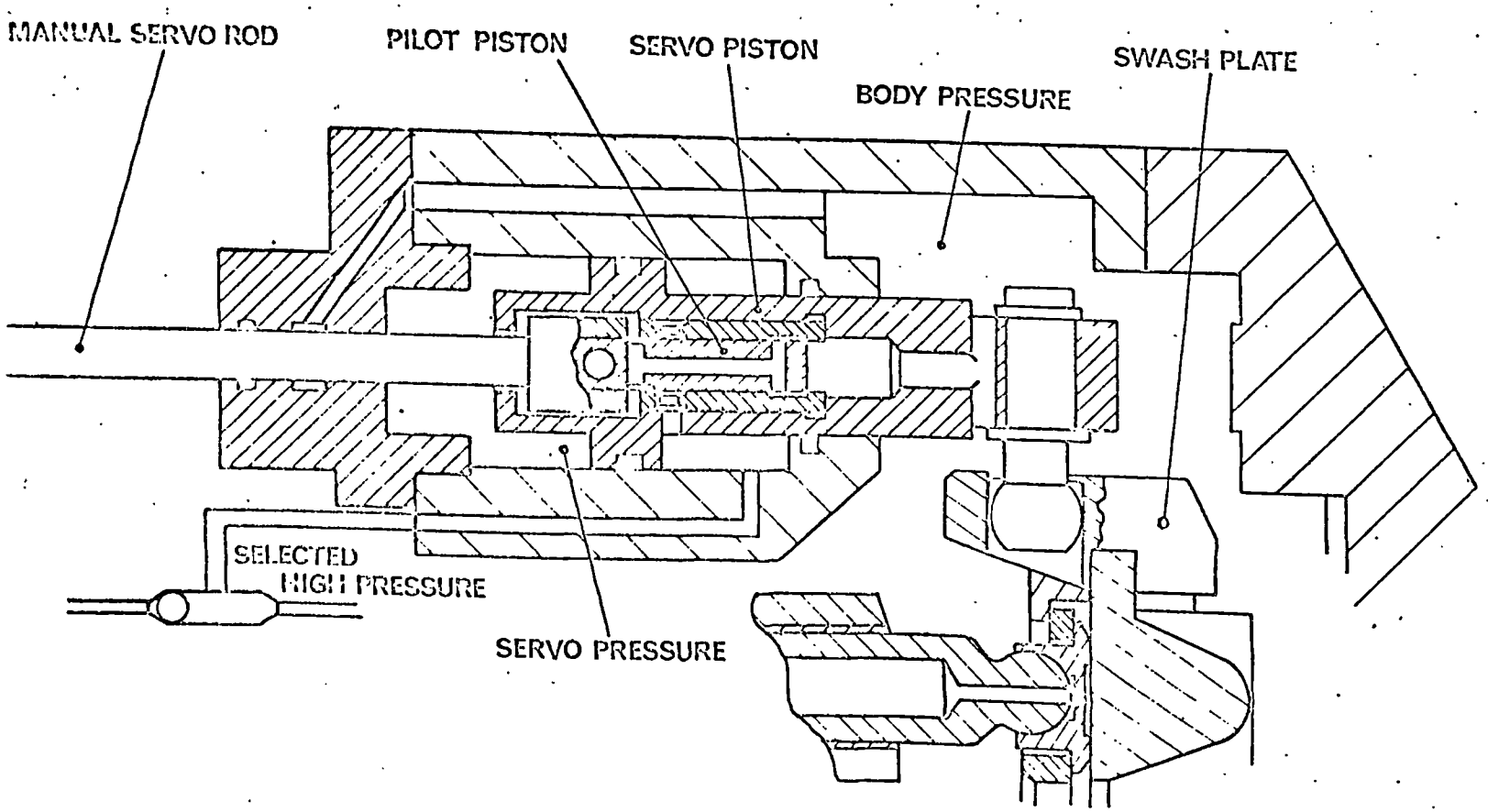

FIGURE 4.11. DIAGRAM OF A MANUALLY OPERATED SERVO ASSISTED VARIABLE ANGLE SWASHPLATE CONTROL

prime mover to run at near constant speed for all design conditions for the hydraulic system. As a result the prime mover can operate under near ideal conditions with the obvious benefits of economy of running costs and the absence of controls for regulating the speed of the prime mover.

4.5 Control of Axial Piston Pumps

The modern axial piston pump often incorporates controls to regulate the flow from the pump, the power demands on the prime mover and the pressure in the hydraulic circuit. These are generally controls which respond to an external signal as in the case of flow control or to the pressure level within the pump for power and pressure control. The external flow control signal may be manual or from some form of controller, for example, an electro-hydraulic controller. The power and pressure controls are generally mechanical in nature with the sensing by spring devices.

Manual methods of varying the angle of tilt of the swash plate may be simple in nature or of more sophisticated design if this is warranted. By using a lever or leadscrew and nut assembly, manual control can be effected and for many applications this is adequate. However the forces to move the swash plate would react directly onto the mechanical assembly and in particular for pumps of large displacement and working at high system pressure, this presents disadvantages as regards accuracy of control, system response and the size of the mechanism required.

Servo assisted control is much more common and by using a valve controlled hydraulic amplifier, high pressure fluid from the pump itself is directed to act on a servo piston to alter the swash plate angle. This is the type of control shown in Fig.4.10, and a diagrammatic sketch of the same control in Fig.4.11. A feedback system ensures that the servo piston follows the movement of the input signal with acceptable levels of accuracy and lag for most industrial applications. The input signal is a proportional input by manual or other means and the servo piston provides the necessary force amplification so that the input signal requires very little force from the controller.

More precise flow control to match changing system requirements is obtained by using an electro-hydraulic controller and an example of this is shown in Fig.4.12. An electrical signal results in an appropriate movement of the armature of an electric torque motor and this movement is transmitted by a spring lever to a first stage hydraulic amplifier using flapper valve control. This moves a spool type directional control valve and hydraulic fluid, frequently supplied at constant pressure by an auxiliary pump, is directed to one side or the other of the main servo piston connected to the swash plate. The resultant servo force moves the swash plate and this movement is sensed by a positional transducer and provides a negative feedback to the torque motor. System stability is achieved when a condition of equilibrium is reached at the servo piston and at the torque motor. This method of flow control gives high levels of accuracy and low response times and allows various forms of remote control from simple rheostatic to radio control to be used. It is also possible to control the flow rate from a pump to a predetermined programme.

A typical constant power control is shown in Fig.4.13. If at a particular pump speed the flow rate from the pump is at a certain level the product of this flow rate and the pump pressure will be the output power of the pump at that instant. Should the pressure rise for any reason, for example, by an increase in the torque on the hydraulic motor or an increase in thrust on a hydraulic actuator, the power demand on the prime mover will also have been increased. Should this happen and the pump is already taking the predetermined level of power from the prime mover, the control senses the change of pressure and reduces the pump flow accordingly by altering the angle of the swash plate and thus the pump displacement. Although for constant power the pressure flow curve would be parabolic and the use of a compression spring would give a linear form of control, by the careful selection of the spring rate and by adjusting the assembled length of the spring, close conformity to the required constant power characteristic can be achieved.

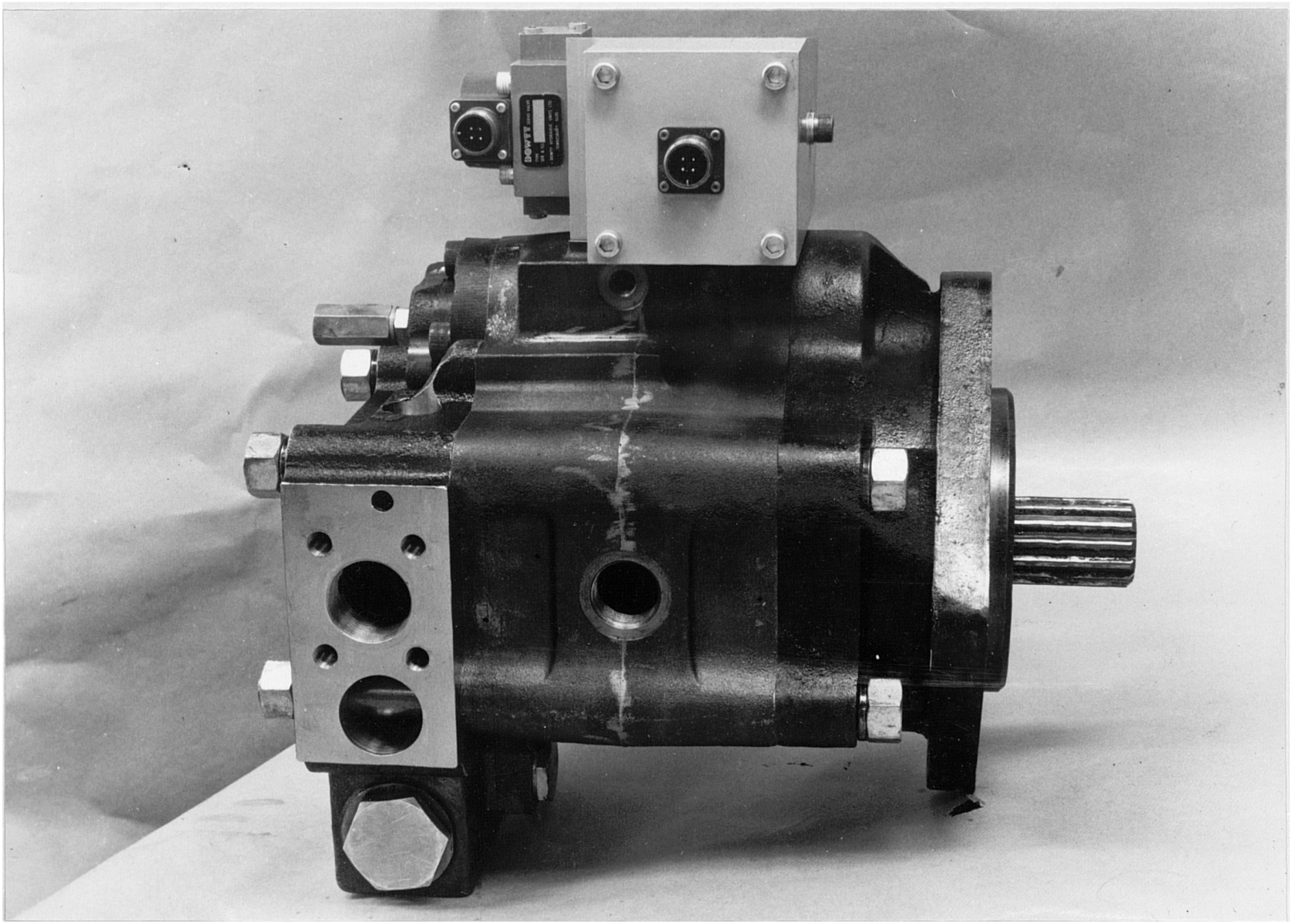

FIGURE 4.12 LUCAS HD 900 AXIAL PISTON PUMP WITH ELECTRO-HYDRAULIC CONTROLLER.

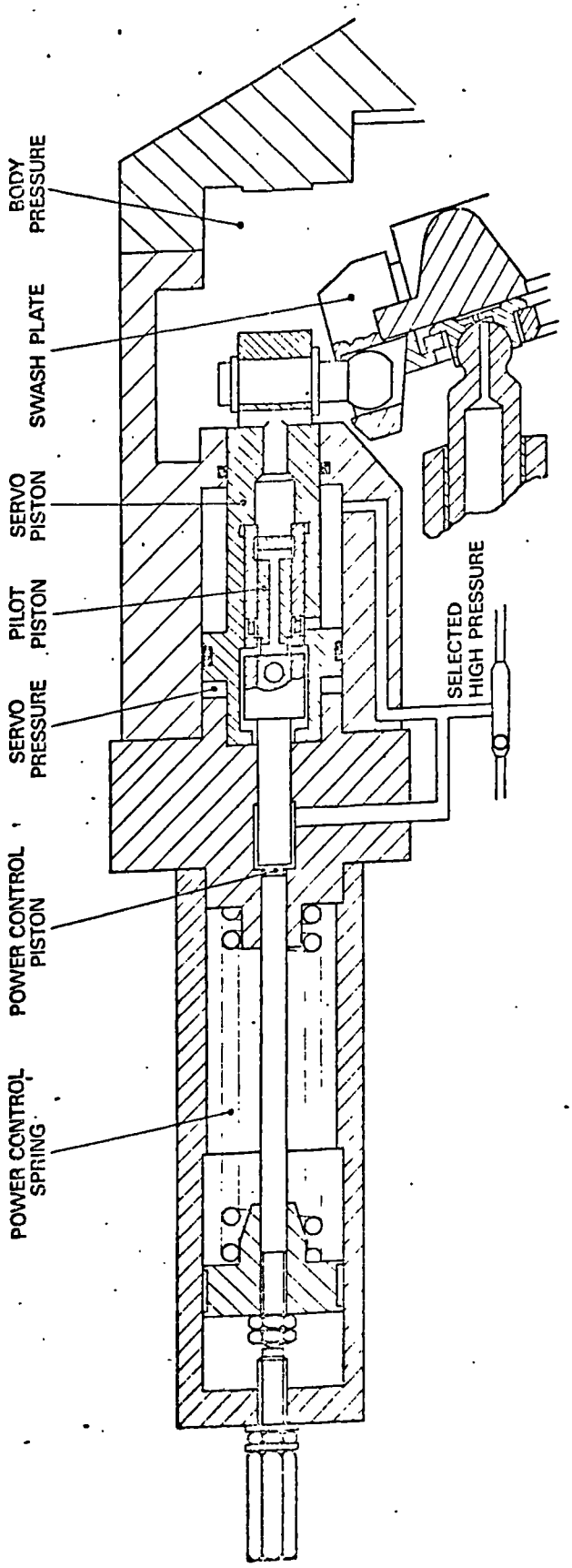

FIGURE 4.13. DIAGRAM OF A CONSTANT POWER CONTROL FOR A SWASHPLATE TYPE AXIAL PISTON PUMP

Constant pressure in a hydraulic system without the power losses associated with pressure relief and regulating valves can be obtained by including constant pressure control on the axial piston pump. Fig.4.14, shows such a control. If the required pressure is exceeded, a push rod allows a ball valve to open on the full piston side of the servo piston. The resultant force on the other side of the piston moves the swash plate to a position of reduced pump displacement and the pressure in the hydraulic system is reduced. On reaching the pressure setting of the control, the ball valve is closed and the system pressure maintained at the required level.

Other controls within the pump are for protecting the hydrostatic transmission system and include high pressure cross-line relief valves to prevent the pressure in the system rising above a predetermined safe level, and the dangers of cavitation at the hydraulic motor due to load overrun and deceleration. Another control could be a low pressure relief valve for ensuring that if a boost pump is used, the pressure developed by this pump is sufficient to open the low pressure selector valves in the main pump to replenish the system of leakage losses. It is also common to include a high pressure selector valve to provide a pressure flow to the flow, power and pressure control valves.

A circuit diagram of a variable displacement pump with manual servo assisted flow control and incorporating the valves described in the last paragraph is shown as part of a complete hydrostatic transmission circuit in Fig.4.7.

4.6 Performance of Axial Piston Pumps

An axial piston pump is essentially a positive displacement unit. This means that for a given swash plate setting, if the pump shaft is rotated one revolution, a volume of hydraulic fluid is pumped out of the pump and that this volume varies relatively little with variations of pressure. Of course some internal leakages do occur which depend on clearances and pressure differentials. Hence the actual displacement is never equal to the theoretical displacement of the pump, but the difference is small.

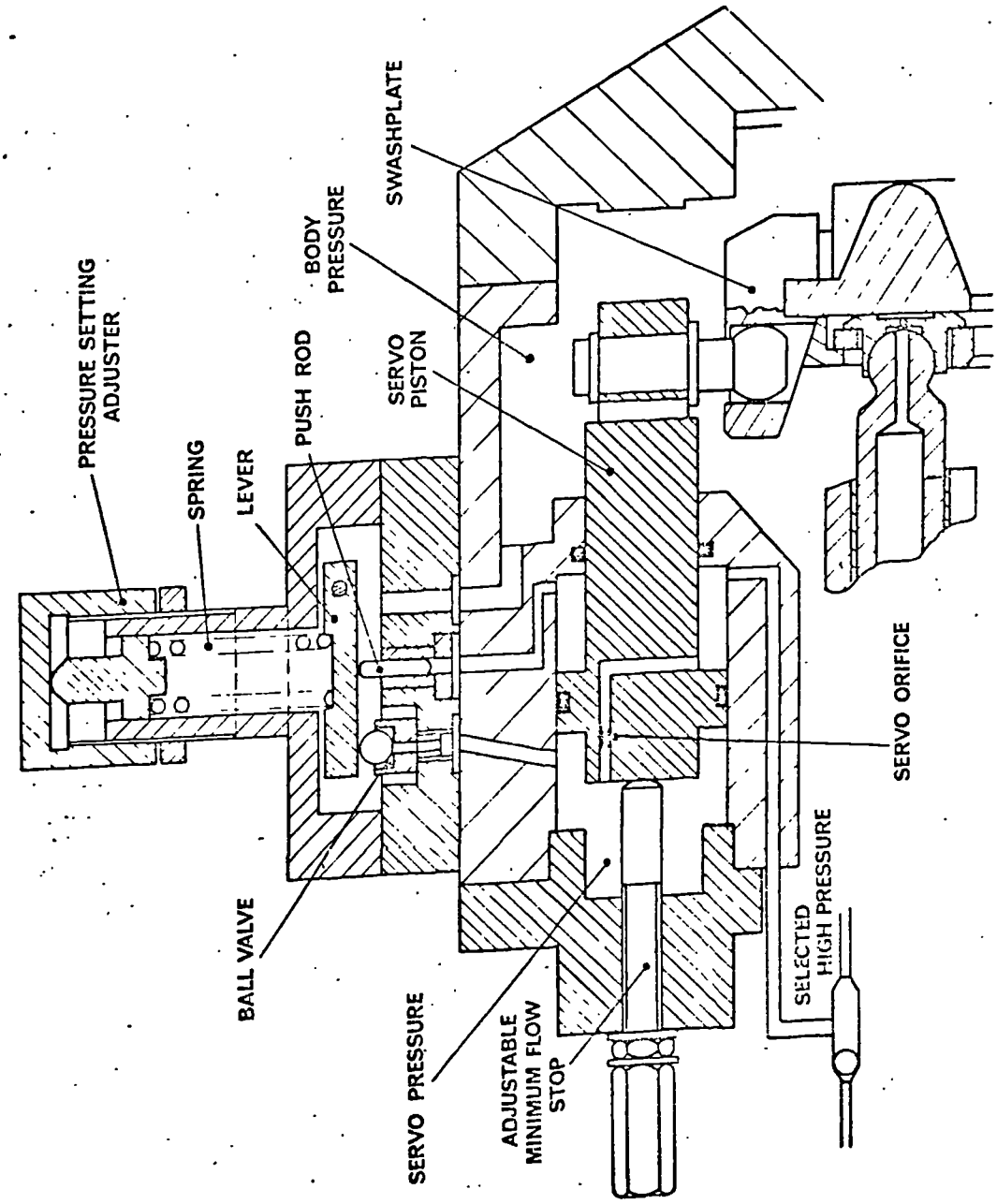

FIGURE 4.14. DIAGRAM OF A CONSTANT PRESSURE CONTROL FOR A SWASHPLATE TYPE AXIAL PISTON PUMP.

Typical performance characteristics for an axial piston pump are shown in Fig.4.15. The curves show the variation of flow rate, input power and overall efficiency for a pump of fixed displacement and running at certain speeds, over a full range of operating pressures. In the case of a variable displacement pump, a set of curves for each setting of the pump displacement would be necessary to completely present the performance characteristics of the pump but in practice curves for maximum displacement setting are adequate for most purposes.

The flow rate curves show the decreases which occur with an increase in pressure but that this is relatively small. In addition to the internal leakages, mechanical losses reduce the efficiency of the pump and the overall efficiencies at the various shaft speeds are indicated by the appropriated curves. Curves for the input power show the effects of the losses by their non-linearity.

An alternative presentation is obtained by plotting iso-power and iso-efficiency curves with flow rate curves against pressure. Fig.4.16, shows a typical set of such curves for the same pump. The advantage of this presentation is that regions of the highest efficiency are readily shown and this can be of considerable assistance in system design.

The efficiencies that can be expected from axial piston pumps depend to a large extent on the quality of the pumps and this is of course reflected in the capital costs of the units. Typical efficiencies for industrial pumps are:

Volumetric Efficiency in excess of 95%
Mechanical Efficiency in excess of 92%
Overall Efficiency in excess of 90%.

It can be seen that the role of the axial piston pump in hydrostatic transmissions is one of prime importance. Improvements in design and manufacture which lead to higher efficiency, greater reliability and improved cost effectiveness, can be expected to lead to an increase in the number of successful applications.

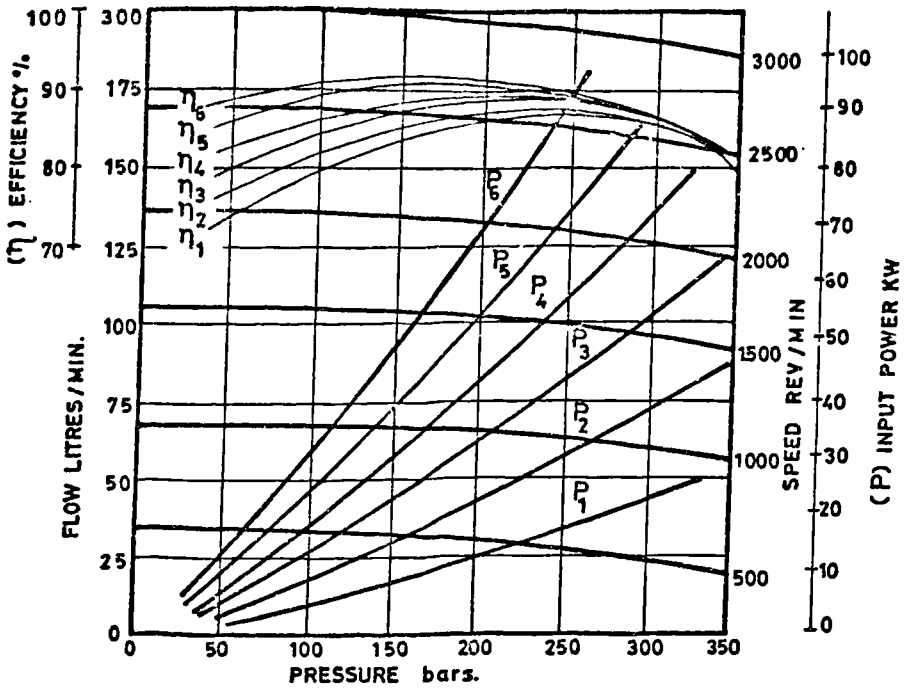

FIGURE 4.15. TYPICAL PERFORMANCE CHARACTERISTICS FOR AN AXIAL PISTON PUMP AT FULL STROKE.

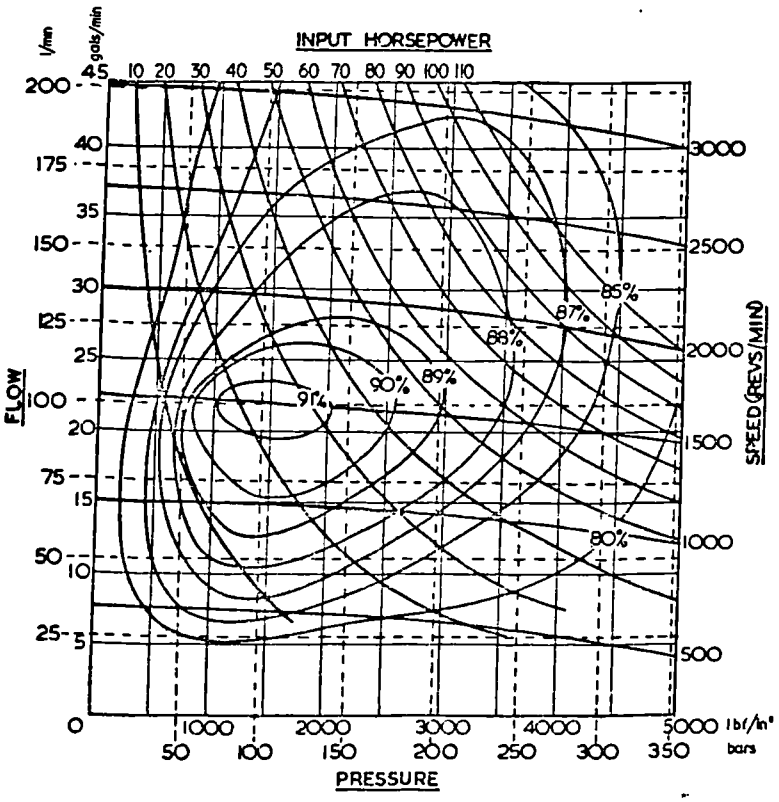

FIGURE 4.16. TYPICAL PERFORMANCE CHARACTERISTICS FOR AN AXIAL PISTON PUMP AT FULL STROKE SHOWING ISO-POWER AND ISO-EFFICIENCY CURVES.

There is evidence that the fluid power industry recognises the need for design and performance prediction methods which lead to improved pump design and this is confirmed by the industrial support for this project.

CHAPTER 5 THEORETICAL DEVELOPMENT OF AXIAL PISTON PUMPS

5.1 Introductory Comments

The design of axial piston pumps and their associated controls require a sound understanding of the theories ranging from the simple concepts of fluid mechanics such as those pertaining to fluid flow through pipes and narrow gaps to those of a more advanced nature involving control theory to estimate the dynamic response of a control system. To present a theoretical background which is of use in the design process, it is essential to closely relate the theory to the operating conditions and performance of the pump or of its controls. This is best done by grouping the theories into four sections: Fluid Mechanics, Mechanical Design, Control Theory and Performance Prediction.

5.2 Fluid Mechanics

An axial piston pump, in common with all positive displacement pumps, does not present special problems in fluid mechanics. Basically the pump draws in hydraulic fluid by the action of developing a pressure inside the pump which is lower than that acting on the fluid at the inlet to the pump and subsequently of forcing the fluid out by developing a pressure inside the pump which is higher than that acting on the fluid at the outlet of the pump.

The conditions which apply can be shown diagrammatically as in Fig.5.1. Hydraulic fluid enters the pump at the inlet port at flow rate Q_{IN} and pressure P_{IN} and passes to the cylinder block via the valve plate. In so doing a pressure loss occurs due to the resistance to flow of the flow path and in particular that of the valve plate. Some small leakage Q_{L1} occurs at the valve plate but this is small and for all practical purposes can be ignored. The theoretical considerations during this stage of suction flow are those of fluid flow and cavitation.

The hydraulic fluid enters the cylinder block at flow rate Q_S and pressure P_S and at the end of the pumping

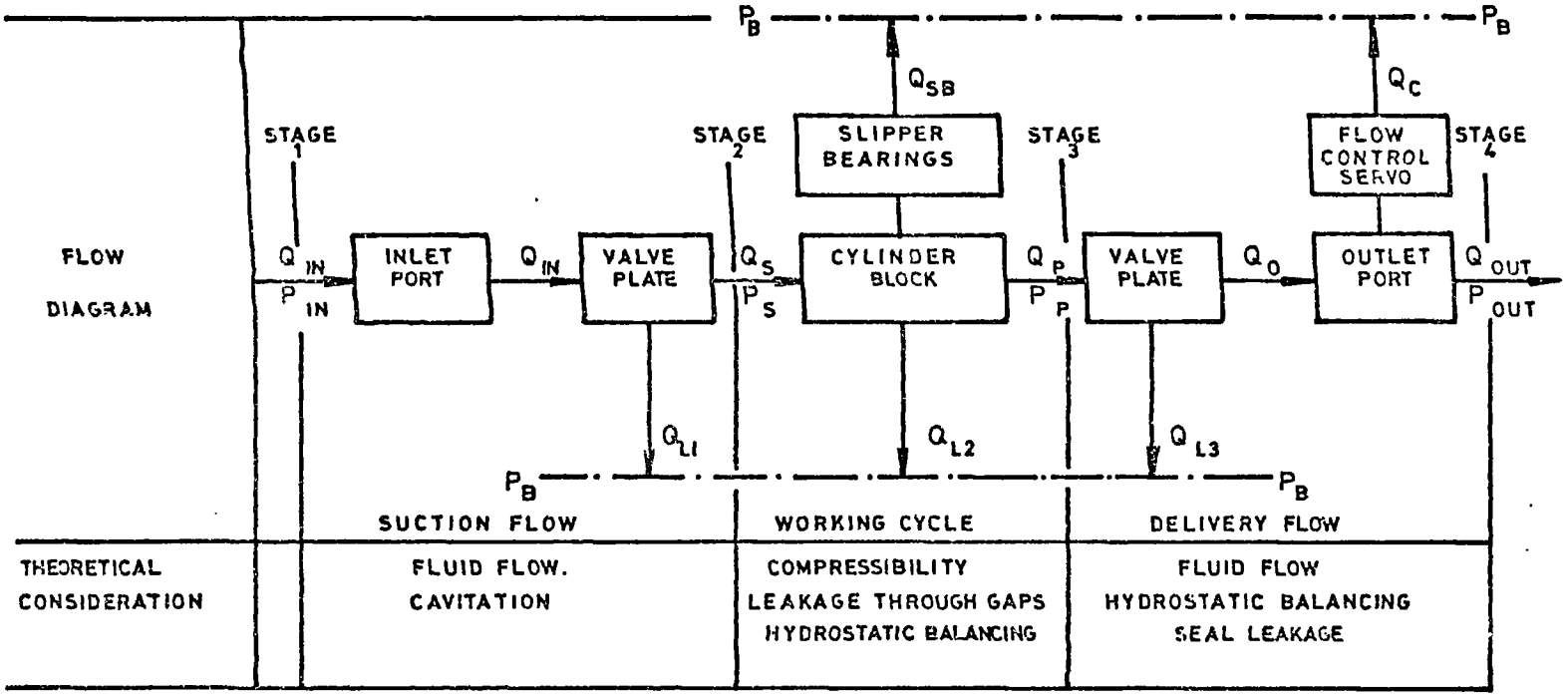

FIGURE 5.1. DIAGRAM OF FLOW CONDITIONS AND THEORETICAL CONSIDERATIONS IN AN AXIAL PISTON PUMP

stroke, the fluid leaves the cylinder block at flow rate Q_P and pressure P_P. Q_P is less than Q_S due to the leakage losses Q_{L2} past the piston and the flow rate Q_{SB} required to provide hydrostatic bearing conditions at the various slipper bearings. Since we are considering volume flow rates as opposed to mass flow rates, Q_P is again less than Q_S because of fluid compressibility. The theoretical considerations which apply during the working cycle are thus concerning leakage through gaps, hydrostatic bearing and compressibility effects.

After leaving the cylinder block with flow rate Q_P and pressure P_P the fluid passes through the valve plate and to the outlet port. Leakage losses Q_{L3} occur at the valve plate and a high pressure bleed-off to a flow control servo piston for positioning the swash plate angle may require a flow rate of Q_C. Q_C will, of course, vary with the rate of change of the swash plate angle but considering a condition of steady pump performance, Q_C will be the leakage rate from the servo. Since the pump body pressure P_B is likely to be of the same order as the pump inlet pressure P_{IN} and if we measure the volume flow rates at the pressures at which they enter or leave the pump, we can write the pump flow equation as:-

$$Q_{OUT} = \left[Q_{IN} - \left(Q_{L1} + Q_{L2} + Q_{L3} + Q_{SB} + Q_C\right)\right] \times \left[1 - \left(\frac{P_{OUT} - P_{IN}}{B}\right)\right] \qquad (5.1)$$

where B is the compressibility modulus for the hydraulic fluid. A common value of B for mineral oils is 12 kilobar which means that if the pump is developing an outlet pressure of 300bar, the outlet flow rate measured at this pressure is $2\frac{1}{2}\%$ less than it would be if measured at ambient pressure corresponding to normal atmospheric conditions.

5.2.1 Fluid Flow

A study of the fluid flow in an axial piston pump is mainly confined to the inlet and outlet ports with the most important consideration being given to the inlet port. Here the main problem will be to make the passages to the cylinder block via the valve plate such that the pressure losses are not excessive; resulting in areas where the pressure is below the vapour pressure of the hydraulic fluid at the working temperature. If such a low pressure did occur the phenomenon of cavitation in the pump would present real problems.

The type of flow in the inlet and outlet passages of the pump is likely to be laminar although in the region of the valve plate, some turbulent flow may occur. The type of flow will be indicated by calculating the Reynold's Number at the particular cross section of the flow path. If the value is below 2000, it can be assumed that the flow is laminar and if above 2500, that the flow is turbulent.

For Circular Flow Paths

$$R_e = \frac{V d}{\nu} \qquad (5.2)$$

where R_e is the Reynold's Number

V is the average velocity in the flow path

ν is the kinetic viscosity of the fluid

$$= \frac{\mu}{\rho}$$

μ is the absolute viscosity of the fluid.

The general expression for the pressure loss through a flow path is -

$$\Delta P = \xi \frac{\rho}{2} \frac{Q^2}{A^2} \qquad (5.3)$$

ξ is a loss coefficient

Q is the volume flow rate

A is a reference cross-sectional area.

For a pipe, tube or equivalent flow path we can write the equation in terms of a friction factor f as -

$$\Delta P = f \frac{\ell \rho Q^2}{2 d A^2} \qquad (5.4)$$

where d is the diameter of the flow path

ℓ is the length of the flow path

and $f = \xi \frac{d}{\ell}$

For Laminar Flow $f = \frac{64}{R_e}$

For Turbulent Flow $f = \frac{0.32}{R_e^{0.25}}$

Which gives for circular flow paths -

Laminar $$\Delta P = \frac{64}{R_e} \cdot \frac{\ell \rho V^2}{2 d} \qquad (5.5)$$

Turbulent $$\Delta P = \frac{0.32}{R_e^{0.25}} \cdot \frac{\ell \rho V^2}{2 d} \qquad (5.6)$$

Localised pressure losses can be estimated using the equation (5.5), but restricting components have relatively high pressure losses and the flow through them is generally turbulent, therefore equation (5.6) is applicable.

a) <u>Orifice Plate</u>

$$\Delta P = \xi \frac{\rho Q^2}{2 A_o} \qquad (5.7)$$

where A_o is the area of the orifice

Guillon (1) suggests the following values of ζ

Orifice with square edges	1.7 to 1.9
Orifice with bevelled upstream edge	1.1
Orifice with both edges bevelled	1.0

b) Abrupt Changes of Cross-Sectional Area

Enlargements

For a flow path which changes from a cross-sectional area A_1, to a cross-sectional area A_2 ; $(A_2 > A_1)$:

$$\Delta P = \left(1 - \frac{1}{\alpha}\right)^2 \frac{\rho Q^2}{2 A_1^2} \qquad (5.8)$$

where α is the coefficient of expansion $= \frac{A_2}{A_1}$

and $\zeta = \left(1 - \frac{1}{\alpha}\right)^2$

Contractions

$$\Delta P = \zeta \frac{\rho Q^2}{2 A_2^2} \qquad (5.9)$$

where β is the coefficient of contraction $= \frac{A_2'}{A_1}$; $(A_2' > A_1)$:

A_2' is the cross-sectional area of the vena contracta.

and $\zeta = \left(\frac{1}{\beta} - 1\right)^2$

Since A_2' is not known we can use values attributed to Oniga (2).

$\frac{A_1}{A_2}$	ENTRY CONDITIONS	β	ζ
>10	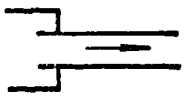 PROTRUDING EDGE. (BORDA MOUTHPIECE)	0·47–0·50	1·3–1·0
	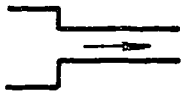 SQUARE EDGE	0·61–0·65	0·4 – 0·3
	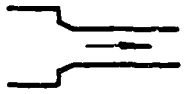 BEVELLED EDGE	0·7 – 0·8	0·20 – 0·06
	 ROUNDED EDGE	0·9	0·012
	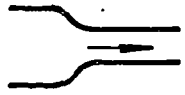 STREAMLINED	0·99	NEGLIGIBLE
ANY VALUE	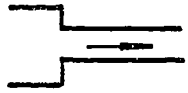 SQUARE EDGE	$0·63 + 0·37\frac{A_1}{A_2}$	$\frac{\frac{A_1}{A_2}-1}{1·7\frac{A_1}{A_2}+1}$

TABLE.5.1. LOSS COEFFICIENTS AND COEFFICIENTS OF CONTRACTION FOR VARIOUS ENTRY CONDITIONS. (AFTER ONIGA)

c) Local Changes in Cross-Sectional Area of Flow Path

Abrupt Increase

* Note Entry Condition

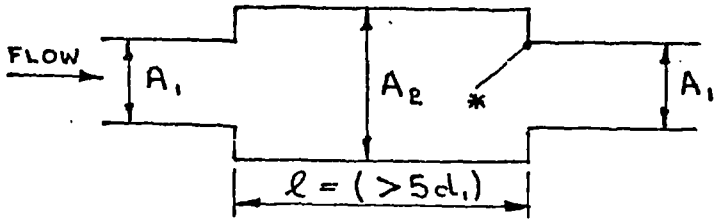

$$\Delta P = \xi \frac{\rho Q^2}{2 A_1^2} \qquad (5.10)$$

where $\xi = \xi_1 + \xi_2$

$$\xi_1 = \left(1 - \frac{1}{\alpha}\right)^2$$

and $$\xi_2 = \left(\frac{1}{\alpha\beta} - 1\right)^2$$

Abrupt Decrease

* Note Entry Condition

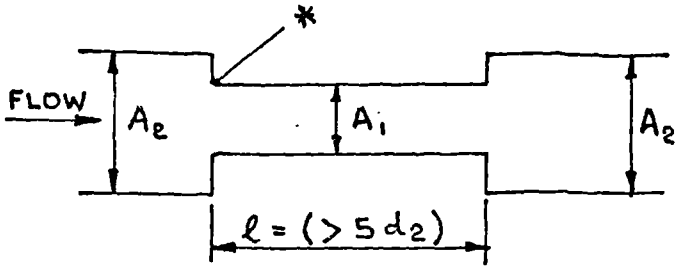

$$\Delta P = \xi \frac{\rho Q^2}{2 A_2^2} \qquad (5.11)$$

where $\xi = \xi_1 + \xi_2$

$$\xi_1 = \left(\frac{1}{\alpha\beta} - 1\right)^2$$

and $$\xi_2 = \left(1 - \frac{1}{\alpha}\right)^2$$

For Non-Circular Flow Paths

Non-circular flow paths are frequently used in axial piston pumps and to estimate the flow conditions it is necessary to distinguish between laminar and turbulent flow. A rough idea of the flow is obtained by calculating the Reynold's Number, by substituting the hydraulic diameter d_H for d in equation (5.2).

Hydraulic Diameter

$$d_H = \frac{4 \times \text{Area of Cross-Section}}{\text{Perimeter of Cross-Section}} \quad (5.12)$$

Non-circular flow paths likely to be encountered are:

Elliptic, Square and Rectagonal.

Elliptic

If $2a$ is the length of the major axis
$2b$ is the length of the minor axis

then Eccentricity $K_e = \sqrt{\frac{a^2 - b^2}{a}}$

and an expression for the periphery of the section is -

$$4a \int_0^{\pi/2} \sqrt{1 - K_e^2 \sin^2 \phi}\, d\phi$$

where ϕ is the angle taken from the minor axis.

By using tables for the values of elliptic integrals the periphery can be found by reading the value of

$$\int_0^{\pi/2} \sqrt{1 - K_e^2 \sin^2 \phi}\, d\phi = F_P$$

for angle θ where $\theta = \sin^{-1} K_e$

and multiplying this by 4a. The periphery can also be found by multiplying twice the major axis by the vertical ordinate to the curve in Fig.5.2, for the eccentricity value K_e.

The area of an ellipse is simply πab, so that the hydraulic diameter is easily arrived at.

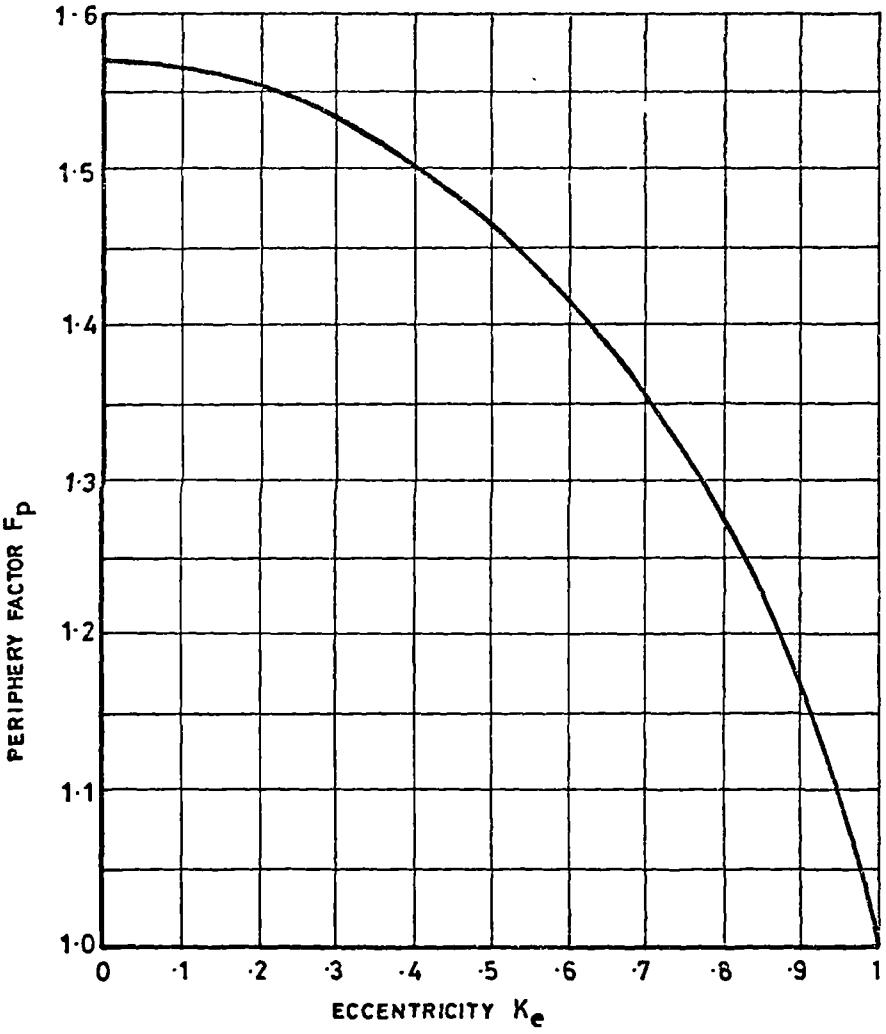

FIGURE 5.2. CURVE OF PERIPHERY FACTOR AGAINST ECCENTRICITY FOR ELLIPSES.

Square and Rectangular

These two shapes present no difficulty in calculating the hydraulic diameter.

Laminar Flow in Non-Circular Flow Paths

Elliptic

$$\Delta P = \frac{4 \mu l (a^2 + b^2)}{\pi a^3 b^3} Q \qquad (5.13)$$

Square

$$\Delta P = 28.4 \frac{\mu l}{w^4} Q \qquad (5.14)$$

where w is the length of the sides.

Rectagonal

When $w \geq h$

$$\Delta P = \frac{12 \mu l}{w h^3} \left[\frac{Q}{1 - \frac{192}{\pi^5 w} \text{TANH} \frac{\pi w}{2h}} \right] \qquad (5.15)$$

When $w \gg h$

where w is the length of the longer side

h is the length of the shorter side.

$$\Delta P = \frac{12 \mu l}{w h^3} Q \qquad (5.16)$$

5.2.2 Cavitation

The conditions which apply at the suction inlet are simply those of obtaining a required fluid flow rate for a relatively small pressure differential. This pressure differential is the difference in pressure between that acting on the fluid at the pump inlet port and that which occurs in the cylinder bores as the pistons are being withdrawn during the suction stroke. The flow rate at a particular instant will depend on the volume displacement of the pump and this in turn is dependent on the piston area, the number of pistons, the stroke and the pump speed.

For design purposes the maximum flow rate is used for designing the pump inlet and the flow path must be of a shape and size that allows the maximum flow rate to pass through to the cylinder bores under the action of a pressure differential less than one atmosphere.

In the event that the resistance to flow reduces the pressure in the flow path to fall to below the vapour pressure of the hydraulic fluid, a condition of cavitation will occur which will have an adverse effect on the pump performance and life. Cavitation is the forming and collapsing of vapour bubbles in the fluid and an immediate consequence is a reduction in the fluid flow rate and the pump performance. When the vapour bubbles reach regions where the local pressure levels are higher than the vapour pressure, the bubbles rapidly collapse and the resulting shock waves produce very high localised pressures of the order of 1 GN/m^2 (3). The formation and collapse of vapour bubbles may occur thousands of times a second; frequencies as high as 1 MHz have been reported by Pearsall (4). Noise is a characteristic of cavitation. If the cavities are small in size it is likely that the noise emission will be of a high frequency and conversely, if the cavities are large it is likely to be of low frequency with the possibility of heavy rumbling and severe vibration.

Another effect of cavitation is that of material erosion. When the cavities collapse the process is so

rapid that temperatures as high as 500°C to 800°C may occur in the material adjacent to the bubble. The combined effect of these thermal and pressure shocks leads to surface cracks probably due to metal fatigue and hence mechanical failure due to erosion of component surfaces.

Since cavitation occurs when the pressure in the fluid reaches a low level, the phenomenon may also be initiated where the local fluid flow velocity is too high. It is therefore necessary to ensure:-

a) that the total pressure loss in the inlet from the inlet port to the cylinder bores does not reduce the inlet pressure for the pump to below a safe level;

b) that care is taken to reduce to a minimum the conditions that lead to high localised fluid velocity;

c) that the viscosity and temperature of the hydraulic fluid which may be used in the pump does not contribute to cavitation.

Unlike in the case of rotodynamic machines, such as centrifugal pumps and turbines, there is little theory which can be applied to axial piston pumps. However, an equation which is an extension to that put forward by Thoma (1881-1943) may be used. Whether cavitation will occur depends on the Net Positive Suction Energy (NPSE) where

$$NPSE = \frac{P_{IN}}{\rho} - g h_s - \frac{P_v}{\rho} \qquad (5.17)$$

P_{IN} is the pressure at the inlet port of the pump under full flow working conditions

P_v is the vapour pressure of the hydraulic fluid at the maximum temperature of the fluid in the inlet flow path

h_s is the height of the pump centre line above the centre line of the pump inlet.

The NPSE can be calculated for the maximum flow rate to the pump and at the maximum viscosity of the hydraulic fluid.

Vapour pressures for a typical hydraulic oil are:-

Temperature ^{o}C	20	40	60	80	100	120	140
Vapour Pressure mbar	9.10^{5}	6.10^{4}	4.10^{3}	2.10^{2}	8.10^{2}	3.10^{1}	8.10^{1}

However, Ishihara (61) has observed small air bubbles appearing in Teresso 52 hydraulic oil at an absolute pressure of 300 to 400 mbar and found that if the pressure reduced to 30 to 50 mbar, the oil boiled violently.

5.2.3 Compressibility Effects

The compressibility of the hydraulic fluid has a significant effect on the operation and performance of an axial piston pump. Since we are concerned with volume flow rates the compressibility may be defined as the specific change in the volume of a fixed mass of fluid at constant temperature for a unit change of pressure:-

$$C = \frac{\Delta V}{\Delta P V}$$

For practical use it is more convenient to express the specific change in volume in terms of the compressibility modulus B where

$$\frac{\Delta V}{V} = \frac{\Delta P}{B}$$

The compressibility modulus depends on the type of fluid, the amount of entrained air and the level of the applied pressure. For pressures in the range 0 to 500bar and for a well deaerated mineral oil, B may be taken as 12 kbar so that if a quantity of the oil is acted upon by a pressure of 500bar, a volume reduction of 4.1% can be expected.

The effect of fluid compressibility is to reduce the volume flow rates to and from the pump. This can be illustrated by considering a single piston and cylinder assembly, with perfect valve switching. At the beginning of the working stroke (BWS) the cylinder assembly contains a volume V_4 of fluid and as the piston moves the pressure rises to P and the volume decreases to V_3

where

$$\frac{V_4 - V_3}{V_4} = \frac{P}{B}$$

At this point the delivery valve opens and the volume of fluid decreases linearly as the piston moves to the end of the working stroke (EWS). At this point the fluid will occupy a volume V_1. If the suction valve now opens, the pressure will fall and in so doing if there is no further intake of fluid, the volume of the fluid must increase to V_2

where

$$\frac{V_2 - V_1}{V_1} = \frac{P}{B}$$

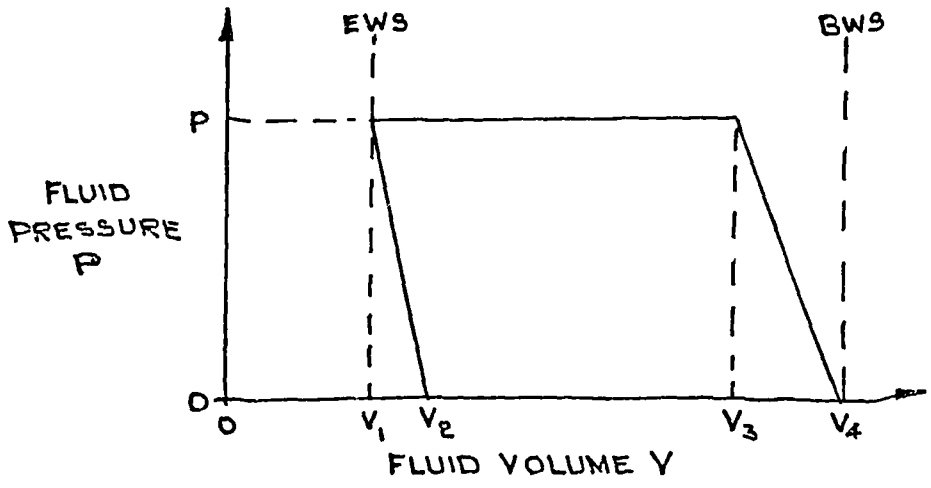

The reduction in the volume flowing from the pump is

$$(V_4 - V_3) = V_4 \frac{P}{B}$$

Since the basic volume is the volume of the cylinder V_c

$$V_c = V_4 - V_1$$

The percentage reduction volume flow from the pump is

$$\frac{V_4}{V_c} \frac{P}{B} 100$$

But V_4 is the working volume of the cylinder plus the volume V_1 between the valve and the cylinder.

Therefore the percentage reduction in volume flow from the pump is

$$\frac{V_1 + V_c}{V_c} \frac{P}{B} 100 \qquad (5.18)$$

Similarly in the case of the flow into the pump the reduction in the volume flow is

$$(V_2 - V_1) = V_1 \frac{P}{B}$$

and the percentage reduction volume flow into the pump is

$$\frac{V_1}{V_c} \frac{P}{B} 100 \qquad (5.19)$$

If the value of V_1 was $\frac{Vc}{4}$, and with P of 150bar, the percentage reduction in flow from the pump would be 1.56%.

In the section on pump performance it is shown that this can represent an appreciable loss of pump flow rate and as such a reduction in pump efficiency.

Fig.5.3, gives curves for finding the percentage volume loss from a pump in terms of the pressure and the ratio of the volumes involved.

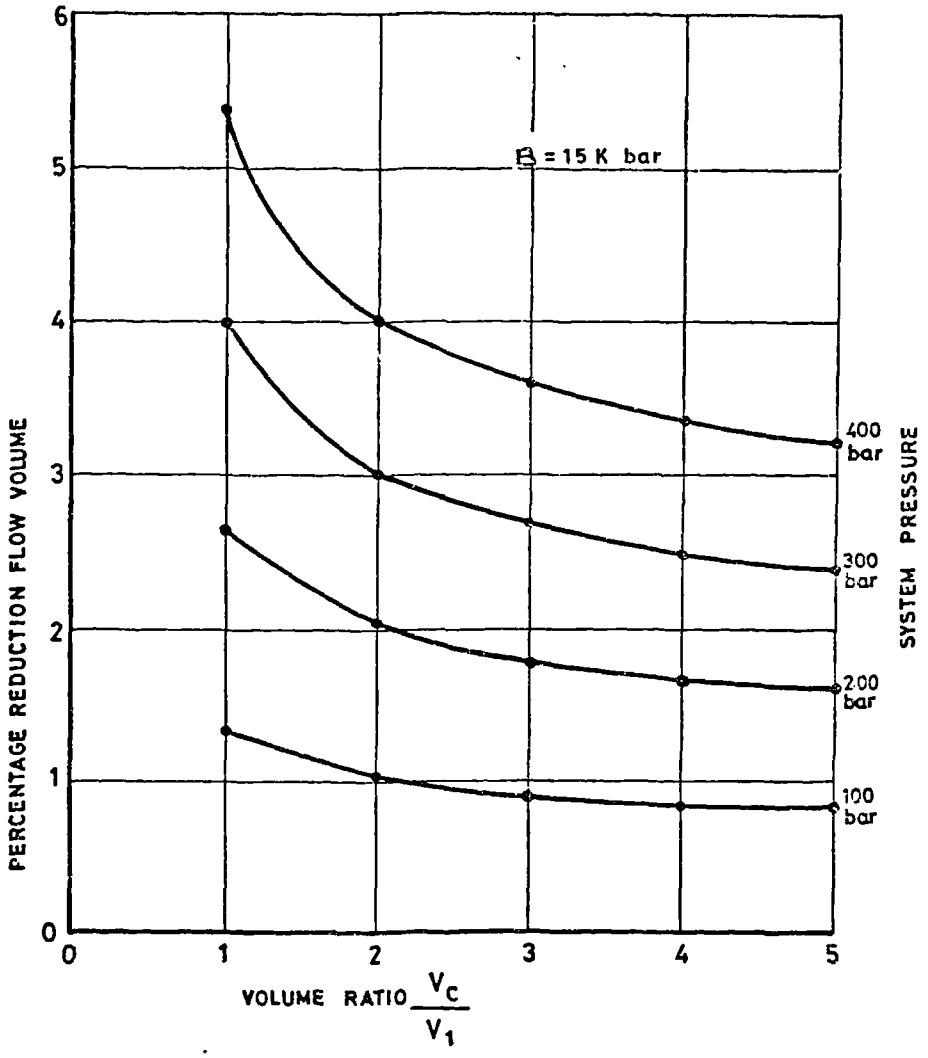

FIGURE 5.3. CURVES SHOWING VALUE OF PERCENTAGE REDUCTION FLOW VOLUME FOR VARIOUS PRESSURE AND VOLUME RATIOS.

5.2.4 Flow Through Gaps

A gap is a narrow clearance separating solid boundaries usually to allow freedom of movement between pairs of components, e.g., pistons and cylinders, valve plates and cylinder faces, slipper bearings and swash plates. In these instances the gaps are filled with hydraulic fluid which also acts as a lubricant. Although the length and width of gaps may vary considerably, in general the height of the gaps is likely to be of the range from 5 to 20×10^{-6}m.

Fluid flow will occur in a gap if either one, or both of two following conditions apply:-

1. there is a pressure differential along the length of the gap. (Poiseuille Flow);
2. relative motion occurs between the walls forming the boundaries to the gap height. (Couette Flow).

At the design stage it is necessary to calculate the rate of fluid flow or the leakage through the gap and the normal and the tangential forces transmitted through the fluid from one component to the other.

The flow is most commonly laminar and the factors affecting the flow conditions are:-

a) the gap height and if this is constant or variable;
b) the viscosity of the fluid;
c) the pressure across the gap;
d) the relative wall movement.

Theory is based on the application of the Navier-Stokes Equations.

$$\frac{dP}{dz} = -\frac{d}{dx}\mu\frac{dv}{dx}$$

where dP denotes a change of pressure

dz denotes a change of position along the gap length

dx denotes a change of position in the gap height

dv denotes a change of fluid velocity

The equation is based on the following assumptions:-

1. the fluid is incompressible;
2. the inertial forces of the fluid are neglected;
3. fluid flow in the direction of the gap height is zero;
4. the fluid velocity is independent of the gap width.

The equations for flow rates due to leakage and the normal and tangential forces acting on the walls of gap configurations commonly encountered in pump design are given on the following pages and are used as appropriate in the design and performance prediction methods.

Parallel Gaps Between Flat Walls

1. With Pressure Differential and with Stationary Walls

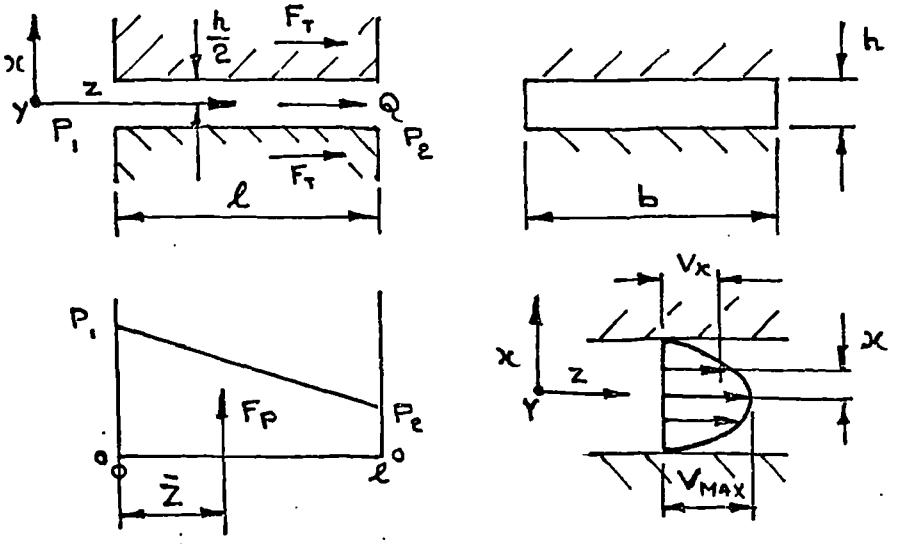

PRESSURE DISTRIBUTION VELOCITY DISTRIBUTION

Mean Fluid Velocity $\bar{V} = \dfrac{(P_1 - P_2)h^2}{12\mu\ell}$ (5.20)

Volume Flow Rate $Q = \dfrac{(P_1 - P_2)bh^3}{12\mu\ell}$ (5.21)

Perpendicular Force on Walls $F_P = (P_1 + P_2)\frac{b\ell}{2}$ (5.22)

Tangential Force on Walls $F_T = (P_1 - P_2)\frac{bh}{2}$ (5.23)

2. With no Pressure Differential and with Wall Motion

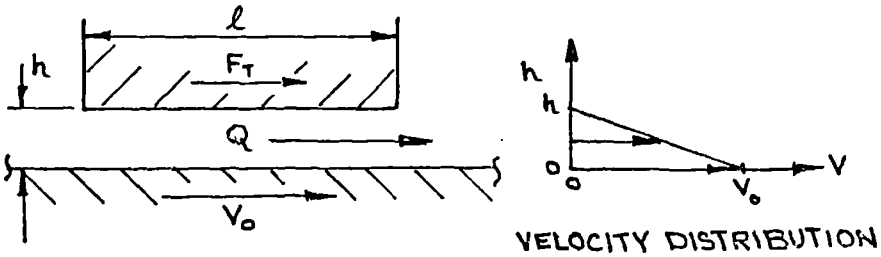

VELOCITY DISTRIBUTION

Volume Flow Rate $Q = \frac{bhV_o}{2}$ (5.24)

Tangential Force on Walls $F_T = \mu V_o \frac{b\ell}{h}$ (5.25)

3. With Pressure Differential and Wall Motion

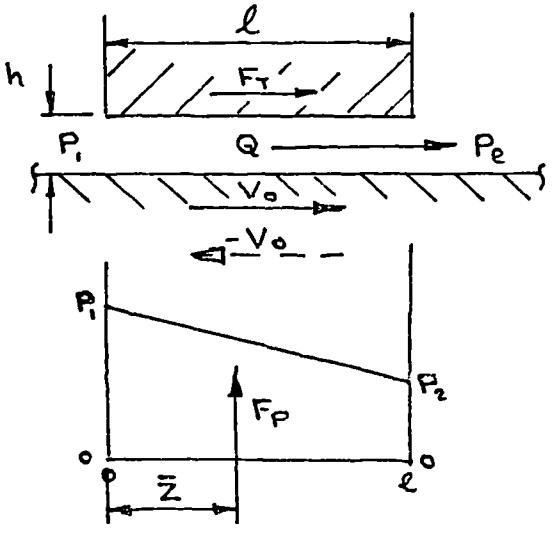

PRESSURE DISTRIBUTION

Volume Flow $Q = \frac{(P_1 - P_2)bh^3}{12\mu\ell} + \frac{bhV_o}{2}$ (5.26)

Perpendicular Force on Walls $F_P = (P_1 + P_2)\frac{bl}{2}$ (5.27)

Tangential Force on Walls $F_T = (P_1 - P_2)\frac{bh}{e} + \mu V_o \frac{bl}{h}$ (5.28)

Annular Gaps Between Cylinders

1. With Pressure Differential and with Stationary Cylinders $(V_o = 0)$

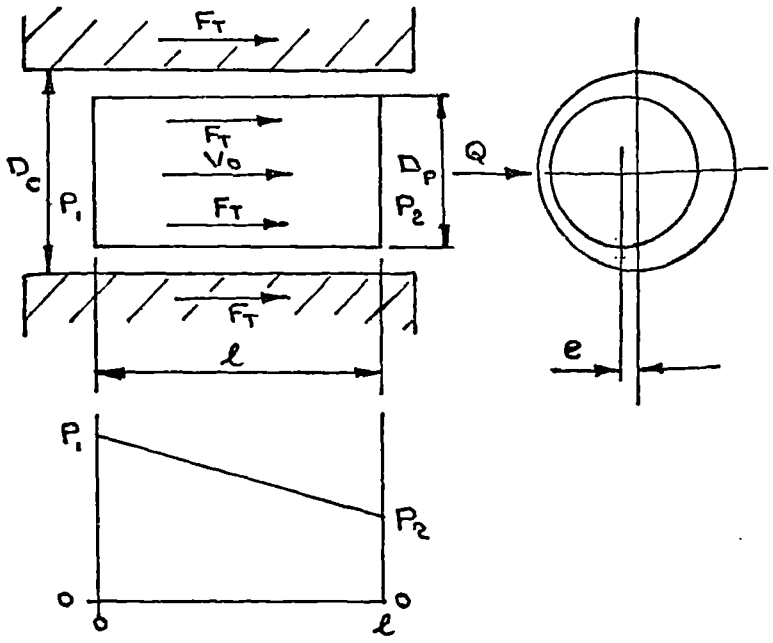

where

D is the mean diameter

$= \frac{(D_c + D_p)}{2}$

C_d is the diametral clearance

$= \frac{(D_c - D_p)}{2}$

e is the eccentricity

Concentric Cylinders

Volume Flow $$Q = \frac{\pi}{96\mu}(P_1 - P_2)\frac{D C_d^3}{\ell} \qquad (5.29)$$

Eccentric Cylinders

Volume Flow $$Q = \frac{\pi}{96\mu}(P_1 - P_2)\frac{D C_d^3}{\ell}\left(1 + \frac{3}{2}\frac{e^2}{\left(\frac{C_d}{2}\right)^2}\right) \qquad (5.30)$$

When the cylinders are fully eccentric, i.e., when $e = \frac{C_d}{2}$ the flow is $2\frac{1}{2}$ times that of the concentric case.

Tangential Force on Walls $$F_T \doteq \frac{\pi}{4} D C_d (P_1 - P_2) \qquad (5.31)$$

2. With no Pressure Differential and with Moving Cylinder

Volume Flow $$Q \doteq \frac{\pi}{4} D C_d V_o \qquad (5.32)$$

Tangential Force on Cylinders $$F_T \doteq 2\pi\mu \frac{D\ell}{C_d} V_o \qquad (5.33)$$

3. With Pressure Differential and with Moving Cylinder

Volume Flow $$Q = \frac{\pi}{96\mu}(P_1 - P_2)\frac{D C_d^3}{\ell}\left(1 + \frac{3}{2}\frac{e^2}{\left(\frac{C_d}{2}\right)^2}\right) \pm \frac{\pi}{4} D C_d V_o \qquad (5.34)$$

Tangential Force on Cylinders $$F_T \doteq \frac{\pi}{4} D C_d (P_1 - P_2) \pm 2\pi\mu \frac{D\ell}{C_d} V_o \qquad (5.35)$$

Variable Height Gaps Between Flat Walls

1. With Pressure Differential and with Stationary Walls

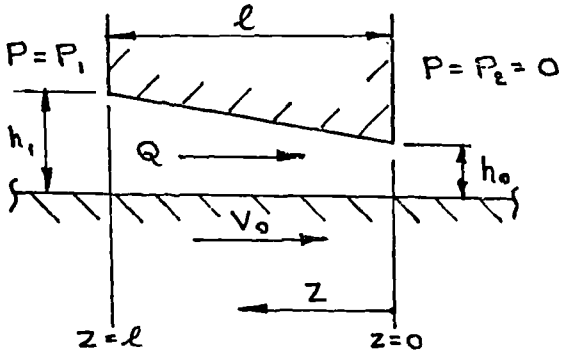

$$h = h_0\left[1 + \delta\frac{z}{\ell}\right]$$

$$h_1 = h_0 + \delta$$

$$\delta = \frac{h_1 - h_0}{\ell}$$

$$\frac{dP}{dz} = \frac{12\mu Q}{bh^3} \quad \text{from (5.20)}$$

$$P(z) = \frac{12\mu Q}{b}\int_0^z \frac{dz}{h^3(z)}$$

$$P(z) = \frac{12\mu Q}{b}\int_0^z \frac{dz}{h_0^3\left[1 + \delta\frac{z}{\ell}\right]^3}$$

substituting $u = \delta\frac{z}{\ell}$

$$P(z) = \frac{12\mu Q\ell}{b h_0^3 \delta}\int_0^u \frac{du}{1+u^3}$$

$$P_1 = \frac{12\mu Q\ell}{b h_0^3}\,\frac{(2+\delta)}{2(1+\delta)^2} \qquad (5.36)$$

$$Q = \frac{P_1 b h_0^3}{12\mu\ell}\,f\left(\frac{h_1}{h_0}\right) \qquad (5.37)$$

Values for $f\left(\frac{h_1}{h_0}\right)$ may be obtained from Fig.5.4.

2. With Pressure Differential and with Moving Wall

$$Q = \frac{P_1 b h_0^3}{12\mu\ell}\,f\left(\frac{h_1}{h}\right) + V_0\frac{hb}{2} \qquad (5.38)$$

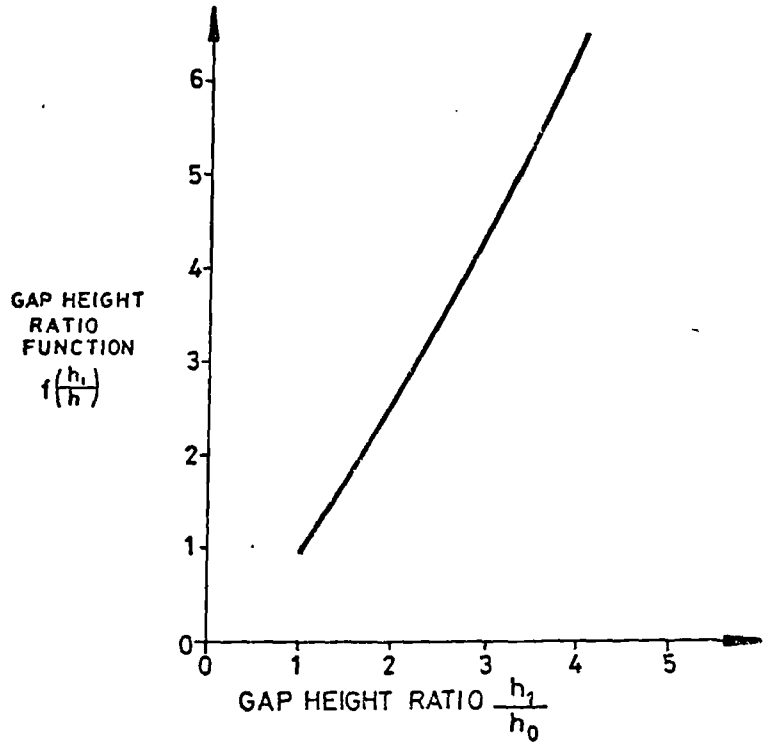

FIGURE 5.4. GAP HEIGHT RATIO FUNCTION FOR GAPS WITH INCLINED WALLS (AFTER THOMA)

5.2.5 Hydrostatic Balancing

Hydrostatic balancing is a means of separating two load carrying surfaces such that relative motion may occur with low frictional losses and with low material wear rates, by using a thin film of a lubricant which has been supplied under pressure from an external source. Examples of hydrostatic balancing in axial piston pumps are at the slipper bearing and swash plate interface where a bleed of fluid from the pressure side of the piston is used to provide a pressure film between the loaded slipper bearing and the swash plate and at the cylinder and valve plate where high pressure fluid leakage provides the film to separate the surfaces.

The load carrying capacity is equal to the product of the effective pressure and the effective area over which the pressure is acting. The frictional force opposing motion is the force required to shear the fluid film. The two examples of a circular pad and a rectangular pad will illustrate the theoretical background to hydrostatic balancing.

a) Circular Pad

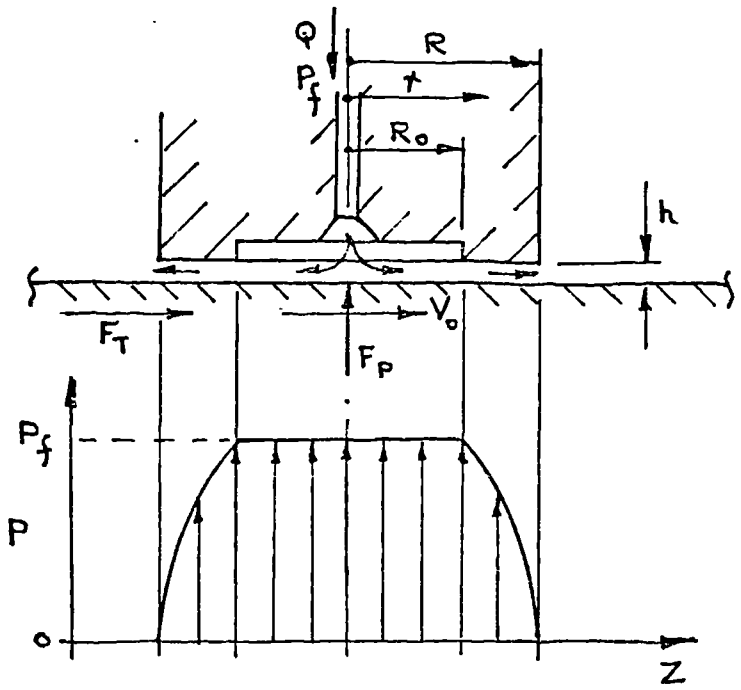

PRESSURE DISTRIBUTION

where

R	is the outside radius of the pad
R_o	is the annulus radius
h	is the gap height
Q	is the volume flow rate
P_f	is the supply pressure
V_o	is the velocity of the pad
F_p	is the separating force

If the pressure external to the pad is zero, the pressure differential across the lips is P_f and as the flow is laminar, from (5.21) -

$$P_f = \frac{12 Q \mu l}{2\pi r h^3} \qquad \text{where } l = dr$$

Then

$$P_f = \frac{6 Q \mu}{\pi h^3} \int \frac{dr}{r}$$

If r LIMITED TO R AND R_o

$$P_f = \frac{6 Q \mu}{\pi h^3} \log_e \frac{R}{R_o}$$

The load carrying capacity will be the sum effect of the pressure times the area acted upon.

$$F_p = \pi R_o^2 P_f + \int_{R_o}^{R} 2\pi r P dr$$

$$= \pi R_o^2 P_f + \frac{12 Q \mu}{h^3} \int_{R_o}^{R} \log_e \frac{R}{r} dr$$

Then

$$F_p = \frac{\pi}{2} P_f \left(\frac{R^2 - R_o^2}{\log_e \frac{R}{R_o}} \right) \qquad (5.39)$$

and $$Q = \frac{\pi h^3 P_f}{6\mu \log_e \frac{R}{R_o}} \qquad (5.40)$$

It will be observed that the load capacity of a circular pad is increased if the area of the annulus is increased relative to the outside radius of the pad. However, the volume flow rate of the lubricant would also be increased.

b) Rectangular Pad

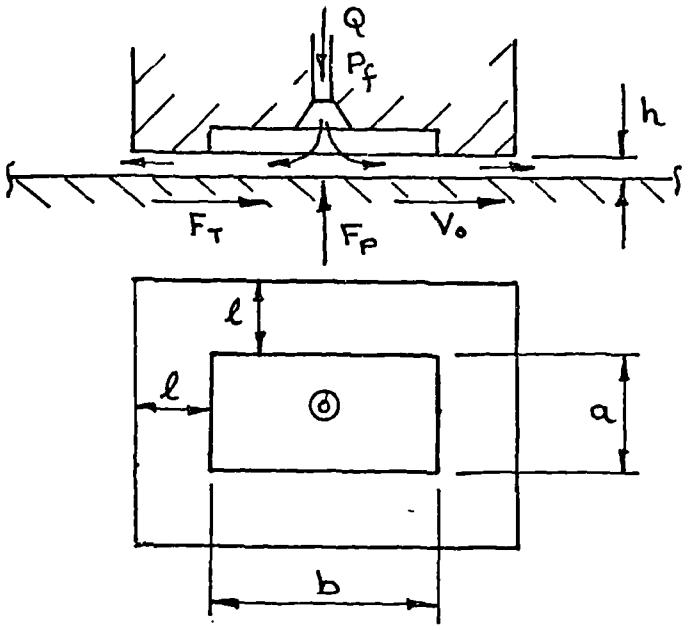

where

a is the length of the recess

b is the breadth of the recess

ℓ is the length of the lands

Then $$F_P = ab P_f + (a+b)\ell P_f \qquad (5.41)$$

and $$Q = \frac{2(a+b)h^3 P_f}{12\mu\ell} \qquad (5.42)$$

The frictional force on the pad is dependent on the viscosity of the lubricant and the velocity of one surface to the other. Since in practical designs the depth of the annulus is many times the design gap height, it may be said that the viscous drag occurs over the area of the lip only, thus from equation (5.25) -

for circular pads

$$F_T = \pi(R^2 - R_o^2)\frac{\mu V_o}{h} \tag{5.43}$$

and for rectangular pads

$$F_T = 2(a+b)\frac{\mu V_o \ell}{h} \tag{5.44}$$

5.3 Mechanical Design

The mechanical design of an axial piston pump involves consideration of several aspects which may be divided into two groups, viz.,

Group 1
- (i) drive and mounting requirements;
- (ii) assembly, installation and maintainability;
- (iii) weight and space restrictions;
- (iv) quality, life and cost.

Group 2
- (v) movement analysis;
- (vi) force analysis and mechanical losses;
- (vii) stress analysis and choice of materials.

The items in Group 1 are non-analytical and do not warrant any treatment here. The theories relating to items (v) and (vii) are well established and may be found in standard works of reference given in the bibliography. The force analysis, however, deserves a full treatment here since it will be used for calculating mechanical losses in the performance prediction method.

5.3.1 Static and Dynamic Force Analysis

Ernst (5), Gerber (6), Korn (7) and Richmond (8), give approximate methods for analysing the forces acting on the piston, slipper bearing and the cylinder. A more precise analysis developed by the author is as follows. Fig.5.5, shows a piston in a cylinder bore and attached to the ball end of the piston is a slipper bearing which bears against the inclined face of a swash plate. Since the pump is rotating, static and dynamic forces are generated within the assembly and these can be grouped as -

1. Pressure forces resulting from the resistance to flow of the fluid within and external to the pump.
2. Inertia forces arising from the acceleration of the moving parts of the pump.
3. Frictional forces which are caused by sliding friction and viscous drag.

The pressure forces originate in the cylinder bore and have the effect of opposing the motion of the piston, loading the cylinder block against the valve plate and of pressurising the cylinder bore. The forces on the piston are transmitted into the slipper bearing and thence to the swash plate assembly. The loading of the cylinder block against the valve plate presents a bearing problem whilst the pressurising of the cylinder bore raises the problems of stress in the cylinder block material.

The inertia forces arise from the linear and centrifugal acceleration of the piston and the slipper bearing. In the main the linear acceleration forces which can vary considerably in magnitude and direction, are transmitted to the swash plate assembly. The centrifugal acceleration forces are fairly constant in magnitude and direction for a constant pump speed and are reacted by the cylinder block and by a couple at the slipper bearing swash plate interface.

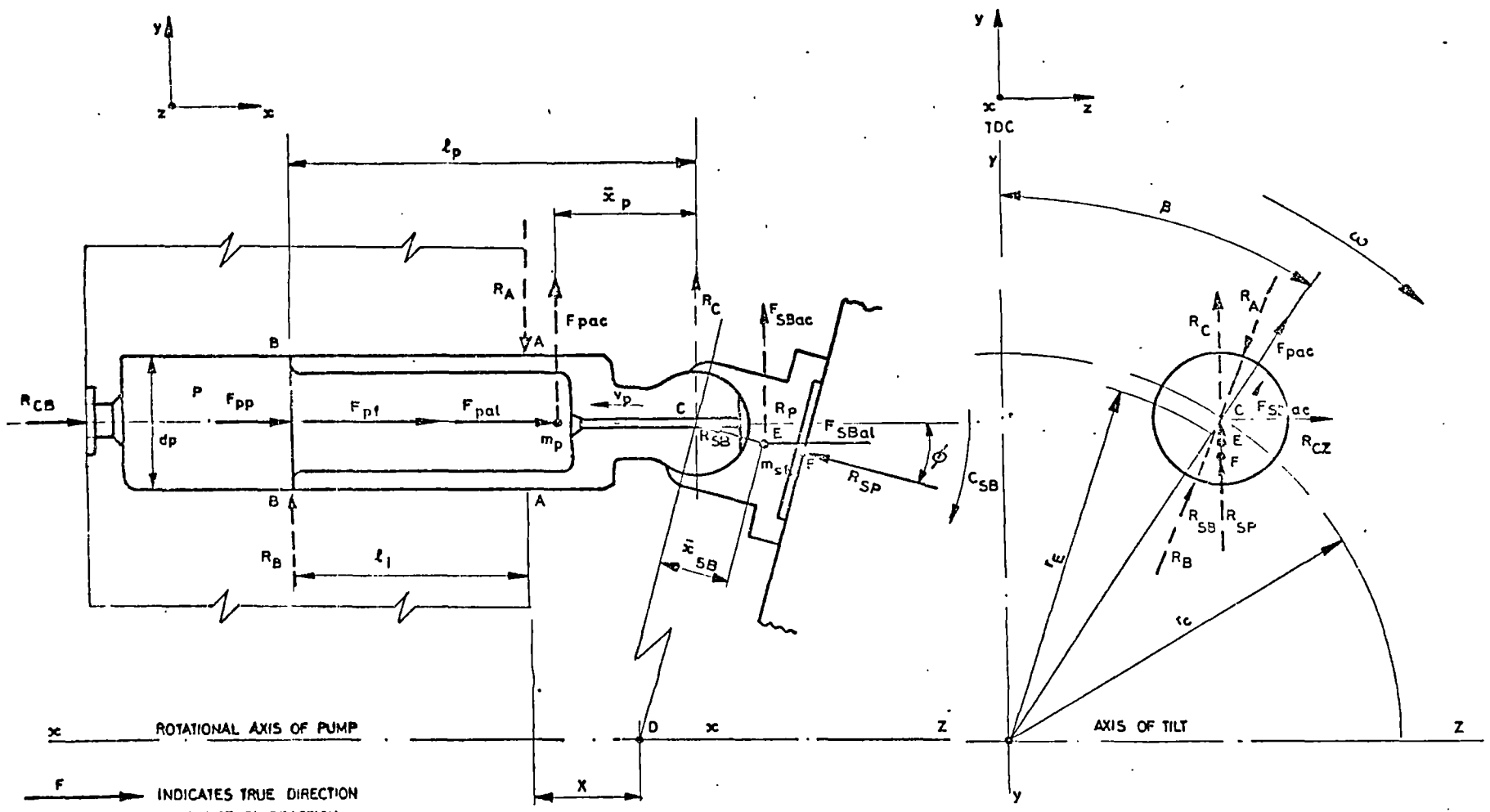

FIGURE 5.5 DIAGRAM SHOWING FORCES, REACTIONS AND COUPLES ACTING ON A PISTON AND SLIPPER BEARING ASSEMBLY.

The frictional forces occur where there is relative motion between parts of the pump and they act in a direction opposing the motion. Such areas are between the piston and the cylinder bore, the piston and the slipper bearing ball joint, the slipper bearing and swash plate surfaces and the cylinder and valve plate faces.

Consider the piston and slipper bearing assembly shown. If the pitch radius of the cylinder bore is r_c, the pump is rotating at ω rad/s and the swash plate angle of tilt is ϕ, when the cylinder bore is at angle β from the top dead centre of the pump we have -

Piston Velocity $$v_p = \omega r_c \tan\phi \sin\beta \quad (5.45)$$

Piston Acceleration $$a_p = \omega^2 r_c \tan\phi \cos\beta \quad (5.46)$$

Length of Piston within Cylinder Bore $$\ell_i = \ell_p - X - r_c \tan\phi \cos\beta \quad (5.47)$$

If the fluid pressure in the cylinder bore is P, the diameter of the piston dp and the piston mass m_p, the forces acting on the piston are -

Pressure Force $$F_{pp} = \frac{\pi}{4} d_p^2 P \quad (5.48)$$

Linear Acceleration Force $$F_{pa\ell} = m_p a_p \quad (5.49)$$

Centrifugal Acceleration Force $$F_{pac} = m_p \omega^2 r_c \quad (5.50)$$

The centrifugal acceleration force can be resolved into components parallel to the Y and Z axes as -

$$F_{pacy} = F_{pac} \cos\beta \quad (5.51)$$

$$F_{pacz} = F_{pac} \sin\beta \quad (5.52)$$

The coulomb friction force F_{Pf} opposing the motion is $(R_A+R_B)f$ where R_A and R_B are the reactions at A and B, and f is the coefficient of friction. Expressing the frictional force in terms of the reactions at A and B we have -

$$F_{Pf} = \left((R_{AY}^2 + R_{AZ}^2)^{1/2} + (R_{BY}^2 + R_{BZ}^2)^{1/2}\right) f$$

Since R_{AZ} will be small compared with R_{AY} and R_{BZ} small compared with R_{BY} we can say -

$$F_{Pf} = (R_{AY} + R_{AZ} + R_{BY} + R_{BZ}) f \qquad (5.53)$$

If C_d is the diametral clearance between the piston and the cylinder bore, the viscous drag on the piston is -

$$F_{PV} = 2\pi d_P \mu \frac{\ell i}{C_d} v_P \qquad (5.54)$$

If E is the centre of mass of the slipper bearing and $\bar{x}_{SB}$ is the distance of E from C the centre of the ball joint, the instantaneous radius of E about the pump axis is -

$$r_E = r_c - \bar{x}_{SB} \sin\phi \cos\beta \qquad (5.55)$$

The acceleration forces acting on the slipper bearing of mass m_{SB} are -

Linear Acceleration Force $F_{SBa\ell} = m_{SB}\omega^2 r_E \tan\phi \cos\beta$ (5.56)

Centrifugal Acceleration Force $F_{SBac} = m_{SB}\omega^2 r_E$ (5.57)

which resolved into components parallel to the Y and Z axes become -

$$F_{SBacY} = F_{SBac} \cos\beta \qquad (5.58)$$

$$F_{SBacz} = F_{SBac} \sin \beta \tag{5.59}$$

If the reaction between the slipper bearing and the swash plate is R_{SP} and between the slipper bearing and the piston at the spherical bearing is R_{SB}

$$R_{SB} = R_{SP} - F_{SBal} \cos\phi + F_{SBacY} \sin\phi \tag{5.60}$$

The reactions on the piston are -

$$R_{AY} = R_{CY} \frac{\ell_p}{\ell_i} + F_{PacY} \frac{(\ell_p - \bar{x}_p)}{\ell_i} \tag{5.61}$$

$$R_{AZ} = F_{SBacz} \frac{\ell_p}{\ell_i} + F_{Pacz} \frac{(\ell_p - \bar{x}_p)}{\ell_i} \tag{5.62}$$

$$R_{BY} = R_{AY} - R_{CY} - F_{PacY} \tag{5.63}$$

$$R_{BZ} = R_{AZ} - F_{SBacz} - F_{Pacz} \tag{5.64}$$

$$R_{CY} = R_{SB} \sin\phi \tag{5.65}$$

$$R_{CZ} = F_{SBacz} \tag{5.66}$$

$$R_P = R_{SB} \cos\phi \tag{5.67}$$

$$= R_{CY} \operatorname{cotan}\phi \tag{5.68}$$

$$= F_{PP} + F_{Pf} + F_{PV} + F_{Pal} \tag{5.69}$$

The reaction acting on the cylinder block parallel to the X axis is -

$$R_{CB} = F_{PP} - F_{Pf} - F_{PV} \tag{5.70}$$

A couple acting about the centre of the spherical bearing at C will result from the acceleration forces on the slipper bearing.

$$C_{SBY} = F_{SBal}\,\bar{x}_{SB}\sin\phi + F_{SBaCY}\,\bar{x}_{SB}\cos\phi \qquad (5.71)$$

$$C_{SBZ} = F_{SBaCZ}\,\bar{x}_{SB} \qquad (5.72)$$

$$C_{SB} = \sqrt{C_{SBY}^2 + C_{SBZ}^2} \qquad (5.73)$$

Relative values of the forces acting on the piston and the slipper bearing can be indicated by plotting non-dimensional factors involving these forces against varying angles of tilt and angles of rotation. The non-dimensional factors are derived by dividing the particular forces by the associated constants. Figs.7.18 to 7.27 inclusive, show these plots. Thus for any known pump, the forces acting at a particular swashplate angle, pump speed and angle of rotation can be readily obtained by reading from the appropriate charts the corresponding values of the non-dimensional factors and by multiplying these by the constant values involved.

5.3.2 Contact Stresses in the Cylinder Bore

In Section 5.3.1, it was convenient to assume that contact between the piston and the bore of the cylinder occurs at only two points A and B and that the point load reactions were R_A and R_B. Since the diametral clearance between the piston and the cylinder bore is very small, the geometrical conformity is high and the concept of point loads and hertzian stresses is not tenable. It is therefore necessary for design purposes to derive a theory for the replacement of these point loads with a pattern of distributed loading such that in addition to satisfying the equilibrium conditions of the piston, the theory will lend itself to an easy and reliable method of estimating the

contact stresses at the interfaces. The levels of these contact stresses will be of paramount importance since excessively high values will lead to unacceptable wear rates of the cylinder bore with loss of pump performance and a reduction in the working life of the unit. The following analytical method has been derived by the author.

It is reasonable to assume that the elastic properties of the cylinder bore material will accommodate the reactions as distributed loads over lengths X_1 and X_2 which are proportional to R_A and R_B respectively.

Point Load Reactions

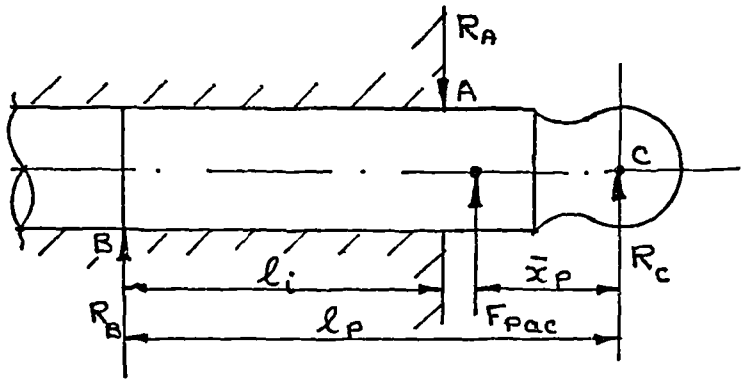

Distributed Load Reactions

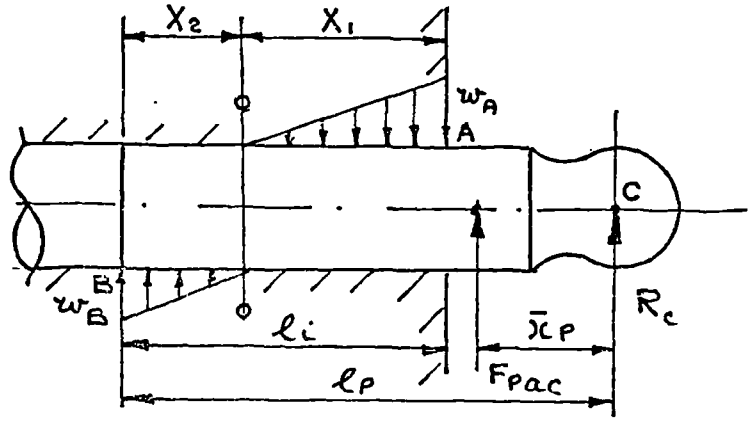

$$X_1 = \frac{R_A}{R_A + R_B}\,\ell_i$$

$$X_2 = \frac{R_B}{R_A + R_B}\,\ell_i$$

For equilibrium -

a) the sum of the external forces acting on the piston must be zero;

b) the sum of the external couples acting on the piston must be zero.

Then if w_A is the distributed load acting on the plane which contains A and w_B is the distributed load acting on the plane which contains point B,

$$w_A \frac{X_1}{2} - w_B \frac{X}{2} \ell - R_c - F_{PAC} = 0$$

and

$$w_A \frac{X_1}{2}\left(\frac{2}{3}X_1 + X_2\right) - w_B \frac{X}{2}\ell \frac{X_2}{3} - R_c \ell_P - F_{PAC}\left(\ell_P - \bar{x}_P\right) = 0$$

to give

$$w_A = \frac{3\left[R_c\left(\ell_P - \frac{X}{3}\ell\right) + F_{PAC}\left(\ell_P - \bar{x}_P - \frac{X}{3}\ell\right)\right]}{\ell_i X_1} \qquad (5.74)$$

$$w_B = w_A \frac{X_2}{X_1} \qquad (5.75)$$

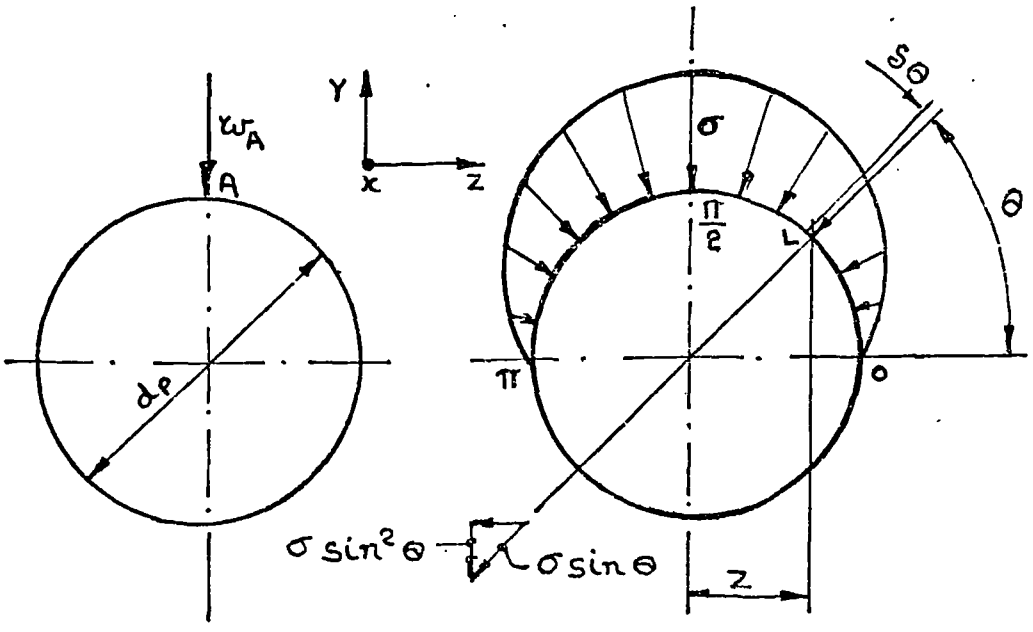

The maximum contact stress will occur in the plane A. Consider a thin lamina of the cylinder block at A and of thickness t., having a distributed load w_A acting on it. The total load in the Y direction will be $w_A t$ and this may be replaced by a redistributed force around the half circumference of the lamina. It is suggested that the distribution is sinusoidal to satisfy the conditions of zero normal stress at $\theta = 0$ & π and a maximum normal stress at $\theta = \pi/2$.

Considering a small elemental area of the circumference at L subtended by the small angle $\delta\theta$ then the elemental area is $\frac{d_p}{2} t \, \delta\theta$ and the projected area in the Y direction is $\frac{d_p}{2} t \cos\theta \, \delta\theta$ Let the stress in the Y direction on the elemental area be σ then the resultant force in the Y direction is $\sigma \, d_p/2 \, t \cos\theta \, \delta\theta$. The total force on the lamina in the Y direction becomes -

$$2\sigma t \frac{d_p}{2} \int_0^{\frac{\pi}{2}} \sin^2\theta \cos\theta \, d\theta$$

LET $u = \sin^2\theta$ $\qquad du = \cos\theta \, d\theta$

$$du = \left[2 \sin\theta \cos\theta\right] d\theta \qquad v = \sin\theta$$

$$\int_0^{\frac{\pi}{2}} \sin^2\theta \cos\theta \, d\theta = \left[uv\right]_0^{\frac{\pi}{2}} - \int_0^{\frac{\pi}{2}} v \, du$$

$$= \left[\sin^3\theta\right]_0^{\frac{\pi}{2}} - 2\int_0^{\frac{\pi}{2}} \sin\theta^2 \cos\theta \, d\theta$$

$$\left[\sin^3\theta\right]_0^{\frac{\pi}{2}} = 3\int_0^{\frac{\pi}{2}} \sin^2\theta \cos\theta \, d\theta = 3 \times \frac{1}{3} = 1$$

THEREFORE $w_A t = \sigma t d_p \times \frac{1}{3}$

AND $\sigma_{MAX} = \sigma_{AT'A'} = \frac{3 w_A}{d_p}$ (5.76)

5.4 Performance Prediction

The performance of an axial piston pump depends on its design features and on the conditions under which it is working. To be able to predict the performance for a range of working conditions is highly desirable and this section sets out the basic theory.

Since a pump is a unit which receives fluid at low pressure and delivers it at a higher pressure, the performance of the pump is very much concerned with flow losses. But the pump also receives mechanical power from a prime mover and delivers most of this as fluid power to the hydraulic system; so that the performance is equally concerned with power losses.

5.4.1 Fundamental Equations Without Losses

The relationships between the physical dimensions of an axial piston pump and the operating variables can be established if the losses within the pump and the effects of compressibility are ignored. The physical dimensions are the diameter of the pistons, the number of pistons in the pump and the length of stroke of the pistons. The operating variables will consist of the volume rate of flow, the operating pressure, the rotational speed, the displacement setting and the torque input to the pump.

The flow rate Q is defined as the volume displacement in unit time and can be expressed as:-

$$Q = n q$$

where n is the number of revolutions of the pump in unit time

q is the volume of fluid displaced per revolution.

Many axial piston pumps have adjustable displacement and the displacement setting can be represented by α where α can vary from zero at the no-flow condition to 1 at the full flow condition.

Then $q = a q_0$

where q_0 is the maximum displacement of the pump

to give $Q = a n q_0$

The operating pressure of the pump will be a function of the resistance to the flow of the hydraulic fluid both within the pump and in the associated external circuit. If the pressure is P the hydraulic energy generated per revolution is given as -

$$E = a P q_0$$

with the theoretical power as $P = a n P q_0$

and the theoretical torque as $M = \frac{a P}{2\pi} q_0$

It is now possible to relate the operating variables, the pump dimensions and the pump performance.

Where d_p is the diameter of the pistons
N_p is the number of pistons
S is the full piston stroke

$$q_0 = \frac{\pi}{4} d_p^2 N_p S \qquad (5.77)$$

$$q = \frac{\pi}{4} d_p^2 a N_p S \qquad (5.78)$$

$$Q = \frac{\pi}{4} d_p^2 a n N_p S \qquad (5.79)$$

$$M = \frac{d_p^2}{8} a P N_p S \qquad (5.80)$$

$$P = \frac{\pi}{4} d_p^2 a P n N_p S \qquad (5.81)$$

5.4.2 Fundamental Equations With Losses

So far the pump has been considered as a loss-free hydrostatic flow generating unit. In this section losses within the pump are taken into account but the compressibility effects ignored. The losses are of two types, Leakage Losses and Torque Losses.

a) Leakage Losses

These are adverse flows through the many sealing gaps in the pump and for the most part these are proportional to the gap areas, the pressure across the gaps and inversely proportional to the lengths of the gaps and the viscosity of the fluid. The effects of the relative movement of the walls of the gaps, e.g., pistons moving in cylinders; have also to be considered. To relate the operating variables to the maximum displacement of the pump, it is convenient to express the leakage losses as a Slip Frequency n_s and in terms of the Flow Loss due to Leakage Slip Q_s as -

$$n_s = \frac{Q_s}{q_o}$$

and the Effective Flow Rate Q_e where

$$\begin{aligned} Q_e &= Q - Q_s \\ &= (\alpha n - n_s) q_o \end{aligned} \qquad (5.82)$$

The relationships between effective flow, displacement setting, rotational frequency, slip frequency and maximum pump displacement is shown as the functional diagram -

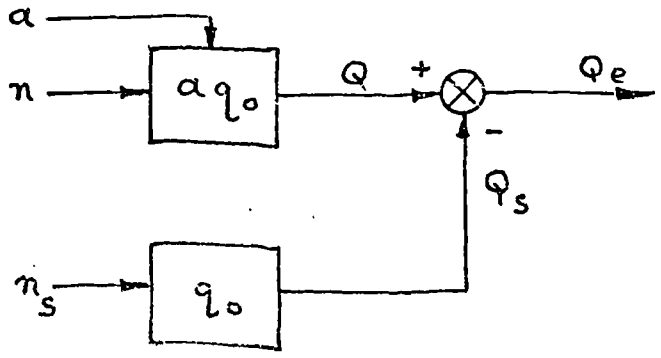

b) Torque Losses

These are due to the frictional effects between the sliding surfaces within the pump and the resistance to flow of the fluid passing through the pump. If the losses are expressed as pressure losses, these can be equated as torque losses and can be related to the maximum displacement of the pump. This in turn facilitates the summation of the leakage and torque losses.

Where M_L is the Torque Loss

P_L is the Pressure Loss

$$M_L = \frac{P_L q_o}{2\pi}$$

And the Effective Torque M_e as -

$$M_e = M + M_L$$

$$= \frac{q_o}{2\pi}\left[\alpha P + P_L\right] \qquad (5.83)$$

The relationships between the effective torque, displacement setting, pressure, pressure loss and maximum pump displacement is shown as the functional diagram -

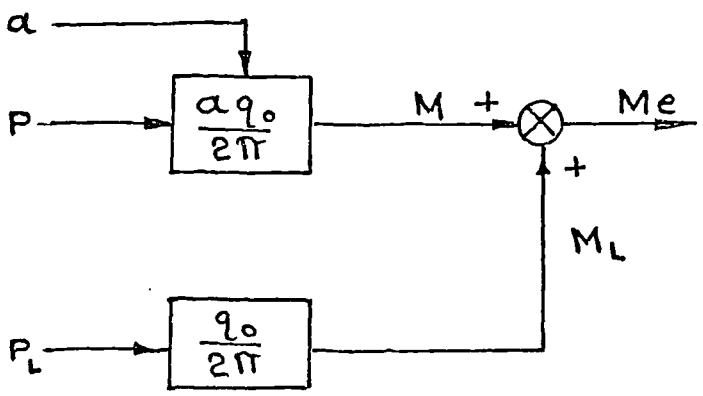

5.4.3 Fundamental Equations for Power and Efficiency

It is now possible to equate the Effective Mechanical Power P_{me} and the Effective Hydraulic Power P_{he} as -

$$P_{me} = 2\pi n M_e$$

$$= \alpha n P q_o + n P_L q_o \qquad (5.84)$$

and

$$P_{he} = P Q_e$$

$$= \alpha n P q_o - n_s P q_o \qquad (5.85)$$

The Volumetric Efficiency is the ratio of the Effective Flow Rate to the Ideal Flow Rate.

$$\eta_v = \frac{Q_e}{Q} = \frac{\alpha n q_o - n_s q_o}{\alpha n q_o}$$

$$= 1 - \frac{n_s}{\alpha n} \qquad (5.86)$$

The Mechanical Efficiency is the ratio of the Ideal Torque to the Effective Torque.

$$\eta_m = \frac{M}{M_e} = \frac{\alpha P q_o}{\alpha P q_o + P_L q_o}$$

$$= \frac{1}{1 + \frac{P_L}{\alpha P}} \qquad (5.87)$$

The Overall Efficiency is the ratio of the Effective Hydraulic Power to the Effective Mechanical Power.

$$\eta = \frac{P_{he}}{P_{me}} = \frac{a n P q_o - n_s P q_o}{a n P q_o + n P_L q_o}$$

$$= \frac{1 - \frac{n_s}{an}}{1 + \frac{P_L}{aP}} = \eta_v \times \eta_m \qquad (5.88)$$

5.4.4 Relationships Between the Slip Frequency, Pressure Losses and the Operating Variables

By testing a pump over its full working range of pressure, speed and displacement setting with hydraulic fluid at constant viscosity at the pump inlet, it is possible to determine values for pressure loss and slip frequency. If the slip frequency is plotted against pressure for various speeds as in Fig.5.6, it will be seen that the slip frequency increases slightly more than proportional to the pressure and that it increases to a small extent with an increase in the pump speed.

The pressure losses can be plotted against the rotational frequency as shown in Fig.5.7, and it will be seen that the pressure loss is made up of three component parts; a constant pressure loss P_{LC} which is independent of pressure and speed, a variable pressure loss $(P_{LV} + P_{Lh})$ which is dependent on the operating pressure and variable pressure loss P_L which is a function of the pump speed.

The constant pressure loss P_{LC} can be attributed to the friction between moving parts at slow speeds and does not include the frictional losses due to the thrust loads arising from a positive working pressure in the pump. The

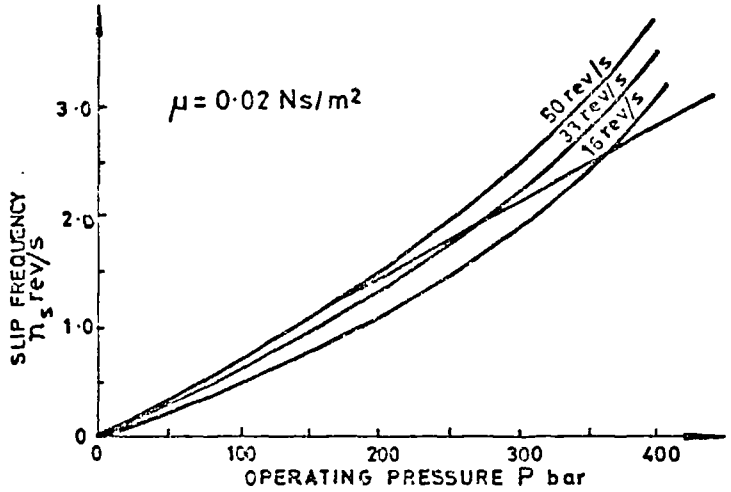

FIGURE 5.6 VARIATION OF SLIP FREQUENCY WITH OPERATING PRESSURE AT CONSTANT VISCOSITY AND FOR VARIOUS PUMP SPEEDS.

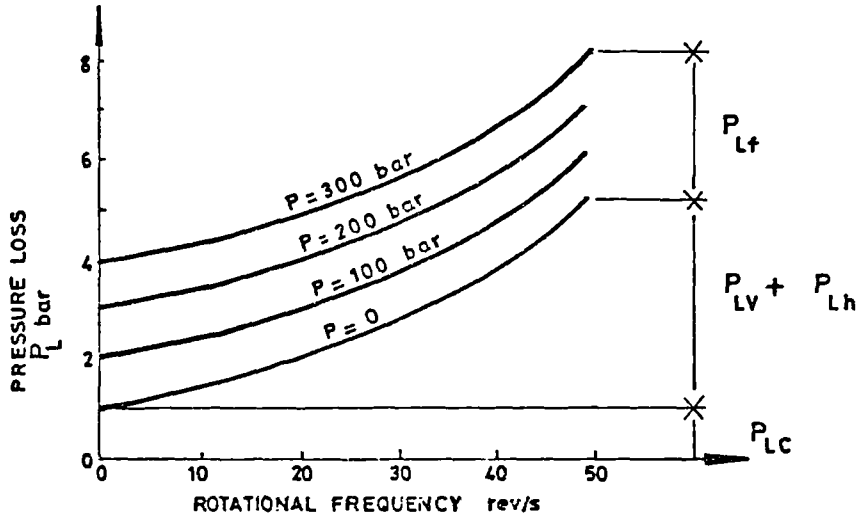

FIGURE 5.7. VARIATION OF PRESSURE LOSS WITH ROTATIONAL FREQUENCY FOR VARIOUS OPERATING PRESSURES.

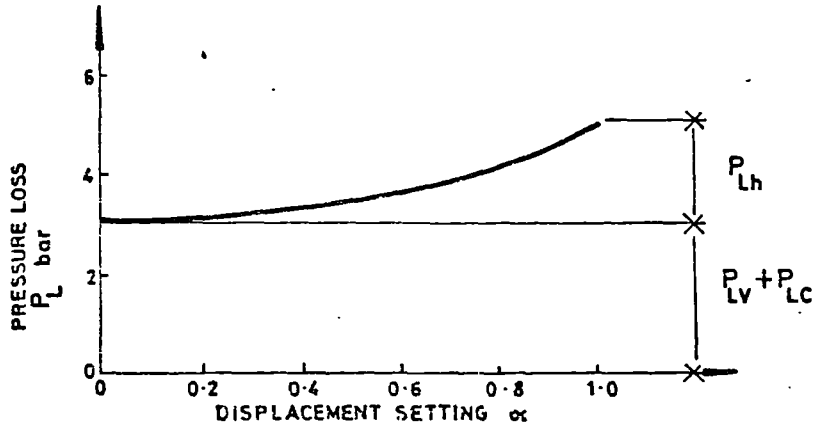

FIGURE 5.8. VARIATION OF PRESSURE LOSS WITH DISPLACEMENT SETTING AT A PARTICULAR PUMP SPEED AND PRESSURE

significance of this loss decreases as the rotational frequency and the operating pressure increase and the scope for reducing the value of P_{LC} by design is limited.

The variable pressure loss $(P_{LV} + P_{Lh})$ is due to viscous friction and hydromechanical losses. The viscous friction loss P_{LV} is caused by fluid shear in the various working gaps and is therefore related to the fluid viscosity and rotational speed as well as the gap dimensions and the effective working radii of the gaps, and as such is amenable to analysis. The hydromechanical loss P_{Lh} is caused by turbulent flow in the various flow paths and churning of the fluid in the pump body. This loss can only be minimised by careful attention to the effects of changes of shape, size and direction of flow paths and to the disturbance aspects of the moving parts of the pump.

5.4.5 Mathematical Models for Pump Performance

Extensive experimental and analytical work by Wilson, W E (U.S.A.), Schlösser, W M J (Holland), and Thoma, J U (Switzerland), has resulted in mathematical models for the losses in hydrostatic pumps and motors. These models relate pump flow rate and input torque to the operating variables and the pump displacement. Various coefficients are used by the three researchers and these have to be obtained by experimental methods. Because of this the models are useful for comparative appraisal of machines of the same basic design but they have only minimal use in indicating probable pump performance at the design stage.

a) Volume Flow Rate

Wilson (9) describes the volume flow rate from a pump as -

$$Q_e = a n q_o - \frac{C_s P q_o}{2\pi\mu} - Q_r \qquad (5.89)$$

where C_s is the coefficient slip

Q_t is the flow loss due to cavitation in the neighbourhood of the pump inlet.

If we assume that measures have been taken in the design of the pump and in the supply of fluid to the pump inlet to eliminate cavitation, Q_r can be equated to zero. Then -

$$\frac{C_s P q_o}{2\pi\mu} = Q_s$$ i.e., the leakage slip flow

The slip coefficient C_s is dimensionless and is based on the sum effect of all the leakage gaps subjected to the pressure differential P.

Schlösser (10) added a leakage component due to fluid inertia forces to Wilson's equation and suggested that the loss is proportional to the root of the pressure and to the inverse root of the fluid density -

$$Q_i = C_i \left(\frac{2P}{\rho}\right)^{1/2} q_o^{2/3}$$

where Q_i is the leakage flow loss due to fluid inertia

ρ is the fluid density

C_i is the coefficient of losses due to fluid inertia

Thoma (11) supports the model put forward by Wilson.

b) Input Torque

Wilson gives the following equation to express the torque required to drive a pump as -

$$M_e = \frac{a P q_o}{2\pi} + C_v \mu n q_o + \frac{C_f P}{2\pi} q_o + M_c \qquad (5.90)$$

where C_v is the coefficient of viscous drag

C_f is the coefficient of dry friction

M_c is the frictional torque which is independent of speed and pressure.

Viscous drag arises from conditions within the pump gaps and fluid bearings as shown by the expression and is proportional to the fluid viscosity and the rotational speed of the pump. Values of the coefficient will depend on dimensions of the gaps and bearings and the radii at which these viscous forces act. The second loss due to dry friction follows the laws of coulomb friction and is therefore independent of the pump speed but dependent on the surface loading and hence on the working pressure. The surface loading is also dependent on the piston area and this is taken care of by including the pump displacement which is the product of piston area and piston stroke, in the expression. The constant torque loss M_C is due to seal friction and similar frictions and may be expressed as the product of the constant pressure loss P_{LC} and the pump displacement.

Schlösser rejects the concept of a constant frictional torque but introduces a loss which takes into account the inertia forces in the fluid including the churning of the fluid by the moving parts of the pump.

$$M_h = C_h n^2 \rho q_o^{5/3}$$

where C_h is the coefficient of hydrodynamic loss.

Thoma supports this part of the torque losses but as an addition to the constant torque loss. To make the hydrodynamic loss suit both fixed and variable displacement pumps, Thoma introduced the displacement setting.

Summary of Mathematical Models for Flow Rate and Input Torque

Flow Rate

Wilson $$Q_e = \alpha n q_o - \frac{C_s P q_o}{2\pi\mu} - Q_r$$

Schlösser $$Q_e = \alpha n q_o - \frac{C_s P q_o}{2\pi\mu} - C_i\left(\frac{2P}{\rho}\right)^{1/2} q_o^{2/3} - Q_r$$

Thoma $$Q_e = \alpha n q_o - \frac{C_s P q_o}{2\pi\mu} - Q_r$$

Input Torque

Wilson $$M_e = \frac{\alpha P}{2\pi} q_o + C_v \mu n q_o + \frac{C_f P}{2\pi} q_o + M_c$$

Schlösser $$M_e = \frac{\alpha P}{2\pi} q_o + C_v \mu n q_o + \frac{C_f P}{2\pi} q_o + C_h n^2 \rho q_o^{5/3}$$

Thoma $$M_e = \frac{\alpha P}{2\pi} q_o + C_v \mu n q_o + \frac{C_f P}{2\pi} q_o + C_h a^3 n^2 \rho q_o^{5/3} + M_c$$

c) Power and Efficiency

The input and output powers of an axial piston pump can be expressed in a similar manner using the mathematical models proposed by Thoma.

Where P_{me} is the power input to the pump

and P_{he} is the power output from a pump

$$P_{me} = 2\pi n M_e \quad \text{and} \quad P_{he} = P Q_e$$

Thus

$$P_{me} = 2\pi n\left[\frac{a P q_o}{2\pi} + C_v \mu n q_o + \frac{C_f P}{2\pi} q_o + C_h a^3 n^2 \rho q_o^{5/3} + M_c\right]$$

and

$$P_{he} = \left[a n q_o - \frac{C_s P q_o}{2\pi\mu} - Q_r\right] P$$

The Volumetric Efficiency

$$\eta_v = \frac{Q_e}{Q} = 1 - \frac{C_s P}{2\pi\mu a n} - \frac{Q_r}{a n q_o}$$

The Mechanical Efficiency

$$\eta_m = \frac{M}{M_e} = \frac{1}{1 + 2\pi C_v \frac{\mu n}{aP} + \frac{C_f}{a} + 2\pi C_h a^2 \frac{n^2 \rho}{P} q_o^{2/3} + \frac{2\pi M_c}{a P q_o}}$$

The Overall Efficiency

$$\eta = \eta_v \times \eta_m = \frac{1 - \frac{C_s P}{2\pi\mu a n} - \frac{Q_r}{a n q_o}}{1 + 2\pi C_v \frac{\mu n}{aP} + \frac{C_f}{a} + 2\pi C_h a^2 \frac{n^2 \rho}{P} q_o^{2/3} + \frac{2\pi M_c}{a P q_o}}$$

CHAPTER 6 FREQUENCY RESPONSE OF AXIAL PISTON PUMP

The Lucas HD900 pump has provision for controlling its output by varying the angle of tilt of the swashplate by means of a servo piston. The control of this movement is either by the use of a manually operated servo valve housed within the servo piston as shown in Fig.4.10, or by the use of an electro-hydraulic controller mounted on the pump body as shown in Fig.4.12, and which in turn controls the flow of hydraulic fluid to the servo piston.

This Chapter attempts to analyse the conditions which pertain to these methods of pump flow control and to present frequency response diagrams and transfer functions such that the performance of the HD900 pump may be estimated under steady state conditions.

By so doing it is hoped that the method will be of value in the estimation of the frequency response of other types of axial pumps.

Fig.4.11, shows the working principles of the manually controlled pump. It will be seen that the system uses a two land, three way spool valve with a bias pressure acting on the head side of an unequal area servo piston. The ratio of the piston areas is two to one and the bias pressure is the pump supply pressure or that of an auxiliary pump. The servo valve may be considered as being of the critical centre (zero lap) type although in fact there is a 0.457mm to 0.686mm overlap which reduces the steady state pump losses and produces an acceptable dead zone. Rectangular orifices are used and the spool and sleeve are lapped to give a diametral clearance of 0.0025mm to 0.0076mm.

The electro-hydraulic controller is shown schematically in Fig.6.1. It incorporates an electrical torque motor with an output proportional to the input current. The motor armature moves a valve flapper towards a nozzle against the resistance afforded by the deflection of a cantilevered spring fixed to the servo valve spool. The fluid flow through the nozzle is diverted causing a hydraulic pressure force to move the spool valve and this in turn directs fluid to the appropriate side of the servo piston.

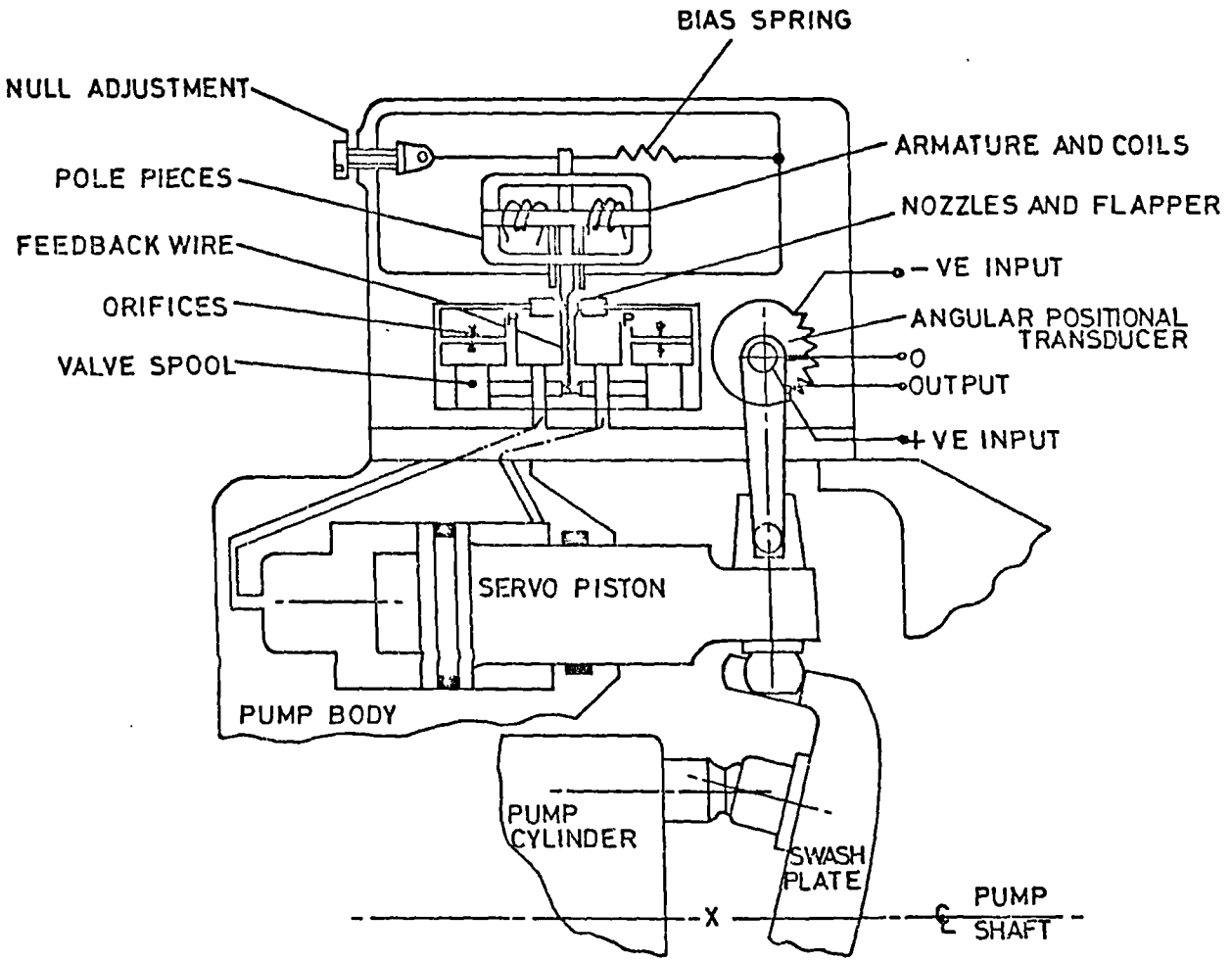

FIGURE 6.1 SCHEMATIC ARRANGEMENT OF ELECTRO-HYDRAULIC CONTROLLER AND SERVO PISTON WITH ELECTRICAL FEEDBACK SYSTEM.

Movement of the servo piston rotates a d.c./d.c. angular positional transducer to provide a feedback voltage to the electro-hydraulic controller. When the desired position of the swashplate is achieved the spool valve will have moved back to near the null point and the flapper valve will be repositioned centrally between the control nozzles.

6.1 Extent of the Analysis

Valve controlled hydraulic servo-mechanisms are used extensively in fluid power and are well described by various authors, e.g., Blackburn, et al (12). In practice, the mechanisms are often heavily loaded and excited by input signals of large amplitude so that the theories based on the linearisation of equations by the small perturbation methods originally attributed to Harpur (13), are far from adequate. In addition, non-linearities such as coulomb friction present difficulties and these are not entirely catered for by the use of describing functions or equivalent viscous damping concepts.

With these problems in mind this work sets out to present analyses of the two types of controls described and in the case of the electro-hydraulic controller to compare the results obtained by these methods with experimental test results, for large amplitude input signals.

Since this work considers only the features and phenomena within the pump itself and its associated controls, consideration of the effects of external influences will be restricted to those of transient system pressure changes. Helgstad, Foster and Bannister (14), have shown that the multi piston pump experiences pressure variations during a working cycle considerably in excess of the 1.25% variation which is frequently quoted for a seven piston pump such as the HD900. It is necessary therefore to assume that the normal supply pressure to the control valves is constant.

The effects of fluid inertia within the pump is also difficult to estimate and although these effects have been investigated by Ainsworth (15), and Streeter and Wylie (16), it is considered that the complexity of the flow paths and

the short lengths of passage involved make the neglect of fluid inertia to be reasonable in this instance.

The value of the bulk modulus can vary greatly depending on the degree of air entrainment. A realistic value is of prime importance since the hydraulic natural frequency of the system is directly dependent on the bulk modulus of the fluid. Merritt (17), suggests a value of 6.9×10^8 N/m^2 and is supported by other sources and will be used in this instance.

The volumes of fluid used in the analysis and other physical dimensions have been derived from manufacturers' drawings and data. It is assumed that no cavitation occurs during the pump operations.

6.2 Analysis of Manually Variable Servo Assisted Stroke Control

The volumetric efficiency of the HD900 pump varies with the system pressure but since 100 bar is considered to be a suitable reference pressure and that at this pressure the volumetric efficiency is of the order of 96%, we can ignore internal pump leakages and compressibility effects and give a linearised equation for the pump displacement q as -

$$q = K x_p$$

where K is a constant for the flow gain of the pump and X_p is the displacement of the servo piston from the zero swashplate angle setting.

The force F_c required to move the swashplate arises from the frictional forces at the swashplate bearings and can be estimated from equations (7.7) and (7.8), by adopting a suitable coefficient of friction for the bearings used. In addition, a force F_L is required to maintain the swashplate at any particular angle of tilt. F_L will vary with the swashplate angle but as its value is low compared to F_c, an average value can be used over the entire range of swashplate angles.

Under conditions of changing velocity of the servo piston and the associated stroke change mechanism, the inertia effects are best considered by finding the equivalent mass M_r on the axis of the servo piston. In addition, there will be viscous damping effects and these can be expressed in terms of a viscous damping coefficient B_p. A schematic diagram of the system is shown in Fig.6.2.

6.2.1 Steady State Conditions for Servo Valve

The equations for pressure flow via the valve openings at 1 and 2 for null conditions, are -

$$Q_L = C_d A_1 \left[\frac{2}{\rho}(P_s - P_c)\right]^{1/2} = C_d W E \left[\frac{2}{\rho}(P_s - P_c)\right]^{1/2} \qquad (6.1)$$

$$Q_L = C_d A_2 \left[\frac{2}{\rho} P_c\right]^{1/2} = C_d W E \left[\frac{2}{\rho} P_c\right]^{1/2} \qquad (6.2)$$

where Q_L = volume flow rate through servo valve at 1 and at 2

C_d = valve flow coefficient

A_1, A_2 = area of flow gap at 1 and at 2

ρ = density of hydraulic fluid

P_s = supply pressure to valve

P_c = control pressure on servo piston

W = area gradient of servo valve ports

E = valve opening = displacement of valve X_v - displacement of servo piston X_p

If small signal response is required, the flow equations can be limited to the regions near the null point and linearised. By defining the null point as being

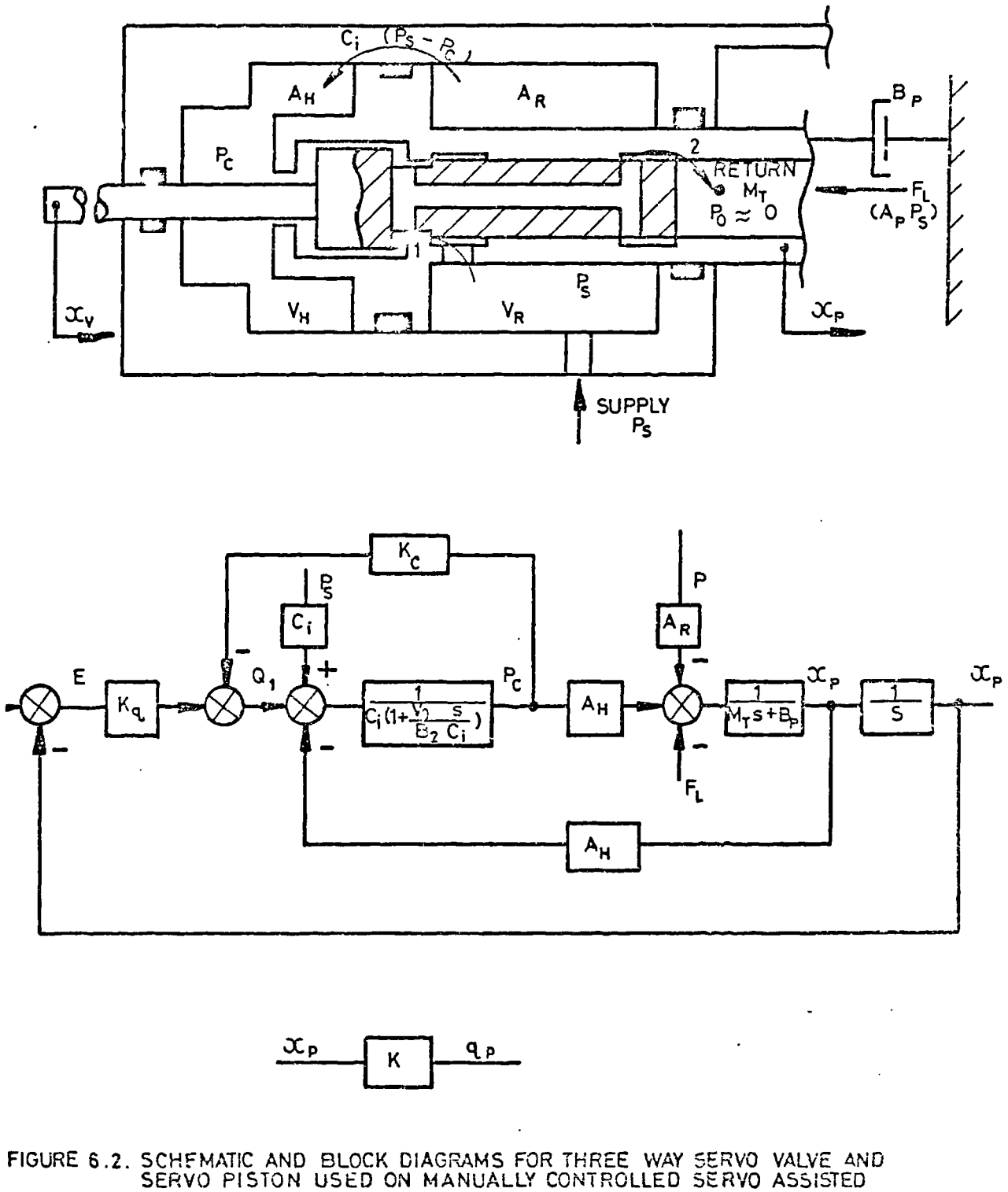

FIGURE 6.2. SCHEMATIC AND BLOCK DIAGRAMS FOR THREE WAY SERVO VALVE AND SERVO PISTON USED ON MANUALLY CONTROLLED SERVO ASSISTED VARIABLE DELIVERY AXIAL PISTON PUMP.

where $Q_L = E = 0$, and since A_H the area of the head side of the servo piston is twice the area of the ram side of the servo piston A_R we can let $P_c = \frac{P_s}{2}$.

The null coefficients of the valve are the flow gain coefficient K_q, the flow pressure coefficient K_c and K_p the pressure sensitivity of the valve. Then by definition -

$$K_q = \left.\frac{\partial Q_L}{\partial E}\right|_c = C_d W \sqrt{\frac{P_s}{\rho}} \tag{6.3}$$

$$K_c = -\left.\frac{\partial Q_L}{\partial P_c}\right|_o = \left.\frac{C_d W E}{P_s}\sqrt{\frac{P_s}{\rho}}\right|_{E=0} = 0 \tag{6.4}$$

$$K_p = \left.\frac{\partial P_c}{\partial E}\right|_o = \left.\frac{P_s}{E}\right|_{E=0} = \infty \tag{6.5}$$

6.2.2 Steady State Conditions for Servo Valve and Servo Piston

The expression for the pressure flow can be rewritten as -

$$Q_L = K_q x_v - K_q x_p - K_c P_c \tag{6.6}$$

and applying the theory of continuity to the control volume V_H we have -

$$Q_L + C_i(P_s - P_c) = \frac{dV_H}{dt} + \frac{V_H}{B}\frac{dP_c}{dt} \tag{6.7}$$

where $V_H = V_o + A_H X_p$ and C_i is the leakage coefficient for the servo piston.

If we consider a small piston movement such that V_o is very large compared to $|A_H X_p|$ we can combine equations (6.6) and (6.7) and Laplace transform to give -

$$Q_L + C_i P_s = A_H s x_p + \frac{V_o}{B} s P_c + C_i P_c \tag{6.8}$$

The force equation for the system is -

$$M_T s^2 x_p = A_H P_c - A_R P_s - B_p s x_p - F_L - \frac{\dot{x}_p}{|\dot{x}_p|} F_c \tag{6.9}$$

Since the sign of F_c depends on the direction of motion on the piston, equation (6.9) is non-linear and solutions can be sought by the use of a) Describing Functions, and b) Equivalent Viscous Damping.

a) The phenomenon of static and coulomb friction can be idealised as in Fig.6.3, where F_S is the static friction force and F the instantaneous friction force. The non-linear element is characterised by a describing function $G_d(\alpha, \beta)$ where a and are ratios relating the dimensions of the non-linearity to the input amplitude M at the non-linear element. The describing function is defined by Merritt (16), as -

$$G_d(\alpha, \beta) \equiv \frac{c_1}{M} \angle \psi$$

if the input is sinusoidal.

The output waveform of the non-linear element is adequately described by the fundamental component of a Fourier series and the effects of harmonics is negligible. The non-linearity is symmetrical and there is no d.c. component but if both static and coulomb friction are considered, there is a phase lag and this can affect system stability. Since

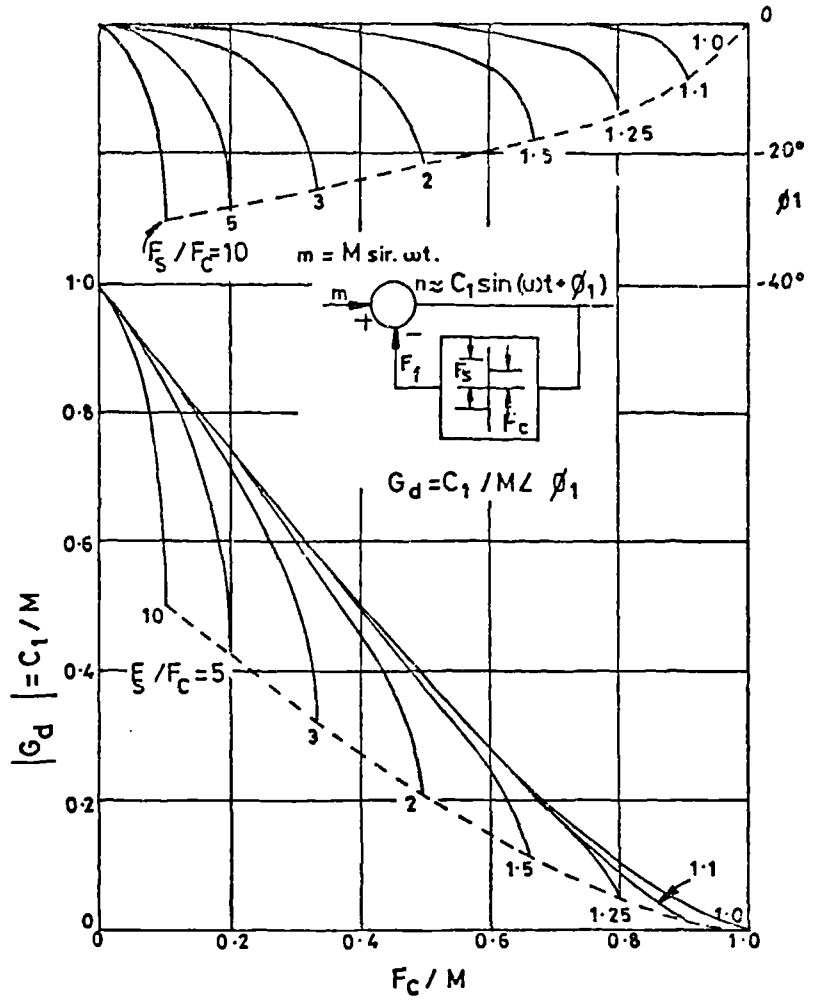

FIGURE 6.3. DESCRIBING FUNCTION FOR A FRICTION NONLINEARITY BASED ON A DOMINANCE OF VISCOUS FORCES.

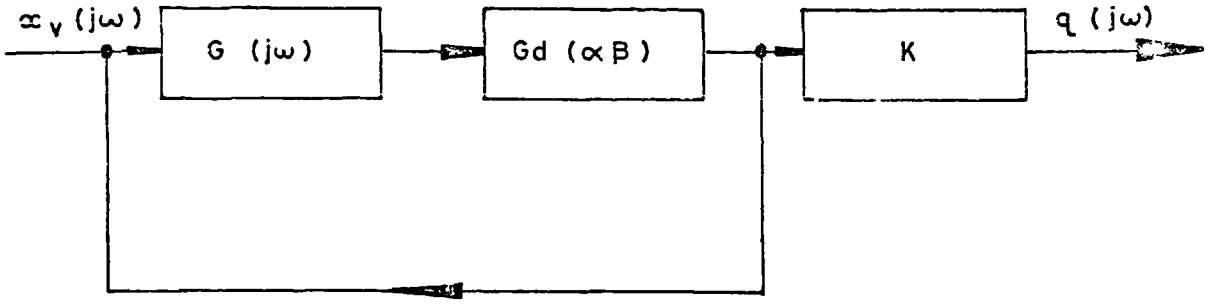

FIGURE 6.4. CLOSED LOOP BLOCK DIAGRAM FOR MANUALLY CONTROLLED PUMP.

one describing function cannot cater for all systems containing non-linearity due to friction, a decision has to be made on which component of the force equation is dominant. Thus describing functions can be used for systems which are -

1. inertia dominant;
2. viscous force dominant;

or in some instances -

3. spring force dominant.

Because of the low equivalent mass of the servo piston/swashplate assembly and the low levels of servo piston acceleration, the system can be considered to be viscous dominant.

Merritt and Gavin (18), have analysed the output waveform as -

$$C_d = \left[\left(\frac{a_1}{M}\right)^2 + \left(\frac{b_1}{M}\right)^2\right]^{1/2} \angle \tan^{-1}\left(\frac{a_1}{b_1}\right)$$

where

$$\frac{\pi a_1}{M} = \left(\frac{F_c}{M}\right)^2 \left[2\frac{F_s}{F_c} - 1 - \left(\frac{F_s}{F_c}\right)^2\right]$$

and

$$\frac{\pi b_1}{M} = \pi - \sin^{-1}\left(\frac{F_s}{M}\right) - \sin^{-1}\left(\frac{F_c}{M}\right) - \frac{F_c}{M}\left[1-\left(\frac{F_c}{M}\right)^2\right]^{1/2} + \frac{F_c}{M}\left(\frac{F_s}{F_c} - 2\right)\left[1-\left(\frac{F_s}{M}\right)^2\right]^{1/2}$$

Fig.6.3 is based on this analysis and can be used to obtain the describing function gain G_d and the phase angle ψ.

6.2.3 Frequency Response of a Manually Controlled Pump by Describing Function Method

The transfer function for the system if the frictional elements are neglected can be obtained by rewriting equation (6.9), as -

$$M_T S^2 x_p = A_H P_c - A_P P_s - F_L - B_P S x_p \qquad (6.10)$$

and since we are concerned only with terms affected by small changes in the variables, P_s can be considered as constant and thereby as zero and by equating (6.6), (6.8) and (6.10) obtain -

$$x_p(s) = \frac{\frac{K_q}{A_H} x_v - \frac{K_T}{A_H^2}\left(1 + \frac{V_o S}{B K_T}\right) F_L}{S\left(\frac{S^2}{\omega_h^2} + 2\frac{\zeta_h S}{\omega_h} + 1\right) + \frac{K_q}{A_H}} \qquad (6.11)$$

where ω_h is the natural frequency $= \sqrt{\frac{B A_H^2}{V_o M_T}}$

and ζ_h is a non-dimensional damping factor such that -

$$\zeta_h = \frac{K_T}{2A_H}\sqrt{\frac{BM_T}{V_o}} + \frac{B_p}{2A_H}\sqrt{\frac{V_o}{BM_T}}$$

where $K_T = K_c + C_i$

Equation (6.11) gives the dynamic response for the servo piston and this can be expressed in terms of the swashplate angle by substituting ϕ (radians) $= \frac{X_p}{\ell_1}$

where ℓ_1 is the distance between the axes of the pump and

of the servo piston. Since the pump displacement is proportional to $\tan \phi$, for small changes of X_p we can substitute q/K

where

$$K = \frac{\pi}{2} \frac{d_p}{\ell_i} r_c N_p$$

The transfer function for the system under steady load is -

$$\frac{x_p(s)}{x_v(s)} = \frac{\frac{K_q}{A_H}}{s\left(\frac{s^2}{\omega_h^2} + 2\frac{\zeta_h s}{\omega_h} + 1\right) + \frac{K_q}{A_H}} \qquad (6.12)$$

and the transfer function for the system if the valve opening remains constant but the load F_L changes, is -

$$\frac{\Delta x_p(s)}{\Delta F_L(s)} = -\frac{\frac{K_T}{A_H^2}\left(1 + \frac{V_o s}{B K_T}\right)}{s\left(\frac{s^2}{\omega_h^2} + 2\frac{\zeta_h s}{\omega_h} + 1\right) + \frac{K_q}{A_H}} \qquad (6.13)$$

Introducing the describing function for friction into the system necessitates substituting $j\omega$ for s in the linear transfer function. If equation (6.12) is expressed as $G_{i(j\omega)}$ and the describing function as $G_d(\alpha, \beta)$, the closed loop response for pump displacement is -

$$\frac{q(j\omega)}{x_v(j\omega)} = K\left[\frac{G_i(j\omega) \cdot G_d(\alpha, \beta)}{1 + G_i(j\omega) \cdot G_d(\alpha, \beta)}\right] \qquad (6.14)$$

Fig.6.4 shows a block diagram for the closed loop system.

6.2.4 Frequency Response of a Manually Controlled Pump by Equivalent Viscous Damping Method

Davies and Lambert (19) have suggested a method of linearising a force equation by replacing the non-linear coulomb friction term by an equivalent viscous friction which absorbs the same amount of energy per cycle.

Considering the motion of the servo piston as sinusoidal -

$$x_p = X_p \sin \omega t \tag{6.15}$$

where X_p is the maximum displacement of the servo piston.

The energy dissipated per cycle by the damping force $B_p \dot{x}_p$ is -

$$W_v = \int_0^{2\pi} \left[B_p \dot{x}_p \right] \frac{x_p}{\omega} \, d(\omega t)$$

$$= \pi \omega B_p X_p^2 \tag{6.16}$$

The energy dissipated by a coulomb force $F_c \frac{\dot{X}_p}{|\dot{X}_p|}$ per cycle is -

$$W_F = \int_0^{2\pi} \left[F_c \frac{\dot{x}_p}{|\dot{x}_p|} \right] \frac{x_p}{\omega} \, d(\omega t)$$

$$= 4 F_c X_p \tag{6.17}$$

By equating (6.15) and (6.16) -

$$B_p = \frac{4 F_c}{\pi \omega X_p} \tag{6.18}$$

and the viscous damping coefficient to represent both the inherent viscous damping effect and the coulomb friction is -

$$B'_p = B_p + \frac{4F_c}{\pi\omega X_p} \qquad (6.19)$$

The frequency response of the system can be described by replacing B_p by B'_p and by using amended values of ζ_h in equation (6.12).

6.2.5 Frequency response of manually controlled servo assisted stroke controlled HD900 pump

It will be seen that considerable variation in the natural frequency and the damping factor for the system will result from changes in the control volume. Such changes can result from:

(i) variations in the mean pump displacement due to changes in the swashplate angle;

(ii) variations in the volume of oil in the system which is at the supply pressure to the servo valve.

Thus it is necessary to relate the frequency response of the pump in a specific application to the mean swashplate angle and to the total volume of oil at the pump supply pressure both within the pump and in the external system.

To indicate the level of control that can be expected from this form of the HD900 pump, Fig.6.5, shows the calculated values for the pump with a pressure generating device such as a pressure relief valve installed:

a) at the pump outlet port tapping;

b) at a distance of one metre from the pump and connected by 30mm bore tubing.

The curves are based on a mean swashplate angle of $7\frac{1}{2}^{o}$ and with a supply pressure of 100 bar. The servo piston amplitude is limited to 0.5mm.

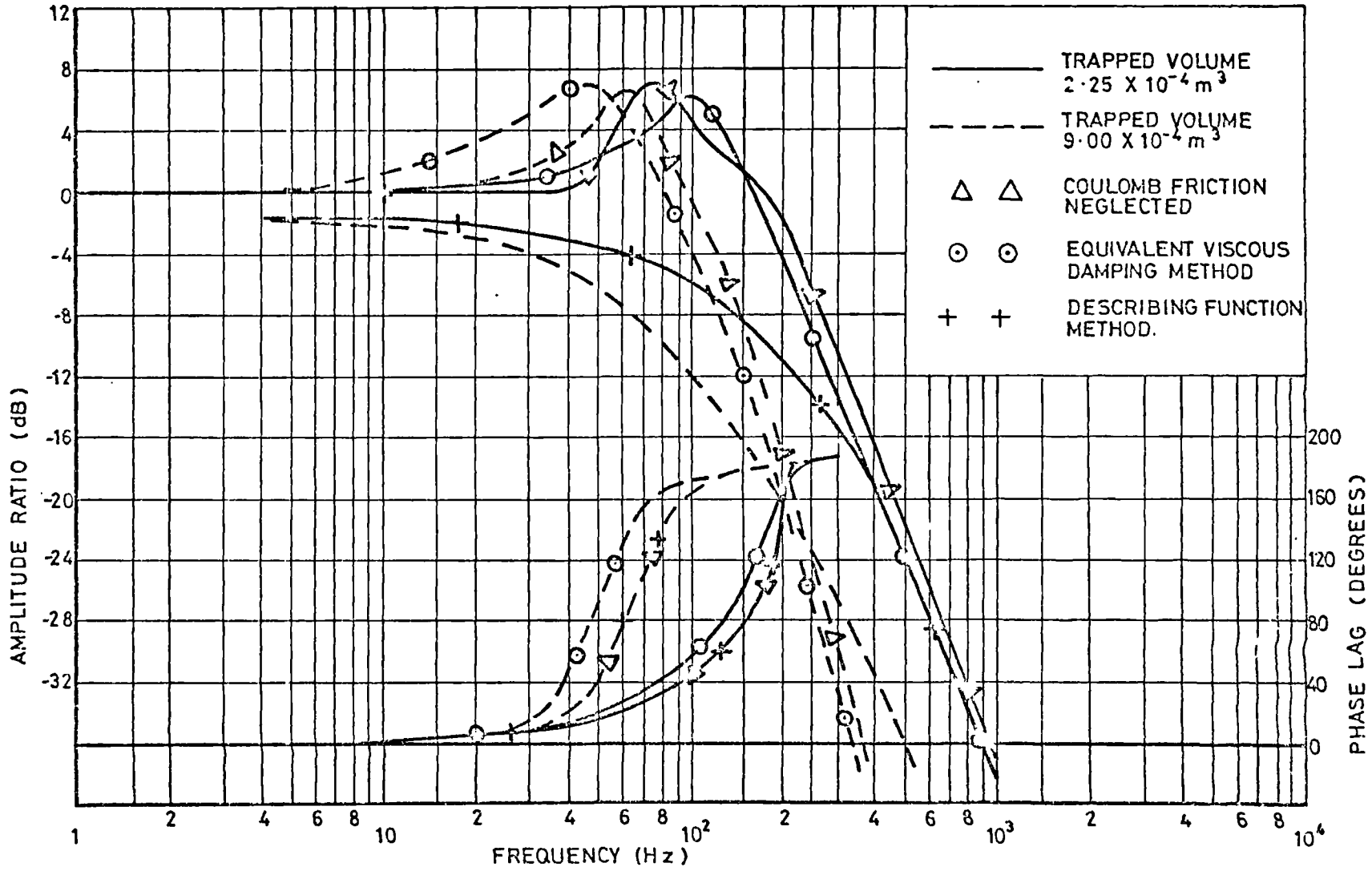

FIGURE 6.5 . PREDICTED FREQUENCY RESPONCE FOR MANUALLY CONTROLLED HD900 PUMP BY VARIOUS ANALYTICAL METHODS.

Data for the Frequency Response of the Lucas HD900 Pump with Manually Controlled Servo Assisted Stroke Control

Area of head side of servo piston	A_H	$= 1.52 \times 10^{-3}\ m^2$
Area of ram side of servo piston	A_R	$= .76 \times 10^{-3}\ m^2$
Valve flow gain coefficient	K_q	$= 1.95\ m^2/s$
Valve flow pressure coefficient	K_c	$= .77 \times 10^{-12}\ m^5/Ns$
Supply pressure	P_s	$= 100$ bar
Density of hydraulic fluid	ρ	$= 875\ kg/m^3$
Valve flow coefficient	C_d	$= .61$
Bulk modulus for hydraulic fluid	β	$= 6.9 \times 10^8 N/m^2$
Viscous damping coefficient	B_p	$=12.15 \times 10^3\ Ns/m$
Area gradient of servo valve ports	W	$=29.92 \times 10^{-3}\ m^2/m$
Total equivalent mass	M_T	$= 2$ kg
Frictional force at 100 bar supply	F_c	$= 1.625 \times 10^3$ N
Static frictional force	F_s	$= 1.25\ F_c$
Swashplate force	F_c	$= 333$ N
Viscosity of hydraulic fluid	μ	$=17.4 \times 10^{-3}\ Ns/m^2$
Piston leakage coefficient	C_i	$= 3 \times 10^{-15}\ m^5s/N$

If the servo piston amplitude is limited to 0.5mm, equivalent viscous damping coefficient -

$$B_p' = 12.25 \times 10^3 + \frac{4.138 \times 10^6}{\omega}$$

Under conditions (a)

Control volume	V_o	$= 2.25 \times 10^{-4}\ m^3$
Natural frequency	ω_h	$= 1880$ rad/s
Damping factor	ζ_h	$= 1.63$

Under conditions (b)

Control volume	V_o	$= 9.00 \times 10^{-4}\ m^3$
Natural frequency	ω_h	$= 940$ rad/s
Damping factor	ζ_h	$= 3.26$

6.3 Analysis of Electro-Hydraulic Stroke Control

The analysis of this form of control can be achieved by considering the system as comprising an electrical torque motor with a first stage hydraulic amplifier and a differential hydraulic piston controlled by a four way servo valve. As in the analysis of the manually controlled stroke control, the effects of coulomb friction can be dealt with separately.

6.3.1 Analysis of Electro-Hydraulic Controller (First Stage)

The electro-hydraulic servo valve used on the HD900 pump is of the two stage type with force feedback. Merritt (16) has derived a transfer function for this type of controller which neglects the pressure feedback to the flapper valve nozzles and the flow forces on the second stage spool valve. In addition, the transfer function requires knowledge of several physical values for the controller under study which would be extremely difficult for a pump designer to obtain from the manufacturer of the controller.

Further works by Zaborszky and Harrington (20), and by Cataldo (21), have overcome some of the shortcomings of Merritt's work but a problem which persists is that of adequately describing the flux density developed within the torque motor. Thayer (22) describes in detail the assumptions which have to be made if the many non-linearities which exist are to be catered for in an analytical method.

It would therefore appear that the best course of action in practical pump design is to base the dynamic response of the controller on the third order transfer function -

$$\frac{Q(s)}{i(s)} = K\left[\frac{1}{s\left(\frac{s^2}{\omega_n^2} + 2\frac{\zeta}{\omega_n}s + 1\right)}\right] \qquad (6.20)$$

where i is the input current to the torque motor, K is the servo valve sensitivity, ω_n is the apparent natural frequency of the controller and ζ the apparent damping ratio of the unit.

Block diagram 6.6, gives a simplified representation of the controller and is tenable if the following assumptions are made.

1. All non-linearities can be approximated by linear expressions or neglected.
2. The armature of the torque motor and the flappers can be treated as a lumped parameter.
3. The supply to the torque motor has infinite impedance.
4. Fluid compressibility and viscosity effects are negligible.
5. Flapper movement is small compared with movement of the valve spool.
6. The forces necessary to move the valve spool are small compared with the pressure force available.

Assumption 6. implies that the pressure differential across the ends of the spool are negligible during dynamic conditions and therefore that the spool mass, friction effects and flow forces can be neglected. Testing the validity of these assumptions on experimental rigs has shown this simplification to be justified.

The natural frequency ω_n of the first stage can be calculated from the effective stiffness of the armature/flapper k_f and ℓ_f the rotational mass of the armature/flapper, where -

$$\omega_n = \sqrt{\frac{k_f}{\ell_f}}$$

The stiffness of the armature/flapper depends on the centering effect of the flexure tube and the decentering effect of the permanent magnetic flux. Thus the value of S_{AF} and M_{AF} can be arrived at by the manufacturer by

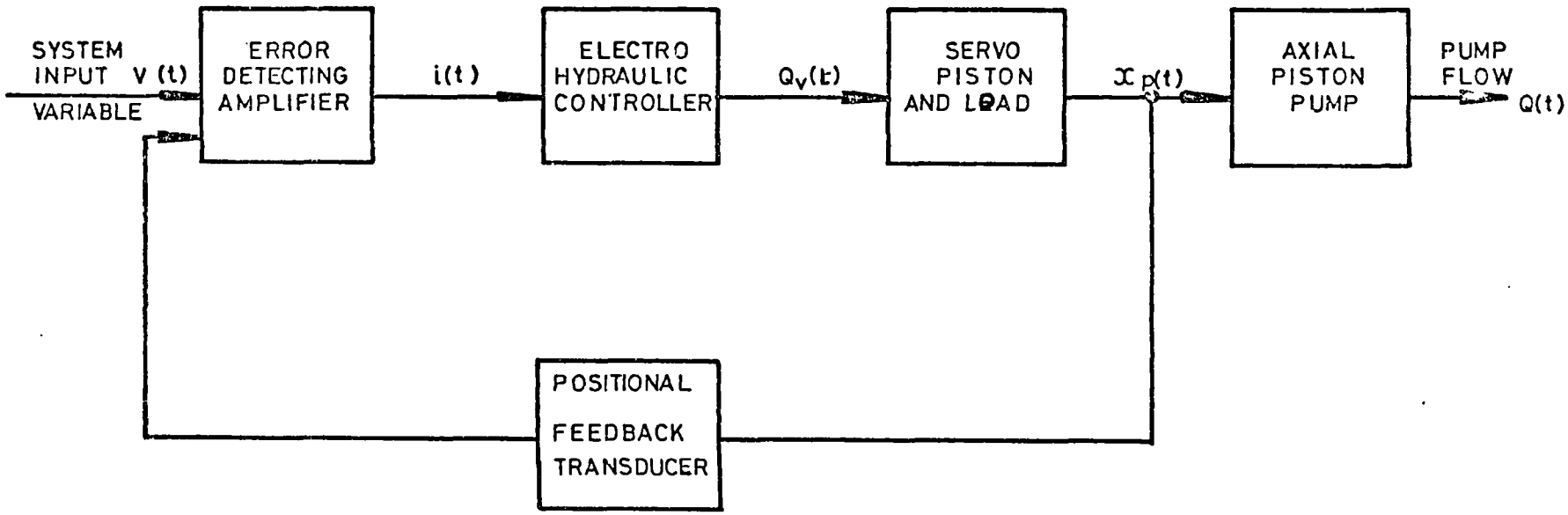

FIGURE 6.6. BLOCK DIAGRAM OF ELECTRO-HYDRAULIC CONTROLLED PUMP.

calculation and test results. The damping force on the armature/flapper is complex and once again reliance must be placed on the manufacturer's data.

$$\zeta_s = \frac{b_f \omega_n}{2 k_f}$$

where ζ_s is the damping ratio of the first stage and b_f is the net damping of the armature/flapper.

The internal loop gain of the servo valve is then -

$$K_v = \frac{K_2 k_w}{k_f A_s}$$

where K_2 is the hydraulic amplifier flow gain and k_w is the stiffness of the feedback wire.

The servo valve static flow gain K_s is then -

$$K_s = K_1 K_v K_3$$

where K_1 is the torque motor gain and K_3 is the flow gain for the spool valve.

The appropriate transfer function for the spool valve displacement is therefore -

$$\frac{x_v(s)}{i(s)} = K_1 K_v \left[\frac{1}{s\left(\frac{s^2}{\omega_n^2} + 2\frac{\zeta_s}{\omega_n} s + 1\right)} \right]$$

(6.21)

6.3.2 Analysis of Servo Valve and Servo Piston

Diagram 6.7 shows the conditions arising at the servo valve and the servo piston.

The flow rate Q_1 to the head side of the piston is given by -

$$Q_1 = C_d W x_v \left[\frac{2}{\rho} (P_B - P_1) \right]^{1/2}$$

(6.22)

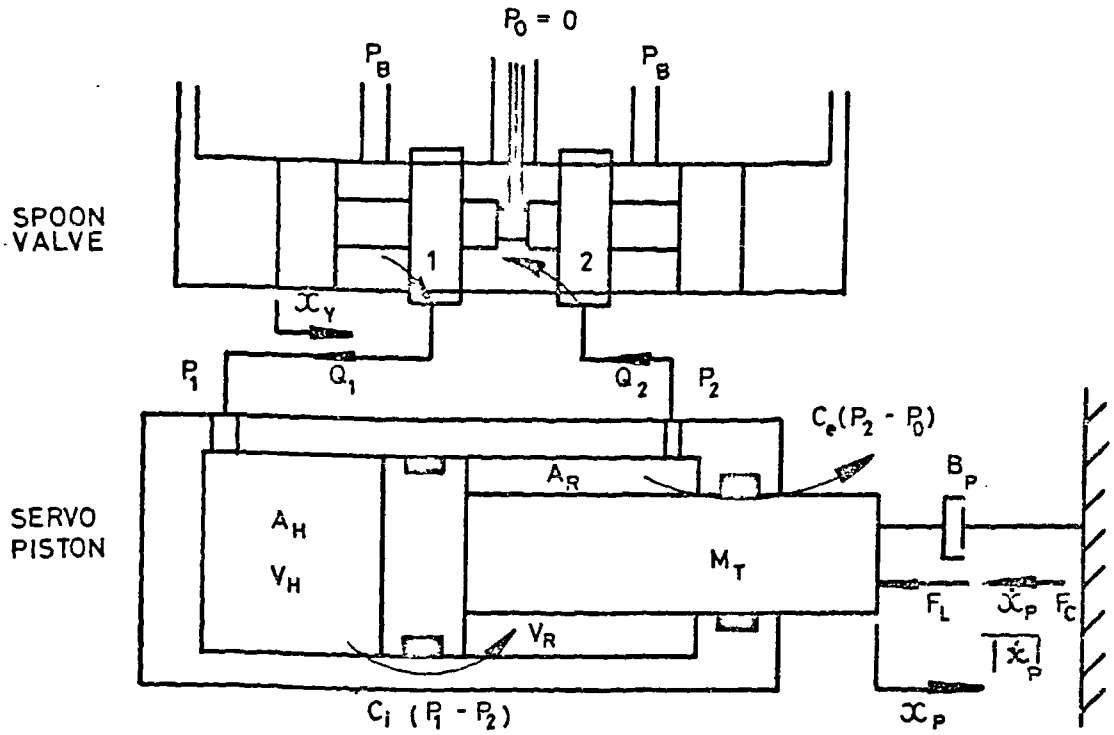

FIGURE 6.7. SCHEMATIC ARRANGEMENT OF ELECTRO - HYDRAULIC SERVO VALVE WITH PUMP SERVO PISTON AND LOADS.

and the flow rate Q_2 to the ram side of the piston by -

$$Q_2 = C_d W x_v \left[\frac{2}{\rho} P_2\right]^{1/2} \tag{6.23}$$

For small perturbations from the null point -

$$Q_1 = \left.\frac{\partial Q_1}{\partial x_v}\right|_0 x_v + \left.\frac{\partial Q_1}{\partial P_B}\right|_0 P_B - \left.\frac{\partial Q_1}{\partial P_1}\right|_0 P_1 \tag{6.24}$$

and

$$Q_2 = \left.\frac{\partial Q_2}{\partial x_v}\right|_0 x_v + \left.\frac{\partial Q_2}{\partial P_2}\right|_0 P_2 \tag{6.25}$$

If P_B is considered constant and introducing valve coefficients, we have -

$$Q_1 = K_q x_v - K_c P_1 \tag{6.26}$$

$$Q_2 = K_q x_v + K_c P_2 \tag{6.27}$$

Since system stability is a minimum when $V_H = V_R = V_o$ (22) continuity considerations for the two sides of the servo piston may be expressed as -

$$-Q_1 - C_i(P_1 - P_2) = A_H \frac{dx_p}{dt} + \frac{V_o}{B}\frac{dP_1}{dt} \tag{6.28}$$

$$C_i(P_1 - P_2) - C_e(P_2 - P_o) - Q_2 = A_R \frac{dx_p}{dt} + \frac{V_o}{B}\frac{dP_2}{dt} \tag{6.29}$$

Neglecting the external leakage term which will be of a low order and combining equations (6.26) to (6.29) -

$$K_q x_v (A_H + A_R) - K_c (A_H P_1 - A_R P_2) = (A_H^2 - A_R^2) S x_p$$

$$+ \frac{V_o}{B} S (A_H P_1 - A_R P_2) + C_i (A_H P_1 - A_R P_2) + C_i (A_R P_1 - A_H P_2)$$

(6.30)

The term $C_i (A_R P_1 - A_H P_2)$ presents considerable mathematical difficulty and since C_i is of a low order and $A_R P_1$ will not be great compared to $A_H P_2$, the term can be neglected.

The hydraulic force on the servo piston is -

$$F_H = A_H P_1 - A_R P_2 \qquad (6.31)$$

and substituting in (6.30), we get -

$$F_H = \frac{K_q x_v (A_H + A_R) - S x_p (A_H^2 - A_R^2)}{K_T \left(1 + \frac{V_o S}{B K_T}\right)} \qquad (6.32)$$

Again, if the coulomb friction is not considered -

$$F_H = M_T S^2 x_p + B_p S x_p + F_L \qquad (6.33)$$

Equating (6.31) and (6.32), we get -

$$x_p(s) = \frac{\frac{3K_q}{A} x_v - \frac{K_T}{A}\left(1 + \frac{V_o s}{B K_T}\right) F_L}{s\left(\frac{s^2}{\omega_{h_1}^2} + 2\frac{\zeta_{h1} s}{\omega_{h_1}} + \tau\right)} \tag{6.34}$$

where -

$$A = A_R = \frac{A_H}{2}$$

$$K_T = K_c + C_i$$

$$\zeta_{h1} = \frac{K_T}{2A}\sqrt{\frac{BM_T}{V_o}} + \frac{B_p}{2A}\sqrt{\frac{V_o}{B M_T}}$$

$$\omega_{h1} = \sqrt{\frac{BA^2}{V_o M_T}}$$

$$\tau = \left(\frac{K_T B_p}{A^2} + 3\right)$$

The transfer function for the system under steady load is -

$$\frac{x_p(s)}{x_v(s)} = \frac{\frac{3K_q}{2A_H}}{s\left(\frac{s^2}{\omega_{h1}^2} + 2\frac{\zeta_{h1} s}{\omega_{h_1}} + \tau\right)} \tag{6.35}$$

The effects of the coulomb friction can again be catered for by the use of a describing function $G_d(a, \beta)$ or by the equivalent viscous damping concept where B_p is replaced by B_p'

The open loop response for the servo valve and the servo piston can be expressed as -

$$\frac{x_p(j\omega)}{x_v(j\omega)} = K_3 K_4 \, G_2(j\omega) \, G_d(a, \beta)$$

where $K_4 \, G_2$ expresses equation (6.35) and the describing function, or as -

$$\frac{x_p(s)}{x_v(s)} = K_3 K_4 \, G_2(s)$$

if the values of ω_{h1}, ζ_{h1} & τ are adjusted to satisfy the equivalent viscous damping requirements.

6.3.3 Frequency Response for Electro-Hydraulic Stroke Controlled Pump

The frequency response for the complete pump with the electro-hydraulic controller can be obtained for small perturbations by combining the transfer functions and the unit gains for the system. Fig.6.8, shows the block diagram for the system, where -

$V(t)$	=	System input variable voltage
$e(t)$	=	System error signal
$i(t)$	=	Controller current
$X_v(t)$	=	Servo valve displacement
$X_p(t)$	=	Servo piston displacement
$q(t)$	=	Change of pump displacement
K_s	=	System open loop gain
K_p	=	Pump flow gain

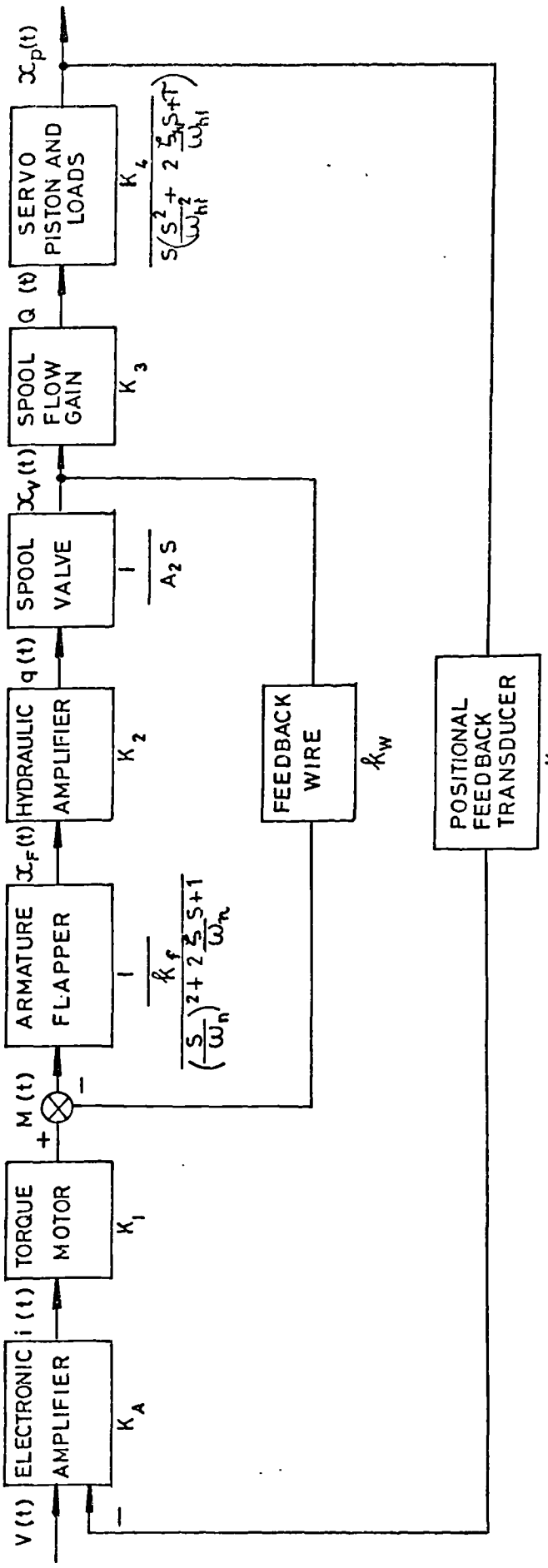

FIGURE 6.8. BLOCK DIAGRAM FOR PREDICTION OF FREQUENCY RESPONSE OF HD900 PUMP WITH ELECTRO-HYDRAULIC CONTROLLER

K_S = System gain

K_A = Electronic Amplifier gain

K_1 = Torque Motor gain

K_2 = Hydraulic Amplifier gain

K_3 = Spool valve flow gain

K_4 = Servo piston and loads gain

K_5 = Inverse of armature flapper stiffness

K_6 = Inverse of spool end area

K_{SV} = Internal loop gain

K_F = Positional feedback transducer gain

$G(s)$ = Time dependent term for complete system

$G_1(s)$ = Time dependent term for first stage hydraulic amplifier

$G_2(s)$ = Time dependent term for spool valve

$G_3(s)$ = Time dependent term for servo piston and loads

$G_{SV}(s)$ = Time dependent term for internal loop.

Then the closed loop transfer function for the first stage of the controller is -

$$K_{sv}\, G_{sv}(s) = \frac{K_5\, G_1(s)\, K_2\, K_6\, G_2(s)}{1 + K_5\, G_1(s)\, K_2\, K_6\, G_2(s)\, k_w}$$

and for the complete system -

$$\frac{x_p(s)}{V(s)} = \frac{K_S\, G(s)}{1 + K_S\, G(s)} = \frac{K_A\, K_1\, K_{SV} G_{SV}(s) K_3\, K_4\, G_3(s)}{1 + K_A K_1 K_{SV} G_{SV}(s) K_3\, K_4\, G_3(s) K_F}$$

(6.36)

Test facilities were set up at the Lucas works for measuring the frequency response of the HD900 pump with a Dowty type 4551-262 electrohydraulic controller. The positional feedback from the swashplate was obtained by using a Penny and Giles type APT25/60 rotary positional transducer.

Figs. 6.9 and 6.10, show the test rig which was basically a standard development test cell and the instrumentation consisted of a signal generator of Keelavite manufacture, a Solartron data logger, a Moseley X-Y plotter and a Southern Instruments UV recorder. The hydraulic circuit was to Fig.6.11.

The HD900 pump was modified and had a linear positional transducer fitted directly to the pump servo piston to indicate swashplate movement.

A series of tests were run with sinusoidal input signals for frequencies up to around 25 Hz and for strokes of 10% and 80% full stroke with the pump running at 2000 rev/min against a working pressure of 137 bar and with the pump inlet boosted to 41 bar.

From the UV traces the amplitude ratio and the phase lag were obtained and plotted in Figs.6.12 and 6.13. Also plotted are the calculated results from the derived transfer function for the system with the method of Nikiforuk and Westlund used to cater for the large signal response. It will be observed that reasonably good agreement was achieved between the experimental and calculated values.

The pump was also subjected in an off load condition to a stepped input signal from 20% to 80% full stroke and Fig.6.14, shows the traces obtained. It will be observed that the overshoot was of the order of 10% and the undershoot some 4%.

The linearity of the swashplate movement to the command signal is shown in Fig.6.15, and excellent results were obtained. Linearity was of the order of 4% and the loop hysteresis was only 3%.

Data for the Frequency Response of the Lucas HD900 Pump with Electro-hydraulic Controller

Area of Head Side of Servo Piston	A_H	=	1.52×10^{-3} m^2
Area of Annulus Side of Servo Piston	A_R	=	0.76×10^{-3} m^2
Test Pump Pressure	P	=	100 bar
Test Pump Speed	N	=	2000 rev/min
Pressure of supply to controller	P_S	=	41 bar
Pressure load on servo piston	F_L	=	333 N
Equivalent mass of servo piston assembly	M_T	=	0.675 kg
Coulomb friction force	F_C	=	1625 N
Control Volume	V_0	=	45×10^{-6} m^3
Leakage coefficient for servo piston	C_i	=	3.0×10^{-15} $m^3/s/N/m^2$
Viscous damping coefficient	B_p	=	12.25×10^3 NS/m

Derived Data

Servo piston and load natural frequency	ω_n	=	4587 rad/s.
Servo piston and load damping factor	ζ_{h_1}	=	$2.045 \times 10^{-4} B'_p$
Equivalent viscous damping coefficient	B'_p	=	$12.25 \times 10^3 + \frac{4F_c}{\pi \omega S}$
Time constant	τ	=	3.016

Data for Dowty Type 4551-262 Electro-hydraulic Controller

Torque motor current rating	i	$= \pm 7.5$ mA
Flapper valve displacement at nozzles	X	$= \pm 0.03$ mm
Spool displacement	X_V	$= \pm 0.457$ mm
Hydraulic amplifier differential flow	ΔQ	$= \pm 2.95$ cm^3/s
Servo valve control flow	Q_L	$= \pm 157.3$ cm^3/s
Torque motor gain	K_1	$= 0.377$ N cm/mA
Hydraulic amplifier flow gain	K_2	$= 968$ cm^3/s cm
Spool valve flow gain	K_3	$= 6.645 \times 10^3$ cm^3/s cm
Spool end area	A_2	$= 0.495$ cm^2
Armature/flapper stiffness	k_f	$= 414$ N mm/mm
Feedback wire stiffness	k_w	$= 36.7$ N mm/mm
Armature/flapper damping	b_f	$= 0.071$ Nm/s mm
Rotational mass of armature/flapper	ℓ_f	$= 1.957 \times 10^{-5}$ N mm/mm s^2
Natural frequency of first stage	ω_n	$= 730$ Hz
Damping ratio of first stage	ζ	$= 0.4$
Servo valve loop gain	K_V	$= 174$ s^{-1}

Data for Penny and Giles Type APT25/60 Feedback Transducer

Transducer sensitivity	K_F	$= 1.06$ mV/degree

Data for Shell Tellus 27 Hydraulic Fluid

Effective bulk modulus	B	$= 6.9 \times 10^8$ N/m^2
Density	ρ	$= 875$ kg/m^3

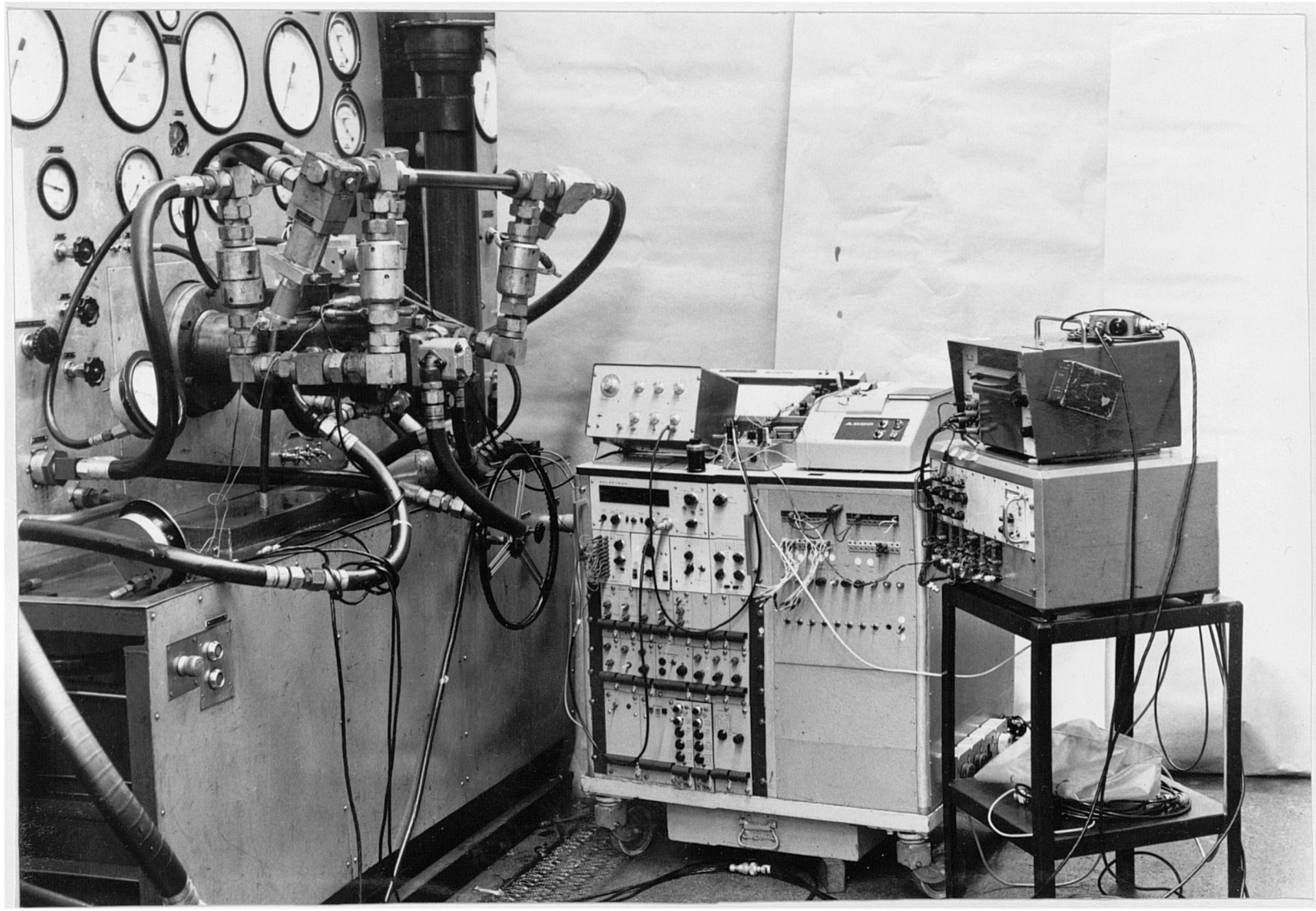

FIGURE 6.9 TEST RIG FOR MEASURING THE FREQUENCY RESPONSE OF THE HD 900 PUMP WITH ELECTRO-HYDRAULIC CONTROLLER.

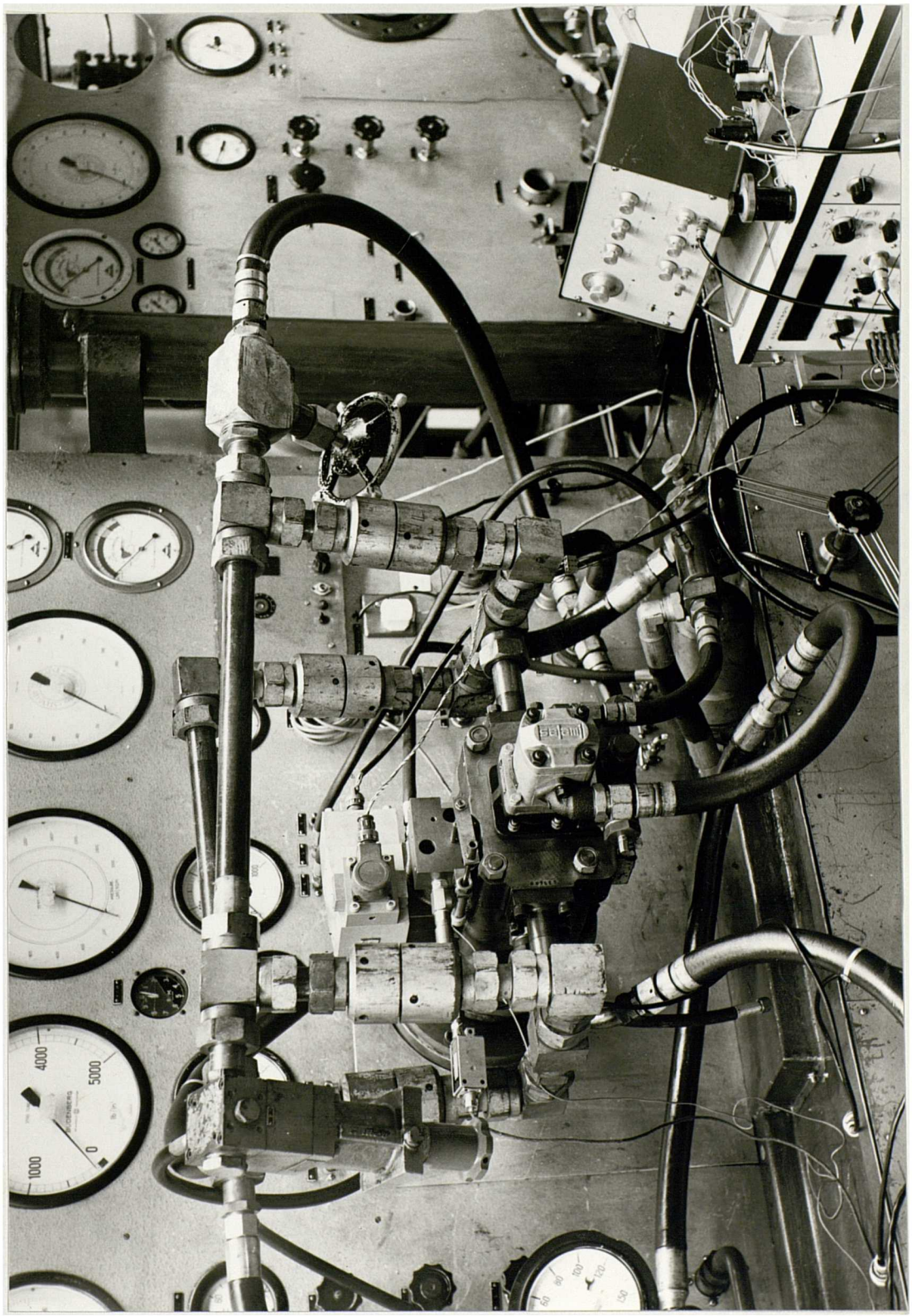

FIGURE 6.10 CLOSE UP OF FREQUENCY RESPONSE TEST RIG.

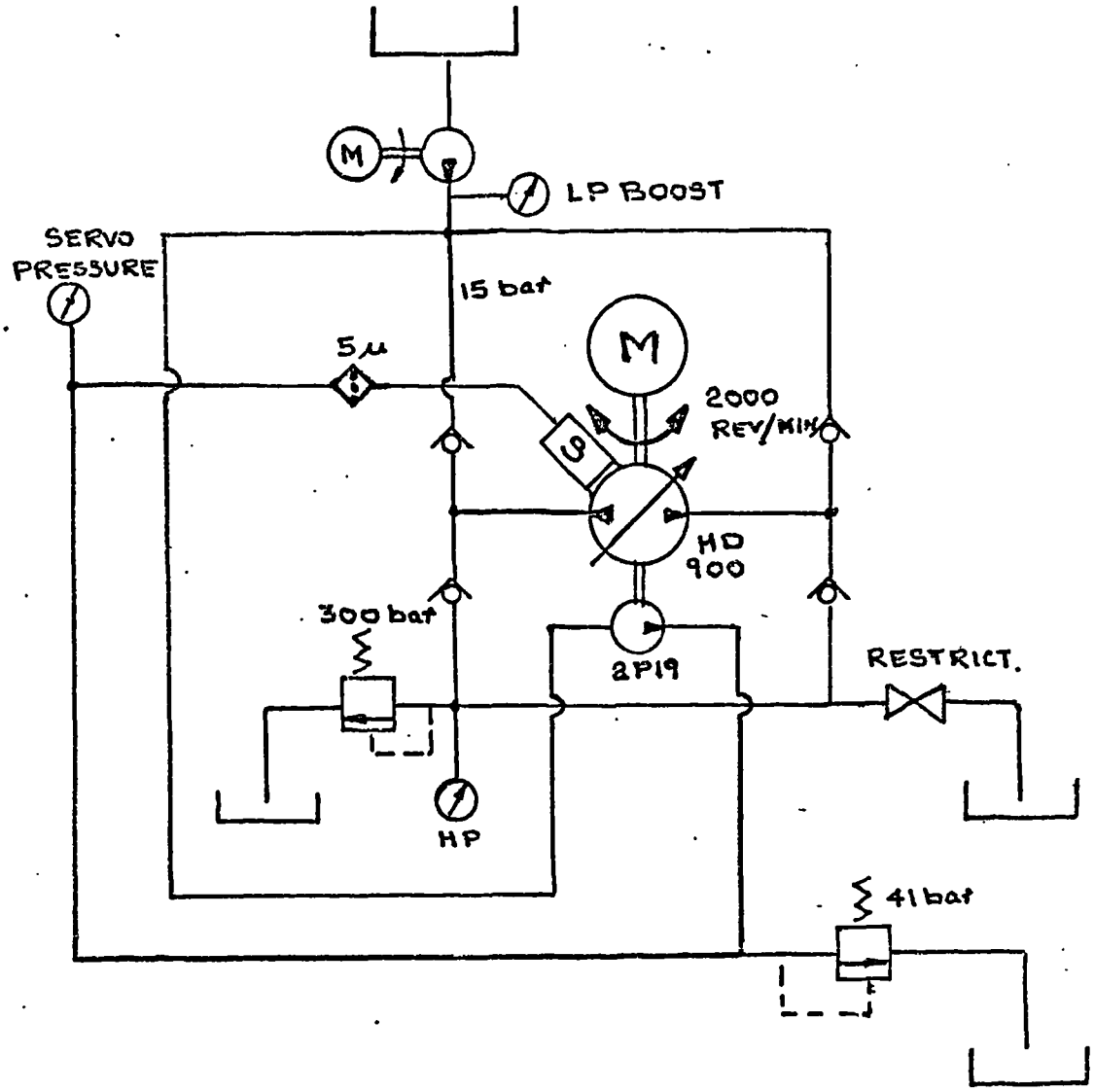

FIG. 6.11 HYDRAULIC CIRCUIT FOR MEASURING THE FREQUENCY RESPONSE OF THE LUCAS HD 900 PUMP.

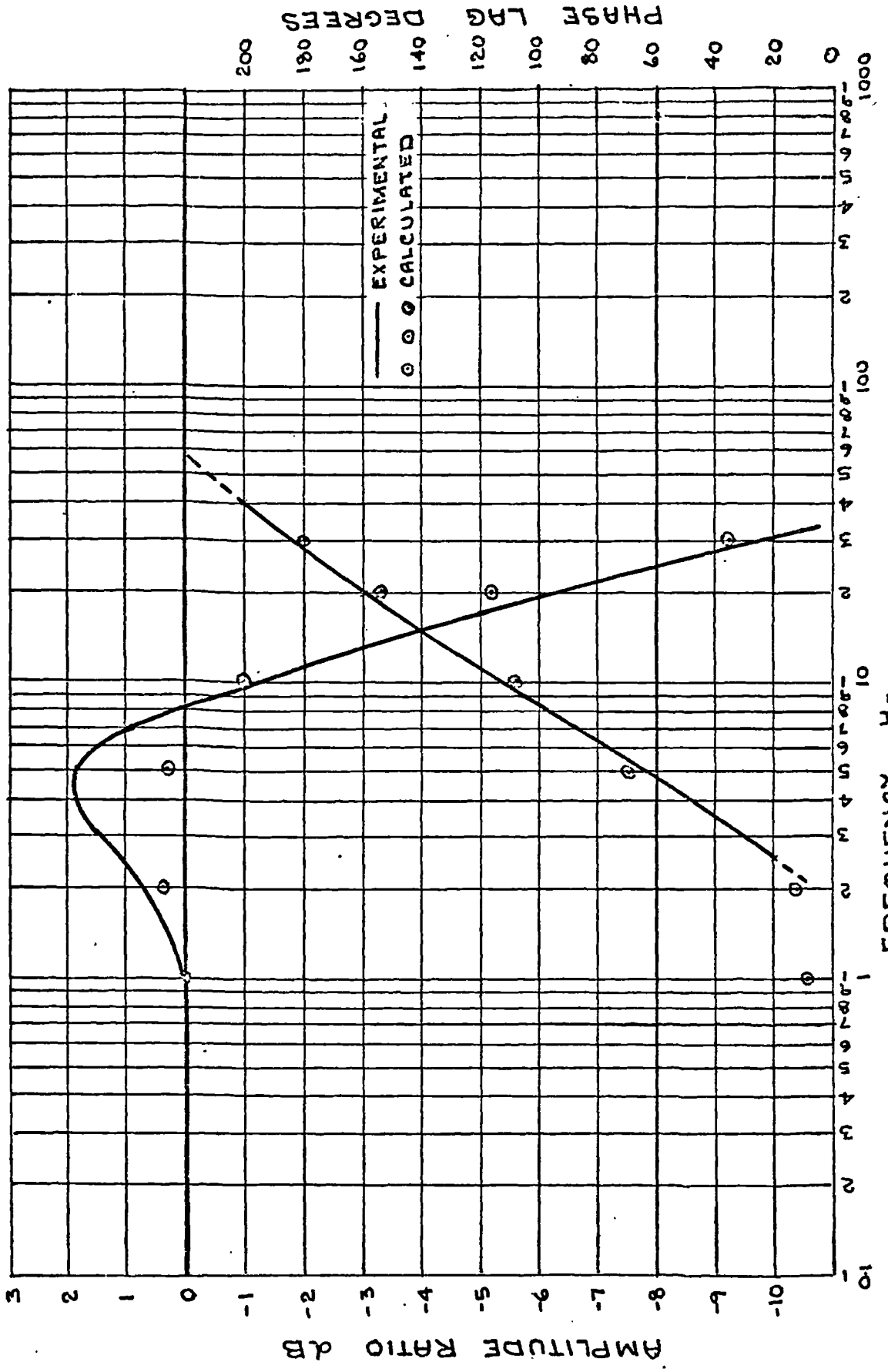

FIG. 6.12 FREQUENCY RESPONSE CURVES FOR HD 900 PUMP AT 2000 REV/MIN, 137 bar WORKING PRESSURE AND 41 bar INLET PRESSURE AND STROKING AT 10% FULL STROKE.

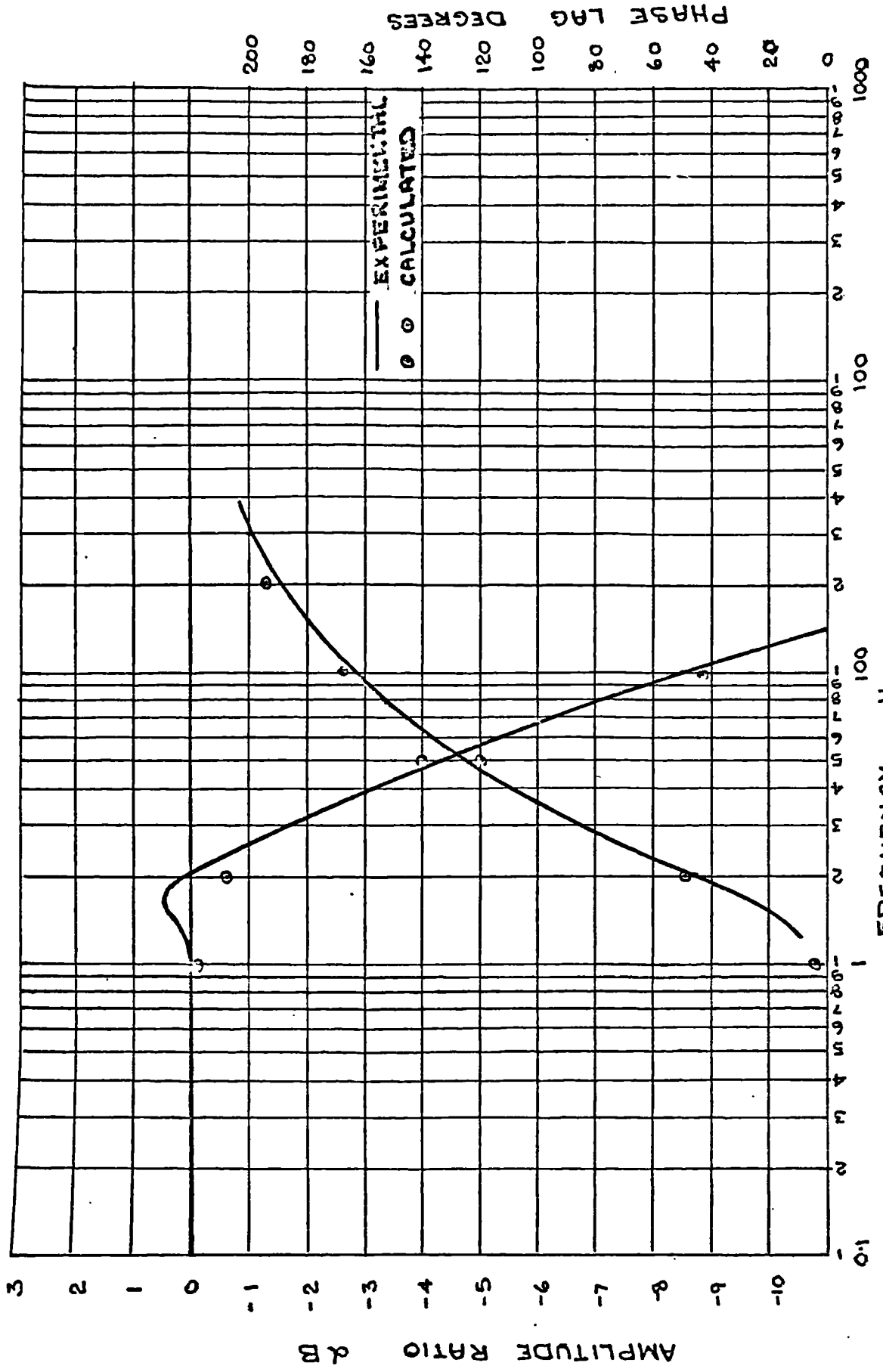

FIG. 6.13 FREQUENCY RESPONSE CURVES FOR HD 900 PUMP AT 2000 REV/MIN, 137 bar WORKING PRESSURE AND 41 bar INLET PRESSURE AND STROKING AT 80% FULL STROKE.

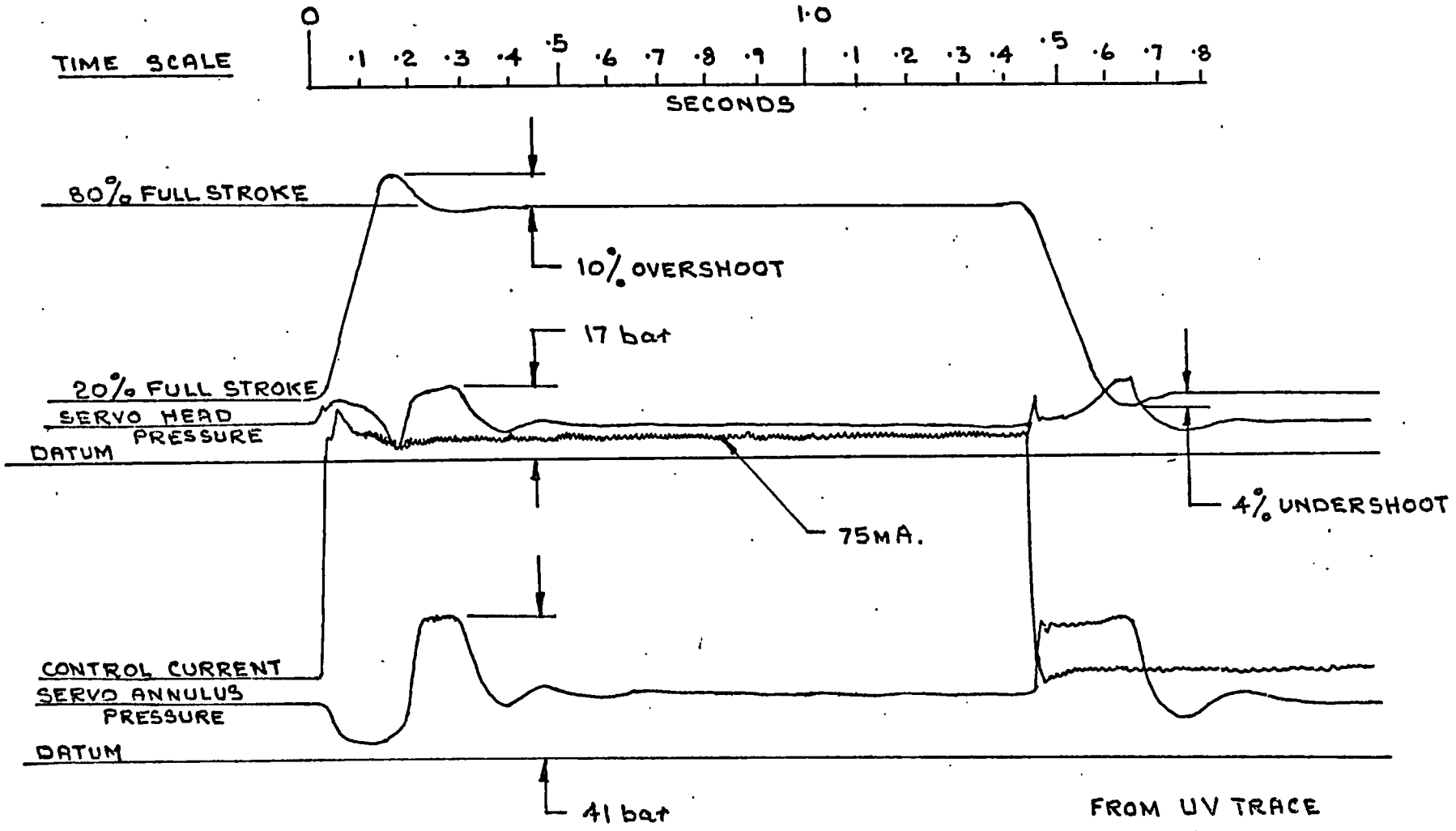

FIG. 6.14 STEPPED INPUT RESPONSE FOR HD 900 PUMP IN OFF LOADED CONDITION.

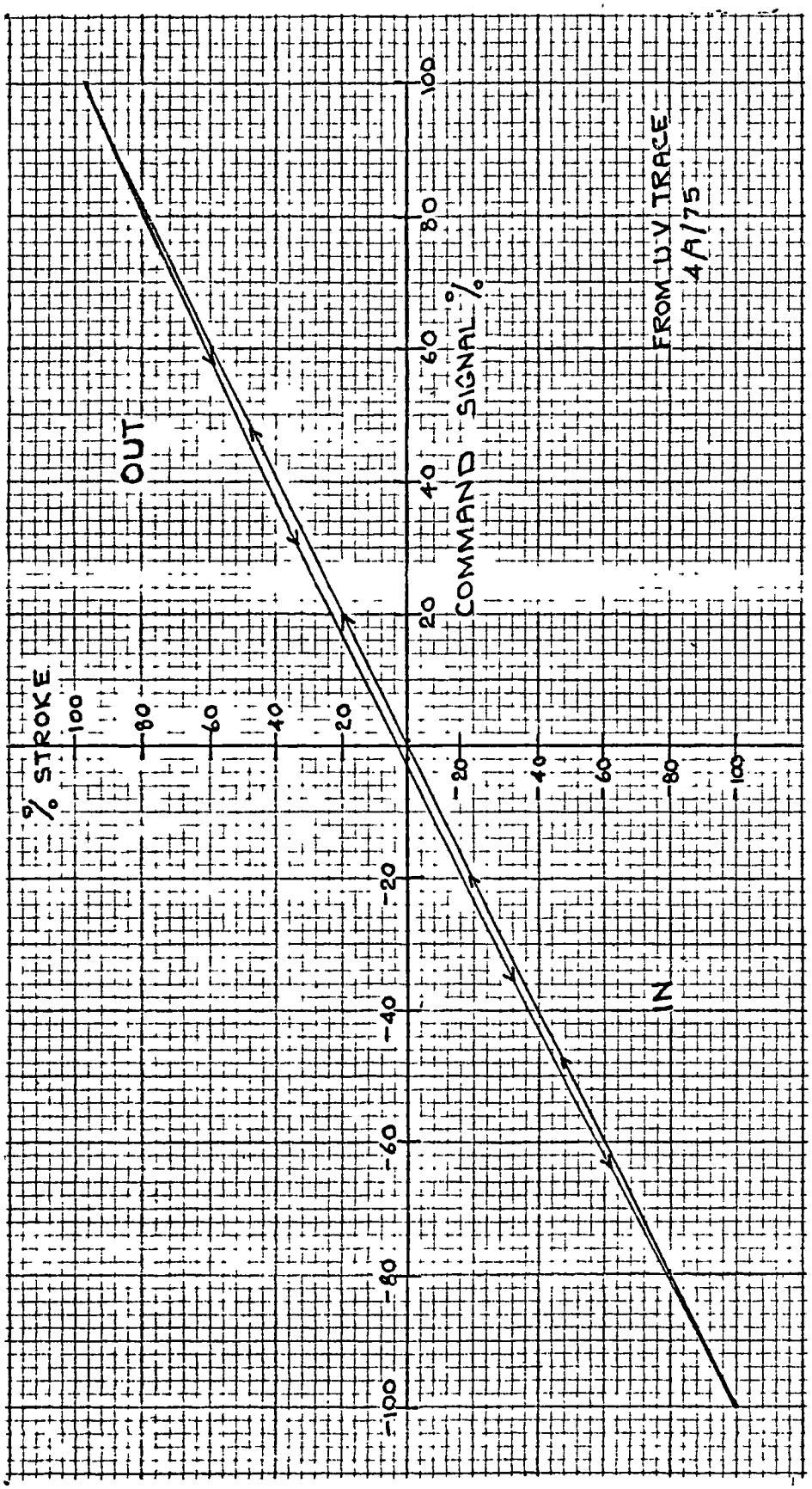

FIG. 6.15 SWASHPLATE DISPLACEMENT CURVE FOR HD 900 PUMP AT 2000 REV/MIN, AT 137 bar WORKING PRESSURE

CHAPTER 7. DESIGN METHOD FOR AXIAL PISTON PUMPS

7.1 Various theoretical aspects of axial piston pump design were developed in Chapter 5. In this chapter a design procedure is outlined. It should be mentioned that design is often regarded as an art combining a broad appreciation of various physical concepts with economic, social and other constraints by the use of intuition and engineering judgment. Here the aim is to put the design of the axial piston pump on a scientific basis, as far as it is practical so to do.

In general, the design process may be divided into two main areas; namely -

(i) conceptual design;
(ii) geometric and functional design.

The conceptual design normally deals with the creation of ideas and the defining of criteria to satisfy the design requirements. As far as the axial piston pump is concerned, these criteria would be based on such design aspects as the drive, mounting requirements, space and weight limitations, installation and maintainability, economic life, prime cost, safety and noise. The geometric design, on the other hand, invariably entails force, movement, strength, rigidity and performance analysis. With these thoughts in mind a logical design method has been developed and the design procedure is shown in Fig.7.1, which serves to identify the various considerations and activities involved.

7.1.1 Design Specification

It is important that the design specification is clear and comprehensive and that it gives all the information necessary for the successful design of the pump. The information it should include can be grouped as:-

(i) non-analytical;
(ii) analytical.

The non-analytical contents would include the size, weight and cost constraints to be adhered to, the method of

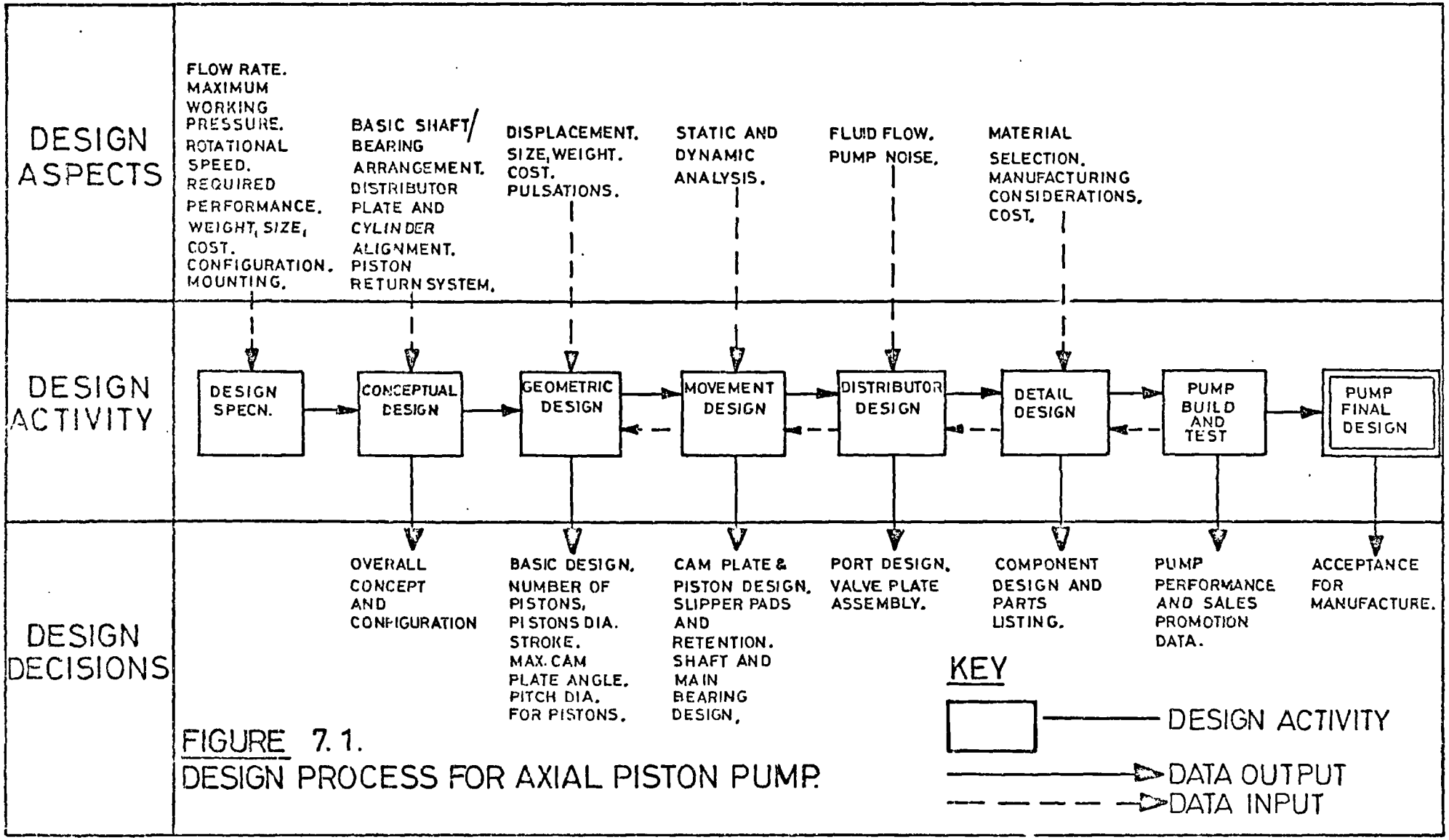

FIGURE 7.1.
DESIGN PROCESS FOR AXIAL PISTON PUMP.

coupling and mounting the pump and an indication of the reliability and service life to be aimed at. Of necessity the intended environment for the pump would be specified and also the acceptable level of pump noise.

The analytical part of the pump specification would include the required performance in terms of flow rate, working pressures, pump speeds and efficiency levels. These would be related to the types of hydraulic fluids to be used together with the viscosity ranges to be accommodated. In addition, the specification would include details of the methods and levels of control to be included in the pump design.

7.1.2 Conceptual Design

The conceptual design will involve consideration of the working principles of the pump and how these can best be integrated into a unit design. The problems involved are many and in few instances do 'best solutions' readily present themselves. Bearing in mind the interrelationship of these problems, the basis for the conceptual design can best be undertaken by considering specific functions within the pump and the relative merits of some possible solutions.

Shaft and Bearing Arrangements

The prime function of the shaft and bearings is to enable the cylinder to be rotated at the required pump speed, in the correct position and with minimum loss of mechanical power. It is also required that the shaft should have the strength and stiffness to carry out this function and that the bearings have an expected service life at least equal to that specified in the design specification.

The shaft presents few problems if a decision is made at this stage on the stiffness required. The problem arises from the asymmetrical loading of the cylinder block against the valve plate because of the grouping of pressurised and unpressurised cylinder bores. This can

result in high leakage losses and also high rubbing contact. Thus the shaft can be designed to have the stiffness necessary to counteract this loading or to have a low stiffness to allow some degree of freedom to the contacting parts to align to one another.

Of necessity the shaft must have the strength to transmit the input torque from the prime mover to the cylinder block but the stiffness of the shaft which gives the desired constraint to the cylinder block will be influenced by the section of the shaft, the distance between the supporting bearings and to some extent by the type of bearings used. These considerations are dealt with in the section on pump shaft design later in this chapter.

By design the axial loads on the bearings can be relatively low with the swash plate and the valve plate loads being reacted into the pump body, but axial location is necessary so that one of the bearings is likely to have an end thrust loading. Rolling element bearings are ideal for the speeds encountered in axial piston pumps because of the low frictional losses, high load capacity and predictable service life. The choice of bearings would be between deep groove ball, plain roller, needle roller, taper roller or self aligning ball or roller bearings.

For moderate speed pumps the practice of supporting the cylinder block in a large roller bearing on the outside of the cylinder block may be considered. With this design a low stiffness shaft is possible and the cylinder is able to align itself with a minimum of constraint at the valve plate interface. Fig.7.2, shows a design incorporating a very stiff shaft with fairly rigid rolling element bearings, whilst Fig.7.3, shows the use of a low stiffness shaft and the cylinder running in a large roller bearing.

Valve Plate and Cylinder Face Alignment

Here the problem is to transfer hydraulic fluid from the inlet port to the cylinder block and from the cylinder block to the outlet port with a minimum of fluid leakage and frictional losses at the valve plate/cylinder block interface.

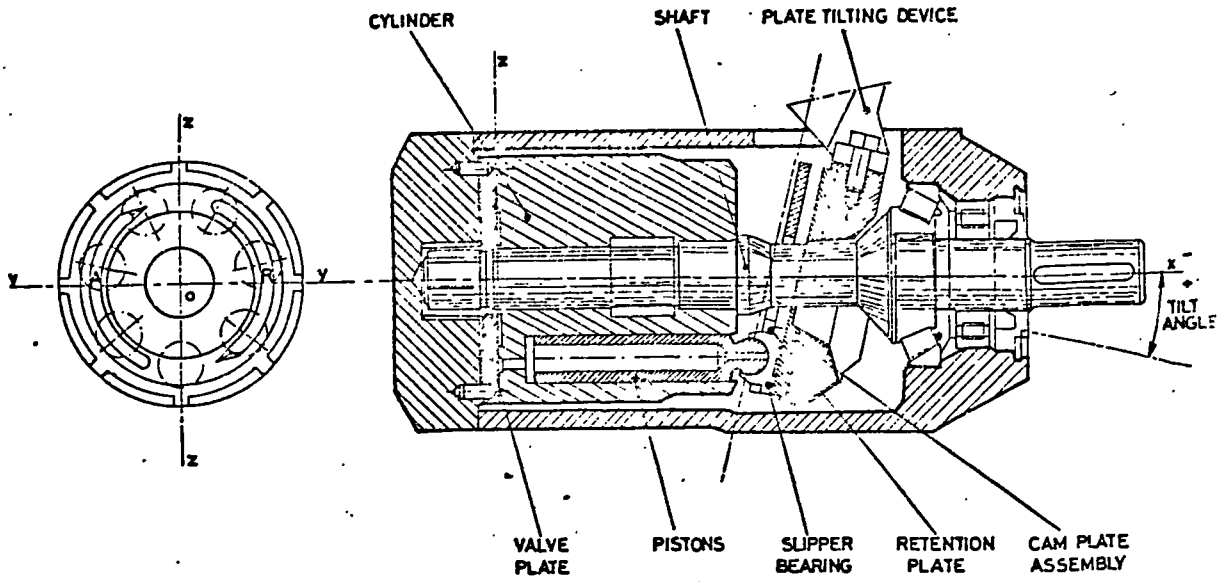

FIGURE 7.2. AXIAL PISTON PUMP DESIGN TO UTILISE A 'STIFF' SHAFT

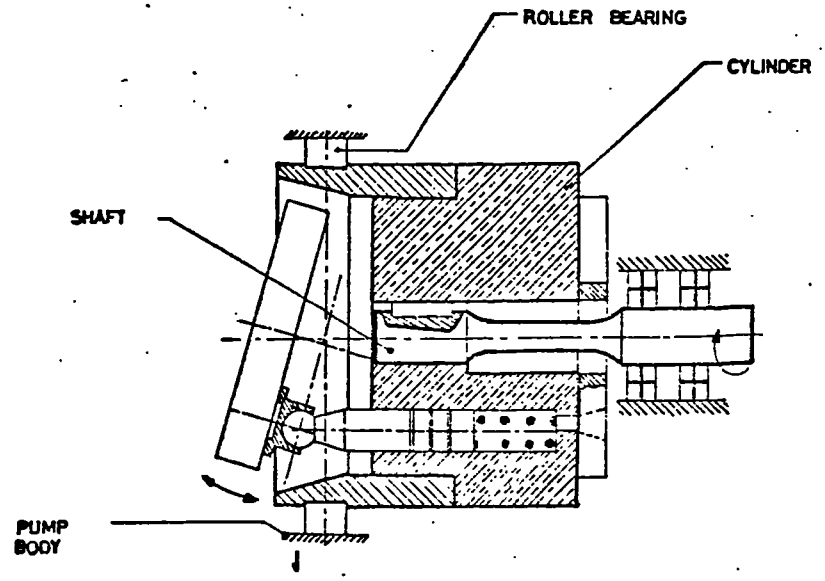

FIGURE 7.3. AXIAL PISTON PUMP DESIGNED TO UTILISE A 'FLEXIBLE' SHAFT

Ideally the design should be such that either the cylinder or the valve plate is in a state of partial suspension so that the small adjusting forces ensure that the contacting surfaces are always loaded against one another to the required degree. Since the surfaces will be hydrostatically balanced, some leakage will occur and this will be dependent on the geometry of the sealing lips. A decrease in the length of the periphery of the lips will be of particular value in reducing the leakage loss.

To illustrate the difficulties that arise and how possible improvements in design may be made, four solutions are described. Fig.7.4, shows an arrangement in which the cylinder block is mounted on the shaft with a minimum of constraint for transverse movement and with the drive from the shaft well away from the cylinder block/valve plate interface. Whilst allowing the surfaces to come into contact, the asymmetric loading tends to increase the gap on the inlet kidney port side and cause excessive leakage. The kidney ports are on much the same pitch circle as the pistons and this tends to make the periphery of the sealing lips considerable. It is also likely that the kidney ports would need to be narrow to provide space for the hydrostatic balancing grooves.

Fig.7.5, shows a somewhat similar design in which the relatively unconstrained cylinder seats onto a spherical valve plate and the pitch radius of the kidney ports is reduced. By design the various external forces on the cylinder block can meet at a point and result in a close contacting condition between the cylinder block and the valve plate. The advantages are appreciable and include the possibility of larger kidney ports. However, the manufacturing difficulties in matching the two spherical surfaces are a distinct disadvantage.

Fig.7.6, shows a design employing hydrostatic balancing of the surfaces. The cylinder block and the valve plate are located between spherical bearings with a fluid feed from the high pressure port loading the surfaces together. This method has much in its favour but the manufacturing problems of the

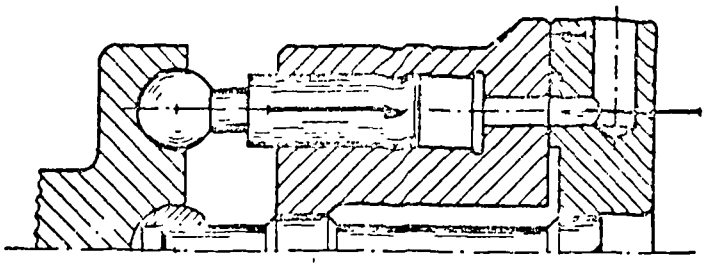

FIGURE 7.4 SUSPENSION OF THE CYLINDER BLOCK WITH KIDNEY PORTS ON THE PITCH RADIUS OF THE CYLINDER.

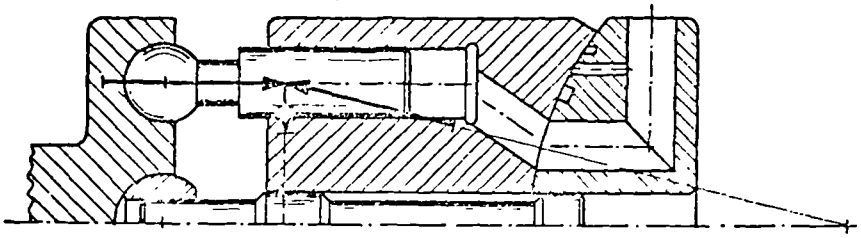

FIGURE 7.5. SUSPENSION OF THE CYLINDER BLOCK WITH KIDNEY PORTS ON REDUCED PITCH RADIUS AND SPHERICAL VALVE FACES FOR COMPENSATION OF THE TILTING MOMENT.

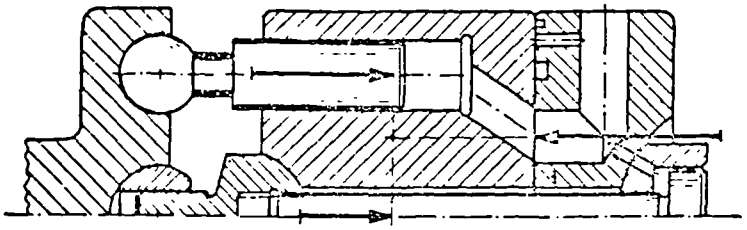

FIGURE 7.6. SUSPENSION OF THE CYLINDER BLOCK WITH KIDNEY PORTS ON REDUCED PITCH RADIUS AND WITH EXPANSION CYLINDER ON THE AXIS.

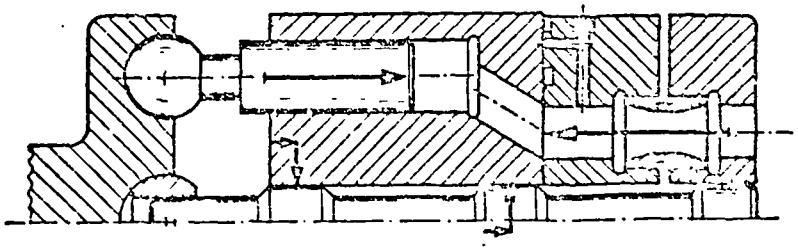

FIGURE 7.7. CYLINDER BLOCK RIGIDLY SUSPENDED ON CENTRAL SPINDLE WITH KIDNEY PORTS ON REDUCED PITCH RADIUS AND WITH FLOATING DISTRIBUTOR.

spherical surfaces should not be underestimated. It is also necessary to feed the balancing piston via non-return valves for a bi-directional pump.

Fig.7.7, shows a rigidly supported cylinder but with a relatively unconstrained valve plate loaded against the cylinder block by hydraulic pressure behind the valve plate. This method presents few manufacturing difficulties and successful designs have been achieved using two sleeves per kidney port.

Methods of Returning Pistons on the Suction Stroke

The return of a piston on the suction stroke presents a number of difficulties and these are increased as the speed of the pump is increased. Although basically the forces are of a low order; particularly if a positive suction head is assured, the space demands of the slipper bearing pad allows very little provision for exerting the necessary return force to the piston. Common practice is for the piston to have a spherical ball end joint with the slipper bearing and the swaging of the skirt of the slipper bearing over the ball of the piston provides adequate strength for the return force. The main difficulty arises in providing adequate bearing contact for the return force having in mind the ellipsoidal loci for the slipper motion.

Various designs are shown in Fig.7.8, Method (a) shows the fitting of a compression spring inside a hollow piston. The spring has to maintain the slipper bearing in contact with the swash plate and in so doing exert a force which is in excess of the acceleration force for the piston/slipper bearing assembly, the viscous and frictional drag on the piston and the force on the piston to draw fluid into the pump. Fortunately when the sum of these forces is at a maximum at the commencement of the suction stroke, the spring is in its maximum compression and is exerting a maximum spring force.

By choosing a spring rate such that at the maximum assembled length the spring force is just in excess of the viscous and frictional drag and the piston force to draw in

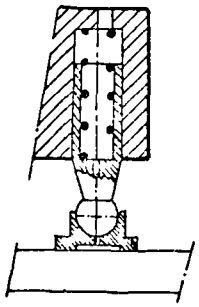

a. PISTON RETURN BY COMPRESSION SPRING INSIDE HOLLOW PISTON

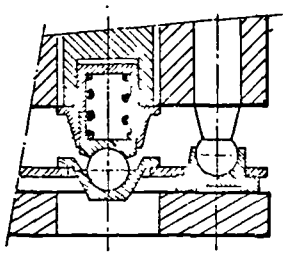

b. PISTON RETURN BY CENTRAL COMPRESSION SPRING

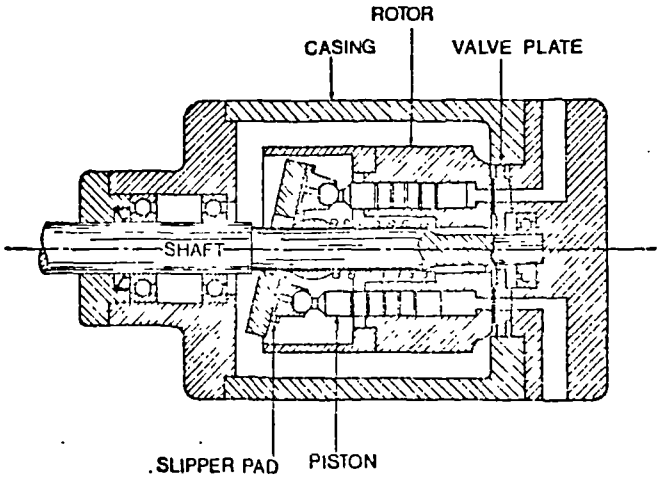

c. PISTON RETURN BY SPRING LOADED SPHERICAL BEARING ON PUMP SHAFT.

FIGURE 7.8. METHODS OF RETURNING PISTON.

the fluid but less than the acceleration force on the piston/slipper bearing assembly, a near optimum condition may be achieved. It will be appreciated that the forces involved are mainly velocity dependent and in theory different springs should be used for differing pump speeds. It is customary to choose a spring rate such that at the maximum assembled length the spring force is one third of the spring force at the minimum assembled spring length. Richmond (18) has presented very comprehensive data and recommendations for the design of piston return springs.

An appreciable disadvantage of this type of piston return is that during the pumping stroke the spring opposes the piston movement and induces an additional resisting torque on the pump shaft. This represents a small power loss which is not present when other piston return methods are used. At the design stage special care is necessary to prevent the coils of the spring being trapped due to lateral instability and the centrifugal forces on the spring.

An alternative design, Fig.7.8(b), employs a heavy duty spring mounted in an assembly fixed to the pump shaft to exert a force onto a steel ball which in turn transfers the thrust through a spherical cap to a piston return plate. The advantages of simplicity and compactness will be very apparent and since the spring is working at near constant length (and loading), a high degree of reliability can be expected. The diagram in Fig.7.8(c), shows a rather similar concept except that a bronze spherical bearing mounted directly onto the pump shaft and loaded by a single compression spring is used in conjunction with a spherical seating in the piston return plate. A high degree of geometrical conformity is achieved and again this method has the advantages of simplicity and reliability.

The Method described in Fig.7.8(d), involves the use of a central location for the piston return plate. In effect a constant clearance regulates the end play of the slipper bearing. Although simple in concept, this method involves some compromise in design since the end play contributes to lost motion and has a small influence on the volumetric displacement of the pump.

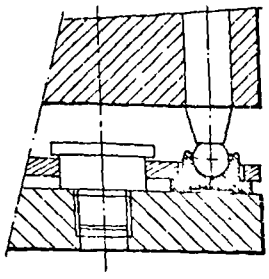

d. PISTON RETURN BY FIXED CENTRAL LOCATION

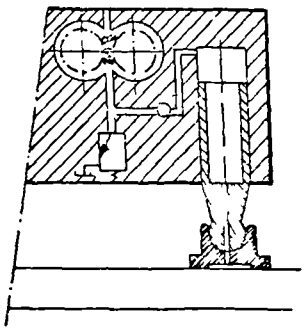

e. PISTON RETURN BY USE OF AUXILLIARY BOOST PUMP

FIGURE 7. 8 (CONT.) METHODS OF RETURNING PISTON.

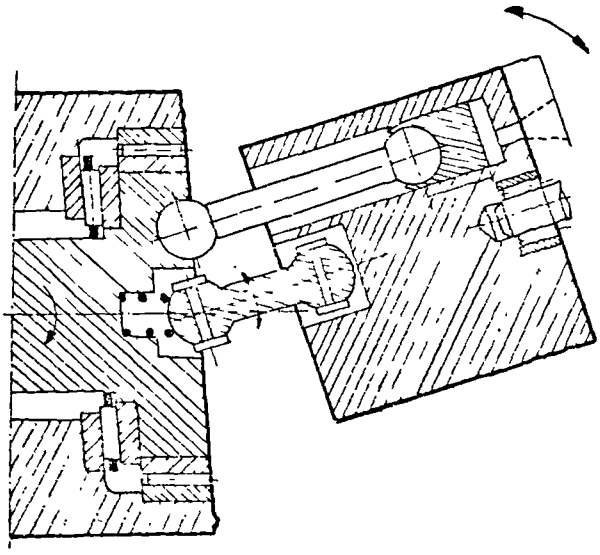

FIGURE 7. 9. TRANSFERENCE OF THRUST FROM PISTON TO SWASHPLATE VIA HOOK'S COUPLINGS.

The Method of Fig.7.8(e), involves the use of an auxiliary boost pump to pressurise the suction line. Whilst this is a feasible proposition and the use of boost pumps for high performance systems is common, the provision of a pump for the sole purpose of returning the pistons would be both expensive and complicated.

Methods of Transferring Thrust from the Swashplate onto the Pistons

Fig.7.2, shows a common method of transferring the thrust from the tilted swashplate to the pistons via a slipper bearing. The working conditions at the slipper bearing/swashplate interface are near ideal since by good design and manufacture, virtually all metal to metal contact can be eliminated by the hydrostatic pad. The thrust to be transmitted is dependent mainly on the pump pressure and the high stiffness characteristic of a hydrostatic bearing pad, ideally caters for changes of pump pressure. However the angle of inclination of the swashplate, the speed of rotation and the mass of the moving parts all affect the level of the thrust.

The second interface between the slipper bearing and the spherical end of the piston presents few design problems. Oscillatory speeds are low compared to the linear speeds between the slipper bearing and the swashplate and a high level of lubrication is obtained by allowing hydraulic fluid to pass into the bearing zone through a bleed line from the pressure side of the piston. However the complete assembly is relatively expensive and warrants consideration of alternative designs. A further disadvantage is that the radial forces on the piston which are reacted into the pump cylinder liner become excessive if the swashplate angle of tilt is in excess of 20°. As a result a restraint is imposed on the piston stroke possible for a particular pitch circle diameter and this generally limits the ratio of stroke to piston diameter to 1.0 or less.

A means of overcoming this constraint is to use an adaption of a Hooke's Coupling for each piston as shown in Fig.7.9. Whilst allowing for tilt angles of as high as 30°

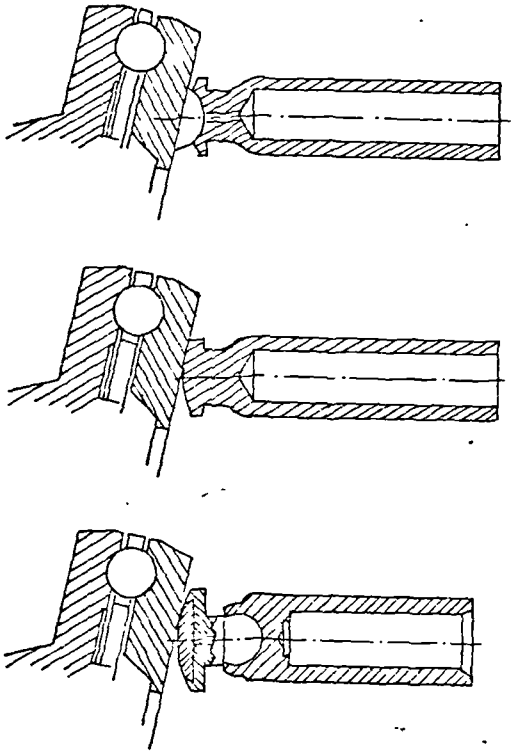

FIGURE 7.10. TRANSFERENCE OF THRUST FROM PISTON TO SWASHPLATE USING ROLLER BEARINGS.

and the use of reasonable piston lengths, considerable difficulty is experienced in designing the couplings to transmit the torque necessary to rotate the swashplate. Because of this a main drive universal coupling is commonly incorporated.

Another method of reducing the sliding motion between the piston assembly and the swashplate is to design for the contact surface of the swashplate to revolve at the pump speed. Fig.7.10, shows three possible arrangements based on the use of a rolling bearing in the swashplate assembly. In general these methods are suitable for low speed, low power pumps where the requirements of size are not so stringent as in high speed, high power pumps. The frictional losses in the rolling bearing are low and the volumetric efficiency is improved by the absence of bleed to a hydrostatic bearing pad as in the case of the pump with slipper bearings.

With the foregoing sections in mind the overall conceptual design of the pump can be arrived at which would form the basis for the geometric or functional design.

7.1.3 Geometric Design

The geometric design of an axial piston pump involves the use of primary design information contained in the design specification. Given the flow rate required at a given pump speed and against a maximum working pressure, the basic pump dimensions can be arrived at. However, it will be important at this stage to consider what effect these dimensions have on other considerations such as size, weight and cost of the pump, the overall pump efficiency and the level of flow pulsations to be expected from the pump.

The basic pump equations are -

$$q = \frac{Q}{n} \tag{7.1}$$

$$q = \frac{\pi}{4} d_p^2 S N_p \tag{7.2}$$

$$D = \frac{\left(1 + \frac{P}{\sigma}\right) d_p}{\sin\left(\frac{180}{N_p}\right)} \qquad (7.3)$$

$$D = S \cot\phi \qquad (7.4)$$

Equation (7.1) is a straightforward relationship between the displacement q, the volumetric flow per revolution of the pump, the flow rate Q and the rotational speed n, and a unique value for q is obtained. Equation (7.2) relates the displacement q with the piston stroke S, the diameter of the pistons d_p and the number of pistons in the pump N_p. A solution requires -

a) a decision on the number of pistons to be used;
b) a relationship to be established between d_p and S.

The number of pistons to be used will influence the flow pulsations to be expected, the size of the pump and the cost of manufacture. These are considered in turn in the following.

Relationship between Number of Pistons and Flow Pulsations

One of the characteristics of an axial piston pump is the cyclic variation of flow rate due to the action of the valves. Although the intensity of the variations may be reduced by increasing the number of pistons in the pump, some fluctuation always remains as a flow ripple or pulsation. The value of this fluctuation is conveniently given as -

$$\frac{Q_{MAX} - Q_{MIN}}{Q_{MAX}} \%$$

Neglecting the very small leakage variations which are dependent on the piston velocity and the length of

piston in the cylinder bore, the rate of flow of a single piston is equal to the area of the piston times the instantaneous piston velocity.

Thus $$Q_{INST} = \frac{\pi}{4} d_p^2 V_p$$

The instantaneous piston velocity is proportional to the piston position which in turn is a function of the rotational position of the pump shaft. This relationship is simple harmonic and can be expressed as -

$$V_p = S \sin \omega t$$

Thus

$$Q_{INST} = \frac{\pi}{4} d_p^2 S \sin \omega t$$

and reaches a maximum value at $\omega t = \frac{\pi}{2}; \frac{3}{2}\pi; \frac{5}{2}\pi$ etc.

Fig.7.11, shows the relationship for a single piston pump. To indicate the flow variation which occurs in multipiston pumps it is convenient to use phasor representation. Fig.7.12, shows this for a single piston pump and Fig.7.13, the maximum and minimum flow rates for a pump having five pistons. Phasor polygons can be constructed for any number of pistons and the maximum and minimum flow rates measured.

The percentage flow variation can be obtained from -

$$\frac{Q_{MAX} - Q_{MIN}}{Q_{MAX}} = 1 - \cos \frac{\pi}{2N_p} \quad \text{for odd numbers of pistons}$$

$$= 1 - \cos \frac{\pi}{N_p} \quad \text{for even numbers of pistons}$$

Fig.7.14, shows that the flow variation for a pump of an odd number of pistons is the same as that for a pump having twice as many pistons. For this reason most axial piston pumps incorporate odd numbers of pistons, usually 7 for Bent Axis and 7 or 9 for Swash Plate Pumps.

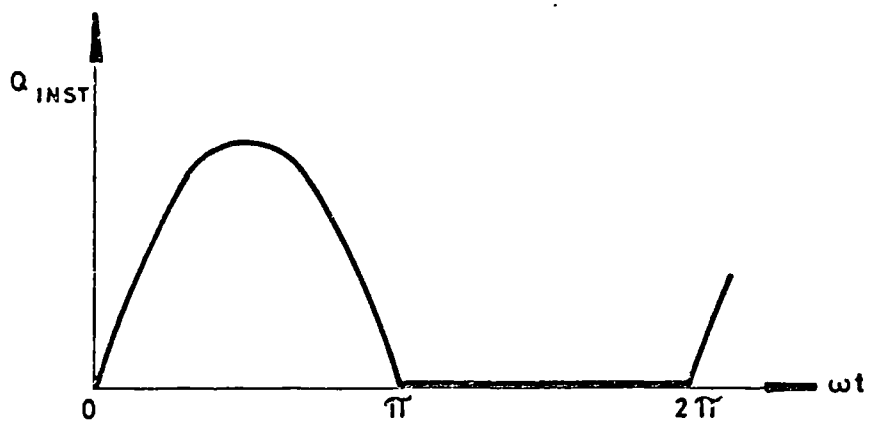

FIGURE 7.11. INSTANTANEOUS DELIVERY OF A SINGLE PISTON AS A FUNCTION OF THE PUMP SHAFT ANGLE.

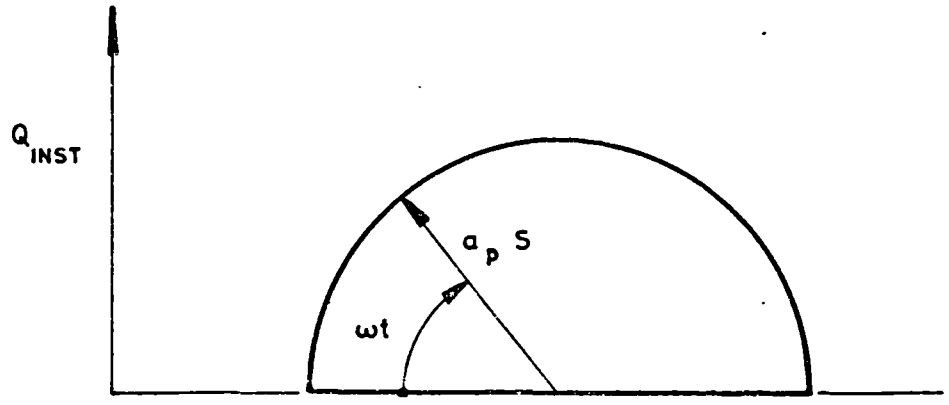

FIGURE 7.12. PHASOR REPRESENTATION OF THE INSTENTANEOUS DELIVERY OF A SINGLE PISTON.

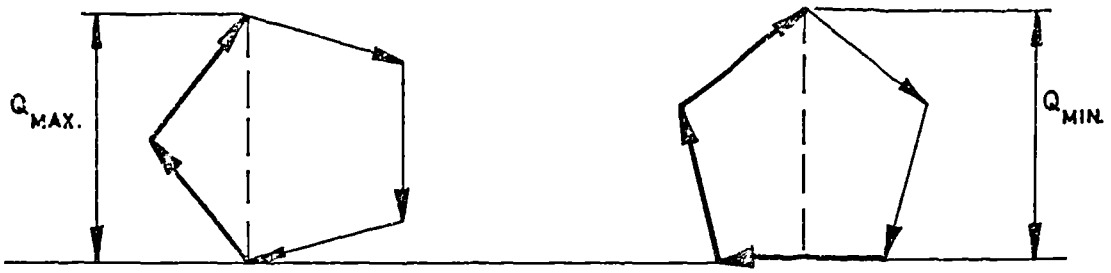

FIGURE 7.13. PHASOR POLYGON FOR A FIVE PISTON PUMP.

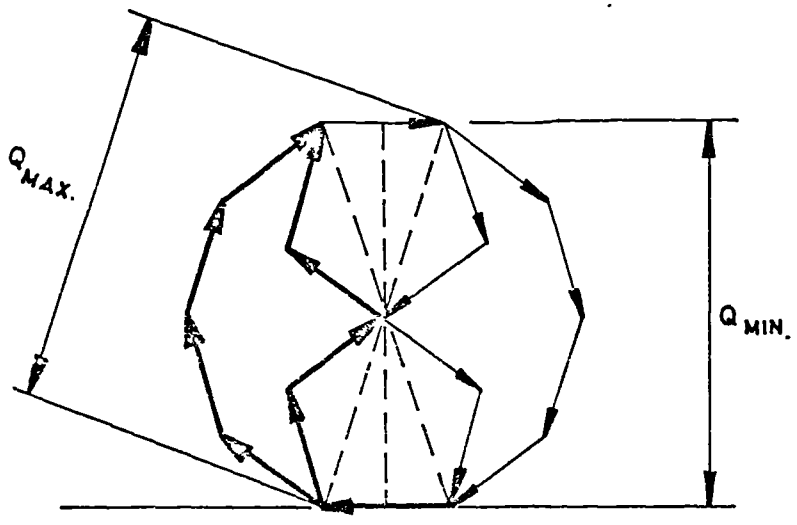

FIGURE 7.14. PHASOR POLYGON FOR A PUMP WITH AN ODD NUMBER OF PISTONS AND FOR A PUMP WITH TWICE NUMBER OF PISTONS.

Table 7.1: Percentage Flow Variation of Multipiston Machines

N_p	1	2	3	4	5	6	7	8	9	10	11
$\frac{Q_{max} - Q_{min}}{Q_{max}}$ %	100		13.4		4.9		2.5		1.5		1.0
		100		29.3		13.5		7.6		4.9	

It is not easy to estimate the effect on the size and the cost of the pump for differing numbers of pistons but in general as the number of pistons is increased, the size of the pump and its manufacturing costs will also increase.

Relationship between Piston Diameter and Stroke

The relationship between the piston diameter and the stroke is complex. Having decided on the number of pistons to employ, the piston diameter and stroke must satisfy equation (7.2). Common practice is to use a ratio $\frac{S}{dp}$ of 0.8 to 1.2. In general if the stroke is kept low the piston velocity and acceleration for a given rotational speed will be correspondingly low and this would mean lower viscous friction losses, lower piston and slipper bearing inertia forces and in all probability a reduction in the wear of the cylinder bores. Cost effects would be minimal but a low length of stroke would somewhat reduce the length of the pump whilst because of the larger piston diameters required, would slightly increase the cross section of the pump.

Relationships between Piston Diameter, Number of Pistons, Pump Pressure and Pitch Circle Diameter of Cylinder Bores

These relationships are expressed in equation (7.3). It will be seen that the P.C.Dia increases as the piston diameter, number of pistons, and pressure is increased but is reduced as the tensile strength of the cylinder block material is increased.

The main design aspects involved are:-

a small pitch circle diameter could result in -

a) insufficient strength between adjacent bores to resist the stresses set up by the fluid pressure;

b) insufficient space for the satisfactory design of the hydrostatic slipper bearings;

c) inadequate length of sealing face lands on the valve distributor plate;

d) impossible to obtain the required stroke without using an excessive swash plate angle. Ref. equation (7.4).

a large pitch circle diameter would result in -

e) increased pump size, weight, rotational inertia and manufacturing costs;

f) increased velocity and therefore increased viscous losses at the slipper bearing/swash plate interface.

The relationships between d_p, N_p, P and σ for a given allowable tensile stress of $180MN/m^2$ are given in Fig.7.15. Fig.7.16, shows the correction factors which would apply for other allowable stress levels.

Relationship Between the Pitch Circle Diameter, the Stroke and the Angle of Tilt of the Swashplate

This relationship is given by equation (7.4). A limiting consideration is that if the angle of tilt exceeds 20°, the radial component of the slipper bearing reaction tends to become excessive and the disturbing couple on the slipper bearing, which is not taken care of by the hydrostatic pad, also becomes a real problem. For these reasons the angle of tilt is usually limited to the range between 15° to 20°.

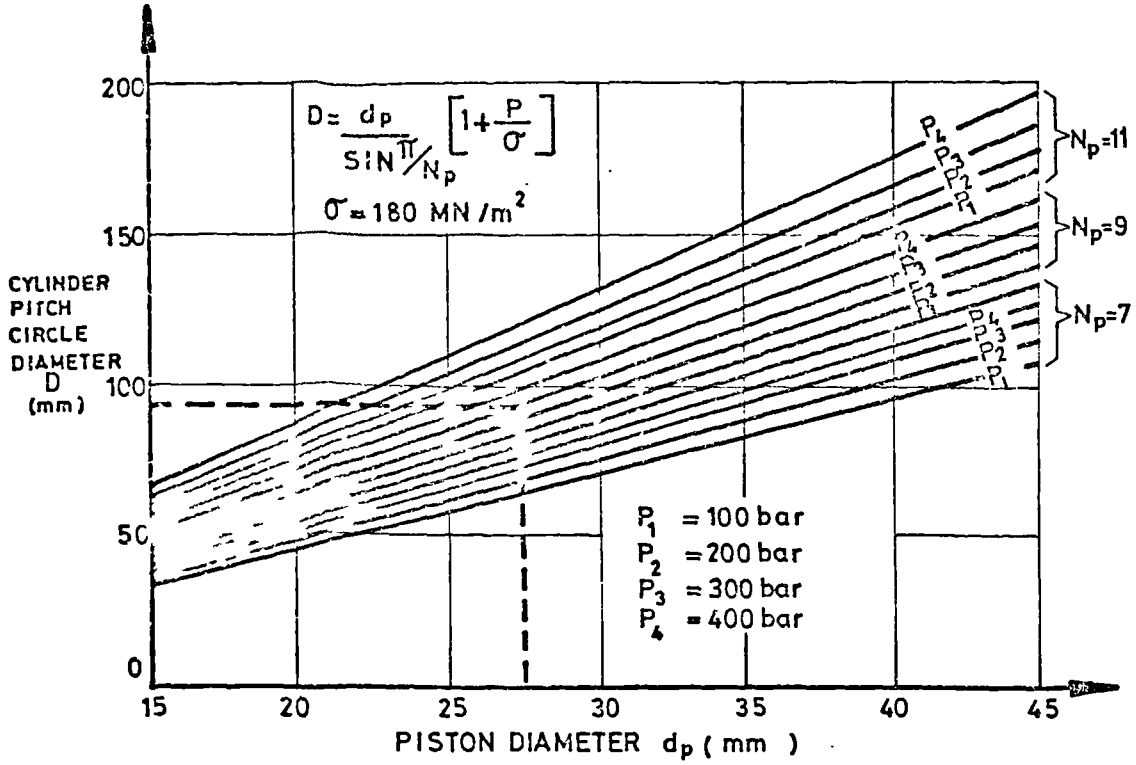

FIGURE 7.15. RELATIONSHIP OF CYLINDER PITCH CIRCLE DIAMETER WITH PISTON DIAMETER. NUMBER OF PISTONS. PUMP PRESSURE AND ALLOWABLE TENSILE STRESS OF CYLINDER MATERIAL.

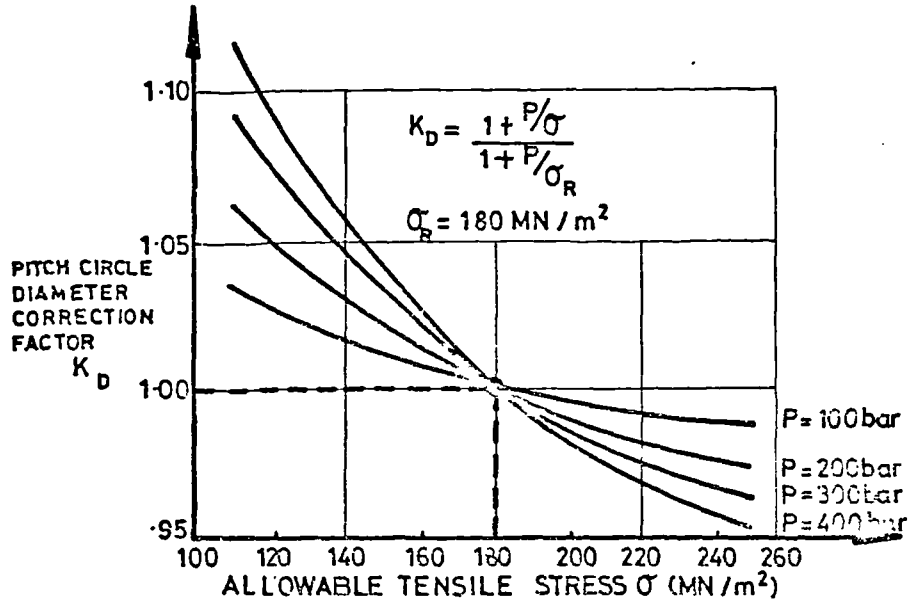

FIGURE 7.16 CORRECTION FACTOR FOR CYLINDER PITCH CIRCLE DIAMETER FOR VARIOUS ALLOWABLE TENSILE STRESSES OF CYLINDER MATERIAL.

Initial Design Chart

To facilitate the choice of the principal design data, Fig.7.17, has been developed. Knowing the volume flow rate Q, the rotational speed n and the pump pressure P, the chart may be used in the choice of the piston diameter d_p, the stroke S, the number of pistons N_p, the pitch circle diameter D and the swash-plate angle ϕ.

The ranges of values covered by the chart are given below.

q	-	0 to 0.40 x 10^{-3} m^3/rev
P	-	100 to 400 bar
dp	-	15 to 45 mm
S	-	12 to 54 mm
Np	-	7, 9 and 11
D	-	25 to 200 mm
ϕ	-	15^o to 20^o

The procedure to use the chart is as follows. Obtain q from equation (7.1), and from this value on the q scale draw a horizontal line to the right to intersect the curve for a chosen value of Np. From this point of intersection draw a vertical line to intersect a chosen $S/_{dp}$ curve. A horizontal line from this point drawn to the left will intersect a scale to give the corresponding piston diameter d_p. Continue this line to the left until it cuts the curve for the required pump pressure. A vertical line downwards from this intersection will in turn cut a curve for the chosen number of pistons. From this intersection draw a horizontal line to the right to obtain a value for the pitch circle D. Also draw a horizontal line from the appropriate point for stroke S and the angle of tilt ϕ to again cut the vertical scale for D. The largest value of so obtained is the required value.

Since this chart is based on an allowable tensile stress in the cylinder block of 180MN/m^2, if any other value is to be used, the design pitch circle diameter will be that already obtained from the chart based on the piston diameter,

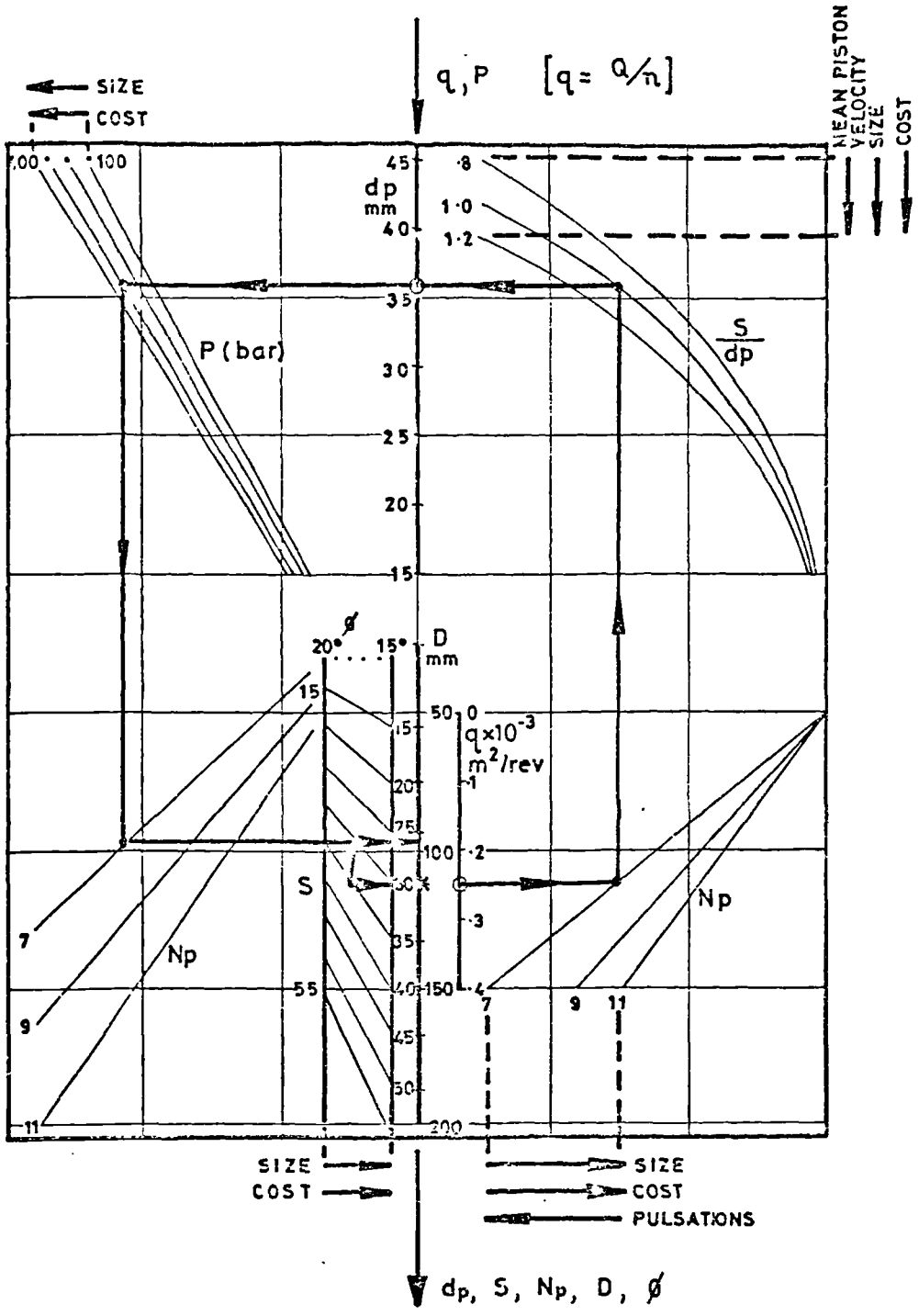

FIGURE 7.17. INITIAL DESIGN CHART FOR AXIAL PISTON PUMPS

the pump pressure and the number of pistons, multiplied by a correction factor K_D from Fig.7.16.

Note that, if the value of D based on the stress considerations exceeds that based on the stroke and the angle of tilt, the angle of tilt should be reduced to correspond.

7.1.4 Movement Design

An important stage in the design process is that of movement design in which an analysis of the operating forces within the pump is used as a basis for designing the moving parts such as the pistons, slipper bearings, swashplate, shaft and main pump bearings. An analysis of the static and dynamic forces, given in Section 5.3.1, makes it possible to calculate the intensity of loading on these components.

To indicate the general intensity and distribution of the forces and reactions in a pump at constant speed but with varying swashplate angles, values were calculated for a high speed pump and plotted as shown in Figs.7.18 to 7.27. The data used in the calculations were:-

Piston Diameter	d_p	= 14 mm
Piston Mass	m_p	= 33 g
Centre of Gravity of Piston	$\bar{x}_p$	= 30 mm
Piston Data Length	X	= 13 mm
Piston Length	ℓ_p	= 43 mm
Slipper Bearing Mass	m_{SB}	= 16 g
Centre of Gravity of Slipper Bearing	$\bar{x}_{SB}$	= 5 mm
Pitch Circle Diameter	D	= 50 mm
Pump Rotation	ω	= 628 rad/s
Absolute Viscosity	μ	= .08 Ns/m^2
Coefficient of Friction	f	= .015
Piston Diametral Clearance	c_d	= .014 mm

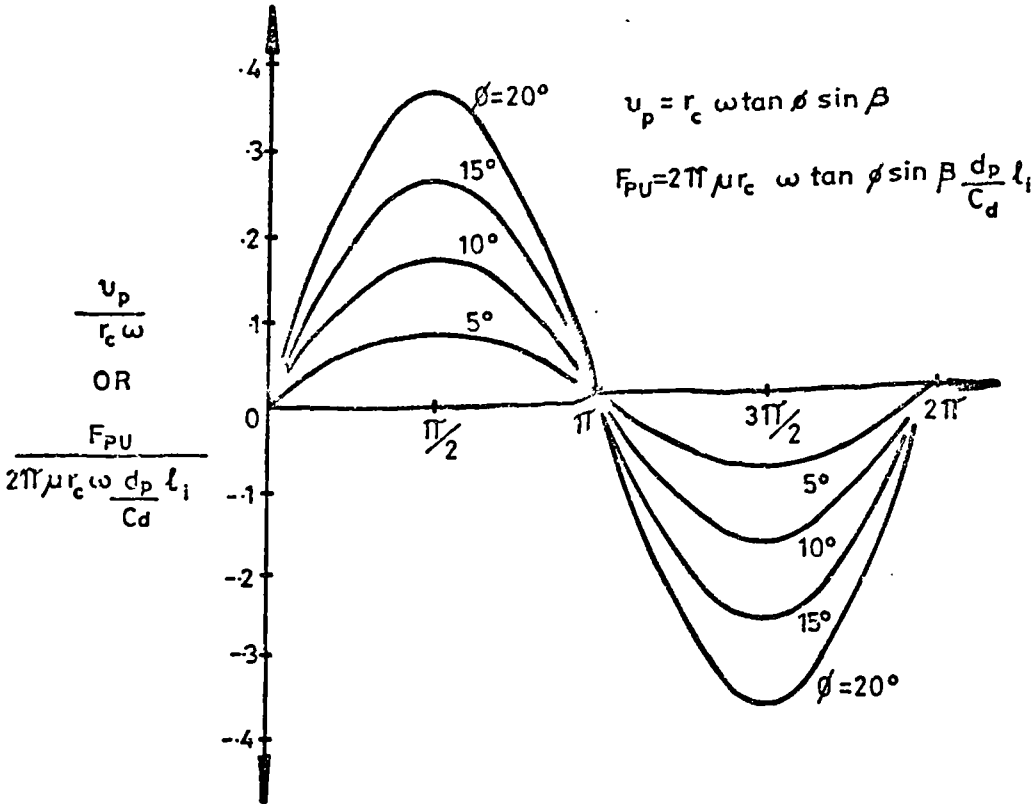

FIGURE .7.18. RELATIVE VALUES OF PISTON VELOCITY AND VISCOUS FORCE ON A PISTON AT VARIOUS TILT ANGLES AND ANGLES OF ROTATION.

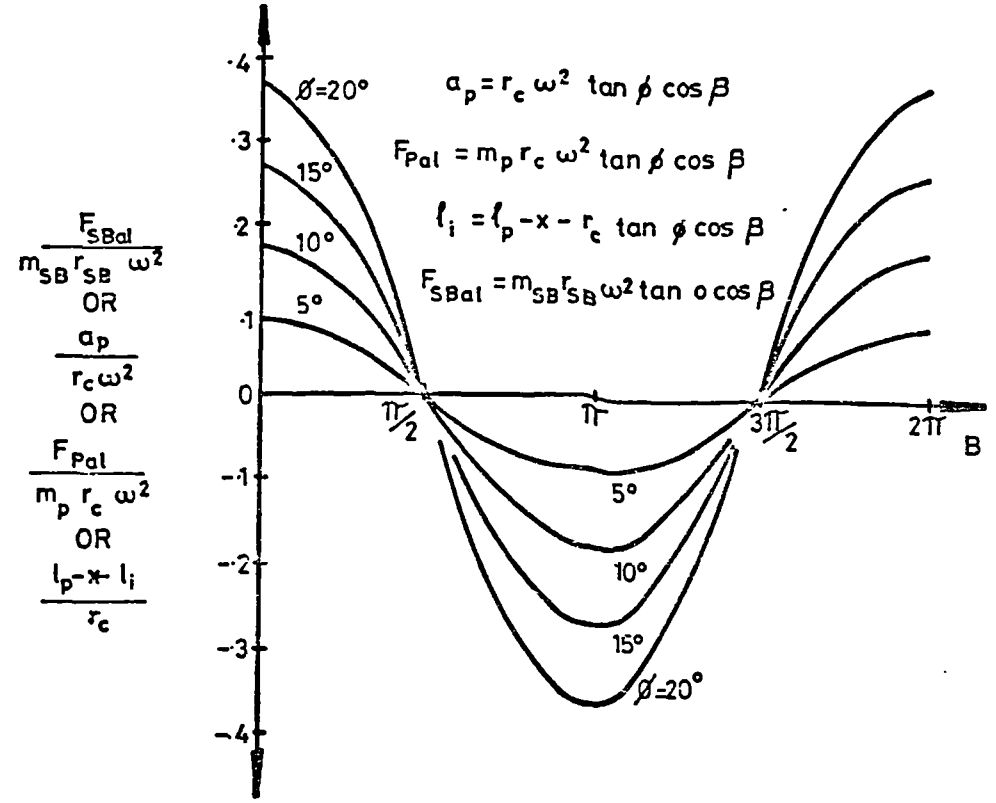

FIGURE 7. 19. RELATIVE VALUES OF PISTON ACCELERATION LENGH OF IMMERSION OF PISTON AXIAL ACCELERATION FORCE ON PISTON AND ON SLIPPER BEARING AT VARIOUS TILT ANGLES AND ANGLES OF ROTATION.

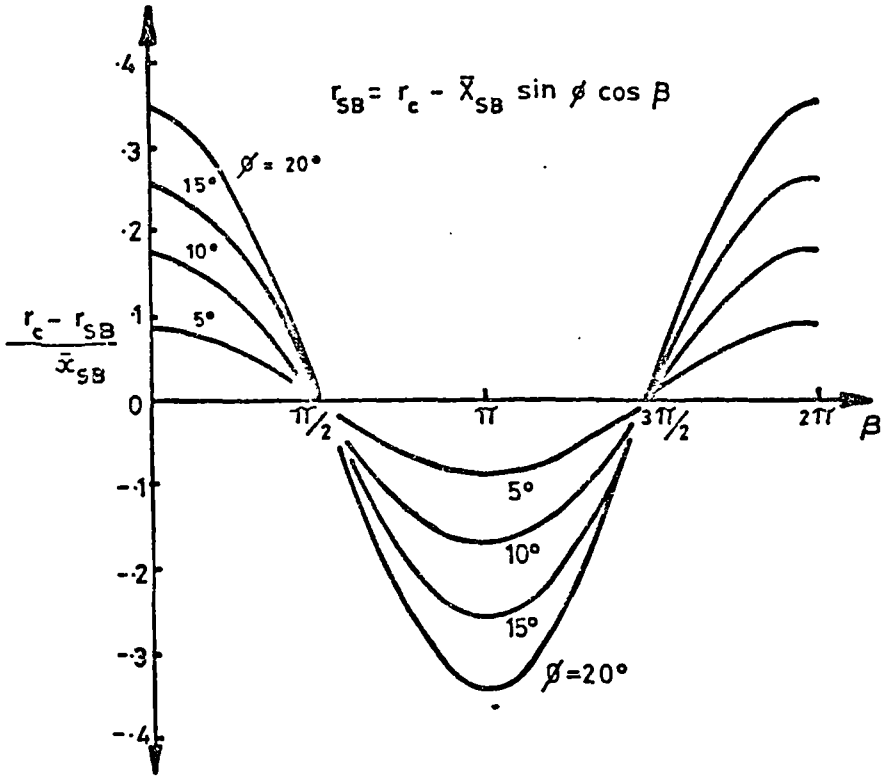

FIGURE 7.20. RELATIVE VALUES OF SLIPPER BEARING RADIUS FOR VARIOUS TILT ANGLES AND ANGLES OF ROTATION.

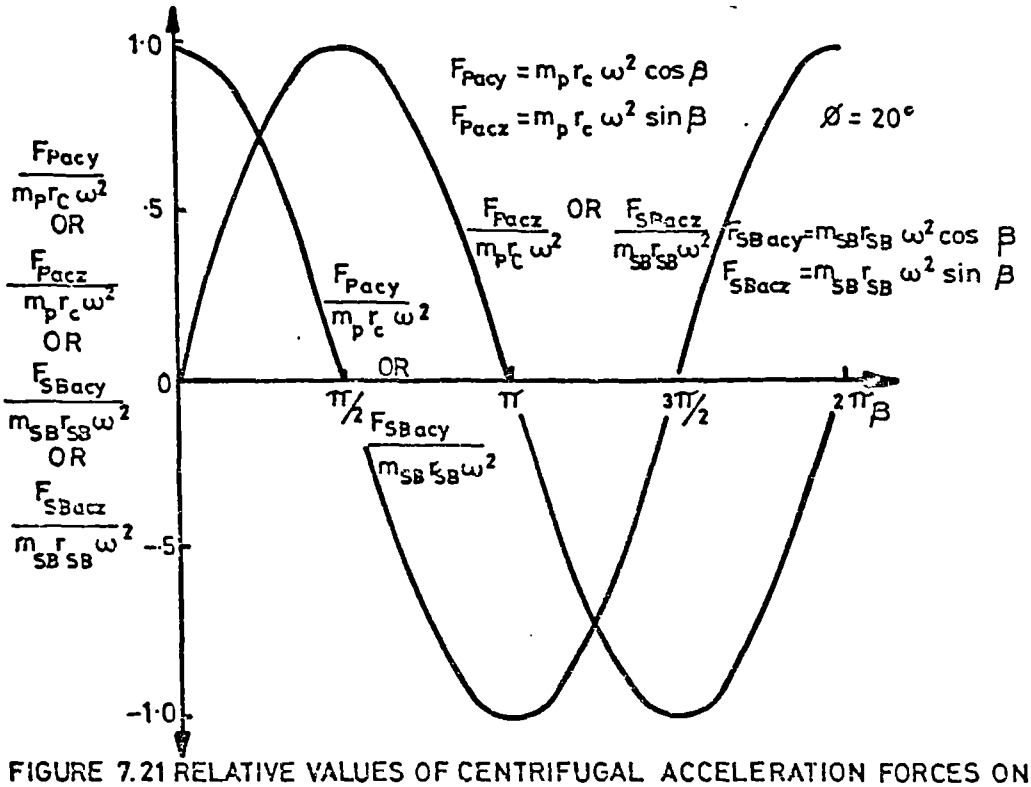

FIGURE 7.21 RELATIVE VALUES OF CENTRIFUGAL ACCELERATION FORCES ON A PISTON AND SLIPPER BEARING AT VARIOUS ANGLES OF ROTATION.

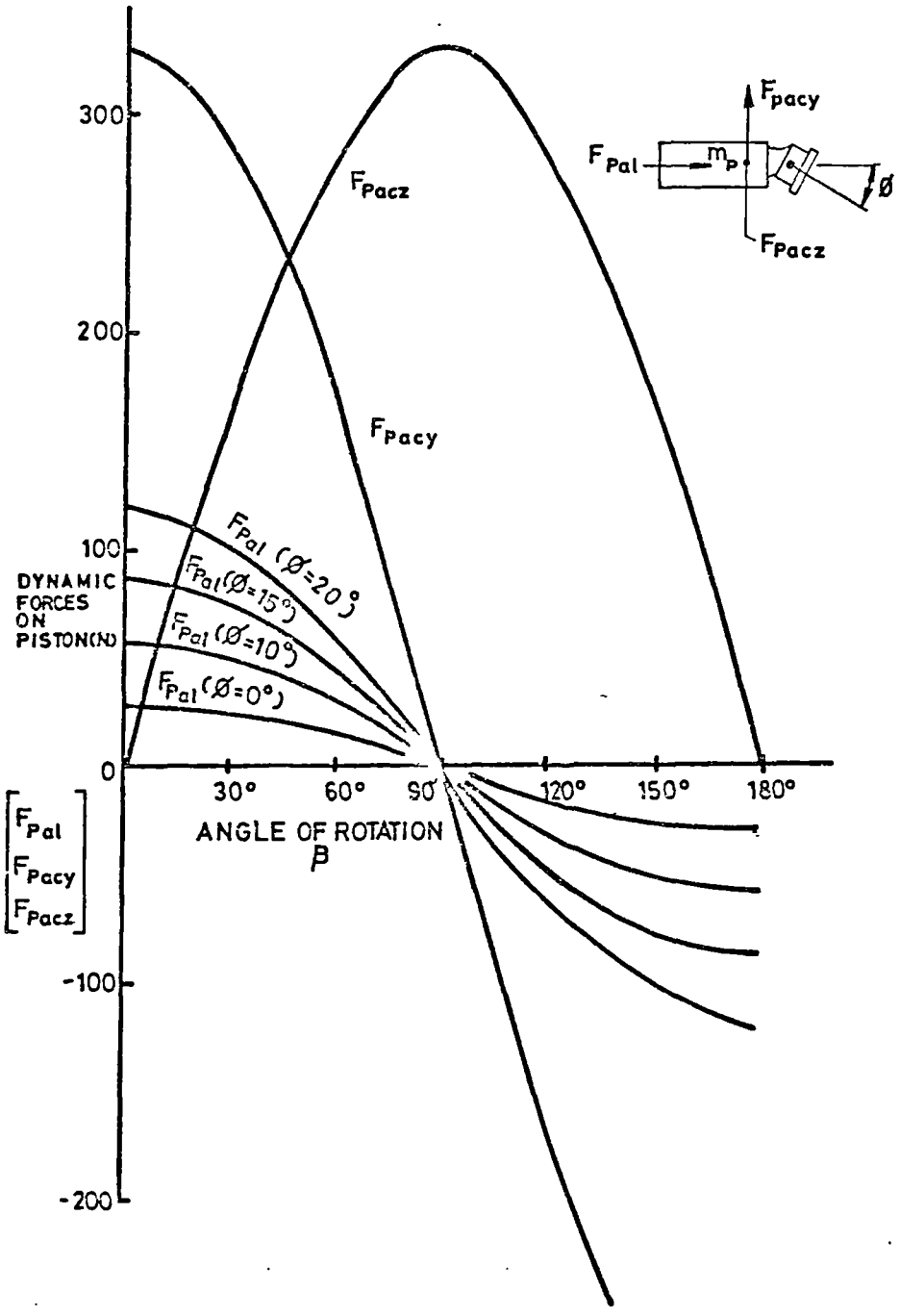

FIGURE 7.22. DYNAMIC FORCES ON A PISTON AT VARIOUS ANGLES OF TILT AND ANGLES OF ROTATION.

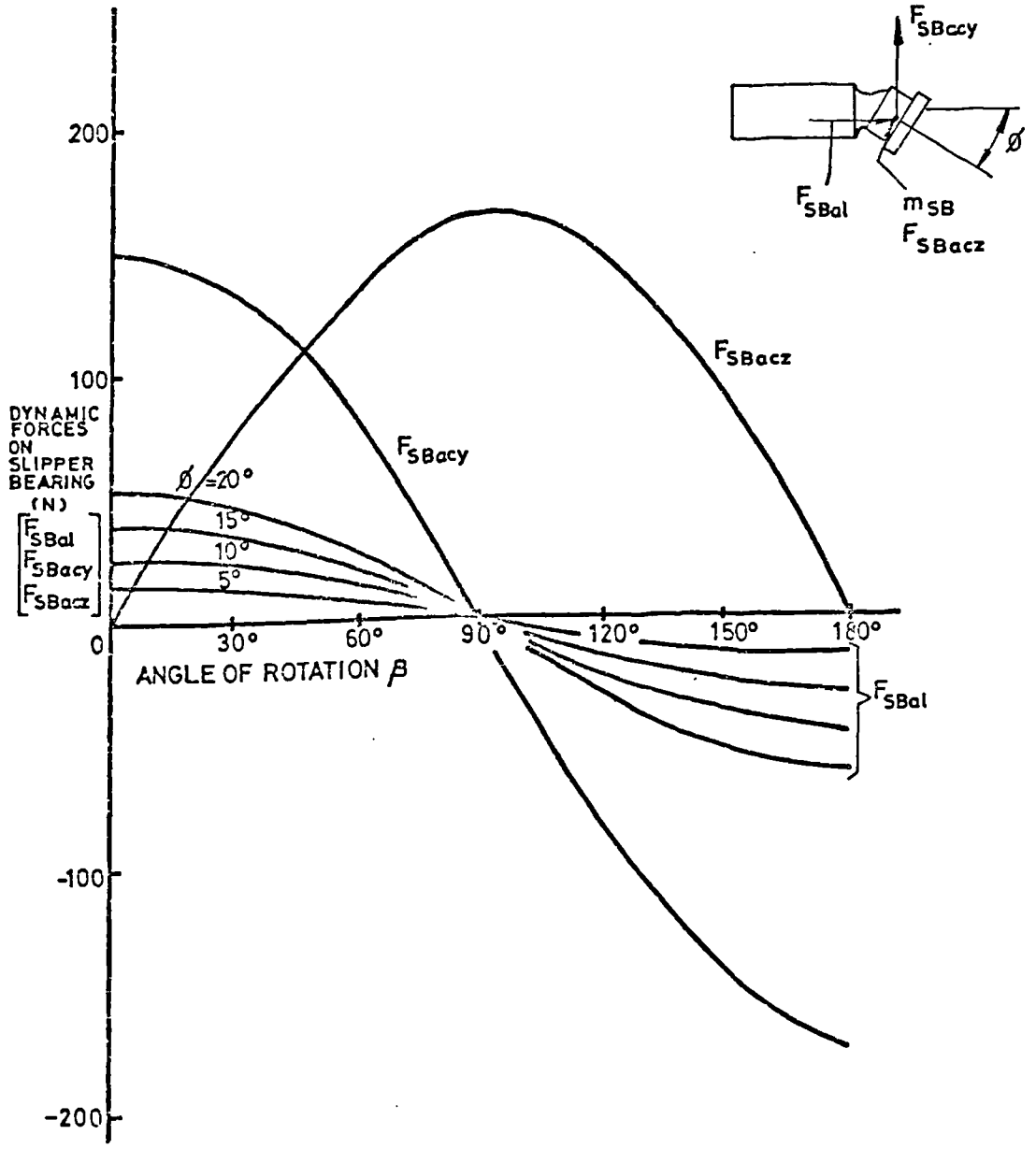

FIGURE 7.23. DYNAMIC FORCES ON A SLIPPER BEARING AT VARIOUS ANGLES OF TILT AND ANGLES OF ROTATION.

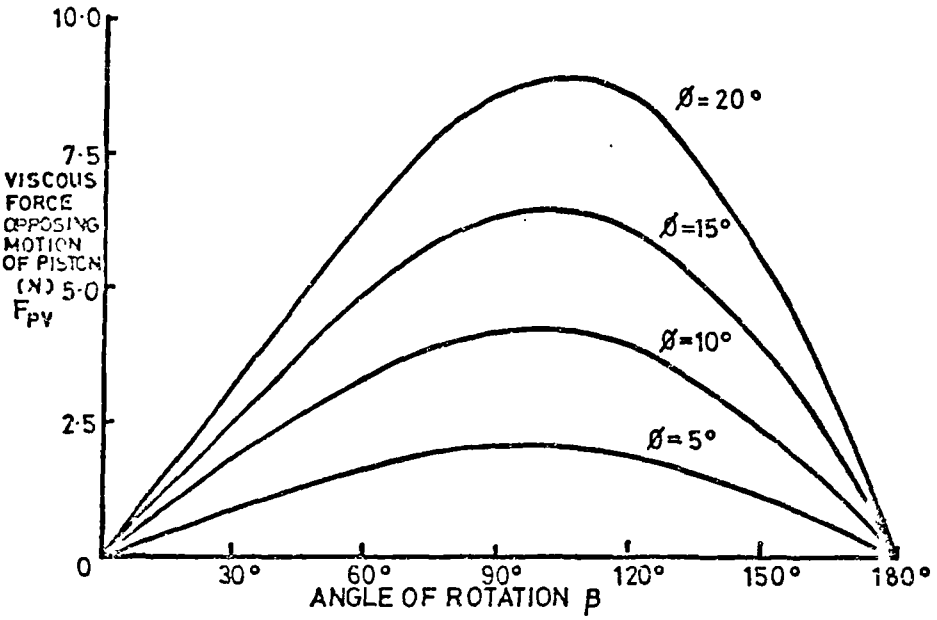

FIGURE 7.24. VISCOUS FORCE OPPOSING MOTION OF THE PISTON AT VARIOUS ANGLES OF TILT AND ANGLES OF ROTATION.

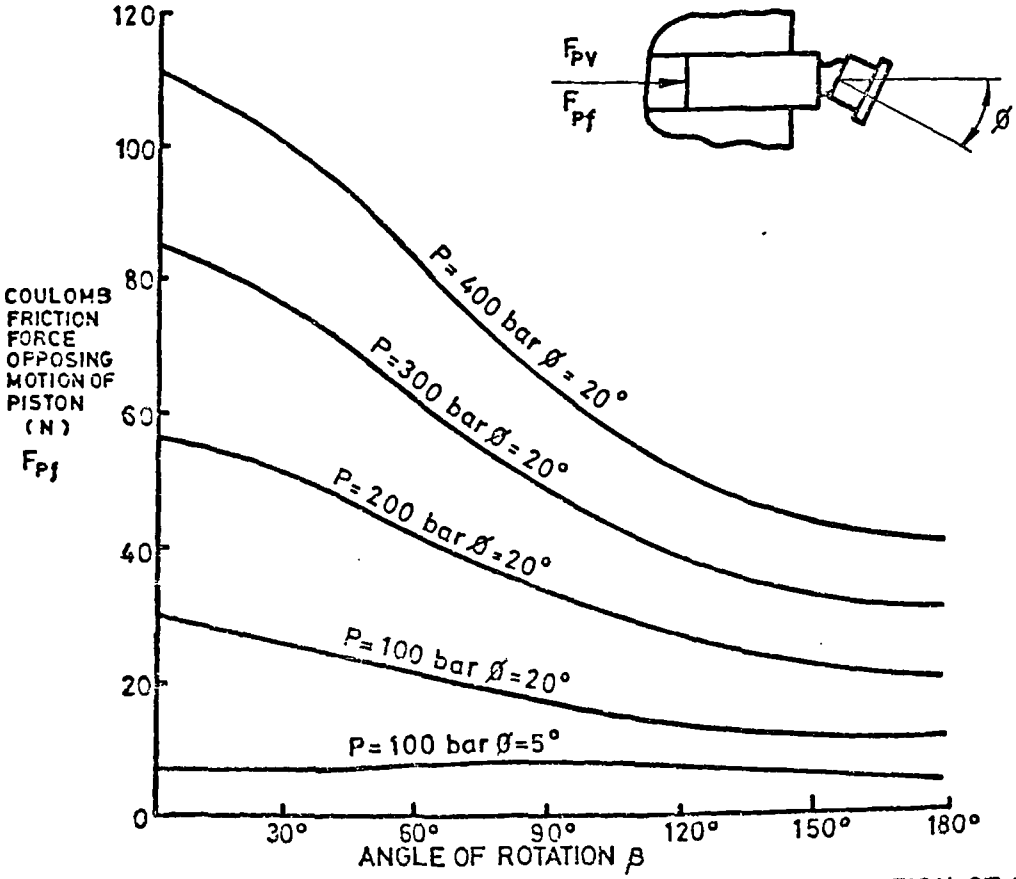

FIGURE 7.25. RELATIVE COULOMB FRICTION FORCE OPPOSING MOTION OF A PISTON AT VARIOUS ANGLES OF TILT AND ANGLES OF ROTATION.

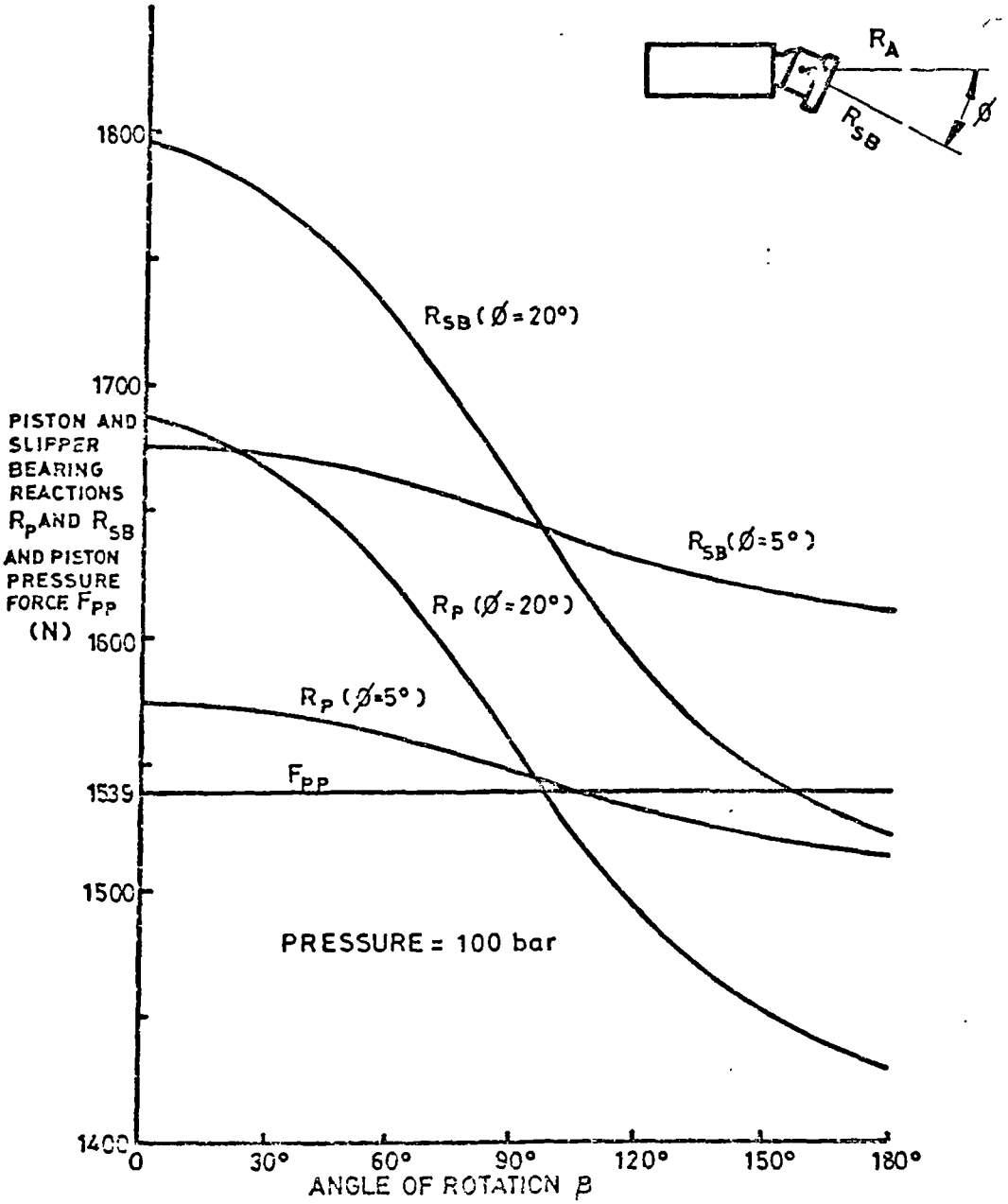

FIGURE 7.26. RELATIVE PISTON AND SLIPPER BEARING REACTIONS AND PISTON PRESSURE FORCE AT VARIOUS ANGLES OF TILT AND ANGLES OF ROTATION.

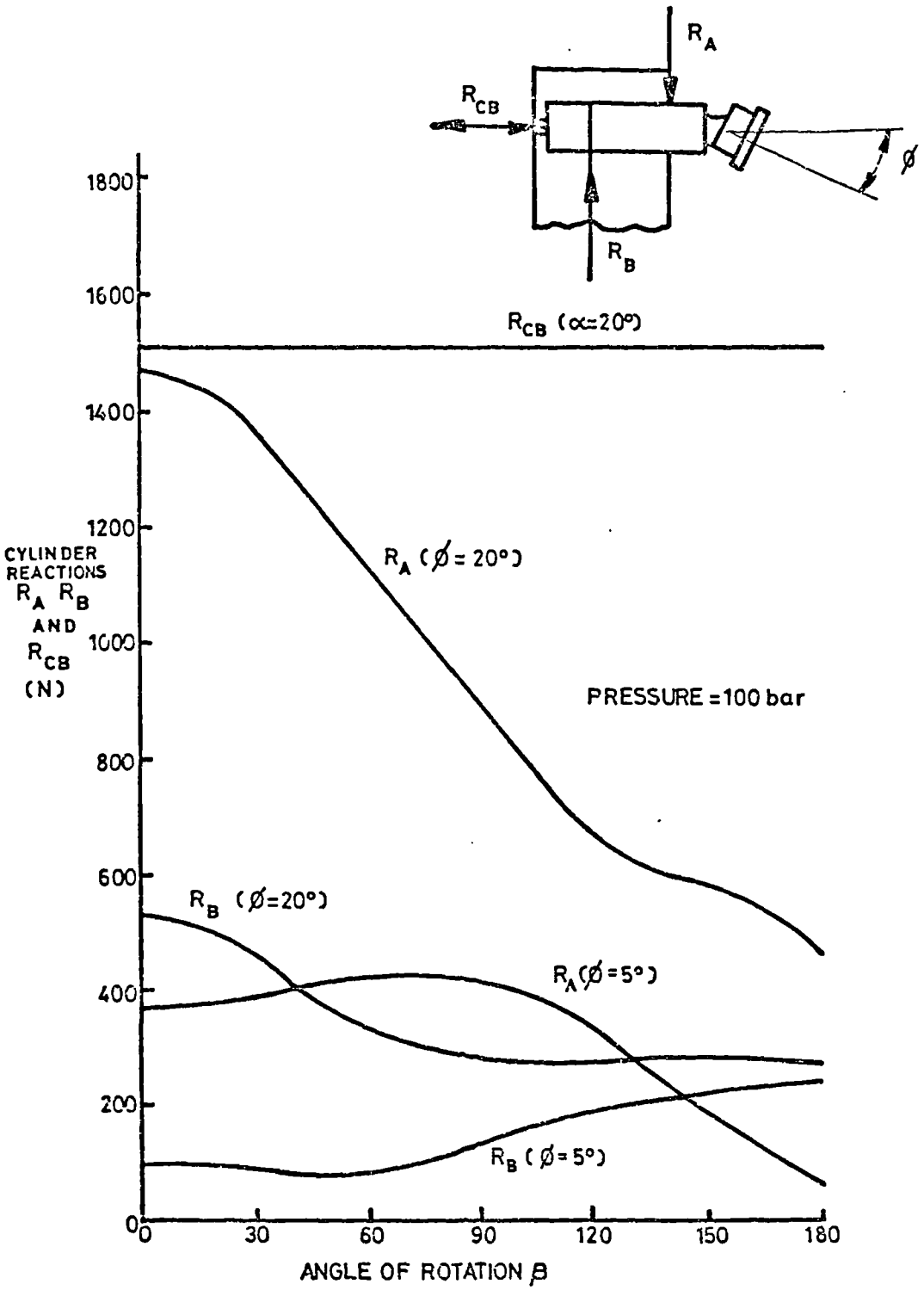

FIGURE 7.27. CYLINDER REACTIONS AT VARIOUS ANGLES OF TILT ϕ AND ANGLES OF ROTATION β

Values were calculated for -

Pump Pressures of 100, 200, 300 and 400 bar

Swashplate Angles of 5°, 10°, 15° and 20°

Close study of these curves will show some interesting trends such as the high levels of coulomb friction at high pressures and swashplate angles and that the reaction R_A between the piston and the cylinder bore rises to be equal to the pressure force of 1539 N on the piston.

Swashplate Design

Very little information has been published on the design of swashplates and that which has been published is of a superficial nature. A design methodology can be formulated by considering the basic features involved, i.e.,

(i) the facility to pivot and in so doing to provide a variable angle of tilt to vary the pump stroke;

(ii) the ability to carry the loads transferred from the slipper bearings and from the swashplate control mechanism;

(iii) the provision of suitable surface conditions at the control surface.

Pivoting may be achieved by mounting the swashplate between trunnion bearings using plain or rolling element bearings. Since the axis of tilt is at right angles to the dead centres axis of the pump, only the bearing on the delivery side of the swashplate will be subjected to appreciable loading. The effects of the forces to return the pistons on the suction stroke may influence the bearing loads but since these are small in value, these forces can be neglected. Fig. 7.28 shows the forces and moments acting on the swashplate and bearings.

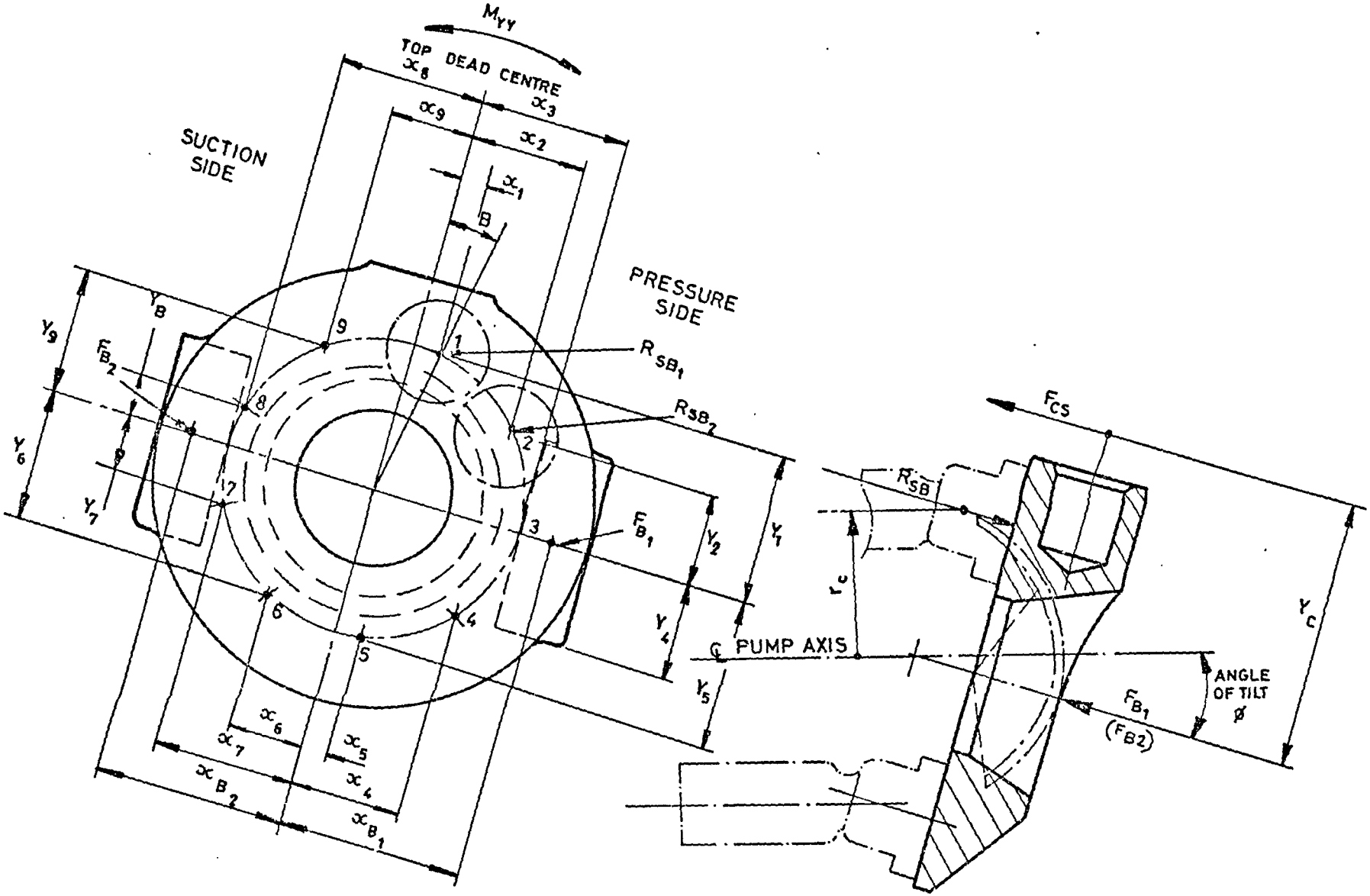

FIGURE 7. 28. FORCES AND MOMENTS ACTING ON SWASHPLATE AND BEARINGS.

At a constant angle of tilt the control force F_{CS} will be small and will vary with the angle of tilt. Variations of this force will occur during a pumping cycle due to:-

(iv) variations in the acceleration forces of the piston and slipper bearing assemblies depending on pump speeds and stroke;

(v) variations of pressure in the pump which occur during a pumping cycle.

The analysis of F_{CS} is therefore very complex but since its value will be small compared to the bearing loads, it may be calculated from the equation -

$$F_{CS} = \frac{\Sigma \left[R_{SB1} Y_1 + R_{SB2} Y_2 + \cdots\cdots R_{SBN} Y_N \right]}{Y_C} \qquad (7.5)$$

where values of Y are positive if referring to reactions above the XX axis and negative for those below.

With a changing angle of tilt, the control force must overcome the frictional resistance of the swashplate bearings and the changing inertial forces. As the frictional component is very much the larger, it is justifiable to equate the new control force as -

$$F_{CD} = F_{CS} \pm \left(F_{B1} + F_{B2} \right) \frac{r_A}{r_C} . f \qquad (7.6)$$

The total bearing loads $F_{B1} + F_{B2}$ can then be calculated from -

$$F_{B1} + F_{B2} \simeq \left(R_{SB1} + R_{SB2} + \cdots R_{SBN} \right) \left(1 + \frac{r_B}{r_C} f \right) + F_{CS}$$

and the individual bearing loads from -

$$F_{B1} = \frac{\left[R_{SB1} (x_B + x_1) + R_{SB2} (x_B + x_2) + \cdots F_{CB} x_B \right]}{2 x_B} \qquad (7.7)$$

$$F_{B2} = \frac{\left[R_{SB1} (x_B - x_1) + R_{SB2} (x_B - x_2) + \cdots F_{CB} x_B \right]}{2 x_B} \qquad (7.8)$$

Gerber (6) has shown that the loci of the centre of the slipper bearings is an ellipse of radius r_e where

$$r_e = \sqrt{r_c \left(1 + \cos^2 \omega t \tan^2 \phi\right)} \qquad (7.9)$$

The worse conditions at the swashplate will occur when the number of pressurised pistons is $\frac{N_p + 1}{2}$ and when the first of these pistons subtends an angle $\beta/2$ with the top dead centre of the pump. Then -

$$\beta = \pi - \left[\left(\frac{N_p + 1}{2}\right) - 1\right] \frac{2\pi}{N_p}$$

$$x_1 = r_{e1} \sin \frac{\beta}{2}$$

$$x_2 = r_{e2} \sin\left(\frac{\beta}{2} + \frac{2\pi}{N_p}\right)$$

$$x_3 = r_{e3} \sin\left(\frac{\beta}{2} + \frac{4\pi}{N_p}\right) \qquad \text{etc.}$$

$$Y_1 = r_{e1} \cos \frac{\beta}{2}$$

$$Y_2 = r_{e2} \cos\left(\frac{\beta}{2} + \frac{2\pi}{N_p}\right)$$

$$Y_3 = r_{e3} \cos\left(\frac{\beta}{2} + \frac{4\pi}{N_p}\right) \qquad \text{etc.}$$

If the pump is for use at high pressure, the loads on the bearings may be such that the use of relatively small diameter trunnion bearings is not practical and it is usual to employ shell bearings of relatively large radius and which provide bearing contact over an arc of some 140°. Using steel backed porous bronze bearings lined with acetal resin co-polymer, the bearing pressure would be generally limited to $140 N/mm^2$ and the coefficient of friction can be taken as .01 to .10.

The loads from the slipper bearings have the effect of creating a bending moment about any diametral axis of the swashplate. A principal bending moment will occur about the YY axis and using classical bending theory, the cross

section on the axis can be determined; i.e.,

$$M_{YY} = \left(R_{SB1}x_1 + R_{SB2}x_2 + - - - R_{SB\left(\frac{N_p+1}{2}\right)}x_{\left(\frac{N_p+1}{2}\right)}\right) \tag{7.10}$$

The swashplate will need to be very rigid to ensure a flat working face for the slipper bearings and therefore the bending stresses will be low. Since little variation of Myy will occur when the pump is running at constant speed and pressure, the variation of stress levels will not be great and metal fatigue is not likely to present problems. In addition to the bending stresses, consideration must be given to the shear stresses that may be present.

Very little surface contact between the slipper bearings and the swashplate is likely during normal running although at 'start-up' and 'shut down', contact will occur resulting in wear of the components. In addition, the couple C_{SB} acting on the slipper bearings may cause some undesirable contact although in all probability hydrodynamic wedge effects will minimise this tendency.

Far greater problems are caused by the presence of foreign particles in the hydraulic fluid and particularly those resulting from wear. Edghill and Rubery (24) give details of the wear that has resulted from hard particles being embedded in the relatively soft surface of the slipper bearings and causing a groove of as much as 2.5mm depth in 1000 hours operation. This means that special care must be taken in selecting the material for the swashplate. Strength and rigidity requirements suggest the use of a ferrous forging with the bearing surfaces nitrided to at least 0.6mm in depth. The working face could be machined to a surface finish of 0.2 micrometres with a flatness of 0.012mm over the entire surface.

Cylinder Block Design

The design requirements of the cylinder block are:-

a) to provide suitable bores for the successful pumping of fluid;

b) to have the strength necessary to resist the hydraulic and mechanical forces involved;

c) to provide a suitable surface for the transference of the fluid to and from the valve plate.

Modern manufacturing methods enable the bores to be produced to meet the requirements of working clearance and interchangeability whilst being economically viable. The levels of working clearances with the piston is fully discussed in the next section. The pistons are loaded against the cylinder bores and the reciprocating motion is best accommodated by non-ferrous bore linings commonly of phosphor bronze or leaded bronze.

The stresses in the metal between adjacent bores can be calculated from -

$$\sigma = \frac{P d_p}{2t} \qquad (7.11)$$

where 2t is the minimum wall thickness between two cylinders -

$$2t = D \sin\left(\frac{\pi}{N_p}\right) - d_p \qquad (7.12)$$

The presence of the non-ferrous liners can be ignored in these calculations if relatively low values of t are used. In any event the conditions imposed by designing the return mechanism for the slipper bearings on the suction stroke will in all probability make it necessary to use a value of D which will result in the wall thickness being even larger than that given by the above equation.

Other strength requirements are those of transmitting the mechanical forces from the shaft which in general are not difficult to accommodate.

The face of the cylinder block which abutts the valve plate must be machined square to the shaft bore and flat within very close limits, e.g., 0.012mm over the entire surface.

It is common practice to float the cylinder block surface away from the valve plate by means of hydrostatic action of the hydrostatic bearing recesses which can be conveniently machined in the valve plate. Because of conditions of friction and wear at start-up and shut-down, a non-ferrous bearing face to the cylinder block may be employed.

The strength, machinability and economic considerations suggest the use of a low carbon cylinder block and since the cylinder contributes appreciably to the weight and rotational inertia of the pump, it is important to keep its size to a minimum. Again because of compressibility losses as discussed in Section 5.2, it is advantageous to reduce the space for hydraulic fluid within the cylinder block to a minimum.

Piston Design

The piston performs the basic function of forcing a quantity of hydraulic fluid along a cylinder bore against a resisting pressure and on the return stroke of drawing a new charge of fluid into the bore for subsequent pumping. So that these functions may be carried out, the piston must satisfy the requirements of:-

a) having a working clearance with the bore of the cylinder block to allow sliding to occur with acceptable levels of fluid leakage and frictional resistance;

b) having the necessary strength to withstand the mechanical and fluid loads imposed on it;

c) having to be of material suitable for the conditions of loading and to resist wear.

Piston Clearances for Axial Piston Pumps

An important consideration in the design of axial piston pumps is the determination of the diametral clearance between the piston and the cylinder bore. If a relatively large clearance is chosen, the leakage losses past the piston will be excessive and this will adversely affect the volumetric efficiency of the pump. On the other hand if the clearance is too small, the viscous drag on the moving piston will be large and will result in a reduced mechanical efficiency. It is thus apparent that there is a real need to optimise the piston clearance for minimum power loss.

During the pumping stroke of a piston the fluid flow rate through the clearance gap is made up of the pressure flow (Poisseuille) and the shear flow (Couette). An expression for the total flow rate past the piston is -

$$Q_s = \frac{\pi}{96} \frac{(P_i - P_e)}{\mu} \frac{d_p C_d^3}{\ell_i} F_e - \frac{\pi}{4} d_p C_d V_p \qquad (7.13)$$

where Q_s is the slip flow rate past the piston

$P_i - P_e$ is the pressure drop across the length of the gap

d_p is the piston diameter

C_d is the diametral clearance of the piston

ℓ_i is the length of piston immersion in the cylinder

F_e is a factor to take care of piston eccentricity

μ is the absolute viscosity of the fluid

V_p is the velocity of the piston.

During the pumping stroke of the piston the values of ℓ_i and V_p will be continuously changing and it is convenient for analytical purposes to substitute average values $\bar{\ell}_i$ and $\bar{V}_p$. For a given pump speed and displacement setting ℓ_i varies as the cosine of angle β and V_p as sin β where β is the angle of rotation of the pump from the top dead centre position.

Then -

$$\bar{l}_i = 0.637\left(l_{i\,MAX} - l_{i\,MIN}\right) + l_{i\,MIN} \tag{7.14}$$

$$\bar{V}_p = 0.637\, V_{p\,MAX} \tag{7.15}$$

It is also apparent from the considerations given to the forces acting on the spherical bearing of the piston that the piston does not take up a position of constant eccentricity along its length but rather of full eccentricity in one direction at the plane of the working face of the piston and varying to full eccentricity in the opposite direction in the plane of the cylinder face. The eccentricity will vary linearly along the immersed length to give an average value of $\bar{e} = \frac{Cd}{4}$

Ernst (5) has given an expression for the eccentricity factor F_e as -

$$F_e = 1 + \frac{3}{2}\left(\frac{2e}{Cd}\right)^2 \tag{7.16}$$

so that for the conditions considered here, $F_e = 1.375$

The viscosity of the hydraulic fluid flowing through the gap will vary considerably. At the face of the piston the pressure effect on the fluid will increase the viscosity to -

$$\mu = \mu_o e^{K_p P} \tag{7.17}$$

where μ_o is the viscosity at zero pressure

μ is the viscosity at pressure P

K_p is the pressure coefficient of viscosity

Along the length of the gap the pressure will decrease and this will in turn reduce the viscosity.

Since the pressure flow through the gap represents a power loss and additional power is lost due to the viscous

drag on the piston, the loss of energy will be manifested in raising the temperature of the fluid in the gap. The heat is mainly removed by the flow of fluid although some will be transmitted through the gap walls into the piston and cylinder block. The rise in the temperature changes the viscosity as -

$$\mu = \mu_o \left[\frac{T_o}{T_o + \Delta T}\right]^{K_T} \tag{7.17}$$

where μ_o is the viscosity at temperature T_o

μ is the viscosity at temperature $T_o + \Delta T$

K_T is the temperature coefficient of viscosity

It will be apparent that the pressure distribution along the length of the gap will not be linear because of the non-linear variation of eccentricity and viscosity. The analysis of the pressure flow is most complex and for design purposes it is more convenient to use an effective viscosity μ_{ef} and to satisfy the theoretical equations given by iteration.

It is suggested that the effective viscosity should be the viscosity at mean temperature and at mean pressure. Then -

$$\mu_{ef} = \mu_o e^{K_p \frac{(P_1+P_2)}{2}} \left[\frac{T_o}{T_o + \frac{\Delta T}{2}}\right]^{K_T} \tag{7.18}$$

The flow rate past the piston is made up of the pressure flow Q_p and the shear flow Q_d and can be expressed as -

$$Q = \frac{1.375\pi}{96\mu_{ef}} (P_1 - P_2) \frac{d_p C_d^3}{\bar{l}_i} - \frac{\pi}{4} d_p C_d \bar{V}_p \tag{7.19}$$

The power loss due to the pressure flow is $Q_p(P_1-P_2)$ and that due to the viscous drag is the product of the force $2\pi \frac{d_p}{C_d} \mu_{ef} \bar{l}_i \bar{V}_p$ and the piston velocity.

$$P_L = P_p + P_s$$

$$P_L = \frac{1.375\pi}{96\mu_{ef}}(P_1-P_2)^2 \frac{d_p C_d^3}{\bar{l}_i} + 2\pi \frac{d_p}{C_d} \mu_{ef} \bar{l}_i \bar{V}_p^2 \qquad (7.20)$$

Then

$$\frac{P_L}{\frac{1.375\pi}{96\mu_{ef}}(P_1-P_2)^2 \frac{d_p^4}{\bar{l}_i}} = \left(\frac{C_d}{d_p}\right)^3 + \frac{192\mu_{ef}^2 \bar{l}_i^2 \bar{V}_p^2}{1.375(P_1-P_2)^2 d_p^4}\left(\frac{C_d}{d_p}\right)^{-1}$$

Differentiating with respect to $\left(\frac{Cd}{dp}\right)$ and equating to zero

$$3\left(\frac{C_d}{d_p}\right)^2 = \frac{192\mu_{ef}^2 \bar{l}_i^2 \bar{V}_p^2}{1.375(P_1-P_2)^2 d_p^4}\left(\frac{C_d}{d_p}\right)^{-2}$$

To give for minimum power loss

$$\left(\frac{C_d}{d_p}\right)_{OPT} = 2.61\sqrt{\frac{\mu_{ef} \bar{l}_i \bar{V}_p}{(P_1-P_2) d_p^2}} \qquad (7.21)$$

However a power loss due to viscous drag also occurs during the suction stroke so that during a full working stroke of the piston the total power loss is $P_L = P_p + 2P_s$

Treating in the same manner as before we have -

$$\left(\frac{C_d}{d_p}\right)_{OPT} = 3.106\sqrt{\frac{\mu_{ef} \bar{l}_i \bar{V}_p}{(P_1-P_2) d_p^2}} \qquad (7.22)$$

And

$$Cd_{OPT} = 3.106\sqrt{\frac{\mu_{ef}\,\bar{\ell}_i\,\bar{V}_p}{(P_1-P_2)}} \tag{7.23}$$

Thus the optimum diametral clearance for a given set of working conditions of pump speed, displacement setting and pressure can easily be determined on the basis of an effective viscosity. Unfortunately any change of $\bar{\ell}_i$, $\bar{V}_p$ and (P_1-P_2) will affect the value of the effective viscosity so that with new working conditions, the effect on the optimum clearance can only be expressed in terms of a new effective viscosity. Using suffixes (1) and (2) to denote values related to conditions 1 and 2 respectively we can use the following relationships.

When the pump pressure changes but the pump speed and displacement setting remains constant:

$$\frac{Cd_{OPT(1)}}{Cd_{OPT(2)}} = \sqrt{\frac{\mu_{ef(1)}\,(P_1-P_2)_{(2)}}{\mu_{ef(2)}\,(P_1-P_2)_{(1)}}} \tag{7.24}$$

When the pump speed changes but the pump pressure and displacement setting remains constant:

$$\frac{Cd_{OPT(1)}}{Cd_{OPT(2)}} = \sqrt{\frac{\mu_{ef(1)}\,N_{(1)}}{\mu_{ef(2)}\,N_{(2)}}} \tag{7.25}$$

When the displacement setting changes but the pump pressure and pump speed remains constant:

$$\frac{Cd_{OPT(1)}}{Cd_{OPT(2)}} = \sqrt{\frac{\mu_{ef(1)}\,\tan^2\phi_{(1)}}{\mu_{ef(2)}\,\tan^2\phi_{(2)}}} \tag{7.26}$$

It is of interest to note that the optimum diametral clearance does not depend on the specific diameter of the piston. However a study of the power loss equation will show that the losses increase with an increase in the piston diameter if all other parameters remain constant.

The effective viscosity may be quickly obtained by using the chart, Fig.7.29, which has been developed from the equation (7.18).

If the pressure is expressed in bars, common values of K_p range from 2.0 to 2.5 x 10^{-3}bar^{-1}. For the temperature range 0° to 70°C, K_T may be reliably taken as 3.

The temperature rise due to the pressure flow losses alone is -

$$\Delta T = \frac{(P_1 - P_2)}{J \rho s} \qquad (7.27)$$

where J is the mechanical equivalent of heat

ρ is the mass density of the fluid

s is the specific heat of the fluid

Using S.I. coherent units, J is 1 and common values of ρ and s are 820 kg/m^3 and 2.09 kJ/kg$^{\circ}$K respectively so that in the absence of specific data, J P S may be taken as 1700kJ/m^3 K. This means that a pressure differential of 100bar will cause a temperature rise due to leakage alone of some 5.88°C.

The chart is also useful for calculating the slip flow and the power losses for a piston assembly. To assist in this process, a flow diagram, Fig.7.30, has been devised for carrying out the calculations in a logical manner.

An estimate of how the pressure, pressure differential and viscosity may vary is obtained by considering the basic pressure flow equation.

$$Q_p = \frac{\pi}{96}(P_1 - P_2)\frac{d_p C_d^3}{\mu l_i}\left(1 + \frac{3}{2}\left(\frac{2e}{C_d}\right)^2\right) \qquad (7.28)$$

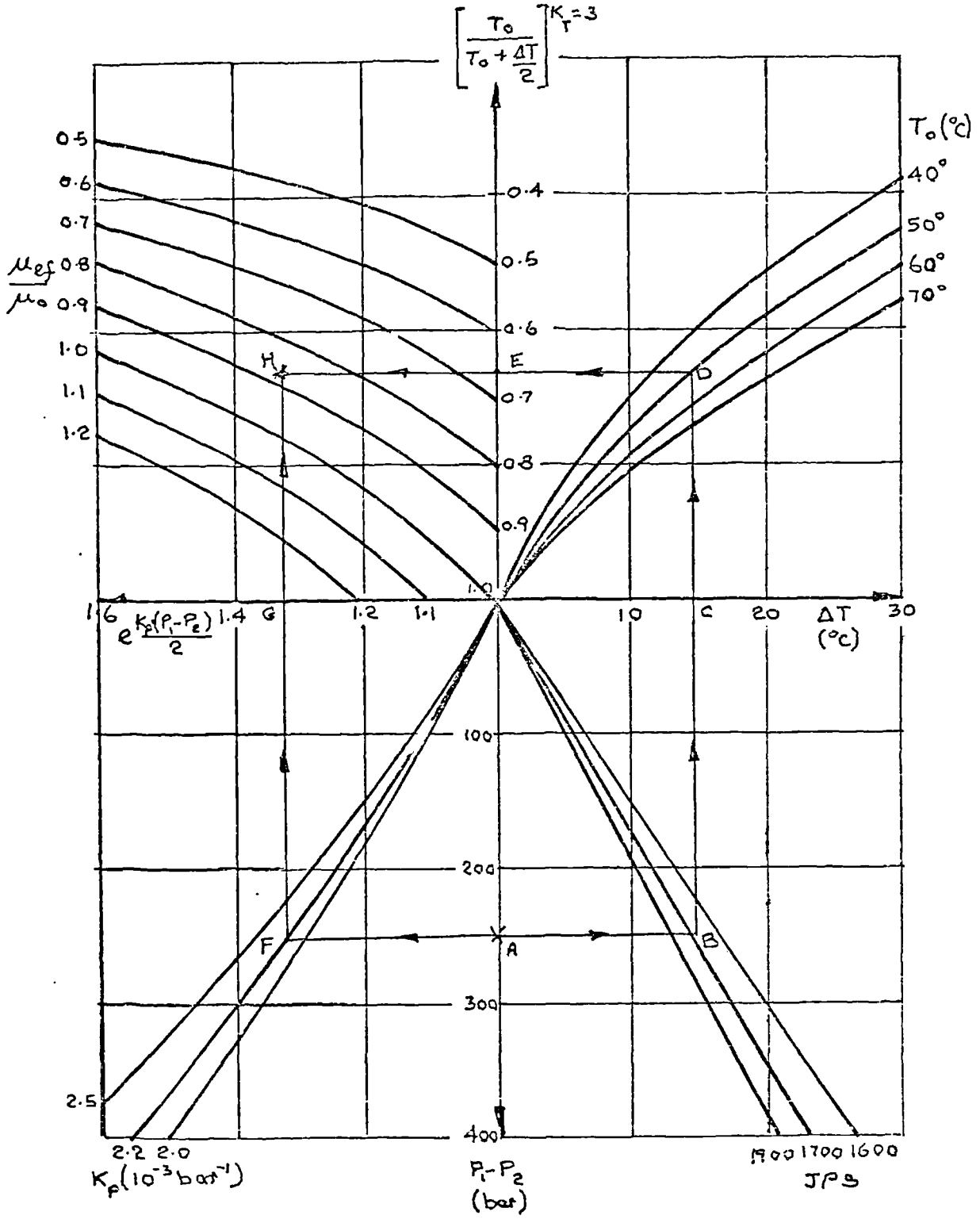

FIGURE 7.29 CHART FOR DETERMINING VISCOSITY RATIO $\frac{\mu_{ef}}{\mu_o}$

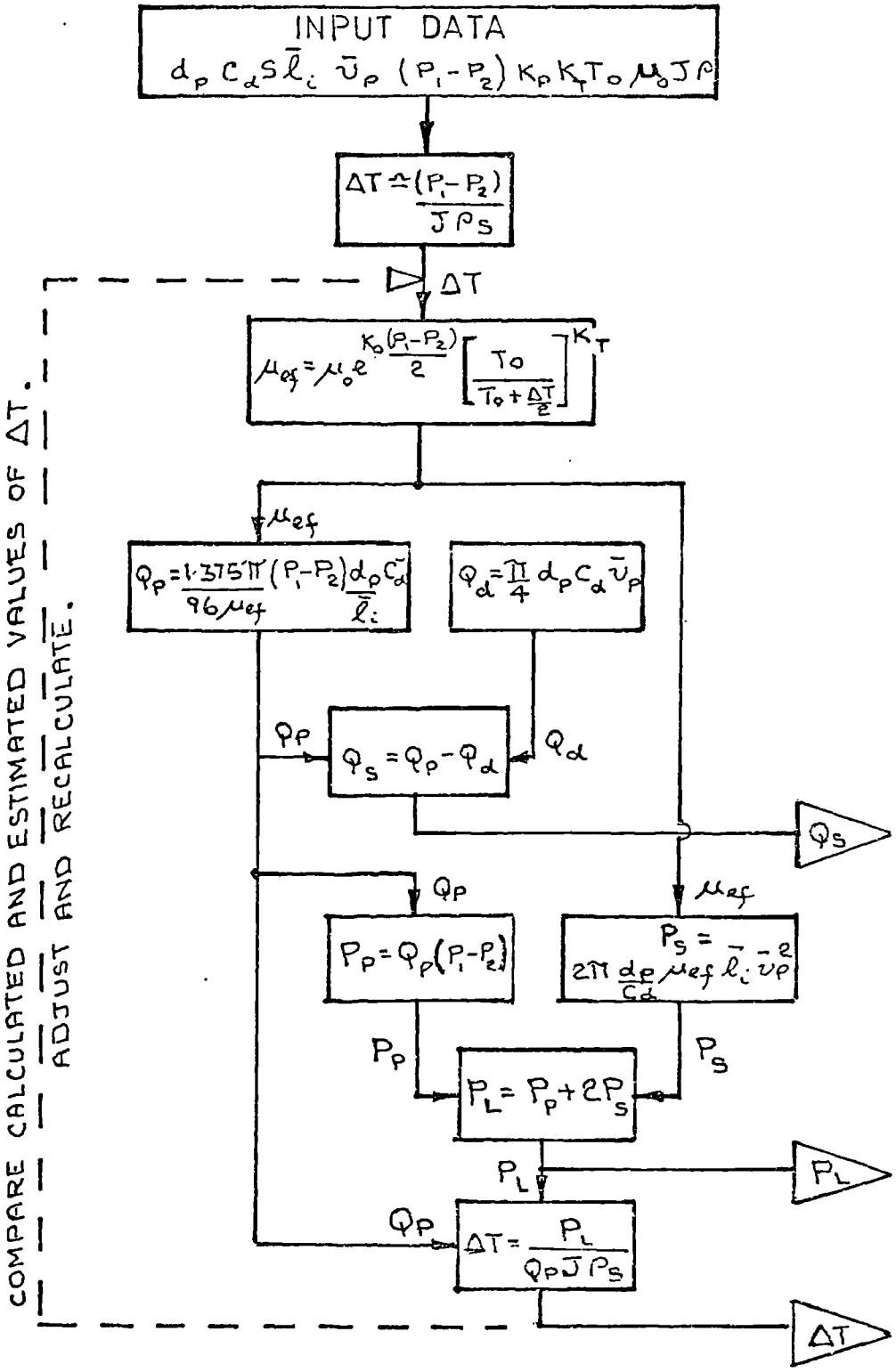

FIGURE 7.30 CHART SHOWING METHOD OF CALCULATING SLIP FLOW RATE, POWER LOSS AND TEMPERATURE RISE AT PUMP PISTON

Although the piston has varying eccentricity with the cylinder bore along its length, the flow rate past any plane distance x from the plane of the working face of the piston is constant. The ratio $\frac{(p_1 - p_2)}{l_i}$ can also be considered as a pressure differential at that plane. Thus if $(1 + \frac{3}{2}(\frac{2e}{Cd})^2)$ is expressed in terms of x we have -

$$\frac{\delta(p_1 - p_2)}{\delta x} = \frac{96\, Q_p \mu}{\pi d_p Cd^3} \quad \frac{1}{6\frac{x^2}{l_i^2} - 6\frac{x}{l_i} + 2{\cdot}5}$$

Let P_2 be 0 and considering initially that the viscosity is constant.

$$\int dp = K_1 \mu Q_p \int \frac{dx}{6\frac{x^2}{l_i^2} - 6\frac{x}{l_i} + 2{\cdot}5}$$

which becomes -

$$P = K_1 \mu Q_p \frac{l_i}{\sqrt{6}} \left[\tan^{-1}\left(\sqrt{6}\frac{x}{l_i} - \frac{\sqrt{6}}{2}\right) + C \right]$$

If P is 0 when $x = l_i$ we have -

$$P = K_1 \mu Q_p l_i \left| \tan^{-1}\sqrt{\frac{6}{2}} - 0{\cdot}886 \right]$$

(7.29)

A curve of $\frac{\sqrt{6}P}{K_1 \mu Q_p l_i}$ against X is shown in Fig.7.31.

Superimposed on the same graph is a curve for the uniform decrease of $\frac{\sqrt{6}P}{K_1 \mu Q_p l_i}$ with X. It will be seen that the effect of the varying eccentricity is to reduce the rate of change of the pressure at the ends of the gap but to increase the pressure differential at the middle zone.

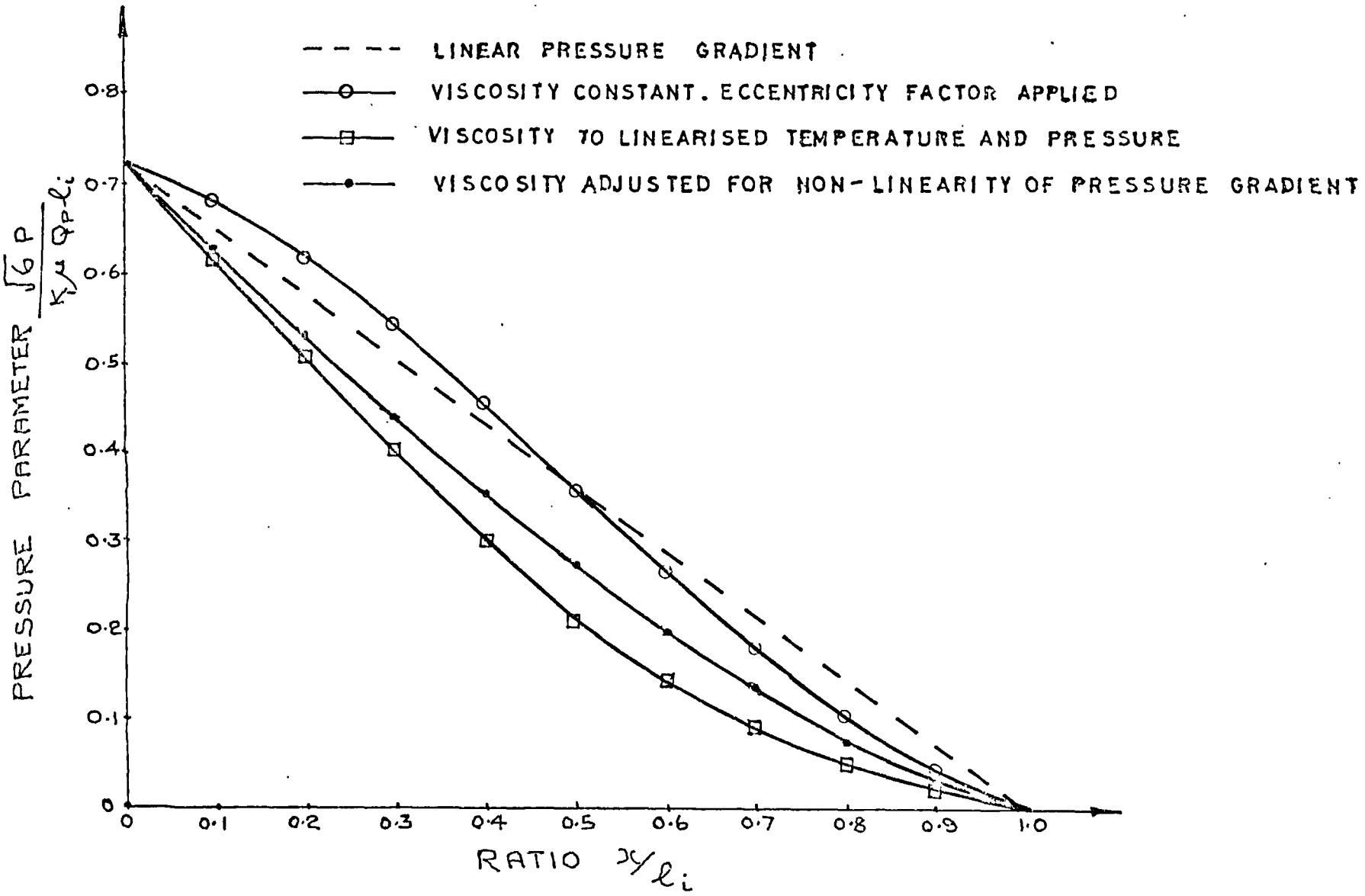

FIGURE 7.31 VARIATION OF PRESSURE PARAMETER WITH DISTANCE ALONG THE LEAKAGE PATH.

This is also clearly shown in Fig.7.32, which shows a series of pressure differential curves plotted against $\frac{x}{\ell_i}$. If we now consider the flow equation but with the viscosity varying with temperature and pressure we have -

$$\frac{\delta P}{\delta x} = K_1 \mu_0 Q_\rho \left(\frac{e^{K_p P} \left(\frac{T_0}{T_0 + \Delta T} \right)^{K_T}}{6 \frac{x^2}{\ell_i^2} - 6 \frac{x}{\ell_i} + 2.5} \right)$$

(7.30)

To solve this equation it is necessary to relate both P and ΔT to X. This is rather difficult but an approximate solution would result if, for the purpose of substitution in the terms affecting the viscosity, the pressure and temperature variation is linearised. Thus let

$$P = P_1 \left(1 - \frac{x}{\ell_i}\right) \quad \text{and} \quad \Delta T = \frac{P_1}{J \rho_S} \cdot \frac{x}{\ell_i}$$

The equation (7.30) now becomes -

$$\frac{\delta P}{\delta x} = K_1 \mu_0 Q_\rho \left[\frac{e^{K_p P_1 \left(1 - \frac{x}{\ell_i}\right)} \left(\frac{T_0}{T_0 + P_1 / J \rho_S} \right)^{K_T}}{6 \frac{x^2}{\ell_i^2} - 6 \frac{x}{\ell_i} + 2.5} \right]$$

(7.31)

This equation when integrated graphically gave a curve which is also shown in Fig.7.31, and which shows that at the beginning of the leakage flow path the relatively high viscosity effect due to the high pressure and the lower temperature, more than offset the effects of high eccentricity and this resulted in a high pressure gradient. The pressure gradient continues to be higher than that of the constant viscosity case until the last third of the gap length when the total effect of the high eccentricity, the reduced pressure effect on the viscosity and the reduction in viscosity due to the higher temperature causes the pressure gradient to fall sharply.

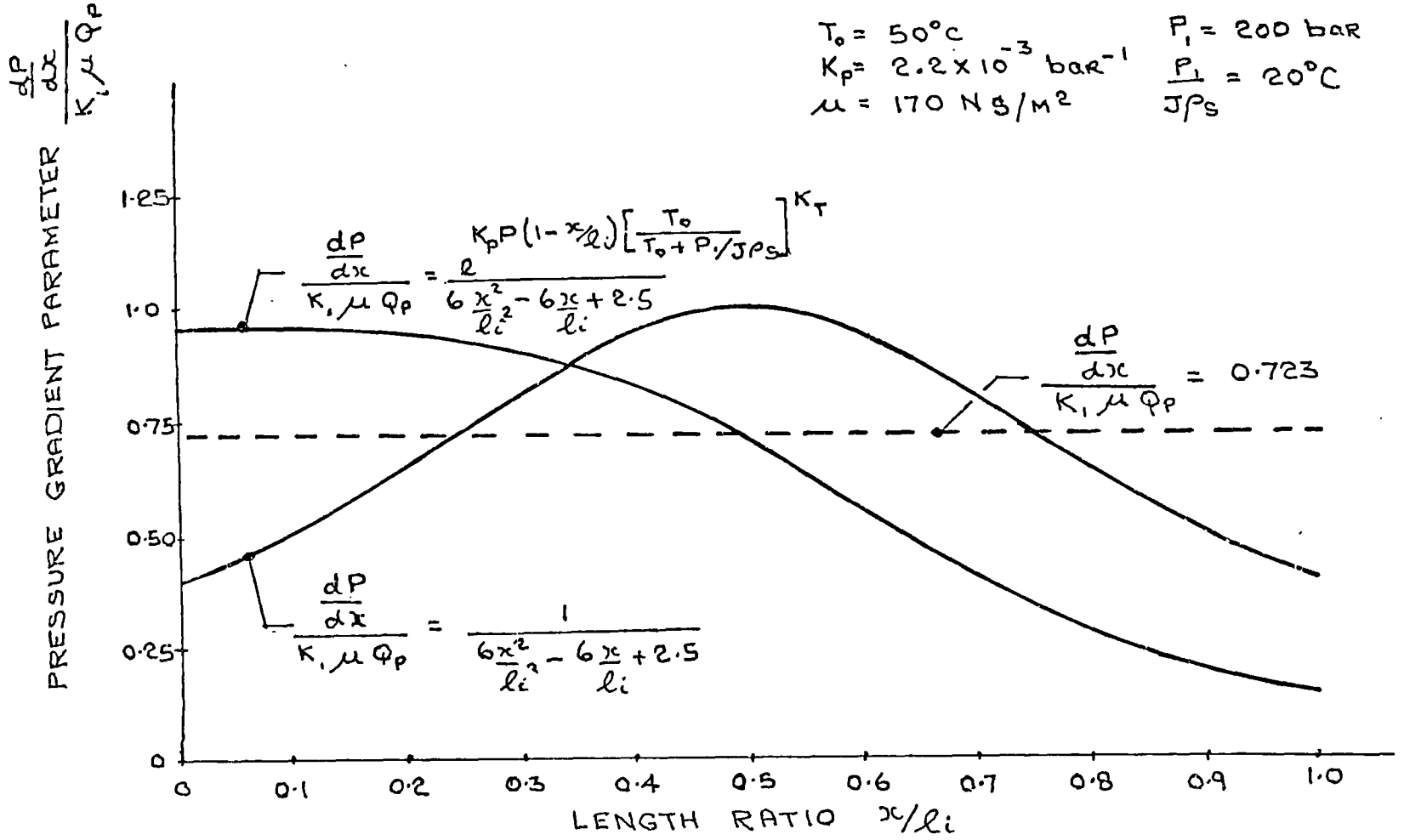

FIGURE 7.32 VARIATION OF PRESSURE GRADIENT PARAMETER WITH DISTANCE ALONG LEAKAGE PATH

By adjusting the value of P in the viscosity term, a final curve for a non-linear pressure distribution has been drawn which, it is considered, is likely to closely approach practical conditions. This investigation lends support to the concept of using an effective viscosity based on the mean pressure and mean temperature in the leakage path.

Several researchers including Wilson (25) and Exline (26) have attempted to relate losses in the piston and cylinder block assembly with changing conditions of diametral clearance, pressure differentials, length of immersion of the piston, piston velocity, fluid viscosity, etc., but with only partial success as far as presenting the findings in a form suitable for design use. Shute and Turnbull (27), however, suggested relating the losses as percentage losses of efficiency as opposed to specific power losses. This is a most useful concept since it enables the designer to readily find the effects of the design changes he is considering.

Taking this concept further to include the effects of variable piston immersion and the power losses during the suction stroke, the following theory is presented in support of an overall design process for piston design.

The percentage loss of efficiency E_p is defined as the percentage of the power developed by a piston during one complete working stroke which is lost due to leakage and viscous shear. Since the theoretical power developed by the piston is the rate of displacement times the working pressures we have -

$$E_p = 100\left[\frac{\frac{1.375\pi(P_1-P_2)^2}{96\mu_{ef}}\frac{d_p C_d^3}{\bar{l}_i} + 4\pi\frac{d_p}{C_d}\mu_{ef}\bar{l}_i\bar{V}_p^2}{\frac{\pi}{4}d_p^2\bar{V}_p(P_1-P_2)}\right] \tag{7.32}$$

which resolves to -

$$E_p = \frac{5.729(P_1-P_2)C_d^3}{\mu_{ef}\bar{l}_i\bar{V}_p d_p} + \frac{1600\mu_{ef}}{(P_1-P_2)}\frac{\bar{l}_i\bar{V}_p}{d_p C_d} \tag{7.33}$$

and rewritten as -

$$E_p = 5{\cdot}73\left(\frac{Cd}{dp}\right)^3 \frac{(P_1-P_2)\,d_p^2}{\mu_{ef}\,\bar{l}_i\,\bar{V}_p} + 1600\left(\frac{dp}{Cd}\right) \frac{\mu_{ef}\,\bar{l}_i\,\bar{V}_p}{(P_1-P_2)\,d_p^2}$$

$$= 5{\cdot}73\left(\frac{Cd}{dp}\right)^3 \lambda_p + 1600\left(\frac{Cd}{dp}\right)^{-1} \lambda_p^{-1} \qquad (7.34)$$

where λ_p is the piston parameter $\dfrac{(P_1-P_2)\,d_p^2}{\mu_{ef}\,\bar{l}_i\,\bar{V}_p}$

Percentage efficiency losses can be calculated from this equation or obtained directly from Fig.7.33, which has been compiled for the general limits of -

(P_1-P_2) up to 400 bar

d_p up to 30 mm

$\bar{l}i$ up to 60 mm

$\bar{V}p$ up to 2m/s

μ_{ef} from 0.01 to 0.20 Ns/m^2

The curves facilitate the estimation of losses for a range of values of $\frac{Cd}{dp}$ and λ_p and two useful curves are superimposed to provide additional information. Curve 'A' shows the values of $\frac{Cd}{dp}$ which give the minimum loss of efficiency for particular values of λ_p. Curve 'B' indicates the value of λ_p which gives the minimum loss of efficiency for particular values of $\frac{Cd}{dp}$.

It will be seen that if optimum piston clearances are used, the percentage losses of efficiency in a low pressure pump will be considerably greater than those in a high pressure pump working with the same diameter of piston, viscosity, length of immersion of piston and piston velocity.

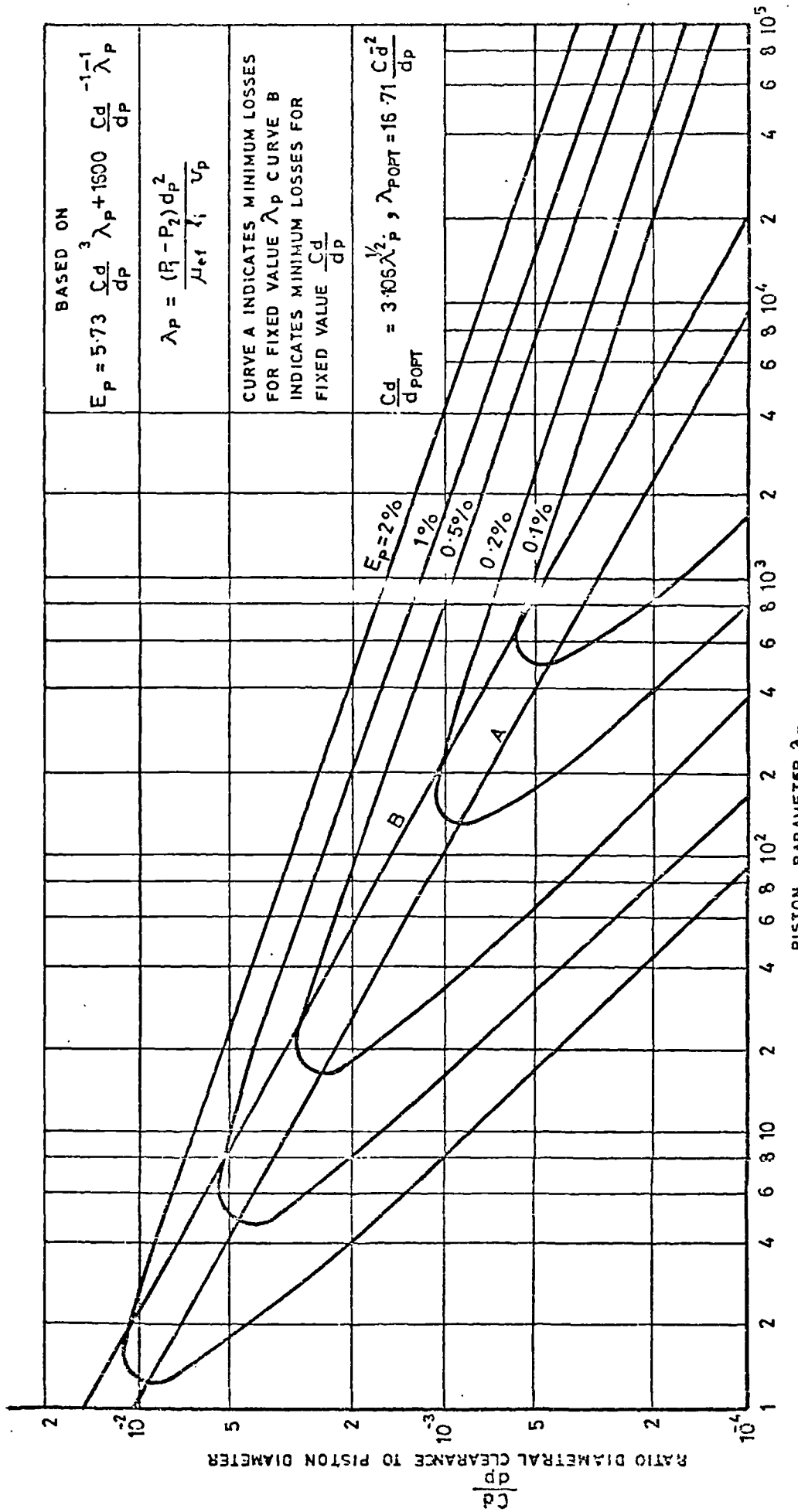

FIGURE 7.33. PERCENTAGE POWER LOSSES FOR AXIAL PISTON PUMP PISTONS

Conversely, all other factors being equal, a high speed pump will experience greater losses than a low speed pump working at the same pump pressure.

Fig.7.34, shows curves for the power losses with variations of piston clearance for the high speed high pressure pump already considered in the section on static and dynamic force analysis.

Reverting to equation (7.34) and substituting for Cd_{OPT} from equation (7.23), we can express the percentage loss of efficiency in terms of the $\frac{Cd}{dp}$ ratio and the ratio of the diametral clearance to the optimum diametral clearance -

$$E_p = 55{\cdot}27 \frac{Cd}{dp}\left(\frac{Cd}{Cd_{OPT}}\right)^2 + 165{\cdot}85 \frac{Cd}{dp}\left(\frac{Cd_{OPT}}{Cd}\right)^2 \qquad (7.35)$$

This equation provides a convenient means of estimating the change of percentage power loss when the diametral clearance varies from the optimum value for example due to manufacturing tolerances or reboring of the cylinder bores. Fig.7.35, has been plotted for a range of $\frac{Cd_{OPT}}{Cd}$ & $\frac{Cd}{Cd_{OPT}}$ values and shows clearly the appreciable variation from the optimum diametral clearance that can occur before the increase in the percentage loss of efficiency is significant. This will be particularly useful in distributing the manufacturing tolerances for the piston diameter and the cylinder bore.

For example, if the $\frac{Cd}{dp}_{OPT}$ for a particular pump is 0.001, then for equal losses of efficiency to occur under extreme conditions of fit, where d_p is the piston diameter and d_c the cylinder bore diameter -

$$C_{d\ MAX} = d_{c\ MAX} - d_{p\ MIN}$$

$$C_{d\ MIN} = d_{c\ MIN} - d_{p\ MAX}$$

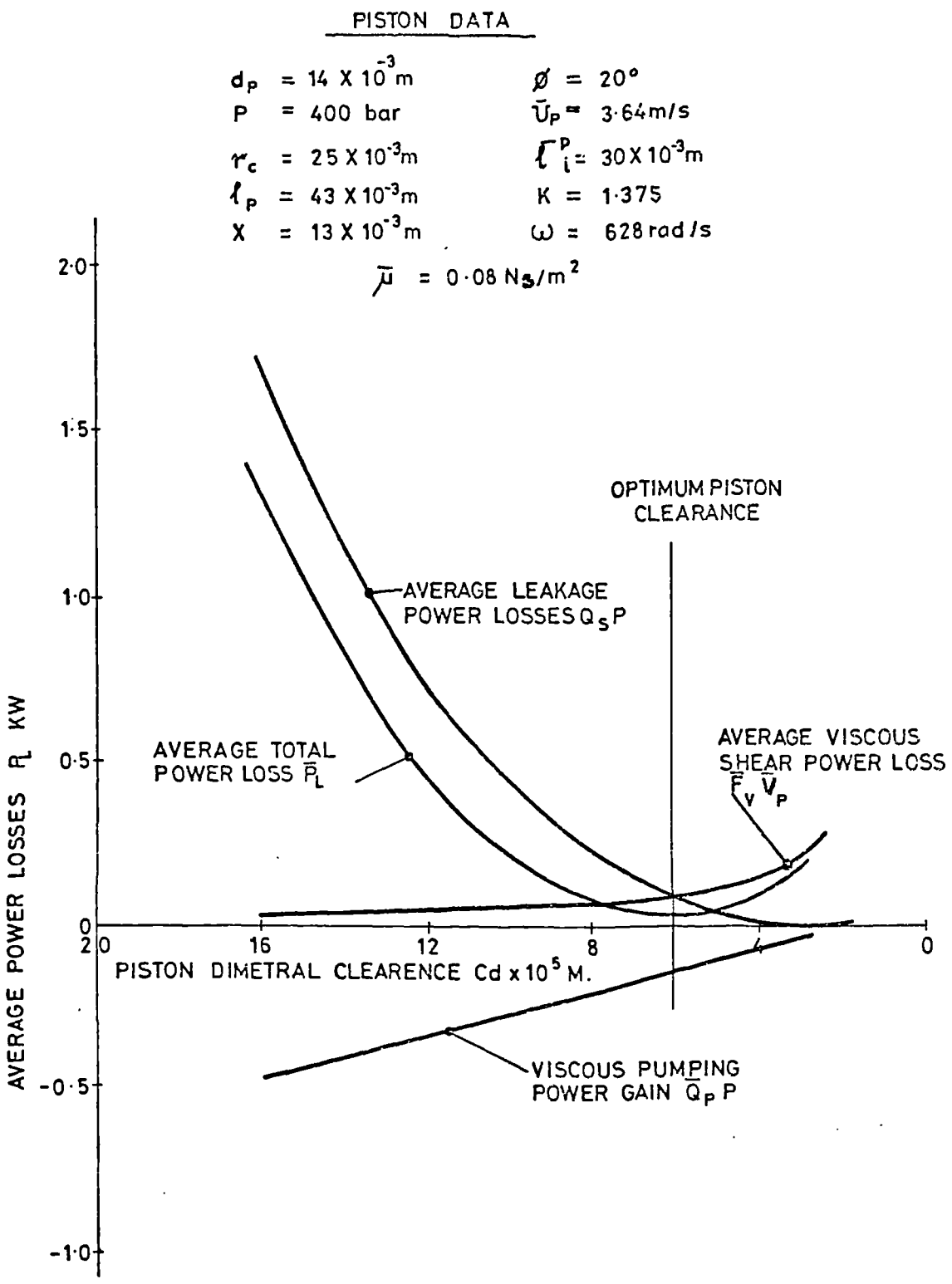

FIGURE 7.34. CURVES OF THE POWER LOSSES WITH VARIATION OF PISTON CLEARANCE

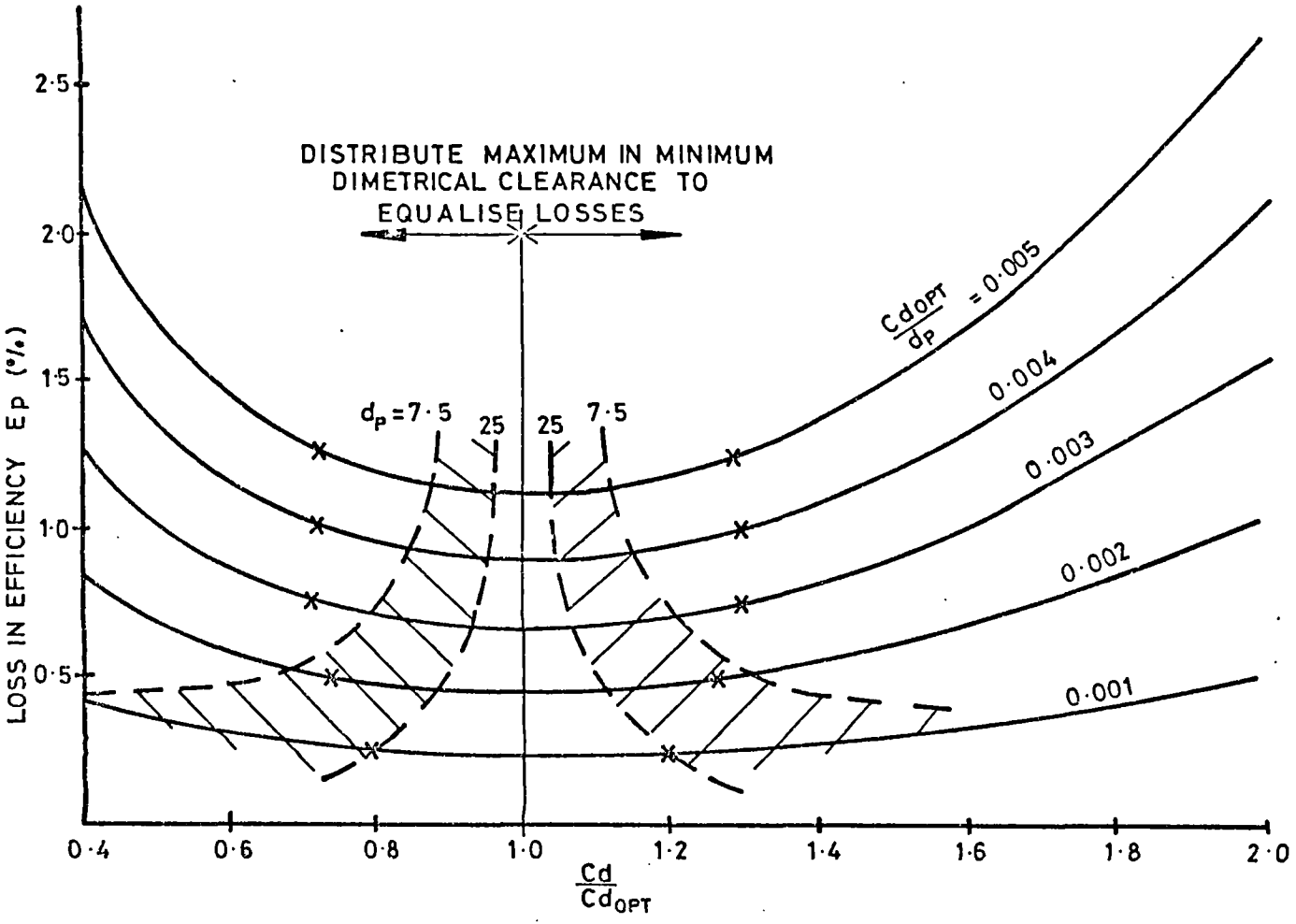

FIGURE 3.35. LOSS OF EFFICIENCY WITH Cd/Cd_{OPT} FOR VARIOUS DIAMETRICAL CLEARANCE TO PISTON DIAMETER RATIOS.

and assuming manufacturing tolerances will allow it, equal losses would occur if -

$$\frac{C_{d\ MAX}}{C_{d\ OPT}} = 1.4$$

$$\frac{C_{d\ MIN}}{C_{d\ OPT}} = 0.8$$

The piston and cylinder bore diameters will require manufacturing tolerances which in turn cause variations to the diametral clearances and as a consequence to the level of power losses in the pump. Fig.7.37, shows part of a chart published by the British Standards Institute (28) and describes the accuracy to be expected from machining inside and outside diameters by grinding and honing.

Fig.7.35, indicates that if the maximum and minimum variations of diametral clearance are equally disposed about the optimum diametral clearance, the resulting percentage losses in efficiency will be very nearly equal. The ratios of the maximum and minimum diametral clearances to the design optimum diametral clearance can then be expressed as -

$$\frac{C_{d\ MAX}}{C_{d\ OPT}} = 1 + \frac{\text{TOTAL TOLERANCE}}{2 d_p} \left(\frac{C_d}{d_p}_{OPT} \right)^{-1} \qquad (7.36)$$

$$\frac{C_{d\ MIN}}{C_{d\ OPT}} = 1 - \frac{\text{TOTAL TOLERANCE}}{2 d_p} \left(\frac{C_d}{d_p}_{OPT} \right)^{-1} \qquad (7.37)$$

Using the tolerances for ground pistons and honed cylinder bores as given in Fig.7.37, values of $C_{d\ MAX}$ and $C_{d\ MIN}$ for a range of piston diameters and $\frac{C_d}{d_p}_{OPT}$ values can be calculated. These are tabulated in Table 7.2, and the results for 7.5mm and 25mm diameter added to Fig.7.35. It will be observed that except for small pistons of about 7.5mm diameter with values of 0.001 and less, it is possible to distribute the manufacturing tolerances to maintain very favourable values of E_p.

Piston Diameter dp	7.5	10	12.5	15	17.5	20	22.5	25
Total Tolerance T.T.	.0094	.0095	.0096	.0097	.0098	.0099	.0100	.0102
$\frac{T.T.}{dp}$	.00125	.00095	.00077	.00065	.00056	.00050	.00044	.00041
$\frac{Cd}{dp}$ OPT = .001	1.625 .375	1.475 .525	1.385 .617	1.325 .675	1.280 .720	1.250 .750	1.220 .780	1.205 .795
.002	1.314 .687	1.238 .762	1.193. .807	1.163 .837	1.140 .860	1.125 .875	1.110 .890	1.103 .897
.003	1.208 .792	1.158 .842	1.128 .872	1.108 .892	1.093 .907	1.083 .917	1.073 .927	1.068 .932
.004	1.156 .844	1.119 .881	1.096 .904	1.081 .919	1.070 .930	1.063 .937	1.055 .945	1.051 .949
.005	1.125 .875	1.095 .905	1.077 .923	1.065 .935	1.056 .944	1.050 .950	1.044 .956	1.041 .959

Table 7.2 Table of $\frac{Cd}{Cd\ OPT}$ MAX and $\frac{Cd}{Cd\ OPT}$ MIN values for a range of piston diameters and $\frac{Cd}{Cd}$ OPT values, based on the accuracy that can be expected for a fine ground piston and a honed cylinder bore.

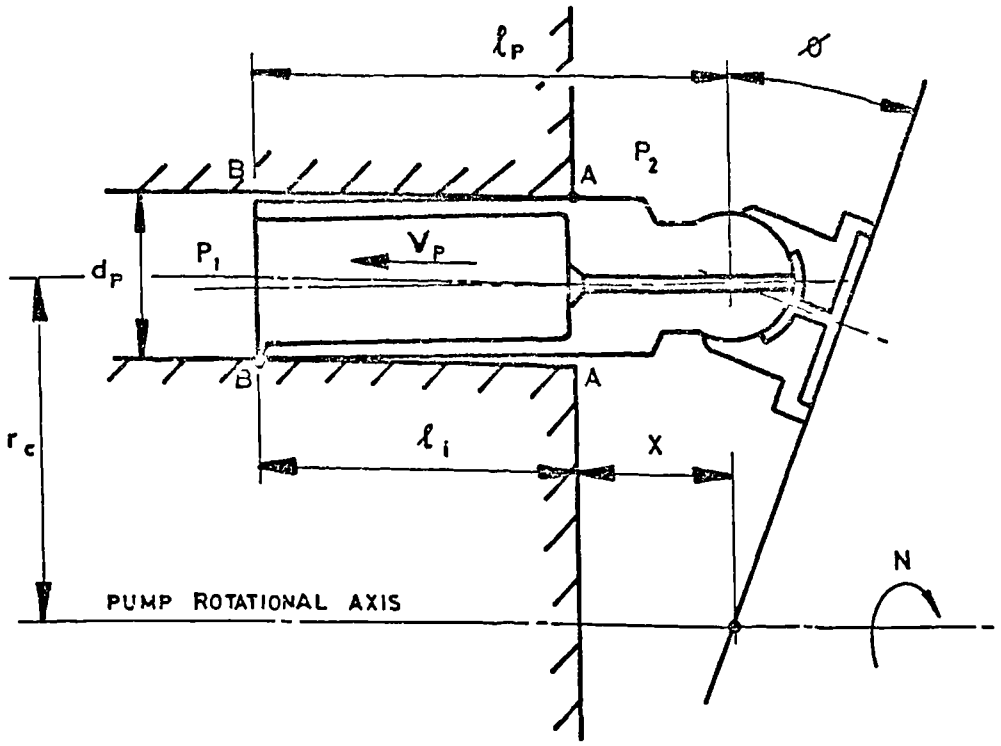

FIGURE 7.36. DIAGRAM OF PISTON AND CYLINDER ASSEMBLY

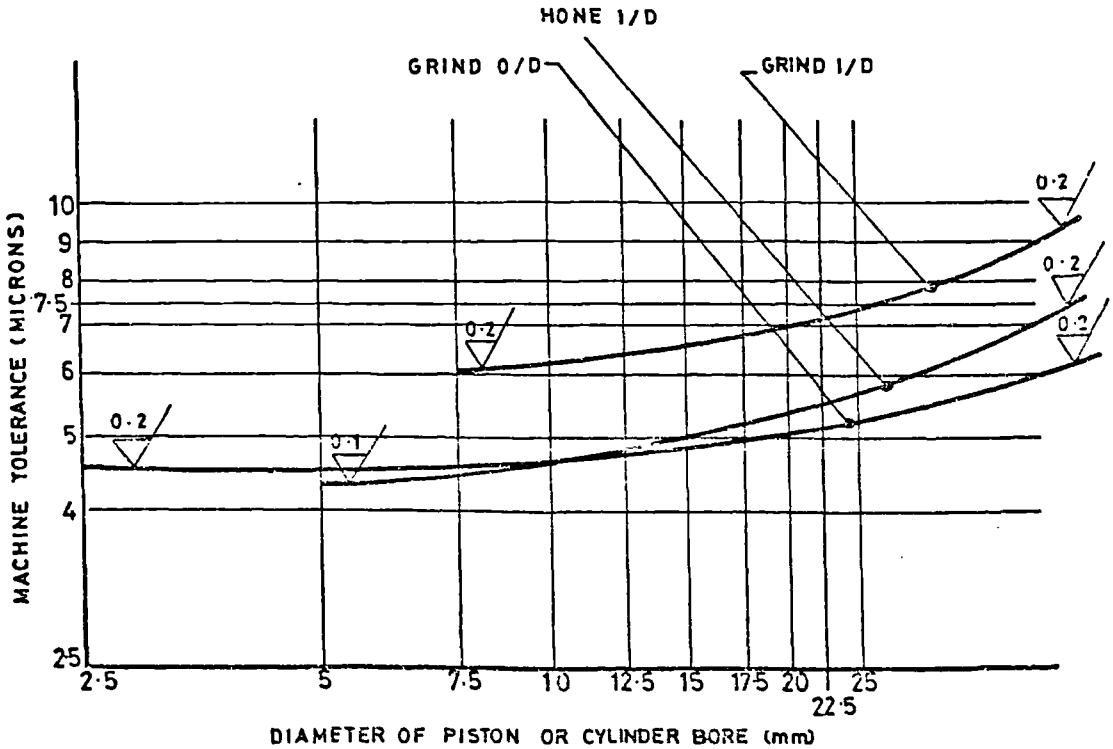

FIGURE 7.37. CHART OF ACCURACY AND SURFACE TEXTURE TO BE EXPECTED FROM GRINDING AND HONING OPERATIONS.

Choice of $\frac{C_d}{d_p}$ Ratio for Full Working Range of Pump

So far the choice of the $\frac{Cd}{dp}$ ratio for a specific set of working conditions has been considered but a pump is more frequently required to function efficiently over a range of speeds, pressures and flow rates governed by swashplate setting.

Referring to equation (7.34), it will be seen that as the mean piston velocity $\bar{V}_p$ is decreased, the pump parameter λ_p is increased and this results in a lower percentage loss of efficiency E_p. If therefore the losses at the piston are acceptable for the maximum swashplate angle, the losses will also be acceptable for all other angles of swashplate tilt. It is common practice for pump manufacturers to quote pump performance at maximum stroke conditions.

As regards the range of pump speed and pressure that must be taken into account, the best $\frac{Cd}{dp}$ ratios will be those that result in the lowest possible average percentage loss of efficiency being achieved.

a) $\frac{C_d}{d_p}$ Ratio for a speed range but with constant pressure and swashplate setting

Equation (7.34) -

$$E_p = 5{\cdot}73\left(\frac{Cd}{d_p}\right)^3 \lambda_p + 1600\left(\frac{Cd}{d_p}\right)^{-1} \lambda_p^{-1}$$

can be integrated with respect to the pump speed N between the limits of N_1 and N_2 and divided by (N_2-N_1) to give the average percentage loss of efficiency E_{pav}

$$E_{pav} = \frac{1}{(N_2-N_1)} \int_{N_1}^{N_2} \left[5{\cdot}73\left(\frac{Cd}{d_p}\right)^3 \lambda_{p1} \frac{N_1}{N} + 1600\left(\frac{Cd}{d_p}\right)^{-1} \lambda_{p1}^{-1} \frac{N}{N_1} \right] dN$$

$$= 5{\cdot}73\left(\frac{C_d}{d_p}\right)^3 \lambda_{P1} \frac{\log n}{(n-1)} + 800\left(\frac{C_d}{d_p}\right)^{-1} \lambda_{P1}^{-1}(n+1)$$

(7.38)

where $n = \frac{N_2}{N_1}$ and λ_{P1} is λ_P at $N = N_1$

Differentiating with respect to $\frac{Cd}{dp}$ and equating to zero will give -

$$17{\cdot}25 \frac{\log n}{(n-1)} \lambda_{P1} \left(\frac{C_d}{d_p}\right)^2 = 800(n+1) \lambda_{P1}^{-1} \left(\frac{C_d}{d_p}\right)^{-2}$$

So that -

$$\frac{C_d}{d_p}_{OPT(N_1 \rightarrow N_2)} = 2{\cdot}610 \sqrt[4]{\frac{n^2-1}{\log n}} \sqrt{\lambda_{P1}^{-1}}$$

(7.39)

b) $\frac{C_d}{d_p}$ Ratio for a pressure range but with constant speed and swashplate setting

Equation (7.34), can again be integrated with respect to pump pressure P between the limits of P_1 and P_2 and divided by (P_2-P_1) to give the average percentage loss of efficiency E_{PAV}

$$E_{PAV} = \frac{1}{(P_2-P_1)} \int_{P_1}^{P_2} \left[5{\cdot}73\left(\frac{C_d}{d_p}\right)^3 \lambda_{P1} \frac{P}{P_1} + 1600\left(\frac{C_d}{d_p}\right)^{-1} \lambda_{P1}^{-1} \frac{P_1}{P} \right] dP$$

$$= 2.865(p+1)\lambda_{P1}\left(\frac{Cd}{dp}\right)^3 + 1600\,\frac{\log p}{(p-1)}\,\lambda_{P1}^{-1}\left(\frac{Cd}{dp}\right)^{-1}$$

(7.40)

where $p = \frac{P_2}{P_1}$ and λ_{P1} is λ_P at $P = P_1$

Differentiating with respect to $\frac{Cd}{dp}$ and equating to zero will give -

$$8.595(p+1)\lambda_{P1}\left(\frac{Cd}{dp}\right)^2 = 1600\,\frac{\log p}{(p-1)}\,\lambda_{P1}^{-1}\left(\frac{Cd}{dp}\right)^{-2}$$

So that -

$$\frac{Cd}{dp}_{OPT(P_1 \to P_2)} = 3.694\sqrt[4]{\frac{\log p}{(p^2-1)}}\sqrt{\lambda_{P1}^{-1}}$$

(7.41)

c) $\frac{C_d}{d_p}$ Ratio for a pressure range and a speed range but with constant swashplate setting

Equation (7.34), can again be integrated with respect to pump pressure P between the limits of P_1 and P_2 and with respect to pump speed N between the limits of N_1 and N_2 and divided by (P_2-P_1) and by (N_2-N_1) to give the average percentage loss of efficiency E_{pav}

$$E_{pav} = \frac{1}{(P_2-P_1)(N_2-N_1)}\int_{P_1}^{P_2}\int_{N_1}^{N_2}\left[5.73\left(\frac{Cd}{dp}\right)^3\lambda_{P1}\frac{P}{P_1}\frac{N_1}{N} + 1600\left(\frac{Cd}{dp}\right)^{-1}\lambda_{P1}^{-1}\frac{P_1}{P}\frac{N}{N_1}\right]dP\,dN$$

$$= 2{\cdot}865\left(\frac{Cd}{dp}\right)^{3}\lambda_{P1}\frac{(p+1)}{(n-1)}\log n + 800\left(\frac{Cd}{dp}\right)^{-1}\lambda_{P1}^{-1}\frac{(n+1)}{(p-1)}\log p \qquad (7.42)$$

where $p = \frac{P_2}{P_1}$; $n = \frac{N_2}{N_1}$ and λ_{P1} is λ_p at $P = P_1$; $N = N_1$

Differentiating with respect to $\frac{Cd}{dp}$ and equating to zero will give -

$$8{\cdot}595\frac{(p+1)}{(n-1)}\log n\,\lambda_{P1}\left(\frac{Cd}{dp}\right)^{2} = 800\frac{(n+1)}{(p-1)}\log p\,\lambda_{P1}^{-1}\left(\frac{Cd}{dp}\right)^{-2}$$

So that -

$$\frac{Cd}{dp}_{OPT\left(\substack{P_1\to P_2\\ N_1\to N_2}\right)} = 3{\cdot}106\sqrt[4]{\frac{(n^2-1)}{(p^2-1)}\frac{\log p}{\log n}}\sqrt{\lambda_{P1}^{-1}}$$

$$= \sqrt[4]{\frac{(n^2-1)}{(p^2-1)}\cdot\frac{\log p}{\log n}}\cdot\frac{Cd}{dp}_{OPT\left(\substack{P_1\\ N_1}\right)} \qquad (7.43)$$

Fig.7.38, shows a set of curves based on equation (7.43) and which enable the easy determination of the optimum diametral clearance for a pump required to satisfy a range of pressures and pump speeds. A comparison between the optimum diametral clearance for a range of pressures and speeds and optimum diametral clearance at the low pressure and speed values is given in Table 7.3.

It will be seen that the effects of optimising for a range of working conditions can be appreciable and can result in a relatively large decrease or increase in the actual piston clearance. The design decision on the pump working range of pressure and speed to be accommodated is a difficult one since as indicated in Fig.7.33, values of

	$\frac{\text{Cd OPT}\begin{pmatrix}P_1 \to P_2\\ n_1 \to n_2\end{pmatrix}}{\text{Cd OPT}\begin{pmatrix}P_1\\ n_1\end{pmatrix}}$			
P	n = 1	n = 2	n = 3	n = 4
1	1	1.777	2.034	2.234
2	.563	1	1.140	1.258
3	.494	.878	1	1.104
4	.448	.796	.907	1

Table 7.3 Table of $\frac{\text{Cd OPT}\begin{pmatrix}P_1 \to P_2\\ n_1 \to n_2\end{pmatrix}}{\text{Cd OPT}\begin{pmatrix}P_1\\ n_1\end{pmatrix}}$

Ratios for a Range of Working Conditions of Pressure & Speed

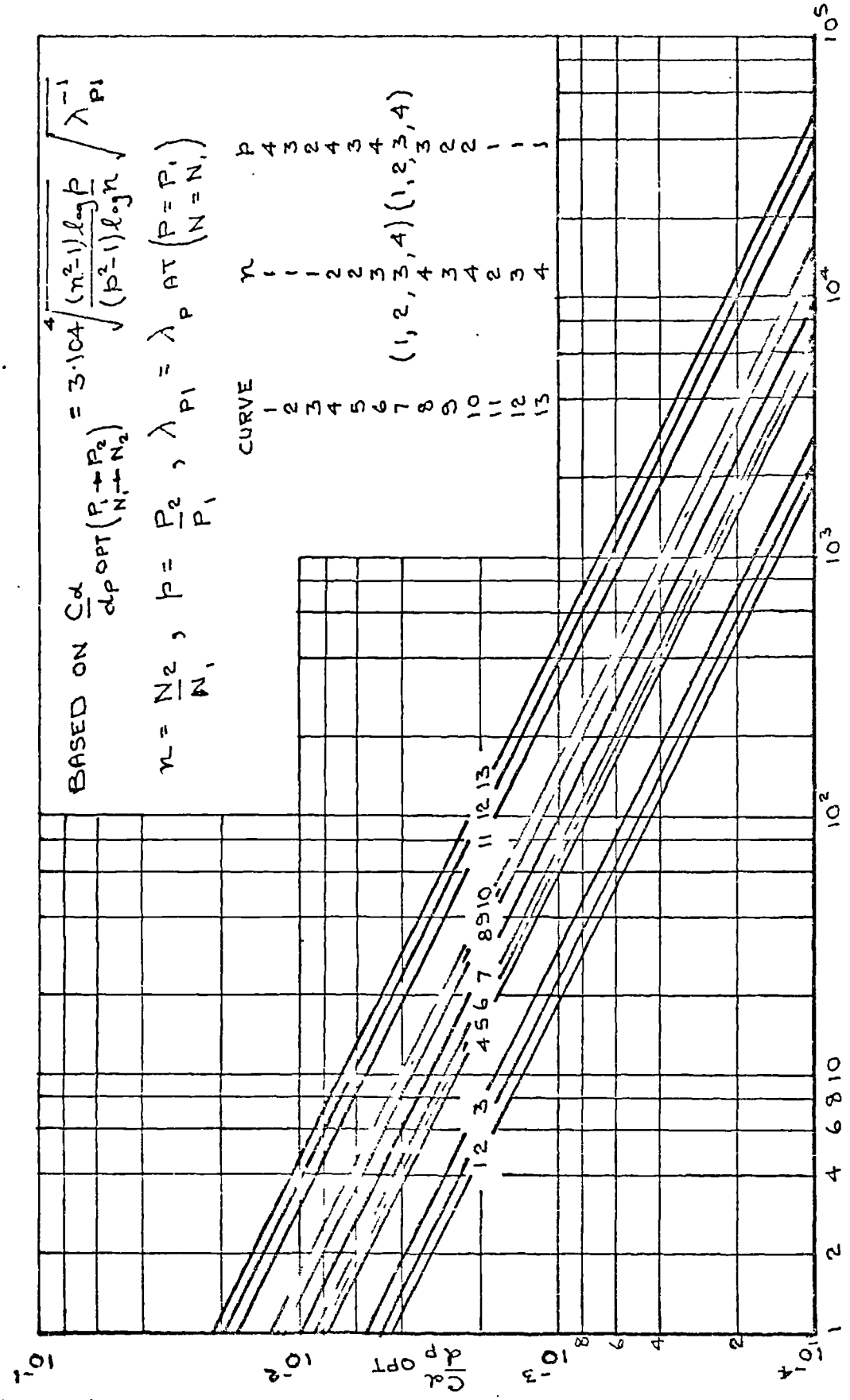

FIGURE 7.38. CURVES FOR OPTIMUM $\frac{C_d}{d_p}$ RATIO FOR A RANGE OF PRESSURES AND SPEED BUT WITH CONSTANT SWASHPLATE SETTING.

$\frac{Cd}{dp}$ away from the optimum values lying on curve A can result in a fairly high percentage increase in losses of efficiency.

Strength of Piston

The piston has to withstand forces arising from the pressure of the hydraulic fluid and dynamic reactions from the slipper bearing and the cylinder bore. A decision has to be made at an early stage of the design process on the possibility of hollow pistons which have a weight advantage over solid pistons. For high speed pumps the lower piston mass will appreciably reduce the inertia forces. However, a disadvantage is that the hollow piston increases the compressibility losses as discussed in Section 5.2.3. Some manufacturers have experimented with hollow steel pistons which have been filled with a strong low density material but reports on this innovation are not encouraging as the manufacturing costs of the piston is appreciably increased.

The stresses induced into solid pistons are easily accommodated by the metal but with hollow pistons care must be taken when deciding on the thickness of the tubular portion. The internal fluid pressure will tend to increase the outside diameter of the piston and induce hoop stresses. Thus the wall thickness must be such that the stresses are within reasonable working limits and the increase in the piston diameter is restricted to maintain adequate working clearance between the piston and the cylinder bore.

Using Thin Wall theory -

$$\text{Hoop stress } \sigma = \frac{P\, d_{pi}}{2\, t_p} \qquad (7.44)$$

d_{pi} = internal diameter of the piston

t_p = wall thickness of the piston

Increase of Piston Diameter

$$\Delta d_p = \frac{\Delta P \, d_{pi}}{2 E \, t_p} \qquad (7.45)$$

E = Modulus of elasticity of piston material

Slipper Bearing Design

Another area of special consideration in the design of axial piston pumps is that of the slipper bearings. Slipper bearings are commonly swaged onto a ball joint at the end of the piston to form a permanent assembly. In operation the slipper bearing transmits thrust from the inclined swashplate to stroke the piston and as this thrust can be of a high order when the pump pressure is high, unless special care is taken in design, the resulting power losses at the slipper bearing and component wear can be far from satisfactory.

For these reasons the slipper bearing is usually in the form of a circular hydrostatic pad and a bleed of fluid from the pressure side of the piston is used to form a load carrying film to separate the surfaces of the slipper bearing and the swashplate. When this is achieved the wear is reduced to that which takes place during the period of start up and stopping the pump when sufficient pressure is not available to lift the slipper bearing away from the swash-plate surface. Again the fluid film will have a low viscous drag which is likely to be less than the coulomb friction if contact occurred between the slipper bearing and the swashplate.

The normal fluid pressure force acting on the slipper bearing from (5.39) is equal to the normal component pressure force on the piston if in the first instance the acceleration and friction forces are ignored. Then -

$$R_{SP} = \frac{\pi}{4} d_p^2 P_1 \sec\phi = \frac{\pi}{8} P_f \frac{(D_2^2 - D_1^2)}{\log_e\left(\frac{D_2}{D_1}\right)}$$

to give -

$$P_f = \frac{2 P_1 d_p^2 \log_e\left(\frac{D_2}{D_1}\right) \sec \phi}{(D_2^2 - D_1^2)} \tag{7.48}$$

If the pressure in the annulus of the pad is maintained constant then from equation (5.40) the flow rate from the pad is -

$$Q_{SB} = \frac{P_f \pi h^3}{6 \mu \log_e\left(\frac{D_2}{D_1}\right)} \tag{7.49}$$

to give -

$$Q_{SB} = \frac{\pi P_1 d_p^2 h^3 \sec \phi}{3 \mu (D_2^2 - D_1^2)} \tag{7.50}$$

where h is the film thickness.

If a capillary hole is used as a control choke then from (5.4) -

$$Q_{SB} = \frac{(P_1 - P_f) \pi d_R^4}{128 \mu \ell_R} \tag{7.51}$$

where d_R is the diameter of the capillary hole and ℓ_R is its length.

The power loss associated with fluid flow due to pressure difference is the product of the pressure and the flow rate and as this occurs only when the piston is pressurised for approximately half a revolution of the pump, this loss is -

$$P_P = \frac{\pi P_1^2 d_p^2 h^3 \sec \phi}{6 \mu (D_2^2 - D_1^2)} \tag{7.52}$$

The viscous drag from the fluid film is given by equation (5.43) and the viscous drag torque will be -

$$M_v = \frac{\pi^2}{2} \frac{\mu}{h} r_e^2 N \left(D_2^2 - D_1^2\right) \tag{7.53}$$

where r_e is the effective radius of the slipper bearing path. Shute and Turnbull (29) have shown that r_e^2 can be expressed as -

$$r_e^2 = r_c^2 \left(1 + f(\phi)\right) \tag{7.54}$$

where

$$f(\phi) = \frac{(\sec\phi - 1)^2}{2} + \ell_{SB}^2 \frac{\tan^2\phi}{2 r_c^2} + \frac{4}{\pi}(\sec\phi - 1)$$

If the fluid gap remains constant during a pump revolution, the viscous drag power loss can be expressed as -

$$P_S = \pi^3 \frac{\mu}{h} r_c^2 \left(1 + f(\phi)\right) N^2 \left(D_2^2 - D_1^2\right) \tag{7.55}$$

A reduction in the viscous drag power loss will result from an increase in the gap during the suction half of the pump rotation when the force on the slipper bearing acts to increase the gap. The increased gap can be controlled by the slipper bearing retention plate.

The theoretical power associated with a slipper bearing during one revolution of the pump is the rate of displacement of the piston times the pump pressure. Thus -

$$P_T = \frac{\pi}{2} d_p^2 r_c N P_1 \tan\phi \tag{7.56}$$

Shute and Turnbull (29) suggest that the performance of a slipper bearing can be expressed as a percentage loss of efficiency, i.e.,

$$E_{SB} = 100 \left[\frac{P_p + P_s}{P_T} \right]$$

Substituting for P_p, P_s and P_T

$$E_{SB} = 100 \left[\frac{\frac{\pi P_1^2 d_p^2 h^3 \sec\phi}{6\mu(D_2^2 - D_1^2)} + \pi^3 \frac{\mu}{h} r_c^2 (1 + f(\phi))(D_1^2 - D_2^2)}{\frac{\pi}{2} d_p^2 r_c N P_1 \tan\phi} \right]$$

or

$$E_{SB} = 33.33 \left(\frac{h}{d_p} \right)^3 \lambda_{SB} \operatorname{cosec}\phi + 1974 \left(\frac{h}{d_p} \right)^{-1} \lambda_{SB}^{-1} \frac{(1 + f(\phi))}{\tan\phi} \qquad (7.57)$$

where

$$\lambda_{SB} = \frac{P_1 d_p^3}{\mu r_c N (D_2^2 - D_1^2)} \qquad (7.58)$$

Percentage efficiency losses can be calculated from this equation or obtained directly from Fig.7.39, which has been compiled for the general limits of -

$(P_1 - P_2)$ up to 400 bar

up to 30 mm

up to 120 mm

up to 60 rev/s

from 0.01 to 0.20 Ns/m^2,

and a swashplate angle of 20°. Figs. 7.40, 7.41 and 7.42 are similar percentage efficiency loss curves for swashplate angles of 15°, 10° and 5° respectively.

BASED ON $E_{SB} = 33{\cdot}33 \left(\frac{h}{dp}\right)^3 \lambda_{SB}$ COSEC $\phi + 1974 \left(\frac{h}{dp}\right)^{-1} \lambda_{SB}^{-1} \left(\frac{1 + f(\phi)}{\text{TAN } \phi}\right)$

$\lambda_{SB} = \frac{P_1 \, dp^3}{\mu_{ef} r_c N (D_2^2 - D_1^2)}$

CURVE A INDICATES MINIMUM LOSSES FOR FIXED VALUES OF λ_{SB}
CURVE B INDICATES MINIMUM LOSSES FOR FIXED VALUES OF $\frac{h}{dp}$

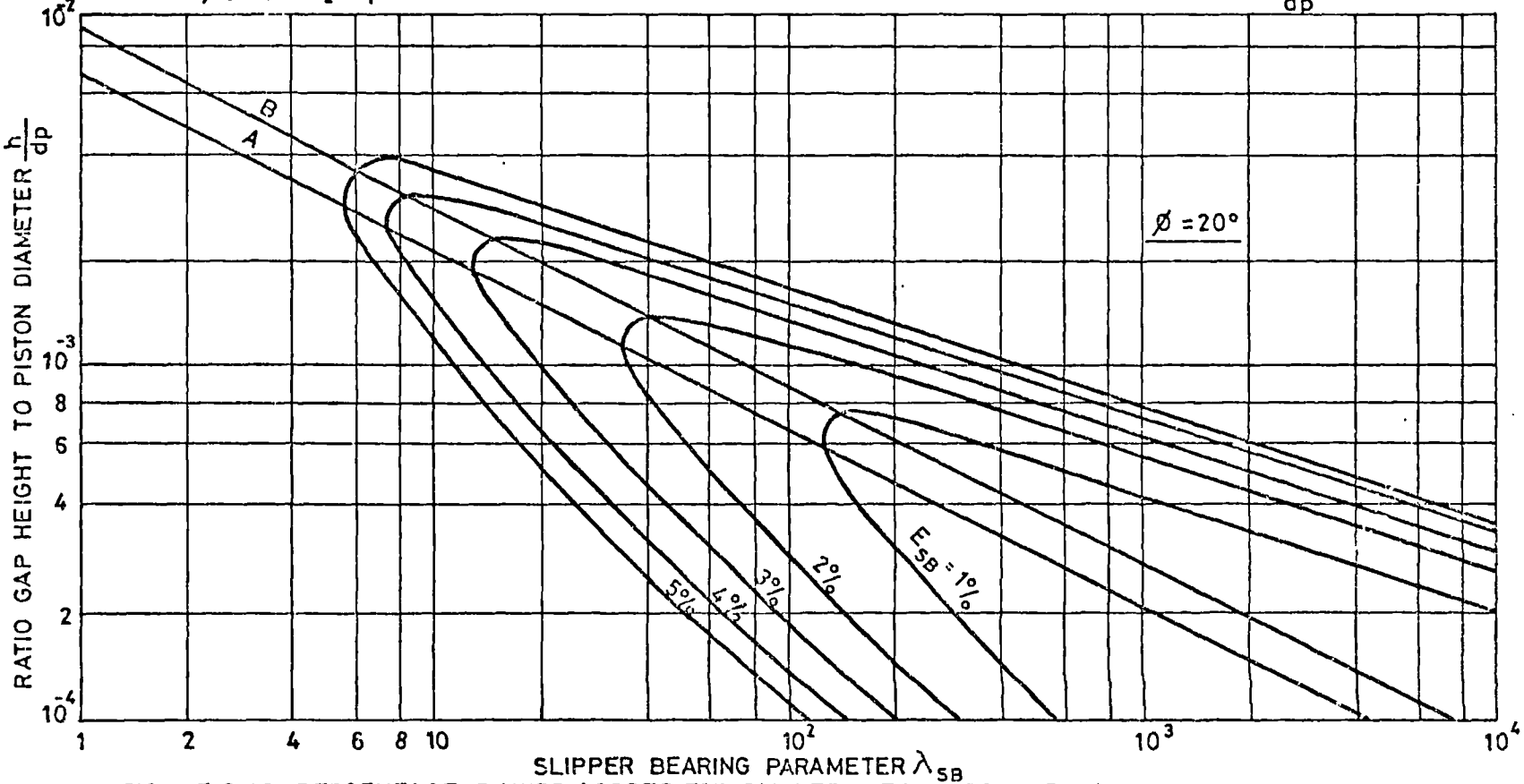

FIGURE 7.39. PERCENTAGE POWER LOSSES FOR SLIPPER BEARINGS WITH 20° SWASHPLATE ANGLE

BASED ON $E_{SB} = 33{\cdot}33\left(\frac{h}{dp}\right)^{3}\lambda_{SB}\,\text{COSEC}\,\phi + 1974\left(\frac{h}{dp}\right)^{-1}\lambda_{SB}^{-1}\left(\frac{1+f(\phi)}{\tan\phi}\right)$

$\lambda_{SB} = \frac{P\,dp^{3}}{\mu_{ef}\,r_c\,N(D_2^2 - D_1^2)}$

CURVE A INDICATES MINIMUM LOSSES FOR FIXED VALUES OF λ_{SB}
CURVE B INDICATES MINIMUM LOSSES FOR FIXED VALUES OF $\frac{h}{dp}$.

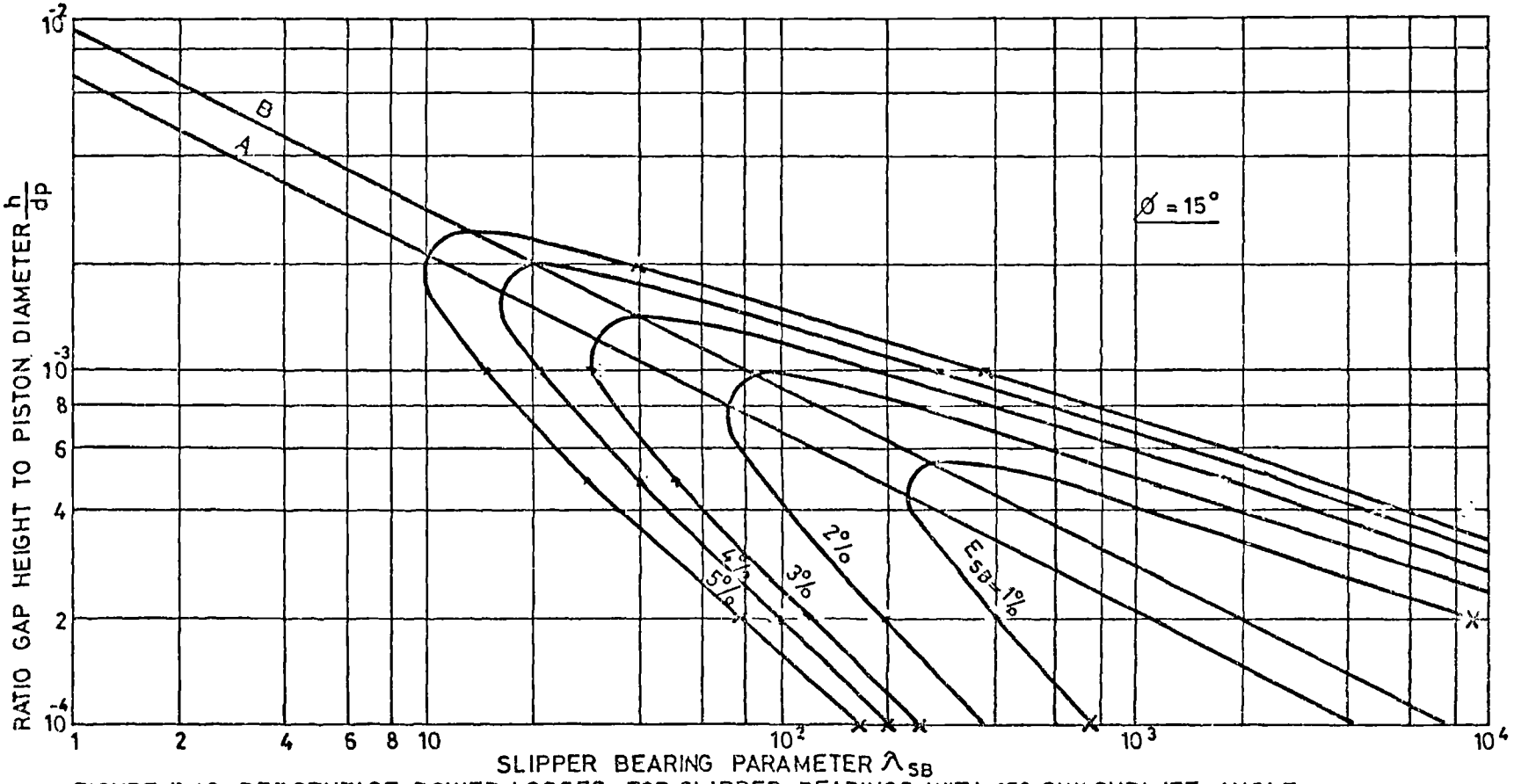

FIGURE 7.40. PERCENTAGE POWER LOSSES FOR SLIPPER BEARINGS WITH 15° SWASHPLATE ANGLE.

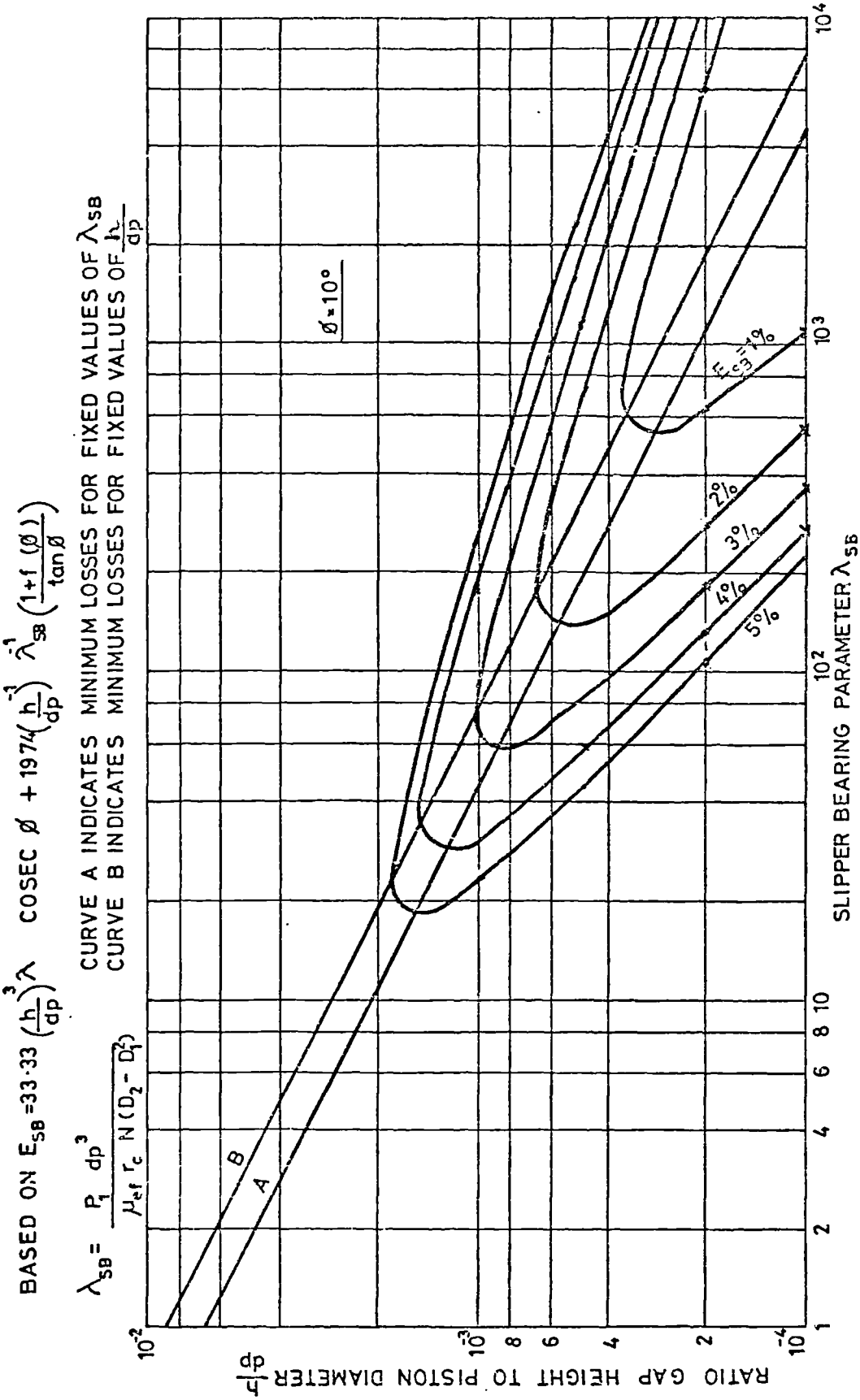

FIGURE 7.41. PERCENTAGE POWER LOSSES FOR SLIPPER BEARINGS WITH 10° SWASHPLATE ANGLE.

BASED ON $E_{SB} = 33{\cdot}33\left(\frac{h}{dp}\right)^{3}\lambda_{SB}\ \text{COSEC}\ \phi + 1974\left(\frac{h}{dp}\right)^{-1}\lambda_{SB}^{-1}\left(\frac{1+f(\phi)}{\text{TAN}\ \phi}\right)$

$\lambda_{SB} = \frac{P_1\ dp^3}{\mu_{el}\ r_c\ N(D_2 - D_1^2)}$

CURVE A INDICATES MINIMUM LOSSES FOR FIXED VALUES OF λ_{SB}

CURVE B INDICATES MINIMUM LOSSES FOR FIXED VALUES OF $\frac{h}{dp}$

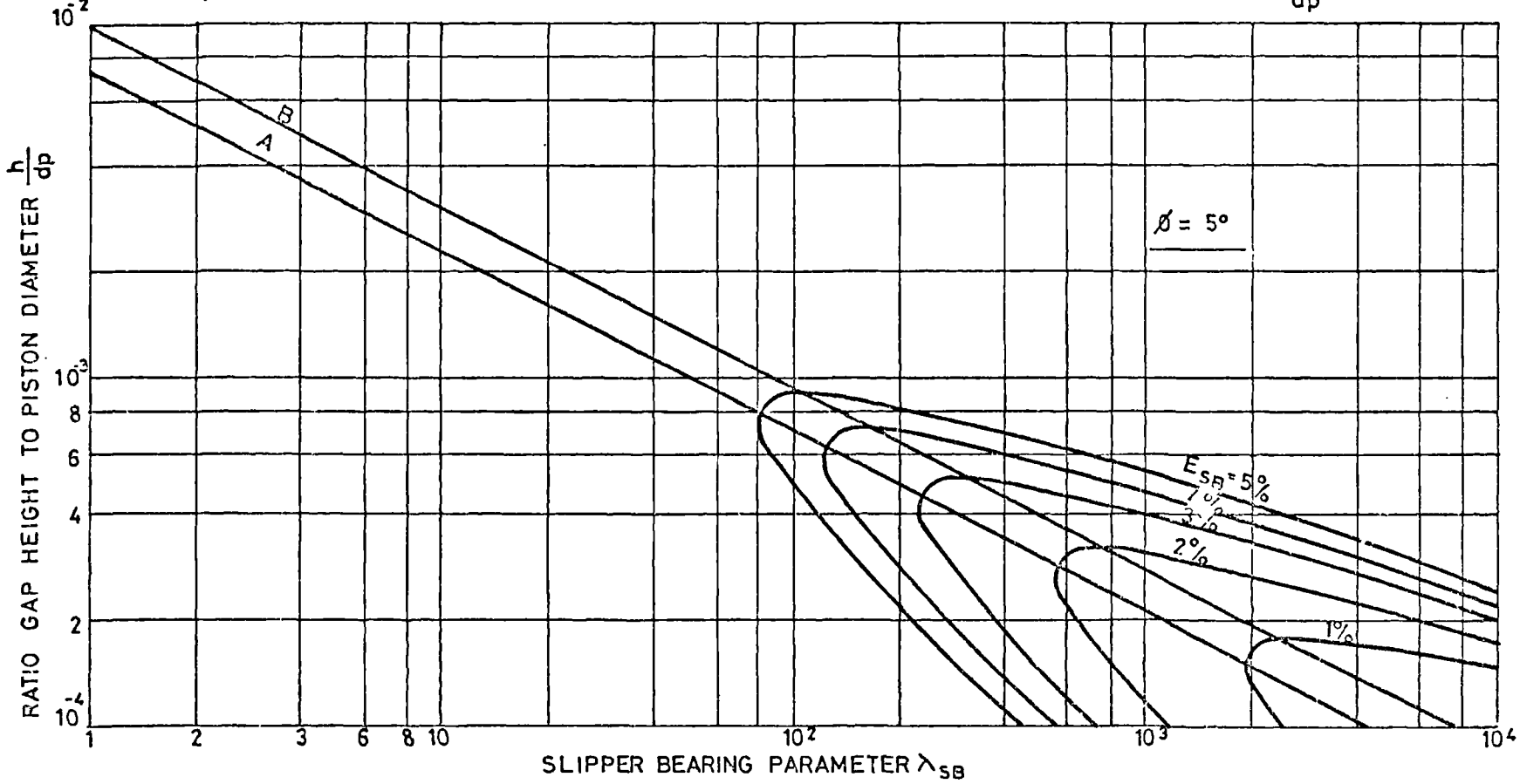

FIGURE 7.42 PERCENTAGE POWER LOSSES FOR SLIPPER BEARINGS WITH 5° SWASHPLATE ANGLE

The optimum $\left(\frac{h}{d_p}\right)$ ratio may be derived by reverting to the power loss equation -

$$P_L = P_p + P_s$$

$$P_L = \frac{\pi P_1^2 d_p^2 h^3 \sec\phi}{6\mu(D_2^2 - D_1^2)} + \pi^3 \frac{\mu}{h} r_c^2 N^2 (D_2^2 - D_1^2)(1 + f(\phi))$$

(7.59)

Then -

$$\frac{P_L}{\frac{\pi P_1^2 d_p^5 \sec\phi}{6(D_2^2 - D_1^2)}} = \left(\frac{h}{d_p}\right)^3 + \frac{\pi^2 \mu^2 r_c^2 N^2 (D_2^2 - D_1^2)(1 + f(\phi))}{P_1^2 d_p^6 \sec\phi}$$

Differentiating with respect to $\left(\frac{h}{d_p}\right)$ and equating to zero -

$$\left(\frac{h}{d_p}\right) = \sqrt[4]{\frac{2\pi^2 \mu^2 r_c^2 N^2 (D_2^2 - D_1^2)^2 (1 + f(\phi))}{P_1^2 d_p^6 \sec\phi}}$$

To give for minimum power loss -

$$\left(\frac{h}{d_p}\right)_{OPT} = 2.108 \sqrt{\lambda_{SB}^{-1}} \sqrt[4]{\frac{1 + f(\phi)}{\sec\phi}}$$

(7.60)

For swashplate angles 0° to 20°, will vary from 1 to 1.017 so that taking an average value of 1.0085 gives -

$$\left(\frac{h}{d_p}\right)_{OPT} = 2.125 \sqrt{\lambda_{SB}^{-1}}$$

(7.61)

In a similar manner an equation for the value of λ_{SB} which will give the minimum power loss for a fixed value of $\left(\frac{h}{d_p}\right)$ can be derived by differentiating equation (7.59) with respect to λ_{SB} and equating to zero. To obtain -

$$\lambda_{SB\,OPT} = 7{\cdot}761\sqrt{\left(\frac{h}{d_p}\right)^{-1}} \tag{7.62}$$

Choice of $\frac{h}{dp}$ Ratio for Full Working Range of Pump

As in the section dealing with the choice of piston diametral clearance to piston diameter ratio for the full working range of speed and pressure, it is also necessary to determine the $\frac{h}{dp}$ ratio for the slipper bearing which will result in the least average percentage loss of efficiency over the full working range of speed and pressure of the pump.

Using similar methods to those developed for piston clearances:

a) $\frac{h}{dp}$ Ratio for a Speed Range but with Constant Pressure.

$$\left(\frac{h}{d_p}\right)_{OPT\,(N_1 \to N_2)} = 1{\cdot}788\sqrt[4]{\frac{n^2-1}{\log n}}\sqrt{\lambda_{SB1}^{-1}} \tag{7.63}$$

where $n = \frac{N_2}{N_1}$ and λ_{SB1} is λ_{SB} at $N = N_1$

b) $\frac{h}{dp}$ Ratio for a Pressure Range but with Constant Speed.

$$\left(\frac{h}{d_p}\right)_{OPT\,(P_1 \to P_2)} = 2{\cdot}528\sqrt[4]{\frac{\log p}{(p^2-1)}}\sqrt{\lambda_{SB1}^{-1}} \tag{7.64}$$

where $p = \frac{P_2}{P_1}$ and λ_{SB1} is λ_{SB} at $P = P_1$

c) $\frac{h}{dp}$ Ratio for a Pressure Range and a Speed Range.

$$\left(\frac{h}{d_p}\right)_{OPT}\left(\frac{P_1 - P_2}{N_1 - N_2}\right) = 2.125\sqrt{\frac{(n^2-1)\log p}{(p^2-1)\log n}}\sqrt{\lambda_{SBI}^{-1}} \qquad (7.65)$$

$$= \sqrt{\frac{(n^2-1)\log p}{(p^2-1)\log n}}\left(\frac{h}{d_p}\right)_{OPT}\left(\frac{P_1}{N_1}\right)$$

The optimum $\frac{h}{dp}$ ratio for a pump to suit a pressure range and a speed range can be readily determined from Fig.7.43. A flow chart is given in Fig.7.44, for determining the Slip Flow, Power Loss and Temperature Rise for a Slipper Bearing.

Slipper Bearing Gap Height

It will be appreciated that the larger the slipper bearing gap height the greater will be the possibility that contact between the pad and the swashplate will not occur during pump operation. An increase in the gap height will reduce the viscous drag losses but at the expense of an increase in the pressure flow losses.

A minimum gap height, however, is indicated by the physical conditions at the slipper bearing/swashplate interface and by the degree of filtration that the pump enjoys. Thus:

a) the design gap height must be greater than the combined roughness of the surfaces and of surface distortion under load. A reasonable manufacturing surface finish for both surfaces is 0.4 μm which gives asperities with trough to peak heights of up to 3.2 μm for ground surfaces. For such conditions, minimum gaps of some 6 μm are indicated.

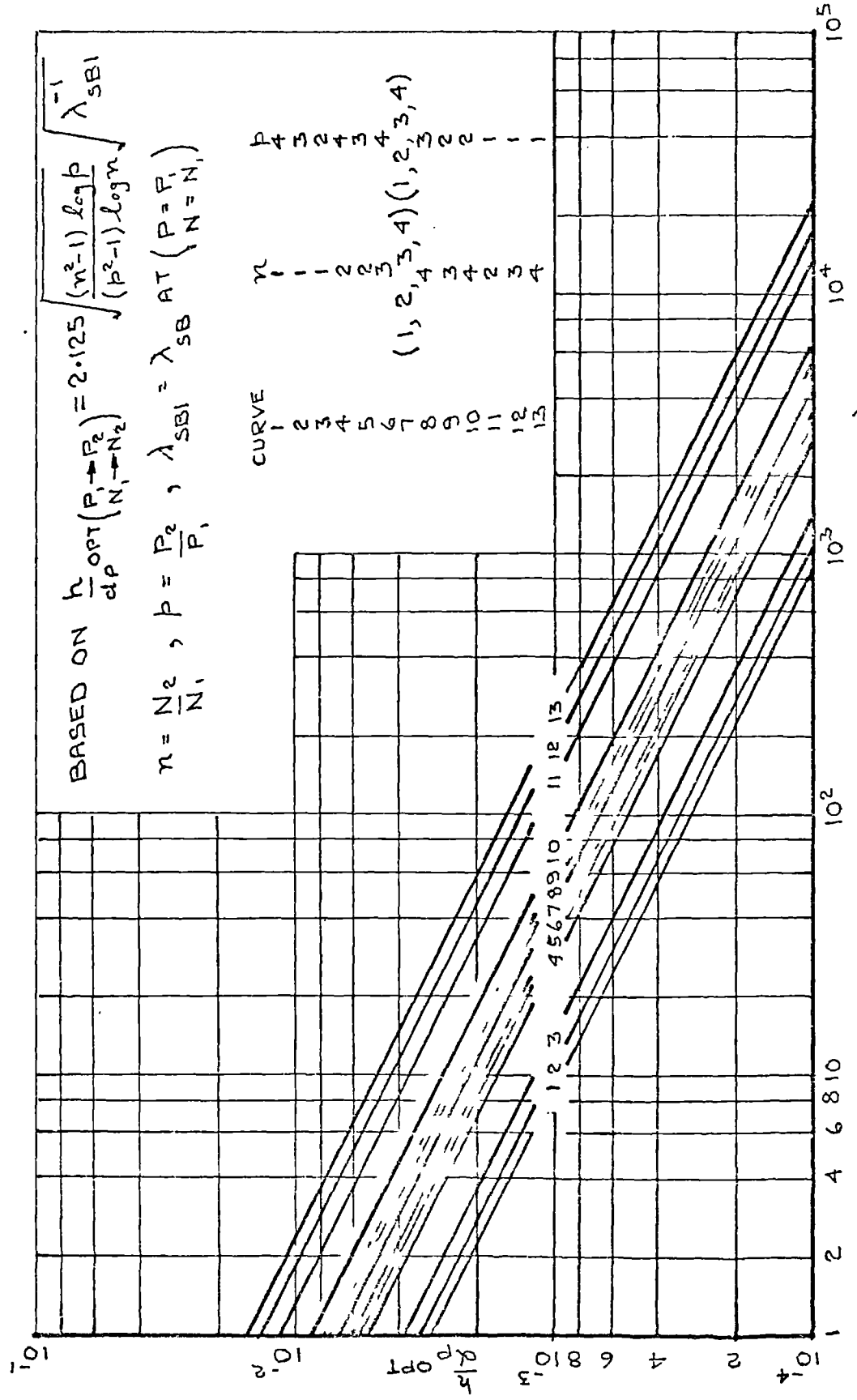

FIGURE 7.43. CURVES FOR OPTIMUM $\frac{h}{d_p}$ RATIO FOR A RANGE OF PRESSURES AND SPEED BUT WITH 20° SWASHPLATE

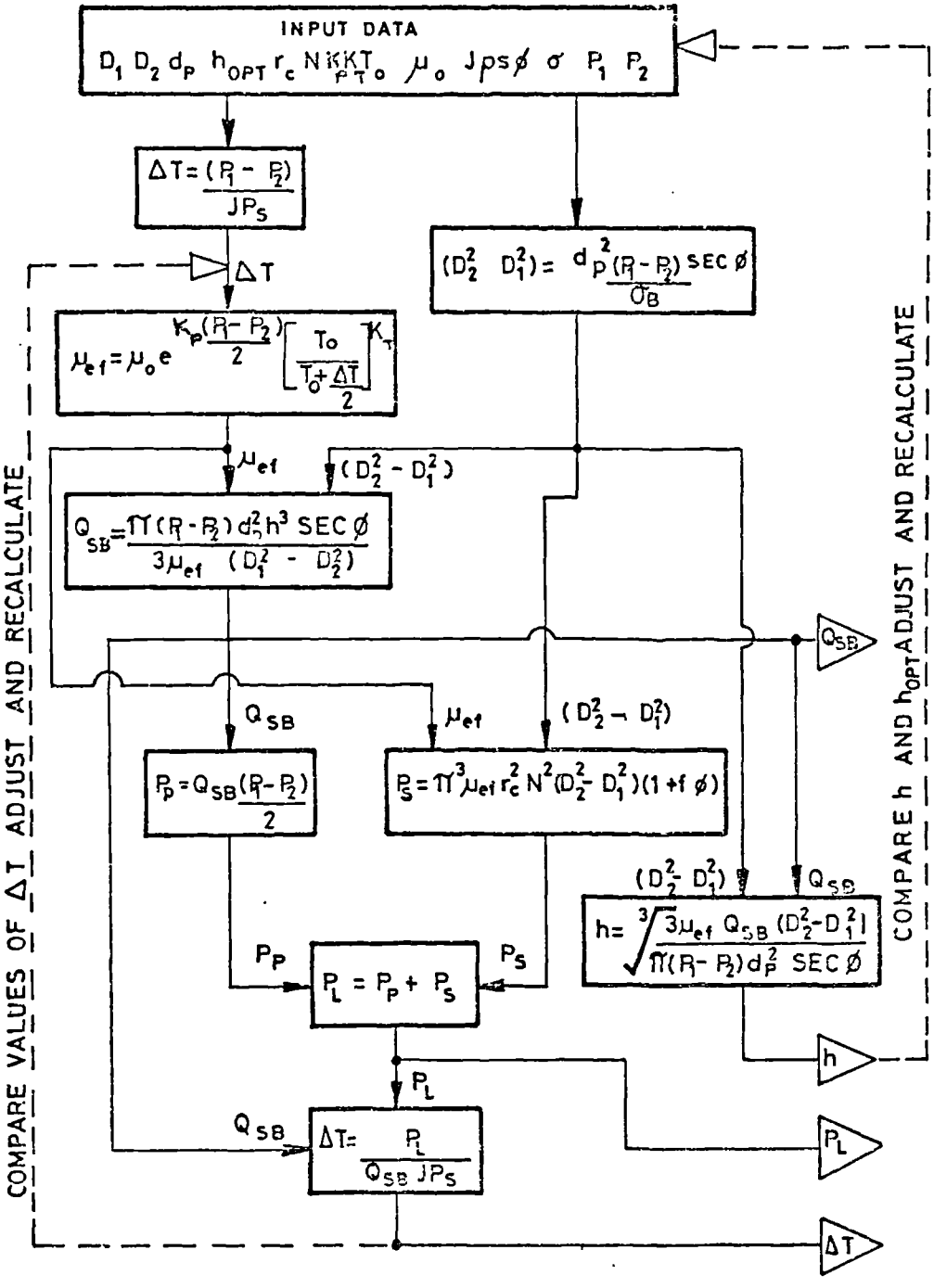

FIGURE 7.44. FLOW CHART FOR DETERMINING THE POWER LOSS, SLIP FLOW AND TEMPERATURE RISE FOR A SLIPPER BEARING.

However, Edghill and Rubery (24) have found surface deterioration of up to 3 μm on axial pump swashplates which suggest a height more closely related to 12 μm. In general it is not difficult to ensure that the swashplate does not distort unduly under load and that changes to the surface flatness is not affected by thermal expansion;

b) the gap height should be larger than the size of the largest contaminant in the hydraulic fluid. This will in the main be controlled by the level of filtration but a possibility will always exist that wear debris will enter the gap without passing through the filter. Large impurities will be unable to enter the gap except via the capillary choke but it is generally agreed that particles just smaller than the gap height can enter and be embedded in the slipper bearing surface to subsequently act as lapping agents against the swashplate surface;

c) heat is generated by the pressure flow and viscous drag losses and the gap height must allow sufficient fluid flow to ensure that the rise in fluid temperature is not excessive. Fluid degradation suggests a limit of 30°C temperature rise;

d) the gap height should be adequate to match the inherent axial and tilting stiffness of the slipper bearing. During a pump cycle axial forces on the slipper bearing will vary appreciably as indicated in Section 5.3.1, and Helgestad, Foster and Bannister (14) have shown the extent to which pressure transients occur. In addition, the slipper bearing couple has to be accommodated by the hydrostatic pressure distribution of the pad and the hydrodynamic

effect on the inclined face of the bearing. Too small a design gap will make this difficult and will result in surface contact despite a high tilting stiffness for the slipper bearing.

In view of these considerations, it would seem that with a level of filtration of 10 μm, a minimum gap height of 12 μm is called for low power pumps whereas with the increased surface speed and power losses of larger units, 15 μm would seem to be more appropriate.

Axial and Tilting Stiffness of Slipper Bearing

The axial and tilting stiffnesses of a slipper bearing will determine the change in the gap height and in the angular attitude of the slipper bearing with changes of load and couple.

Considering the force on a piston as consisting only of the pressure component and neglecting frictional and inertial forces, then F_p can be expressed as -

$$F_p = \frac{\pi}{8} P_f \frac{(D_2^2 - D_1^2)}{\log\left(\frac{D_2}{D_1}\right)} \cos\phi \qquad (7.66)$$

But the volume flow rate through the slipper bearing is given by equations (7.49) and (7.50) so that -

$$\frac{\pi P_f h^3}{6\mu \log\left(\frac{D_2}{D_1}\right)} = \frac{(P_1 - P_f)\pi d_R^4}{128 \mu l_R}$$

Equating these equations gives -

$$F_p = \frac{\pi P_1 d_R^4 (D_2^2 - D_1^2) \cos\phi}{8\left[\frac{64}{3} h^3 l_R + d_R^4 \log\left(\frac{D_2}{D_1}\right)\right]} \qquad (7.67)$$

The axial stiffness S_{SB} can be defined as $\frac{\partial F_p}{\partial h}$ and so -

$$S_{SB} = -\frac{3\pi}{8}\left[\frac{P_1 d_R^4 (D_2^2 - D_1^2)\cos\phi}{\frac{64}{3} h^4 \ell_R}\right] \tag{7.68}$$

Shute and Turnbull (30) express this conveniently as -

$$S_{SB} = -3\frac{F_p}{h}\left[1 + \frac{2 d_p^2 \log\left(\frac{D_2}{D_1}\right)}{(D_2^2 - D_1^2)\cos\phi}\right]$$

where from equation (7.48) -

$$\frac{P_f}{P_1} = \frac{2 d_p^2 \log\left(\frac{D_2}{D_1}\right)}{(D_2^2 - D_1^2)\cos\phi}$$

so that -

$$S_{SB} = -3\frac{F_p}{h}\left[1 + \frac{P_f}{P_1}\right] \tag{7.69}$$

It will be seen that the axial stiffness increases with the pump pressure P_1 so that transient forces on the slipper bearing due to non-pressure sources are better accommodated at the higher pump pressures. Again it will be seen that an increased ratio of the outside diameter to recess diameter for the slipper bearing will also increase the bearing stiffness.

Since a pump must generally work over a range of pressures, speeds and swashplate angles it is convenient to consider the slipper bearing in terms of an axial stiffness coefficient $\bar{S}_{SB}$ where -

$$\bar{S}_{SB} = \frac{S_{SB}}{\left(-\frac{F_R}{h}\right)}$$

$$= 3\left[1 + \frac{P_f}{P_1}\right] \tag{7.70}$$

Fisher (31) and Bennett (32) have shown that if the bearing surface of a slipper pad is inclined to the surface of a swashplate, an inherent righting moment is produced. In Section 5.3.1, it was seen that a couple C_{SB} is produced on a slipper bearing due to the mass of the slipper bearing being eccentric to the spherical bearing. Again in operation, a disturbing couple will result from the viscous drag between the slipper bearing and the swashplate of value -

$$M_{SB} = \frac{\pi^2}{2} \frac{(D_2^2 - D_1^2)}{h} \mu N r_c \ell_{SB} \tag{7.71}$$

Couples C_{SB} and M_{SB} are basically acting at right angles to one another with M_{SB} as the major component.

Fisher (31) derived an expression for the righting moment as -

$$M'_{SB} = \pi P_f D_2^3 \left[f_1\left(\frac{D_1}{D_2}\right)\varepsilon + f\left(\frac{D_1}{D_2}\right)\varepsilon + \cdots \right] \tag{7.72}$$

where ε is the ratio of the angle of tilt to that at which contact would occur between the slipper bearing and the swashplate, and where -

$$f_1\left(\frac{D_1}{D_2}\right) = \frac{3}{256} \left[\frac{\left(1 + \left(\frac{D_1}{D_2}\right)^2\right)\left(1 - \left(\frac{D_1}{D_2}\right)^2\right)}{\log\left(\frac{D_2}{D_1}\right) - 4\left(\frac{D_1}{D_2}\right)^2} \right]$$

and $f_2\left(\frac{D_1}{D_2}\right)\varepsilon^3$ is so small that it can be neglected.

The tilting stiffness can be defined as -

$$S'_{SB} = \left. \frac{\partial M}{\partial \varepsilon} \right|_{\varepsilon \longrightarrow 0}$$

so that

$$S'_{SB} = \pi P_f D_2^2 f_1\left(\frac{D_1}{D_2}\right) \tag{7.73}$$

Substituting for P_f from equation (7.48) -

$$S'_{SB} = \frac{3\pi P_1 d_p^2 D_2}{128 \cos\phi}\left[\left(1+\left(\frac{D_1}{D_2}\right)^2\right) + \frac{4\left(\frac{D_1}{D_2}\right)\log\left(\frac{D_2}{D_1}\right)}{\left(1-\left(\frac{D_2}{D_1}\right)^2\right)}\right]$$

and the tilting stiffness coefficient $\bar{S}'_{SB}$ as -

$$\bar{S}'_{SB} = \frac{D_2}{d_p}\left[\left(1+\left(\frac{D_1}{D_2}\right)^2\right) + \frac{4\left(\frac{D_1}{D_2}\right)\log\left(\frac{D_2}{D_1}\right)}{\left(1-\left(\frac{D_1}{D_2}\right)^2\right)}\right] \qquad (7.74)$$

where

$$\bar{S}'_{SB} = \frac{S'_{SB}}{\frac{3\pi P_1 d_p^3}{128\cos\phi}}$$

Curves presented by Shute and Turnbull (30) give variations of axial and tilting stiffness coefficients with slipper bearing and piston parameters. It will be seen that the tilting stiffness increases with the pump pressure and with the outside diameter of the slipper bearing.

Pump Shaft Design

The pump shaft design must cater for:

a) a variety of prime movers with differing torsional characteristics;

b) a maximum level of torque and bending moment;

c) an acceptable working life during which time combinations of torque and bending stresses will occur many thousands of times.

The coupling of the pump shaft to the prime mover will require special consideration. For the type of pump under consideration, direct drive is likely without the need to accommodate high overhanging loads. Economically a keyed shaft has advantages but the likelihood of premature

fatigue failure is high. It would therefore seem that the drive should be through a splined shaft end, preferably of the involute tooth type which offer the following advantages:

i) maximum strength at the root diameter;

ii) the self centering action of the flank profiles equalising bearing and shear stresses in the splines;

iii) ease of manufacture by a number of multi cutting edge methods.

Since the involute spline is critical in shear a reliable spline torque capacity T_S can be obtained from -

$$T_S = \frac{L_s D_s^2 \tau_a}{1.273} \qquad (7.75)$$

where L_s is the length of the splines

D_S is the pitch diameter of the splines

τ_a is the allowable shear stress.

It is reasonable to assume that the pump shaft will experience cycles of combined loading in excess of 10^6 times during its working life and for this reason the sizing of the shaft should be on the basis of the endurance limit σ_e for the cyclic stress component and considering steel as a ductile metal, on the basis of the yield stress σ_Y for the steady stress component.

For a solid shaft of diameter d_s the nominal maximum torsional stress τ and maximum bending stress σ acting on the extreme fibres of the shaft material are -

$$\tau = \frac{16T}{\pi d_s^3} = 5.1 \frac{T}{d_s^3} \qquad (7.76)$$

$$\sigma = \frac{32\,M}{\pi d_s^3} = 10.2\,\frac{M}{d_s^3} \qquad (7.77)$$

Peterson (33) has suggested on the basis of Mises criteria for strength, that the shaft design should be based on $1.33\,\sigma_Y$ for the steady stress component, thus taking into account the redistribution of stress; and the fatigue strength reduction factor K_f for the cyclic stress component, where

$$K_f = q\,(K_c - 1) + 1$$

and q is the notch sensitivity factor

K_c is the stress concentration factor.

Design data for $\sigma_Y\ \sigma_e\ q$ & K_c is available under References (34), (35).

Thus for a shaft subject to a combination of steady torque T_o and a fully reversing bending moment M_v

$$d_s = 2.17\sqrt[3]{n\sqrt{0.422\left(\frac{T_o}{\sigma_Y}\right)^2 + \left(\frac{K_f M_v}{\sigma_e}\right)^2}} \qquad (7.78)$$

Depending upon the accuracy to which T_o and M_v have been determined, the factor of safety n of 2 to 3 may be satisfactory.

It is also necessary to consider the lateral and the torsional stability of the shaft assembly.

For lateral stability the mass of the cylinder block M_{cy} may be idealised as acting at a point to give a static deflection of the shaft of -

$$\delta_{ST} = \frac{M_{CY}\,g\,l^3}{48\,E\,I} \qquad (7.79)$$

where ℓ is the distance between the bearing centres

E is Young's Modulus for the shaft material

I is the second moment of area of the shaft cross section about a diameter.

Then the natural frequency -

$$\omega_n = \sqrt{\frac{k}{M_{CY}}}$$

where

$$k = \frac{M_{cy}g}{\delta_{ST}}$$

Thus the critical speed is -

$$N_c = 187.7\sqrt{\delta_{ST}} \text{ REV/MIN.}$$

(7.80)

The design of the shaft should be such that the shaft critical speed is appreciably higher than the maximum operating speed of the pump.

Because of the relatively short length of the shaft, torsional stiffness and stability are seldom causes of concern and will not be considered further in this work. A suitable reference on this aspect of design is Reference (36).

7.1.5 Distributor Design

Valve Plate Design

The valve plate presents a number of problems in design which can be related to its function and to the conditions which occur in this region of the pump. The prime function of the valve plate is to transfer the fluid from the inlet port of the pump to the suction cylinders and from the discharging cylinders to the pump outlet port. For this to be achieved efficiently, minimum fluid flow and leakage losses are essential. In addition it is necessary for the valve plate to function with a minimum of mechanical losses and wear.

Common practice is to incorporate two kidney slots in the valve plate, the one being in direct communication with the pump inlet port and the other with the pump outlet port. The extent of the slots around a common pitch circle is such that when a cylinder bore is in a mid position between the two slots, as at t.d.c. and b.d.c., adequate inter slot lands are present to prevent the short circuiting of high pressure fluid from the cylinder to the pump inlet or from the outlet port to a suction cylinder bore.

Early designs as reported by Ernst (5) and others suggested that if the angle subtended by the ends of the kidney ports exceeded the angle subtended by the cylinder flow passage by some 4^{o} to 6^{o}, adequate sealing resulted if the theoretical contact pressure force between the cylinder block and the valve plate was some 15% of the pressure force due to half of the pistons being under pressure. In addition the radial width of the valve plate lands enclosing the kidney slots can be generous in the absence of space restrictions, to resist leakage from the high pressure slot.

A secondary function of the valve plate is to react some or all of the axial forces on the cylinder block due to the pressure forces on the pistons and any spring loads which occur. Also to be reacted are the dynamic forces in the pump. It will be appreciated that with an odd number of pistons and with the variation of dynamic loads which occur during a pump

revolution, considerable cyclic changes in the reaction of the valve plate will occur and that these will make analysis of the problems of force balancing less than easy.

For design purposes it is convenient to apply simplified theory to these problems. The fluid pressure in the discharge kidney slot will exert a hydrostatic balancing force against the cylinder block. In addition since the valve lands act as face sealing surfaces, some leakage to the pump body pressure is inevitable and this in turn will extend the hydrostatic balancing across these lands. The angular deviation of adjacent leakage flow paths across the lands will be small in the limit and it is reasonable to assume a linear pressure differential.

Numerous designs have been proposed for the satisfactory force balancing with minimum leakage losses and these have been reviewed by Shute and Turnbull (37). Ernst proposes a semi-empirical method and uses a 'pressure factor' concept to account for the non-linear pressure distribution across the lands. Saitchenko (38) has derived a simple form of analysis and this has been used in the design calculations in this work.

Guidance on the desirable level of force balancing is given by Saitchenko (38), Ernst (5) and Guillon (1). Saitchenko proposes that the high pressure piston force on the cylinder block should exceed the hydrostatic balancing force on the valve plate by at least 15% and that the moment of the piston forces about the pump t.d.c. and b.d.c. axis should exceed the balance moment of the valve plate by at least 15%. Guillon suggests that adequate force balance exists if it is considered that the valve plate slots each extend for 180° and that the valve plate balance force is from 5% to 15% less than the average total piston force. Franco (39) has derived equations for the radial variation in pressure distribution but does not take into account the pressure field between the two kidney ports. Mauroschat (40) has attempted an analytical approach to the problem but his findings lead to appreciable mathematical difficulties.

Shute and Turnbull (41) have described a method of finding the effective fluctuation of hydrostatic force on a valve plate by an analogue technique based on the use of electrically conducting paper and find that for a valve plate of normal design (i.e., one not incorporating any form of decompression grooves), the effective port length is approximately 194° for half of the time and 154° for the other half. The mean effective length is therefore 174° which indicates an error of only 3% if an effective length of 180° is assumed. To indicate the variation of pressure across the valve plate and the variation of the position of the centre of pressure of the valve plate and the piston forces, refer to Figs.7.45 and 7.46.

A considerable amount of research has been devoted to the balancing of the valve plate by additional hydrostatic bearing pockets with associated capillary control. Leading this interesting field of design are H. Thoma (42), J. Thoma (43), Blok (44) and Propofiev (45). The inherent stiffness characteristics of this form of bearing are attractive in view of the variation of forces that occur. Palmer (46) has shown that small hydrostatic bearings in the valve lands can provide stiffnesses of the order of 10^{6} N/mm. However, since the allowable changes of gap between the valve plate and the cylinder block is of the order of 10^{-3} mm, the practical values of stiffness are of the order of only a few hundred newtons per 10^{-3} mm displacement. This is, however, beneficial and may result in an increased use of such designs in future pump designs.

There is general agreement that as in the case of plain face seals in which researchers such as Mayer (47), Nau (48) and Vogelpohl (49) have found positive clearance gaps at conditions of high contact loading of up to 85% of the pressure to be sealed, so in the case of underbalanced valve plates, clearances have been reported by many researchers including Nau and Brangs (50). Using the particularly suitable B.H.R.A. valve plate test rig, Nau found that the minimum film thicknesses during a series of tests with normal type valve plates were of the order of 500 micro inch (0.0127 mm)

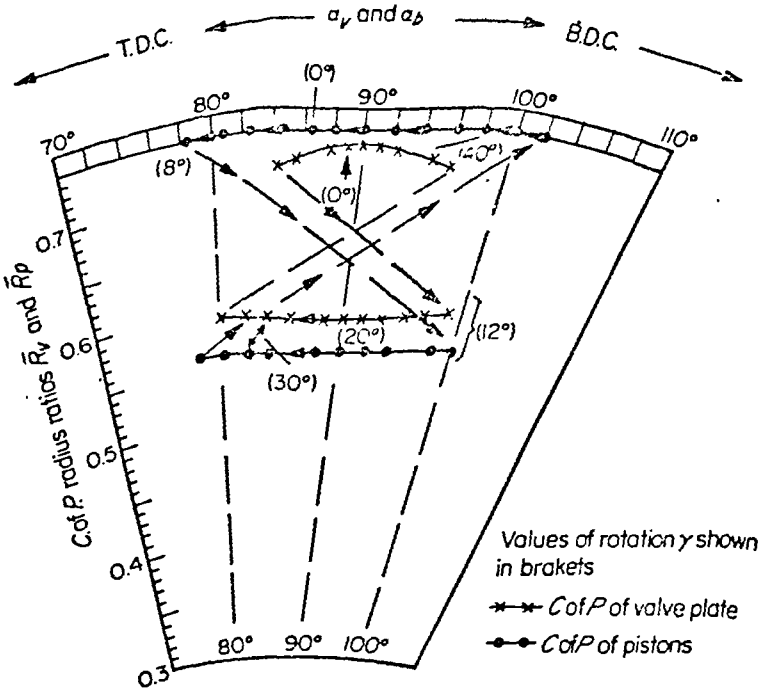

FIGURE 7.45. VARIATION OF PRESSURE DISTRIBUTION AROUND THE ENDS OF A VALVE PLATE PORT.

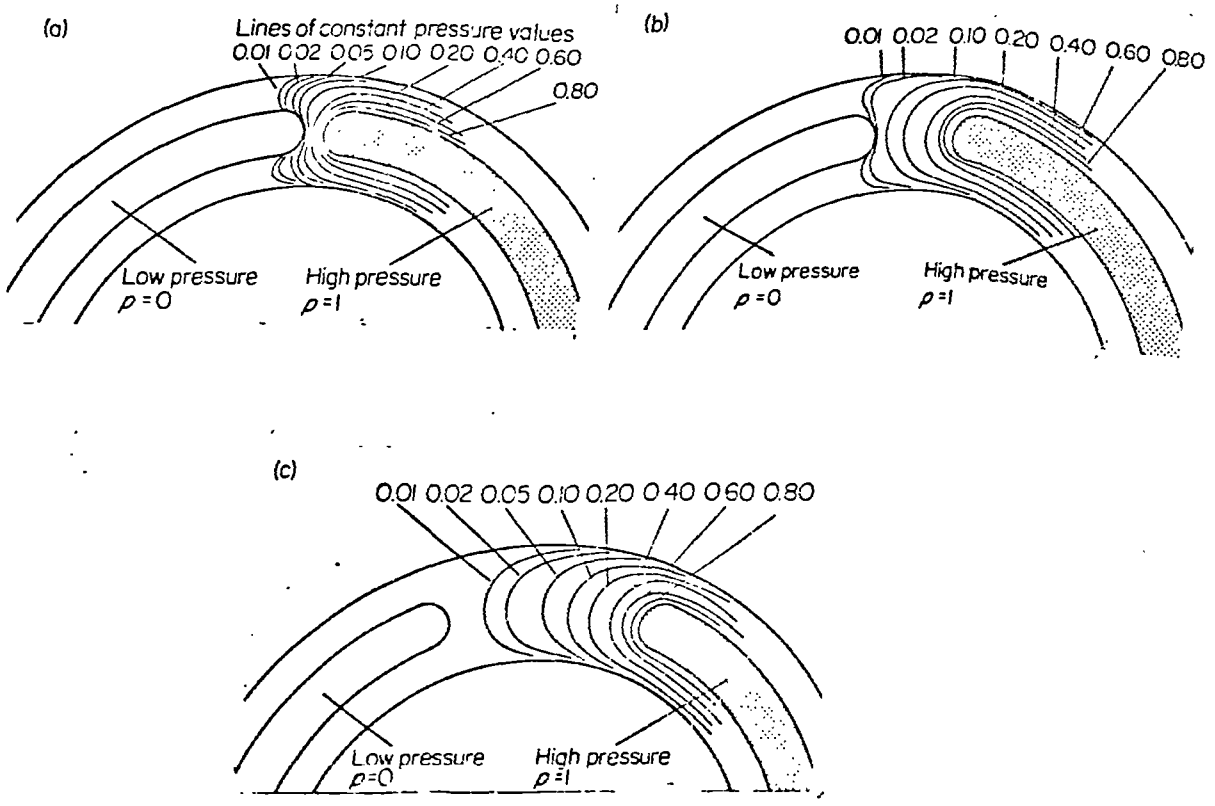

FIGURE 7.46. VARIATION OF POSITION OF CENTRE OF PRESSURE OF A VALVE PLATE AND PISTON FORCES

and that the clearances rose rapidly with a decrease in specific loading to some 2000 micro inch (0.051 mm). Brangs has measured gaps of 0.020 mm on industrial pumps. These findings have confirmed the presence of some hydrodynamic lubrication in valve plate force balancing and Shute and Turnbull (51) have studied the variations of the net load on a valve plate as the rotor rotates and have indicated the relative levels of hydrostatic and hydrodynamic balancing.

It is apparent that the analysis of the conditions pertaining to the valve plate/cylinder block interface are, to say the least, complex. Even if satisfactory theory could be derived, and Thoma suggests that this is not possible, the mathematical tools would be unwieldy from the designer's point of view. There is little doubt that the recommendations of Saitchenko, Ernst and Guillon do result in some very satisfactory designs, especially where the essential ingredient of past experience is available. It is also apparent that only assumptions can be made of the working gap on which to base decisions on surface accuracy and texture and to use in the estimation of hydraulic and mechanical performance.

Various hypotheses have been put forward to account for the hydrodynamic force generated in the gap. Researchers such as Thoma (43) and de Raucourt (52) have proposed the existence of 'thermal wedges' and 'viscosity wedges' but Dowson and Hudson (53) have shown that the large loads carried by parallel thrust bearings are not indicated by these theories. Swift (54) as long ago as 1946, suggested that thermal distortion of the surfaces have an appreciable effect and this has more recently been confirmed by Neal (55). There is little doubt that the asymmetric loading of a valve plate can be expected to assist in the establishment of a physical wedge flow path despite the fact that many modern designs incorporate floating elements to reduce the tendency for unwanted surface separation. On the Lucas HD900 pump under consideration, shaft deflections of up to 0.15 mm have been recorded which, in the absence of effective floating of the valve plate, would result in an appreciable surface separation. It must also be borne in mind that the surface flatness tolerances are generally of the order of 0.010 mm,

the same value as that found by Nau for minimum gap height. It would not seem improbable that much of the hydrodynamic effect is initiated by undulations in the surfaces of the valve plate and the cylinder block.

Vogelpohl (49) has suggested that a hydrodynamic gap between plain face seal surfaces can be described by the equation -

$$C^2 = C_1 \mu \frac{V b}{P_c}$$

where C is the height of the gap, V is the velocity of the rotating surface at mean radius, b is the radial width of the seal, P_c is the contact pressure of the sealing surfaces and is a constant dependent on the geometric features of the surfaces. In the case of a valve plate it is suggested here that since the mean velocity is proportional to the pump speed n and the contact pressure is a function of the pump pressure P_1 and the balance factor B_{FVP} we can write -

$$C^2 = \frac{C_2 \mu n b}{P_1 (1 - B_{FVP})}$$

Heinze (56) and Boon (57) have recorded satisfactory estimations of face seal leakage from the equation -

$$Q_S = \frac{\pi d_E C^3 P_1}{12 \mu b}$$

where d_E is the diameter at the entry to the radial annulus. Leakage in a valve plate can be expected across both lands which enclose the pressure kidney slot and if in place of d_E the appropriate length of entry is substituted we have -

$$Q_{SVP1} = \frac{\theta C^3 P_1}{6\mu} \left[\frac{D_{L3}}{(D_{L4} - D_{L3})} + \frac{D_{L2}}{(D_{L2} - D_{L1})} \right]$$

where θ is the angle in radians subtended by the ends of the kidney slot.

To take the analysis further it is necessary to obtain values for C. Based on the findings of Nau and Brangs it is here suggested that the following assumptions are made.

1. That at the maximum pump pressure and at one tenth of the maximum pump speed, the value of C be taken as 0.012 mm.

2. That at the maximum pump speed and at one tenth of the maximum pump pressure, the value of C be taken as 0.020 mm.

If $\bar{n}$ is the ratio of the pump speed to the maximum pump speed and $\bar{P}$ is the ratio of the pump pressure to the maximum pump pressure, we can find values of C from the expression -

$$\underset{(\text{MICRON})}{C} = 1.2 \times 10^{-3} + 3 \times 10^{-3} \bar{n} + 5 \times 10^{-4} \frac{\bar{n}}{\bar{P}} \tag{7.81}$$

as shown in Fig.7.47.

An additional leakage will occur due to Couette flow. It can be assumed that the flow is from the trailing end of the pressure kidney slot and can be expressed as -

$$Q_{SVP2} = \frac{\pi}{8} C n \left(D_{L3}^2 - D_{L2}^2 \right)$$

The total slip flow from the valve plate is then -

$$Q_{SVP} = \frac{\theta C^3 P_1}{6\mu} \left[\frac{D_{L3}}{(D_{L4} - D_{L3})} + \frac{D_{L2}}{(D_{L2} - D_{L1})} \right] + \frac{\pi}{8} C n \left(D_{L3}^2 - D_{L2}^2 \right) \tag{7.82}$$

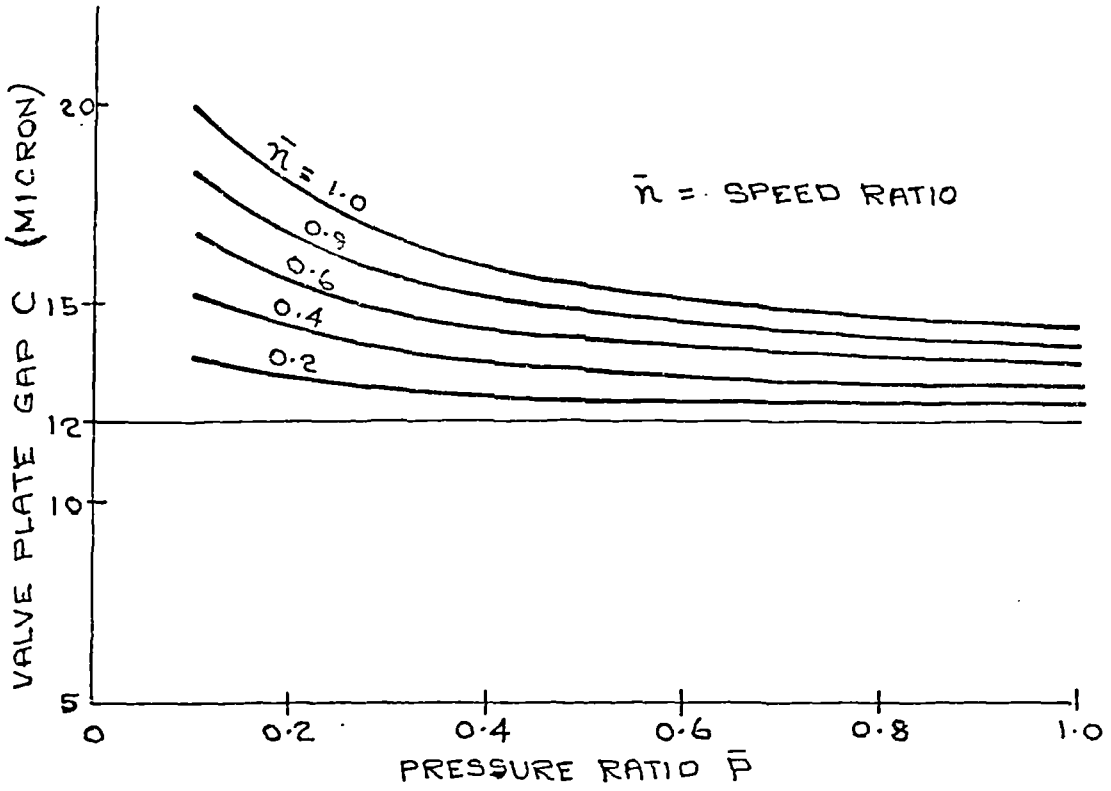

FIGURE 7.47. PROPOSED VALVE PLATE GAP FOR VARIOUS VALUES OF PUMP SPEED RATIO $\bar{n}$ AND PUMP PRESSURE RATIO $\bar{P}$

Valve Timing

'Ideal' valve timing can be described as the condition when the delivery kidney port is opened at the instant the pressure in the pumping cylinder is equal to the pump discharge pressure and when the suction kidney port is opened to a suction cylinder at the instant the pressure in the suction cylinder is equal to the pump inlet pressure. Since during a pumping stroke the rise of pressure in the cylinder bore will depend on the trapped volume, the bulk modulus of the fluid, the leakage past the piston and slipper bearing assembly and the pump speed, the theoretical determination of the conditions for ideal timing is complex. Helgestad, Foster and Bannister (14) have successfully derived non-linear simultaneous equations for the flow rate and pressure gradients in the inlet and discharge chambers and the piston/cylinder space and solved these to find the angle for perfect precompression of the fluid on the delivery stroke. They found a very wide range of port timing is required if a pump is to operate with ideal timing over a full range of pressure and swashplate angle but that the pump speed was only important if the leakage is important, i.e., for small swashplate angles.

They also found that for a given swashplate angle, the variation of the port angle for ideal timing with pressure was approximately linear over appreciable pressure ranges and this confirms the suitability of some pump designs which have provision for rotating the valve plate by a spring loaded cylinder connected to the pump outlet port.

The use of restrictor grooves overcomes to some extent the difficulties of obtaining near ideal timing, since the high resistance to flow on initial opening modulates the transfer flow rates. It would seem that satisfactory designs could result from having zero lap between the valve plate restrictor grooves and the cylinder ports at t.d.c. and b.d.c. and that the length of each groove extends some 4° to 6° of angular rotation to give adequate sealing as discussed earlier in this section. This angle should also ensure that at the instant of valve opening the pressure conditions are such as to give good valve timing over a wide band of pump working conditions.

Pump Noise

Consideration of ways of reducing the noise emission from an axial piston pump is an important stage in the design process. Pump noise is caused by the cyclic variations of fluid pressure and flow in the pump flow paths and by strains in the pump parts due to fluctuating loads. These effects cause vibrations which are transmitted by the hydraulic fluid and the pump structure and are emitted as liquid borne and air borne noise.

Fig.7.48, shows an adaptation of a noise analysis scheme by Willenkens (58) which identifies the aspects which affect the level of noise from a pump. It will be seen that the air borne noise is dependent on the total design of the pump and is therefore directly related to the design decisions made during the design process. The liquid borne noise is mainly related to pump performance and particularly to the fluctuations of flow and pressure levels.

Considering initially the air borne noise it is apparent that any means of reducing the effects of the fluctuating loads will be beneficial. Thus for a given load cycle, reduction of working clearances and an increase in structural strength of the loaded components will reduce the effects of cyclic changes in the applied loads. Typical of such working clearances are those controlling the separation of the slipper bearings and the swashplate during the suction stroke. An increased structural rigidity can also be expected to reduce the air borne noise although this will be at the expense of pump weight and manufacturing cost. A small improvement can be expected by using rubbing bearings in place of rolling element bearings particularly for high speed pumps but in the main the high load capacity, life prediction and ease of installation of rolling bearings is likely to outweigh the noise reduction considerations.

Vibration measurements around a pump casing show that harmonics of the piston frequency are predominant and some noise reduction will result from prestressing the swashplate in the direction of the piston loads. With a variable displacement pump, the frictional loads of the swashplate pivots assist in noise reduction.

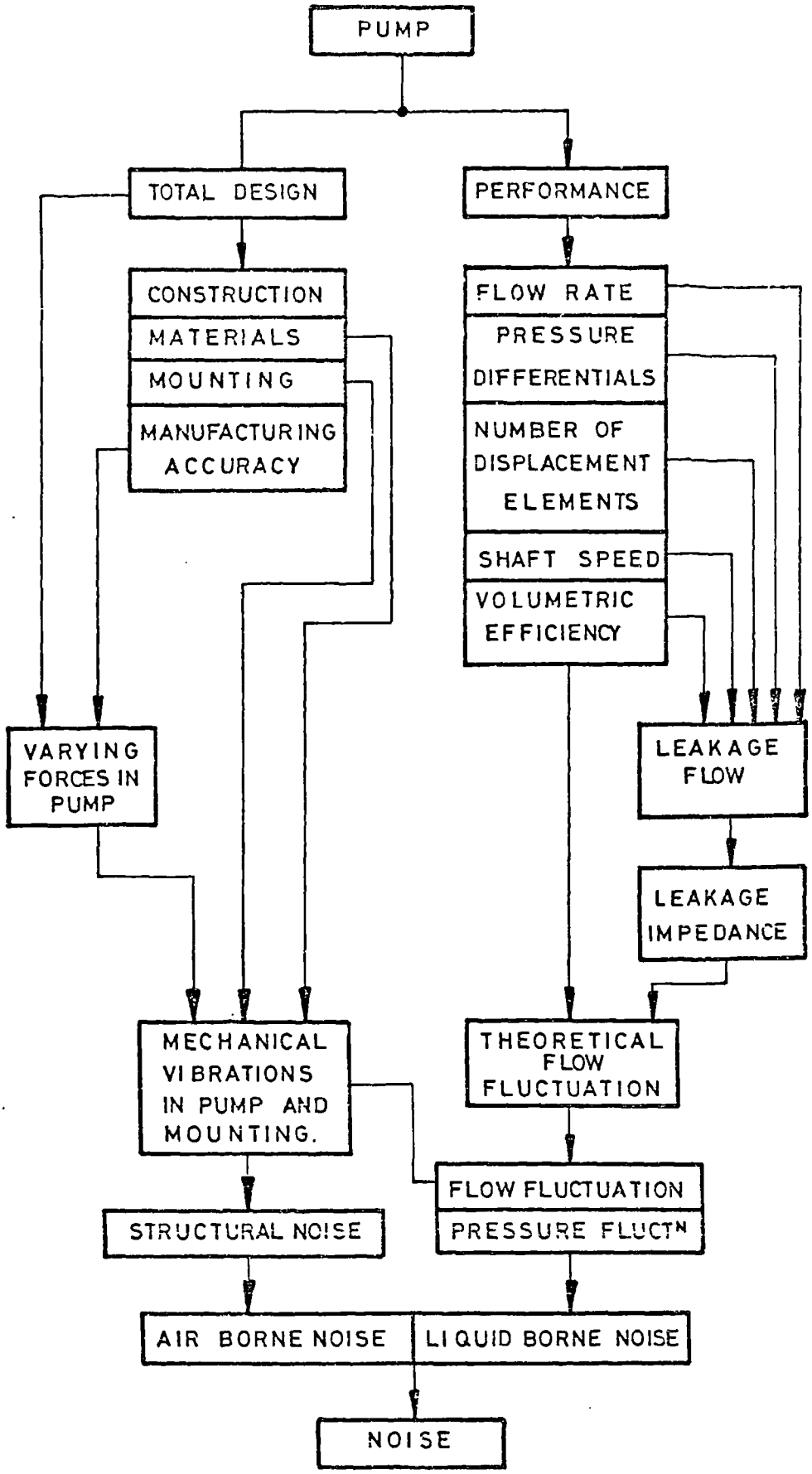

FIGURE 7.48. ASPECTS WHICH INFLUENCE THE LEVEL OF NOISE EMISSION FROM AN AXIAL PISTON PUMP

The mounting of the pump will also influence the transmission of air borne noise and the use of effective anti-vibration mountings will obviously be beneficial in the case of foot mounted pumps. An appreciable advantage is obtained by flange mounting the pump since a major component of the vibrating forces are then acting normal to the mounting face.

A final consideration is that of materials for the pump components, and in particular, for the pump body and end plates. The vibration damping properties of the ferrous metals and especially those of cast iron makes these materials first choices for all but low weight pump designs.

The liquid borne noise is very dependent on pump performance and therefore with flow rates and pressure differentials. These in turn are related to the number of displacement elements, (piston and slipper bearing assemblies in the case of axial piston pumps), and the shaft speed which will in turn determine the frequency of the noise generated. A major source of noise in axial piston pumps however is also related to fluid compression. If all internal leakages are neglected, it is necessary for a pump to rotate through some 12^{o} to compress a cylinder charge to say, 140 bar, and for some pumps with large trapped volumes this may be nearer 20^{o} of rotation. To enable the fluid to flow into the hydraulic system in general, the pressure of the hydraulic fluid in the pump cylinder must be at a somewhat higher pressure than the system pressure. If the fluid was incompressible the discharge would be gentle but because of compressibility severe shock is created resulting in a pressure overshoot as indicated in Fig.7.49. The severity of the shock is dependent on the pump speed, piston stroke, the trapped volume and the level of leakage from the pumping cylinder to the pump discharge port across the valve plate/cylinder block interface. Helgestad, Foster and Bannister (14) (59) have made valuable contributions to the understanding of the noise generation and the calculation of the associated pressure transients in axial piston pumps together with the effects of port timing and of incorporating restricting

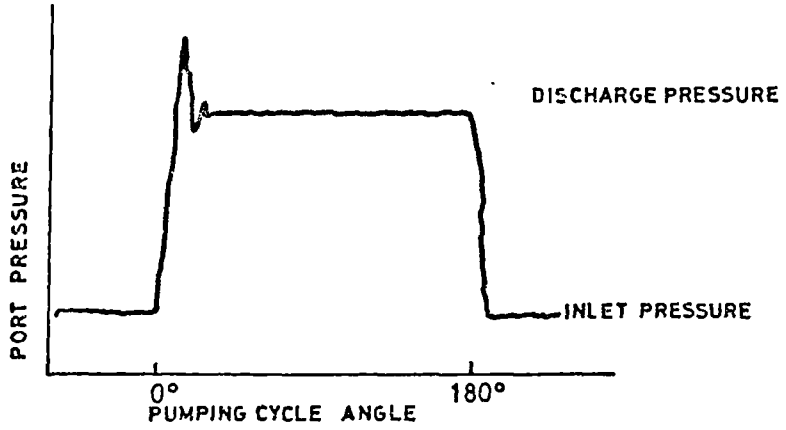

FIGURE 7.49. PRESSURE OVERSHOOT IN A PUMPING CYLINDER DUE TO BACKFLOW FROM DISCHARGE PORT

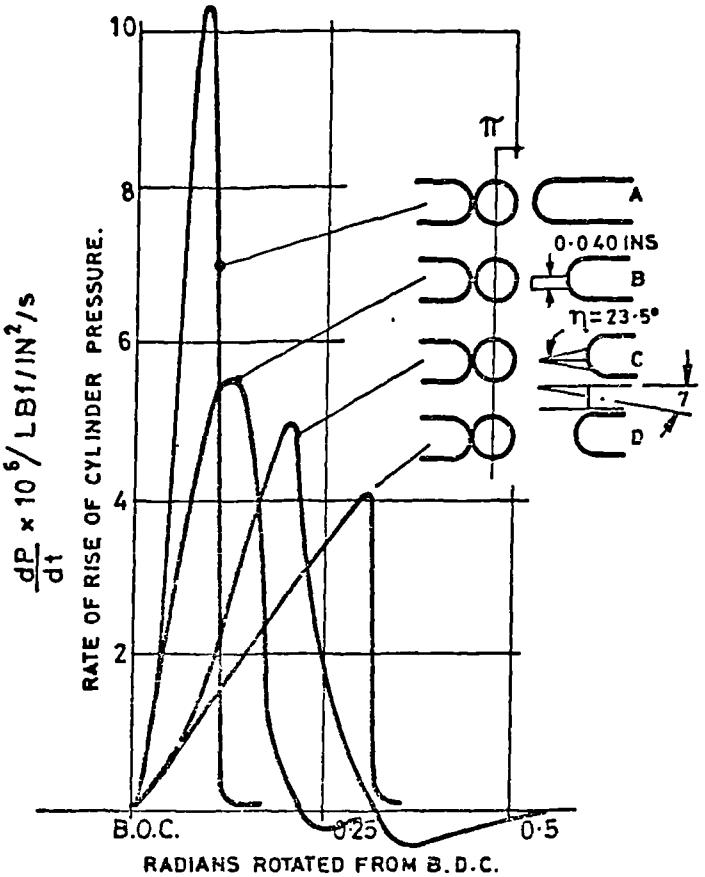

A STANDARD PORT PLATE
B PORT PLATE WITH PARALLEL ENTRY SLOTS
C PORT PLATE WITH TRIANGULAR ENTRY SLOTS
D PORT PLATE SET TO GIVE 'IDEAL' TIMING

FIGURE 7.50 RATE OF RISE OF CYLINDER PRESSURE AGAINST ROTATION FROM B.D.C. FOR VARIOUS PORT CONFIGURATIONS

grooves at the ends of the kidney ports in the valve plate. Fig.7.50, shows the rate of rise of cylinder pressure in a Lucas ID500 pump for valve plates with:-

a) plain ports with no restricting grooves;
b) parallel slot restricting grooves;
c) triangular slot restricting grooves;
d) plain ports set at 'Ideal Timing'.

In addition to the pressure rise in the discharge port similar pressure transients can occur in the suction port if the high pressure fluid remaining in the cylinder bore suddenly expands into the inlet chamber if the valve opens too soon or the fluid remaining in the cylinder bore is expanded to too low a pressure level, causing cavitation, if the port opens too late.

For design purposes their main recommendations are:-

(1) for a pump rotating in one direction and operating at a substantially constant pressure and flow, it is better to use a port plate without silencing grooves. The port timing should be such that full precompression and pre-expansion is achieved on delivery and suction strokes respectively. The cut-off at the end of each of the kidneys should be exactly at b.d.c. or t.d.c. as appropriate;

(2) for a pump operating in one direction, but under varying output conditions, triangular silencing grooves should be used to optimise the pressure transients at some chosen operating conditions. A final design can only be achieved by trial and error, but use of a computer can reduce the problem to manageable proportions;

(3) for a bi-directional pump, parallel slot restrictors at each end of each kidney slot are desirable. The design of these is relatively simple; by choosing the width so that the pressure drop is equal to the boost pressure at the maximum flow conditions, cavitation is avoided, but at the same time, some degree of control of the pressure transient is maintained.

7.1.6 Detail Design

The success of the entire design process will depend on the quality of the detail design. As already indicated, the axial piston pump is a complex machine with many factors affecting the important design aspects of performance, life, weight and manufacturing costs.

The design of each component will require the utmost care in material selection, treatment, manufacturing methods and accuracies, and in ease of assembly and maintainability. It would be inappropriate here to state in detail the factors affecting component design as these are well developed in many publications. However, it is appropriate to emphasise the desirability that component design should receive the fullest support in the form of quality of staff, level of supervision and checking, and above all, that it should not be a hurried activity.

The axial piston pump calls for the use of design skills of a high order, but as in virtually all design activity, simplicity of concept and manufacture must be a guiding aim.

7.2 Design of Pump to Given Specification

To demonstrate the use and effectiveness of the design method, a pump of the same specification as that for the Lucas type HD900 was designed.

Design Specification

A variable displacement bidirectional axial piston pump to satisfy the performance -

Volume flow rate per 1000 rev/min	...	68 litres/min
Maximum peak pressure	...	350 bar
Maximum continuous pressure	...	280 bar
Maximum operating speed	...	3000 rev/min.

The pump is to be capable of operating efficiently with a wide range of hydraulic fluids as commonly used in industrial hydraulic systems and with ambient temperatures of $-20^{\circ}C$ to $80^{\circ}C$.

The pump is to have the facility for incorporating fixed capacity, manual variable capacity and electro-hydraulic remote control. Integrated in the pump assembly are to be the necessary valves for facilitating the use of these controls, together with provision for mounting suitable boost pumps and relief and replenishing valves.

The pump is to be suitable for close flange mounting to a prime mover with the shaft extension splined to S.A.E. involute splines standards. Alternative shaft end with a parallel key is also to be made available.

The dry weights of the pump should not exceed -

Fixed capacity unit	...	66kg
Manually controlled variable capacity unit	...	86kg
Electro-hydraulic controlled variable capacity unit	...	100kg.

The pump is to be as compact as possible with particular regard being paid to the ease of installation and maintenance. The pump is intended for use in a wide range of industrial and transportation applications and must satisfy the highest levels of quality and reliability called for in these areas of fluid power. Particular attention must be paid to ensuring that the pump is cost effective.

Conceptual Design

Referring to the assembly drawings No.8812345, sheets 1 and 2, it will be seen that the new pump design, designated Type JD900 is of similar basic design to the HD900. This is intentional as it was felt that if the JD900 incorporated wide differences in conceptual design, this would make comparisons difficult and would in all probability not further the task of demonstrating the effectiveness of the design method.

The JD900 is designed around a two bearing shaft which has ample strength to carry the torque loading of the pump but with only moderate deflectional stiffness. Double row spherical roller bearing races have been chosen for a 30,000 working hour life at maximum continuous pressure and at 0.65 maximum pump speed.

DRG No **885923** QUOTE LATEST ISSUE No

THIRD ANGLE PROJECTION

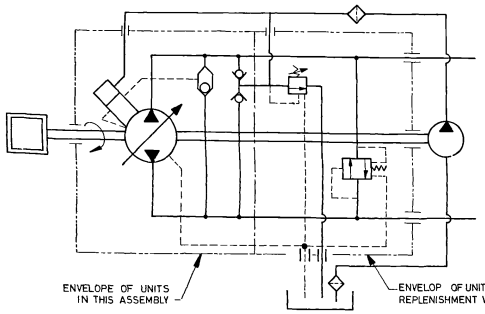

CIRCUIT DIAGRAM FOR PUMP AND INTEGRATED CONTROLS

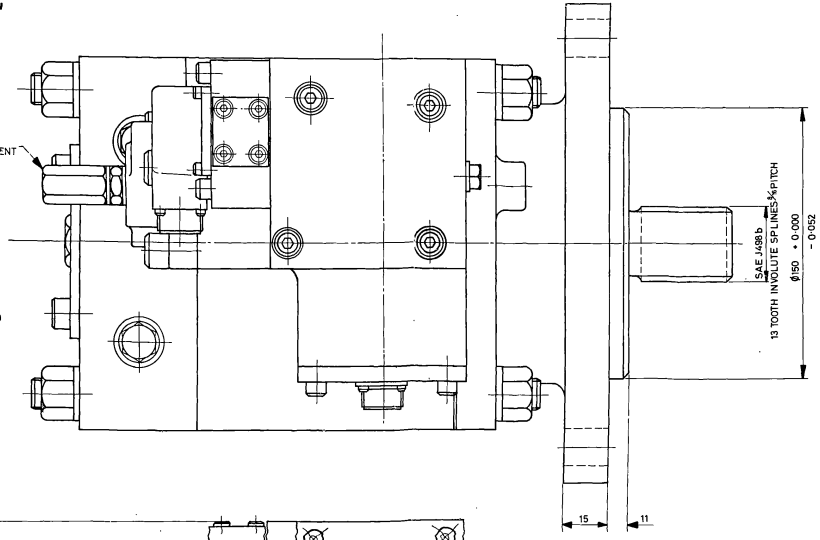

PERFORMANCE DATA

TYPICAL FOR UNIT WITH MINERAL OIL $1{\cdot}74 \times 10^{-3}$ Ns/m² AT 50°C.
VOLUME FLOW RATE AT 100 P.M. - $6{\cdot}8 \times 10^{-5}$ m³
MAXIMUM OPERATING SPEED 3000 R.P.M.
MAXIMUM PEAK PRESSURE 350 bar.
MAXIMUM CONTINUOUS PRESSURE 280 bar.
TEMPERATURE RANGE 20°C TO 80°C
MAXIMUM BODY PRESSURE 4 bar.
MINIMUM INLET PRESSURE FOR MAXIMUM CONDITIONS SHOULD NOT BE LESS THAN 3·5 bar ABOVE BODY PRESSURE.

PUMP DRY WEIGHT.

STANDARD UNIT 94 kg.
LIGHT ALLOY. VERSION 82 kg.

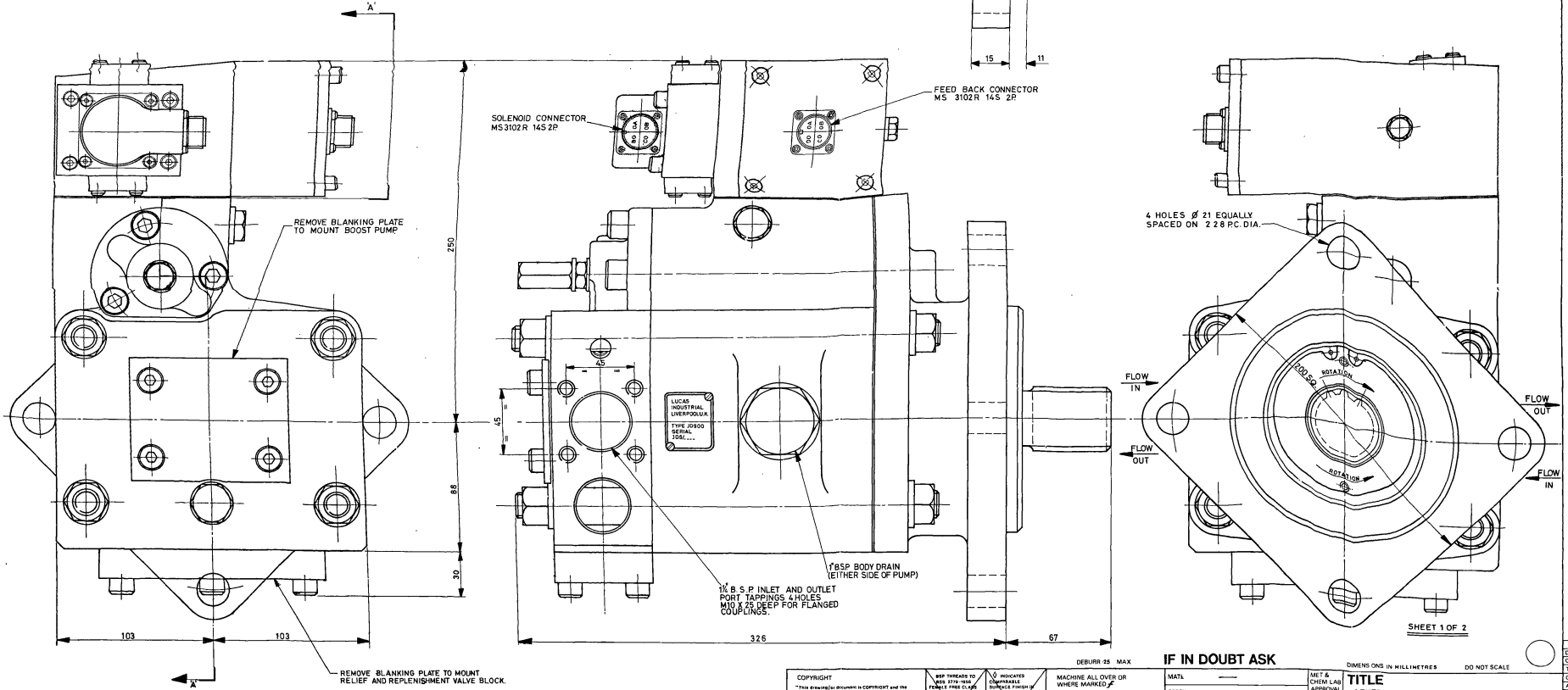

SHEET 1 OF 2

MANUFACTURING METHOD TO BE APPROVED BY LIE PRODUCTION ENGINEERING DEPT.

BSP THREADS TO BSS 3779-1966 FEMALE FREE CLASS MALE MED CLASS BSF THREADS TO BSS 84-1965 MEDIUM CLASS BA THREADS TO BSS 93-1951 MEDIUM CLASS METRIC ISO THREADS TO BSS 3643-1953 OR I.S.O. STANDARDS

◇ INDICATES COMPULSORY SURFACE FINISH IN MICRIN. INCHES (UCA) ▽ INDICATES ACTUAL SURFACE FINISH IN MICRO INCHES (UCA) ALL DIMENSIONS ARE AT 20°C UNLESS OTHERWISE STATED

MACHINE ALL OVER OR WHERE MARKED ✓

LIMITS

FRACTIONAL DIMENSIONS ± 1/64 DECIMAL DIMENSIONS ± 0·010 ANGLES ± 1/2° CONCENTRICITY TOLERANCE = ½ HALF-TOTAL TOLERANCE (TYP.) (SUM OF TOLERANCES)

DEBURR .25 MAX

IF IN DOUBT ASK

DIMENS ONS IN MILLIMETRES DO NOT SCALE

MAT'L	
SPEC'N	
TREAT MENT	
FINISH	

MET & CHEM LAB APPROVAL

LUCAS INDUSTRIAL EQUIPMENT

SCALE FULL.

TITLE

GENERAL ARRANGEMENT OF TYPE JD 900 AXIAL PISTON PUMP WITH ELECTRO-HYDRAULIC FLOW CONTROLLER.

DRAWN	W.J.B.
CHECKED	
TRACED	A.RODDY
CHECKED	
APPROVED	
DATE	8/77
SUPERSEDES	
SIMILAR TO	
REF. DRG. NO	
FIRST USED ON	
DRG No.	885923
QUOTE LATEST ISSUE No.	

MODIFICATION OR ALT. NOTE	DATE	ISSUE

THIS DRAWING MAY ONLY BE ALTERED IF THE PART REMAINS INTERCHANGEABLE / IF NOT INTERCHANGEABLE A NEW DRAWING NUMBER MUST BE TAKEN

A.O.

DRG No **885923** QUOTE LATEST ISSUE No.

THIRD ANGLE PROJECTION

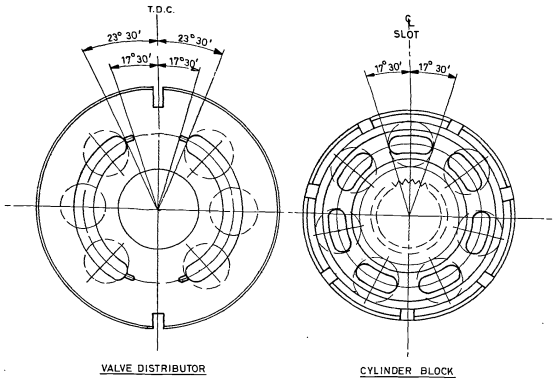

VALVE DISTRIBUTOR

CYLINDER BLOCK

VIEWS ON VALVE PLATE AND CYLINDER BLOCK SHOWING PORT CONFIGURATIONS AND BEARING LANDS.

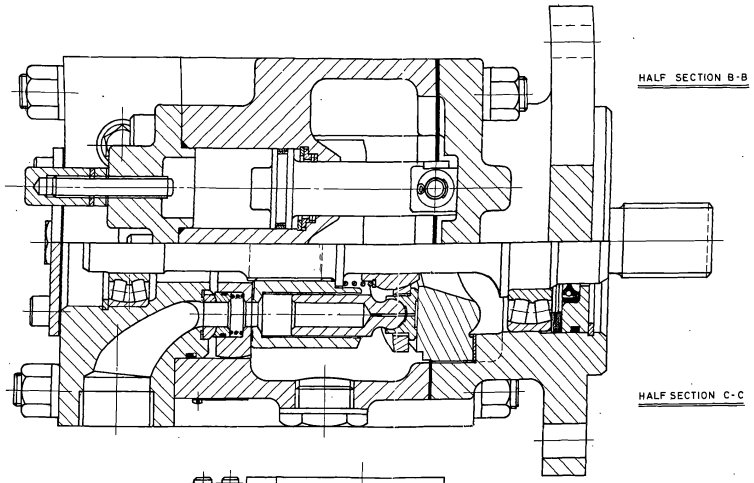

HALF SECTION B-B

HALF SECTION C-C

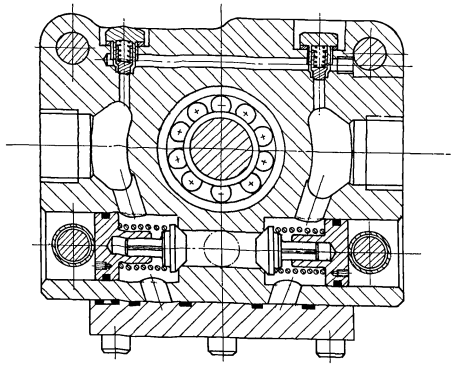

PART SECTION D-D

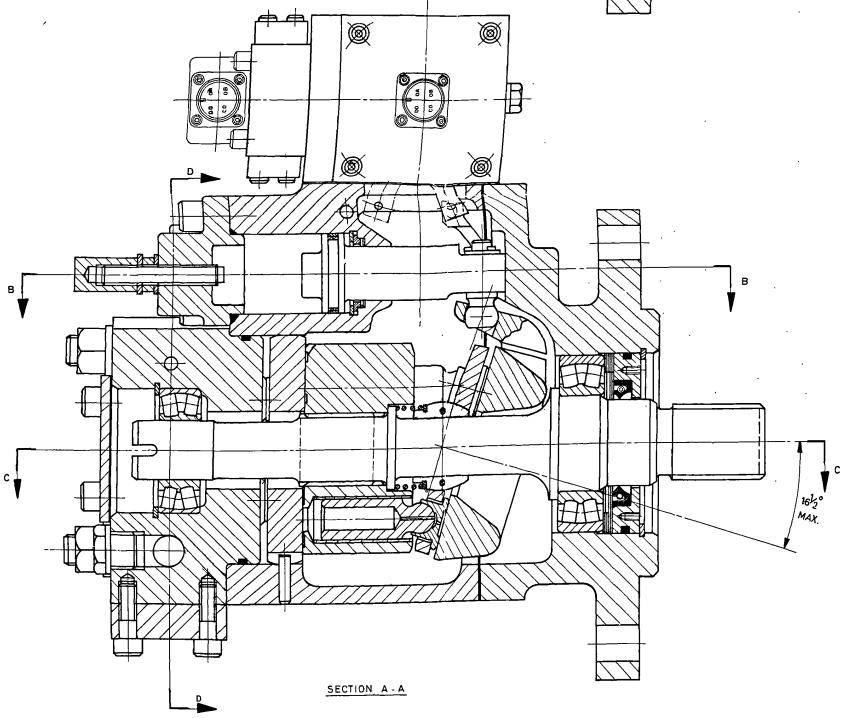

SECTION A-A

SHEET 2 OF 2

MANUFACTURING METHOD TO BE APPROVED BY L.I.E. PRODUCTION ENGINEERING DEPT

DEBURR .25 MAX

IF IN DOUBT ASK

DIMENSIONS IN MILLIMETRES DO NOT SCALE

BSP THREADS TO BSS 2779: 1956
FEMALE FREE CLASS
MALE RED CLASS
BSP THREADS TO BSS No. 1956
MED SM CLASS
BA THREADS TO BSS 93/601
FEMALE NORMAL FIT
MALE CLOSE FIT
UNC THREADS TO BS 1580: 1953
OR I.S.E. STANDARDS

◊ INDICATES MACHINABLE SURFACE FINISH IN MICRO INCHES (CLA)
▽ INDICATES ACTUAL SURFACE FINISH IN MICRO INCHES (CLA)
ALL DIMENSIONS EXCLUSIVE OF PLATING AND BEFORE PLATING UNLESS OTHERWISE STATED

MACHINE ALL OVER OR WHERE MARKED ✓

LIMITS
FRACTIONS-DIMENSIONS & HKS DEC MAL DIMENSIONS & SOS ANGLES ± 30'
CONCENTRICITY-TOLERANCE = ± HALF-TOTAL TOLERANCE (THE SUM OF TOLERANCES)

MATL	
SPECN	
TREAT MENT	
FINISH	

MET & CHEM LAB APPROVAL

LUCAS INDUSTRIAL EQUIPMENT

SCALE FULL

TITLE
GENERAL ARRANGEMENT OF TYPE JD900 AXIAL PISTON PUMP WITH ELECTRO-HYDRAULIC FLOW CONTROLLER.

DRAWN	W.J.B.
CHECKED	
TRACED	A.M.R.
CHECKED	
APPROVED	
DATE	8/77
SUPERSEDES	
SIMILAR TO	
REF DRG NO.	
FIRST USED ON	

DRG No **885923** QUOTE LATEST ISSUE No.

MODIFICATION OR ALT NOTE	DATE	ISSUE

THIS DRAWING MAY ONLY BE ALTERED IF THE PART REMAINS INTERCHANGEABLE ▽ IF NOT INTERCHANGEABLE A NEW DRAWING NUMBER MUST BE TAKEN

A0

The valve plate is of partially balanced design with a balance factor of 0.89. A maximum assembly clearance between the valve plate and the cylinder block is limited to 0.400mm by shimming at the shaft extension end bearing. The valve plate has suction and delivery kidney ports with decompression grooves at each end for bi-directional operation. Transference of the hydraulic fluid to and from the valve plate is by means of six sprung bobbins seating on spherical inserts pressed into the pump valve block.

The pistons are actuated by slipper bearings on an inclinable swashplate which is located in two 120° shell bearings to give direct load reaction into the pump end housing. The slipper bearings are returned by a substantial return plate located on a split spherical bearing on the pump shaft which in turn is preloaded by a high rate compression spring.

Geometric Design

It was decided to use seven pistons since the 2.5% flow variation was not considered excessive for the applications envisaged for the pump. Using the 'Initial Design Chart' Fig.7.17, with $q = 6.8 \times 10^{-5} m^3/rev$ and $N_p = 7$, a piston diameter of 23.00mm, a stroke to piston ratio of 1.0 was chosen which resulted in a pitch circle diameter of 80.00mm and a maximum swashplate angle of just under $16\frac{1}{2}°$. These values were considered suitable for a low cost, low weight design with the advantage of a reasonably low swashplate angle. It was also felt that the maximum allowable hoop stress of 180 MN/m^2 would not be difficult to achieve in the cylinder block.

Movement Design

A design layout resulted in the adoption of the design of pump as shown in the general arrangement drawings. The swashplate is of 3% Ni Cr forged steel with the working surfaces case hardened to a depth of 0.5 to 0.6mm, surface ground to 0.2 micrometres and with a flatness tolerance of 0.012mm T.I.R. Generous bearing lands gave a maximum bearing pressure of only 40 MN/m^2 on the acetal lined, porous bronze, steel backed shell bearings.

The pistons have an effective length of 56.5mm terminating in a 17mm diameter spherical bearing which gave a maximum bearing pressure of 74MN/m^2 with the slipper bearings. The pistons are of 1½% Ni Cr Mo steel heat treated to condition T, and hard chrome plated to a depth of 0.010mm with a surface finish of 0.2 micrometres. Although of hollow design, no attempt was made to design for reduced piston clearance with increasing pressure. The result was a piston mass of 0.127kg and gave design values of -

Maximum Piston Velocity	...	3.72 m/s
Maximum Piston Acceleration	...	1169 m/s^2
Maximum Piston Acceleration Force	...	148.9 N.

It was decided to optimise the piston diametral clearance for the pressure range 100 to 200 bar and for a speed range of 1000 to 2200 rev/min as this was considered to most suitably cover the majority of possible applications including the use of four and six pole induction motors and industrial type I.C. engines. On this basis the piston diametral clearance was limited to 0.025mm to 0.040mm.

The slipper bearings were designed to provide full off balancing and the design gap was chosen to give optimum power losses over the range of pressure and speed used for determining the piston diametral clearance. Design data for the slipper bearings is -

Outside diameter of slipper bearing	...	28.550mm
Diameter of slipper bearing recess	...	17.500mm
Diameter of slipper bearing choke	...	0.800mm
Length of slipper bearing choke	...	3.500mm
Design slipper bearing clearance	...	0.015mm

An analysis of the static and dynamic forces in the pump gave the following maximum values at 350 bar and 3000 rev/min.

Maximum Piston Velocity	...	3.722 m/s
Maximum Piston Acceleration	...	1169.4 m/s^2
Maximum Piston Pressure Force	...	14.54 kN
Maximum Piston Acceleration Force	...	148.5 N
Maximum Piston Centrifugal Force	...	501.4 N
Maximum Slipper Bearing Reaction	...	15.38 kN
Maximum Cylinder Bore Reaction	...	8.96 kN

Distributor Design

The ports were designed to give smooth fluid flow between the cylinder block and the $1\frac{1}{4}$" B.S.P. tappings. This was achieved by the careful profiling of the cored holes in the end block and by maintaining clean flow conditions through the valve plate bobbins.

The valve plate utilises two kidney ports each spanning 133° of the cylinder piston bores pitch circle diameter. The kidney slots in the cylinder block each subtended an angle of 35° which allowed 6° for basic sealing in the absence of restrictor grooves. The restrictor grooves are 4mm wide by 2mm deep of rectangular cross section with fully rounded ends to facilitate manufacture.

The valve plate is of traditional design with sealing lands to provide the balance factor of 0.89. Additional bearing contact area is afforded by auxiliary vented lands.

Detail Design

The cylinder block is of 0.35 C steel with the cylinder bores lined with leaded bronze liners. The face of the cylinder block which seats against the valve plate is also lined with the same type of bronze to a depth of 1.50mm. The surface finish of the bores and the cylinder face is 0.2 micrometres and a flatness tolerance of 0.012mm is applied to both the cylinder block face and that of the valve plate.

The cylinder is mounted onto the pump shaft by means of 40mm straight sided splines and the shaft is of 1½% Ni Cr steel heat treated to condition U. Using equation (7.75) with the allowable shear stress at 0.5 the ultimate shear strength, the splined end of the shaft has a torque capacity of 1273 Nm which gives a design factor of safety of 3.2 for the maximum working torque. This is considered adequate to take the peak cycling torques to be expected from I.C. engines, even if only three cylinder engines are used.

The highest combined stresses occur in the spline relief adjacent to the location shoulder and using equation (7.78) with a safety factor of n=3 gave a diameter of 32.4mm compared with 36mm as used in the design.

The natural frequency of the shaft and the cylinder block was estimated as 3890 rev/min which is sufficiently higher than the maximum pump speed as to be considered satisfactory.

The maximum deflection of the shaft due to pressure forces was calculated as 0.127mm which amounts to 0.03mm at the periphery of the cylinder block. It was considered that the valve plate design with the transfer bobbins can adequately accommodate this cycling deflection.

7.3 Appraisal of Pump Design

Long periods of study of the existing H.D.900 pump convinced the author that the quality of design was of a very high order and that at the best only relatively few improvements could be expected in a new design. As a result most of the aspects raised in this appraisal may be considered of minor importance and no doubt debatable.

The JD900 is appreciably smaller in size whilst maintaining the basic requirements of mounting, shaft end and port sizes. The relevant dimensions are:

	HD900	JD900
Overall length ..	425mm	393mm
Overall width of body ..	240mm	206mm
Overall height of body ..	389mm	369mm

The JD900 is lighter than the HD900 in all its forms. An example of this is that the JD900 complete with electro-hydraulic controller is estimated to weigh 94kg, whereas the HD900 in the same form weighs 118kg.

Because of reduced lengths of cylinder block and shaft the rotating masses of the JD900 are appreciably less than that of the HD900. In addition, it is thought that the use of a split spherical bush with a relatively light compression spring would considerably ease the assembly of this part of the pump. The spherical bush also eliminates the use of the piston return plate assembly and this should result in an appreciable cost saving. Because of this design the swashplate is also smaller and simpler on the JD900.

The use of valve plate bobbins on the JD900 will possibly increase the manufacturing cost in this region but this is somewhat offset by the elimination of the intermediate plate between the cylinder block and the valve plate on the HD900.

Few differences exist in the shaft and bearing design for the two pumps. Because of the reduced bearing centres of the JD900 its shaft is somewhat more stiff than that of the HD900, but the relative values are likely to have little effect on the overall design.

The servo piston design is the same for both units but by specially designing the pump body to take the electro-hydraulic controller an improvement can be claimed for the JD900 in that the main pump body can be used for any of the standard Lucas controllers without modification. Thus for the full range of pump configurations only two bodies may be provided. That shown for variable delivery pumps and a simpler version for fixed displacement pumps.

The integrated valves are in the main of similar design and no special features are worthy of mention except that the author's own experience in valve design led to the poppet valves having fewer geometric tolerancing featured than those of the HD900 pump.

It was found that conditions at the piston, slipper bearings and valve plate of the HD900 were very close to those

suggested in the design process of this report. The piston clearances, slipper bearing gaps and valve plate balancing of both pumps are therefore very similar. One possible adverse feature of the JD900 is a small reduction in the length of piston immersion at the beginning of the pumping stroke and although the resulting bearing stresses were acceptable, a more detailed consideration would be given to this in the event of the design being implemented.

It is possible that a small improvement in overall performance can be expected from the JD900. This is mainly due to a reduction in the torque losses due to -

a) smaller effective radius for the slipper bearings;

b) lower reaction loads in the main bearings;

c) lower hydrodynamic losses in the outlet port flow path;

and in the slip losses due to -

d) lower compressibility losses due to a reduction in the volume of fluid between the valve plate and the cylinder.

As indicated in Chapter 8, the performance of the JD900 was not estimated using the performance prediction method as it was felt that the differences that could be expected would not be significant.

The design of the JD900 has served to demonstrate the usefulness and validity of the proposed design method. In conjunction with the proposed performance prediction method it should be possible for a competent designer to produce satisfactory pump designs with appreciably reduced development time and costs.

CHAPTER 8. PERFORMANCE PREDICTION METHOD FOR AXIAL PISTON PUMPS

It has been shown in the sections devoted to the design of axial piston pumps that it is possible at the design stage to optimise for minimum power losses for specific working conditions within the pump. The benefits to be derived from this capability are obvious and should greatly aid the designer in achieving the design specification.

However an axial piston pump invariably has to satisfy performance requirements over a wide range of operating conditions and in particular of pressure, speed, viscosity and displacement setting. The mathematical models of Wilson, Schlösser and Thoma, as discussed in Section 5.5, present methods of performance prediction which depend heavily on empirical coefficients Unless a pump of similar design has been tested and the coefficients derived, the mathematical models would not be available for use at the design stage of a new pump. In any event the scaling of the coefficients would tend to reduce their validity. As a result the mathematical models are mainly of academic interest and are little used in practical design.

A performance prediction method which made use of loss coefficients based on theoretical considerations as opposed to experimental results would overcome this difficulty and could provide a useful design aid. A close study of the effects on pump performance of the physical dimensions of the pump would enable a theoretical basis to be derived for calculating the specific values of the coefficients for varying operating conditions. It was recognised that this hypothesis could be tested by calculating the performance of a pump over its full working conditions and testing the results obtained against the experimental pump performance. Close agreement between the theoretical and experimental results would indicate a significant step forward in pump performance prediction.

The mathematical models of the three researchers closely agree with one another. Schlösser and Thoma had

the undoubted advantage of more accurate and sophisticated measuring equipment than that enjoyed by Wilson, and their work has to a large extent survived a critical examination by Kronenbourg (60). Schlösser indicates a leakage loss due to fluid inertia effects but this is not supported by Thoma on the grounds that Schlösser's equation shows this loss to be proportional to the root of the pump pressure and this would, together with the slip leakage, give a total leakage which increases less than proportionally with pump pressure. Tests on hydrostatic pumps and motors of all types invariably indicate leakages which increase more than proportionally with pressure. Schlösser's leakage loss due to fluid inertia is rejected in this work on the grounds that to match experimental results, the coefficient C_i would be negative in value and this would indicate a flow from a low pressure zone to a high pressure zone.

Schlösser includes a torque loss term for hydrodynamic effects within the pump and this constitutes an important improvement on the models of Wilson. However Schlösser failed to relate this loss to the pump displacement setting and this was included by Thoma. In addition Thoma included the constant pressure loss due to seal friction and similar losses not affected by pressure or viscosity.

It was therefore decided that Thoma's mathematical models would be chosen as the framework for the pump performance prediction method.

Thoma's models can be expressed by the two equations -

$$Q_e = a n q - \frac{C_s P q}{2\pi\mu} - Q_f$$

and

$$M_e = \frac{a P q}{2\pi} + C_v \mu n q + \frac{C_f P q}{2\pi} + C_h a^3 n^2 \rho q^{5/3} + M_c$$

No attempt has been made to deal with the flow loss due to cavitation at the pump inlet, Q_r as besides being virtually indeterminate, the loss would not be present in a properly engineered installation where a positive suction head can be expected by incorporating a boost pump or by gravitational means.

8.1 Performance Prediction Method

Slip Flow (Leakage)

In an axial piston pump leakage can be expected at the piston/cylinder bore, slipper bearing/swashplate and valve-plate/cylinder block interfaces. Since the various leakage flows will be from pump pressure P_1 to pump body pressure P_2 the coefficient of slip C_S can be considered as made up of the three sub-coefficients for the three parallel flow paths. Then -

$$C_s = C_{sp} + C_{ssb} + C_{svp}$$

where the suffixes relate to the three interfaces already identified. In addition there is an apparent leakage due to fluid compressibility. This can be denoted by the coefficient C_{sc}. An obvious difficulty arises from the changes of viscosity in the leakage paths due to pressure and temperature changes. This is fully discussed in Section 7.1.4 where it is proposed that an effective viscosity μ_{ef} should be used in such instances and where μ_{ef} is expressed by the equation -

$$\mu_{ef} = \mu_o e^{K_p \frac{P}{e}} \left[\frac{T_o}{T_o + \frac{\Delta T}{e}} \right]^{K_T}$$

and $\frac{\mu_{ef}}{\mu}$ is designated $\bar{\mu}$ and can be evaluated by using Fig.7.29.

Then if the total slip leakage is Q_S it can be expressed as -

$$Q_s = Q_{sp} + Q_{ssb} + Q_{svp} + Q_{sc}$$

Piston Slip Flow Coefficient C_{SP}

$$C_{sp} = Q_{sp} \cdot \frac{2\pi\mu}{q_p}$$

From equation (7.19) and on the basis that half the pistons are pumping at a particular time -

$$Q_{sp} = \left[\frac{1.375\pi P}{96\mu_{ef}\bar{l}_i} d_p C_d^3 - \frac{\pi}{4} d_p C_d \bar{V}_p\right]\frac{N_p}{2} \qquad (8.1)$$

then -

$$C_{sp} = \frac{d_p C_d N_p}{q}\left[0.141\frac{C_d^2}{\mu\bar{l}_i} - 2.467\frac{\mu}{P}\bar{V}_p\right] \qquad (8.2)$$

Slipper Bearing Slip Flow Coefficient C_{SSB}

If during the pumping stroke a clearance exists between the faces of the slipper bearing and the swashplate, leakage flow will occur. The presence of a gap is indicated by the balance factor B_{FSB} where

$$B_{FSB} = \frac{\text{Hydrostatic Force on Slipper Bearing}}{\text{Piston Pressure Force on Slipper Bearing}}$$

$$= \frac{(D_2^2 - D_1^2)\cos\phi}{2 d_p^2 \log_e\left(\frac{D_2}{D_1}\right)} \qquad (8.3)$$

If $B_{FSB} > 1$ a gap will result and the leakage flow is calculated from equation (7.50) and (5.24).

Then if -

$$C_{SSB} = Q_{SSB} \frac{2\pi\mu}{qP}$$

and on the basis that half the slipper bearings are loaded at a particular time -

$$Q_{SSB} = \frac{\pi^2 P d_p^2 h^3 N_p \sec\phi}{6\mu_{ef}(D_e^2 - D_i^2)} + \frac{\pi}{2} t_e D_i h n N_p \qquad (8.4)$$

to give -

$$C_{SSB} = \frac{\pi^2 d_p^2 h^3 N_p \sec\phi}{3\mu(D_e^2 - D_i^2)q} + \frac{\pi^2 \mu t_e D_i h N_p n}{qP} \qquad (8.5)$$

If $B_{FSB} < 1$ then assume h to be 0.0025mm, on the basis that it is probably somewhat less than the expected 0.0032mm asperity height of a ground surface.

Valve Plate Slip Flow Coefficient C_{SVP}

If when a pump is working a gap exists between the valve plate and the cylinder face, leakage flow will occur. As discussed in Section 7.1, for virtually all pump designs a clearance will be present due to the combined effects of hydrostatic and hydrodynamic forces. The magnitude of the gap will depend on the geometric features of the interface, the working pressure and speed of the pump and the valve plate balance factor B_{FVP} where -

$$B_{FVP} = \frac{\text{Hydrostatic Force on Valve Plate}}{\text{Total Piston Pressure Force and Spring Force on Cylinder}}$$

$$= \frac{\pi P \left(D_{L4}^2 + D_{L3}^2 - D_{L2}^2 - D_{L1}^2 \right)}{16 \left(\frac{\pi}{8} \alpha_p^2 N_p P + F_s \right)} \qquad (8.6)$$

If $B_{FVP} > 1$ the gap height will be C_{MAX} and if $B_{FVP} < 1$ the gap height can be obtained from Fig. (7.47).

Then if -

$$C_{SVP} = Q_{SVP} \frac{2\pi\mu}{P_q}$$

from equation (7.82) -

$$Q_{SVP} = \frac{\Theta C^3 P}{6\mu_{eff}} \left[\frac{D_{L3}}{(D_{L4} - D_{L2})} + \frac{D_{L2}}{(D_{L2} - D_{L1})} \right] + \frac{\pi}{8} Cn \left(D_{L3}^2 - D_{L2}^2 \right) \qquad (8.7)$$

to give -

$$C_{SVP} = \frac{\Theta \pi C^3}{3\mu q} \left[\frac{D_{L3}}{(D_{L4} - D_{L2})} + \frac{D_{L2}}{(D_{L2} - D_{L1})} \right] + \frac{\pi^2 C \mu n}{4 P q} \left(D_{L3}^2 - D_{L2}^2 \right) \qquad (8.8)$$

Fluid Compressibility Slip Flow Coefficient C_{SC}

If V_o is the volume of fluid trapped between the valve plate and a piston when the piston is at mid-stroke, the total volume V_4 trapped at the beginning of the pumping stroke is -

$$V_4 = V_o + \frac{\pi}{8} \alpha_p^2 r_e \tan \phi$$

From equation (5.18) the decrease in volume flow for a single piston per pumping stroke is $V_4 \frac{P}{B}$

Then the decrease in volume flow rate for the entire pump is Q_{SC} where -

$$Q_{SC} = V_4 \frac{P}{B} N_p n$$

$$= \left(V_o + \frac{\pi}{8} d_p^2 r_e \tan \phi\right) \frac{P}{B} N_p n \qquad (8.9)$$

Since -

$$Q_{SC} = C_{SC} \frac{P_{q-}}{2\pi\mu}$$

$$C_{SC} = \frac{2\pi\mu N_p n}{Bq} \left[V_o + \frac{\pi}{8} d_p^2 r_e \tan \phi \right] \qquad (8.10)$$

Torque Losses

Torque losses will occur in a number of regions. At the piston/cylinder bore, slipper bearing/swashplate and valve plate/cylinder block interfaces, viscous drag will result in torque losses whereas in the shaft bearings and in the case of an under-balanced valve plate of slipper bearing, surface contact will create dry or contact friction torque losses. Torque losses will also result from the fluid flow conditions, in the pump ports and ducts and these are frequently turbulent. These are hydrodynamic losses and are augmented if rolling element bearings are used by the hydrodynamic torque losses within the bearings. Frictional contact at sealing surfaces where the contact pressure remains unchanged with changes of pump pressure, contribute further to the torque losses.

Since for each type of torque loss, the total loss is the sum of the individual losses, the related torque loss coefficient is made up of the individual torque loss for that specific region of the pump and can be conveniently identified by appropriate suffixes.

Viscous Torque Loss

If the total viscous torque loss M_V is expressed in terms of the individual viscous torque losses, then -

$$M_V = M_{VP} + M_{VSB} + M_{VVP}$$

It will be recognised that if a particular interface has less than full hydrostatic balancing, the torque loss will be due to contact friction and must be taken care of in that part of the analysis.

The overall viscous drag coefficient is expressed as -

$$C_V = C_{VP} + C_{VSB} + C_{VVP}$$

The component viscous drag coefficients are discussed in the following sections.

Piston Viscous Drag Coefficient C_{VP}

$$C_{VP} = \frac{M_{VP}}{\mu n q}$$

From equation (7.20) and on the basis that all the pistons contribute to the viscous drag losses -

$$M_{VP} = 2 \frac{d_P \mu_{ef} \bar{l}_i \bar{V}_P^2 N_P}{C_d n} \qquad (8.11)$$

then -

$$C_{VP} = 2 \frac{d_P \bar{\mu} \bar{l}_i \bar{V}_P^2 N_P}{C_d n^2 q} \qquad (8.12)$$

Slipper Bearing Viscous Drag Coefficient C_{VSB}

Viscous drag will occur if a fluid film separating the slipper bearing and swashplate faces exists. The presence of such a film is indicated by the Slipper Bearing Balance Factor B_{FSB}

If $B_{FSB} > 1$

$$C_{VSB} = \frac{M_{VSB}}{\mu n q}$$

From equation (5.43) and on the basis that all the slipper bearings contribute to the viscous drag losses -

$$M_{VSB} = \frac{\pi^2}{4} \mu_{ef} N_p r_e^2 n \left(D_e^2 - D_i^2\right) \left[\frac{1}{h} + \frac{1}{h_{MAX}}\right] \tag{8.13}$$

Then -

$$C_{VSB} = \frac{\pi^2}{4} \frac{\mu}{q} N_p r_e^2 \left(D_e^2 - D_i^2\right) \left[\frac{1}{h} + \frac{1}{h_{MAX}}\right] \tag{8.14}$$

If $B_{FSB} < 1$

Under these conditions viscous drag will only occur because of the suction slipper bearings. Then -

$$M_{VSB} = \frac{\pi^2 \mu_{ef} N_p r_e^2 n \left(D_e^2 - D_i^2\right)}{4 h_{MAX}} \tag{8.15}$$

and

$$C_{VSB} = \frac{\pi^2 \mu N_p r_e^2 \left(D_e^2 - D_i^2\right)}{4 q h_{MAX}} \tag{8.16}$$

Valve Plate Viscous Drag Coefficient C_{VVP}

$$C_{VVP} = \frac{M_{VVP}}{\mu n q}$$

If the Valve Plate Balance Factor B_{FVP} is greater than one, it can be taken that the gap height will be C_{MAX}. Then on the basis that the viscous drag occurs at the valve lands only, from equation (5.25) we can write -

$$M_{VVP} = \frac{\pi^2 \mu_{ef} n}{16 C_{MAX}} \left[D_{L4}^4 - D_{L3}^4 + D_{L2}^4 - D_{L1}^4 \right] \tag{8.17}$$

to give -

$$C_{VVP} = \frac{\pi^2 \mu}{16 C_{MAX} q} \left[D_{L4}^4 - D_{L3}^4 + D_{L2}^4 - D_{L1}^4 \right] \tag{8.18}$$

If $B_{FVP} < 1$ the gap height C can be estimated from equation (7.81) and by substituting C for C_{MAX} we have -

$$M_{VVP} = \frac{\pi^2 \mu_{ef} n}{16 C} \left[D_{L4}^4 - D_{L3}^4 + D_{L2}^4 - D_{L1}^4 \right] \tag{8.19}$$

and -

$$C_{VVP} = \frac{\pi^2 \mu}{16 C q} \left[D_{L4}^4 - D_{L3}^4 + D_{L2}^4 - D_{L1}^4 \right] \tag{8.20}$$

Torque Loss Due to Coulomb Friction

Frictional torque losses will result from loaded contacting surfaces with relative motion. Instances within an axial piston pump are -

1. Between the pistons and the cylinder bores.
2. Between the slipper bearings and the swashplate.
3. Between the valve plate and the cylinder block.
4. Between the shaft bearing components.
5. Between the slipper bearing and the piston ball end.

It has already been suggested that a fluid film capable of supporting the applied loads exists between the valve plate and the cylinder block so that the coulomb frictional losses at this interface can be taken as zero. It will also be apparent that the frictional losses in the piston/slipper bearing ball joint will be of a low order and are not considered further in this work.

Thus if the total frictional torque loss is

$$M_f = M_{fP} + M_{fSB} + M_{fB}$$

and the overall coefficient of dry friction is C_f we have -

$$C_f = C_{fP} + C_{fSB} + C_{fB}$$

The component dry friction coefficients are discussed in the following sections.

Piston Dry Friction Coefficient C_{fP}

As shown in Section 5.3.1, contact friction occurs between the pistons and cylinder bores. This frictional force will vary appreciably during the pumping cycle and this will result in cyclic torque variations. The contact forces are low during the suction stroke and can be neglected in this instance but during the pumping stroke

their value can be high at the beginning of the stroke and fall to a much lower value at the end of the stroke.

Simplified equations for the reactions R_A and R_B are -

$$R_A = \frac{\pi}{4} d_p^2 P_1 \frac{l_p}{l_i} \tan\phi$$

$$R_B = \frac{\pi}{4} d_p^2 P_1 \left(\frac{l_p - l_i}{l_i}\right) \tan\phi$$

to give a total contact reaction of R_P where -

$$R_P = \frac{\pi}{4} d_p^2 P_1 \left(2\frac{l_p}{l_i} - 1\right) \tan\phi$$

and a piston friction force F_{fP} of -

$$F_{fP} = \frac{\pi}{4} d_p^2 P_1 f_B \left(2\frac{l_p}{l_i} - 1\right) \tan\phi$$

The resulting frictional torque M_{fP} for a single piston during the pumping stroke can be described as -

$$M_{fP} = \frac{\pi}{4} d_p^2 P_1 f_B r_c \left(2\frac{l_p}{l_i} - 1\right) \tan^2\phi \sin\beta$$

and since the mean value of this torque is obtained by integrating M_{fP} with respect to rotation angle β between the limits of $\beta = \pi$ and $\beta = 0$ the mean frictional torque for half the pistons is expressed as -

$$\bar{M}_{fP} = \frac{N_p}{2\pi} \int_0^{\pi} M_{fP} \, d\beta$$

to give for half the number of pistons in the pump -

$$M_{fP} = d_p^2 P_1 f_B N_p r_c \left[\left(\frac{2 l_p}{r_c \tan\phi}\right) \log_e \left(\frac{l_p - X + r_c \tan\phi}{l_p - X - r_c \tan\phi}\right) - 2\right] \times \tan^2\phi \qquad (8.21)$$

Since -

$$\bar{M}_{fP} = C_{fP} \frac{P_q}{2\pi}$$

then -

$$C_{fP} = \frac{\pi d_p^2}{4q} f_B N_p r_c \tan^2\phi \times \left[\left(\frac{2l_p}{r_c \tan\phi}\right) \log_e \left(\frac{l_p - X + r_c \tan\phi}{l_p - X - r_c \tan\phi}\right) - 2\right] \quad (8.22)$$

Slipper Bearing Dry Friction Coefficient C_{fSB}

If the design of a slipper bearing results in an underbalanced condition, dry friction losses will occur. The balance condition can be expressed in terms of the slipper bearing balance factor B_{FSB}.

If $B_{FSB} > 1$ *it can be assumed that no contact occurs* between the slipper bearing and the swashplate.

Then - $M_{fSB} = 0$

and - $C_{fSB} = 0$

If $B_{FSB} < 1$ the out of balance force being carried by the surface contact is -

$$\frac{\pi}{4} d_p^2 P (1 - B_{FSB}) \sec\phi$$

Then on the basis that half of the pump pistons are pumping at a particular instance -

$$M_{fSB} = \frac{\pi}{8} d_p^2 P (1 - B_{FSB}) f_B r_e N_p \sec\phi \quad (8.23)$$

Since -

$$C_{fSB} \approx M_{fSB} \frac{2\pi}{Pq}$$

$$C_{fSB} = \frac{\pi^2}{4} \frac{d_p^2}{q} (1 - B_{FSB}) f_B r_e N_p \text{SEC}\phi$$

(8.24)

Pump Bearings Dry Friction Coefficient C_B

The frictional torque in the pump bearings is the sum of two components M_o and M_1 where M_o is due to hydrodynamic losses and M_1 is due to conditions at the loaded contact surfaces.

M_1 which is load dependent and is the predominant bearing torque loss at low speeds results from the elastic deformation of the bearing elements and the partial sliding that occurs at the loaded contact surfaces. M_1 can be expressed as -

$$M_1 = f_1 g_1 P_o d_m$$

where f_1 is a factor depending on the bearing design and bearing load (see Appendix 2)

g_1 is a factor depending on the direction of the bearing loads (see Appendix 2)

P_o is the equivalent static bearing load (see Appendix 2)

d_m is the mean diameter of the bearing.

All the necessary data for calculating the equivalent static bearing load is given in bearing manufacturers' catalogues.

The radial and axial loads on the bearings can be expressed in terms of the pump pressure as indicated in Appendix 1, so that in turn the bearing frictional torque can also be expressed in terms of the pump pressure.

If M_{fB} is the total frictional torque of the pump bearings, then -

$$C_{fB} = \frac{2\pi M_{fB}}{P q}$$

to give for a two bearing pump -

$$C_{fB} = \frac{2\pi}{Pq}\left[f_{11} g_{11} P_{01} d_{m1} + f_{12} g_{12} P_{02} d_{m2} \right] \qquad (8.25)$$

where suffixes 1 and 2 refer to bearing 1 and 2 respectively.

Hydrodynamic Torque Loss

The hydrodynamic torque losses in a pump are made up of the losses due to pressure drops in the various flow paths, the churning of the hydraulic fluid in the pump body and the hydrodynamic torque losses in the pump bearings. Unfortunately the complexity of the flow paths in terms of cross-sectional areas, changes of section and changes of direction makes only an approximate evaluation possible.

The losses due to the churning of fluid in the pump body are indeterminate and of necessity will not be considered further in this analysis.

Thus the total torque losses due to hydrodynamic effects can be expressed as -

$$M_h = M_{hFP} + M_{hB}$$

and the overall coefficient of hydrodynamic torque loss as -

$$C_h = C_{hFP} + C_{hB}$$

Flow Path Hydrodynamic Coefficient C_{hFB}

In a well designed pump the various flow paths are likely to be of reasonably generous proportions to facilitate fluid flow. The length of the flow paths will be small so that the individual pressure losses due to 'pipeline losses' can also be expected to be small. In addition the provision of a positive head at the pump inlet port can be said to remove the inlet flow path losses from the considerations of the pump performance. It is therefore suggested that losses in the pump flow paths consist solely of pressure losses due to change of section in the passages on the pressure side of the pump.

From (5.9) the pressure loss ΔP due to a change in cross-section of a flow path is given as -

$$\Delta P = \frac{\xi \rho}{A_2^2 2} a^2 q^2 n^2$$

The total pressure loss ΔP_T is $\Sigma \left(\frac{\xi}{A_2^2}\right) \frac{\rho}{2} a^2 q^2 n^2$

The hydrodynamic torque loss is then -

$$M_{hFP} = \Sigma \left(\frac{\xi}{A_2^2}\right) \frac{\rho}{4\pi} a^3 q^3 n^2 \qquad (8.26)$$

and since -

$$C_{hFP} = \frac{M_{hFP}}{a^3 n^2 \rho q^{5/3}}$$

$$C_{hFP} = \Sigma \left(\frac{\xi}{A_2^2}\right) \frac{q^{4/3}}{4\pi} \qquad (8.27)$$

Bearing Hydrodynamic Coefficient C_{hB}

The hydrodynamic torque loss M_o in a rolling element bearing is independent of load and predominates in a high speed, lightly loaded bearings and can be evaluated from the expression -

$$M_o = f_o (\nu n)^{2/3} d_m^3$$

where f_o is a factor dependent on the bearing design and mode of lubrication (see Appendix 3)

ν is the kinematic viscosity of the lubricant.

Since the bearings are completely submerged in the hydraulic fluid, factor f_o must be taken as that recommended for oil bath lubrication with a vertical shaft.

The hydraulic fluid will not be under pressure but will be at a temperature somewhat higher than that at the inlet port.

For a pump with two bearings -

$$M_{hB} = \left[f_{o1} d_{m1}^3 + f_{o2} d_{m2}^3 \right] \left(\frac{\mu n}{\rho} \right)^{2/3} \qquad (8.29)$$

and since -

$$C_{hB} = \frac{M_{hB}}{a^3 n^2 \rho q^{5/3}}$$

Then -

$$C_{hB} = \frac{\mu^{2/3}}{a^3 n^{4/3} \rho^{5/3} q^{5/3}} \left[f_{o1} d_{m1}^3 + f_{o2} d_{m2}^3 \right] \qquad (8.30)$$

Constant Torque Loss

Constant torque loss will occur at the pump seals which are frequently of the rotary lip seal variety. Thoma expresses this loss in terms of a pressure loss but as the direct torque loss is easily estimated from seal manufacturers' catalogues, it is proposed not to perpetuate this concept. Typical curves for the torque losses in rotary lip seals in a 'run in' condition are shown in Fig.8.1.

A useful range of values is likely to be for seal diameters from 25mm to 75mm diameter and a mathematical equation to fit the seal manufacturers' empirical curve is -

$$-M_c = 1.58 \times 10^{-4} d_s^2 + 5.66 \times 10^{-4} d_s \quad (Nm) \qquad (8.31)$$

where d_s is the seal diameter in mm.

Performance Prediction Calculations

Having derived the values of the various coefficients and that of the constant torque, the effective flow rate Q_e and the input torque M_e of the pump can be calculated at any set of working conditions. Further simple calculations will result in value for the volumetric efficiency η_v, the mechanical efficiency η_m and the overall efficiency η.

Fig.8.2, shows a flow chart for the systematic calculation of the predicted performance and this chart will greatly assist the writing of computer programs.

It will be seen that the specific values of the coefficients will provide a clear indication of the losses suffered in particular areas of the pump and should greatly assist in improving the design if the pump performance is not up to the specified levels.

It is appreciated that the flow chart does not accommodate all axial piston pump design variations, e.g., spring return pistons, but with the theory derived in the test it should be easy to make the minor amendments necessary within the framework of the method.

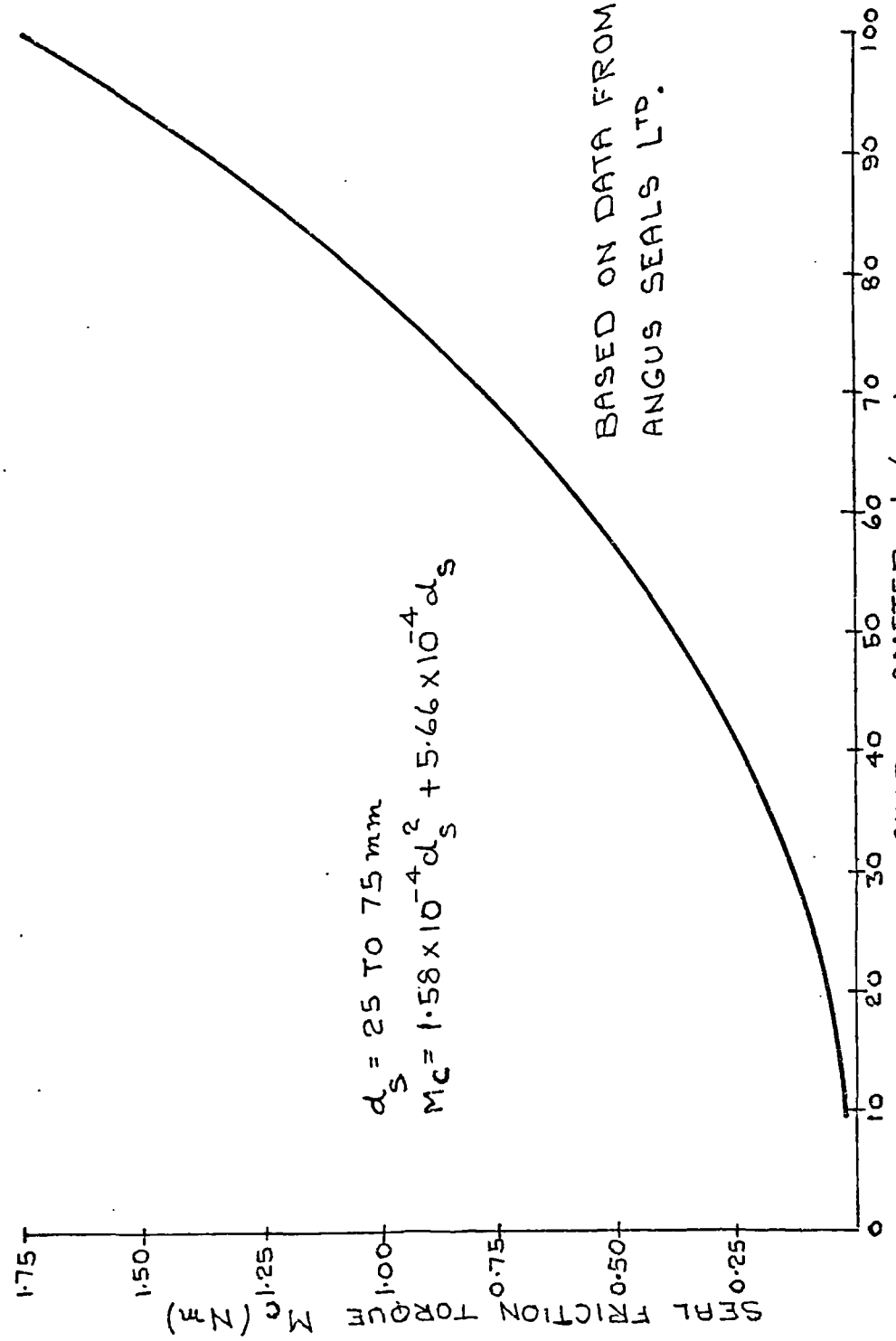

FIGURE 8.1. FRICTIONAL TORQUE IN ROTORY LIP SEALS.

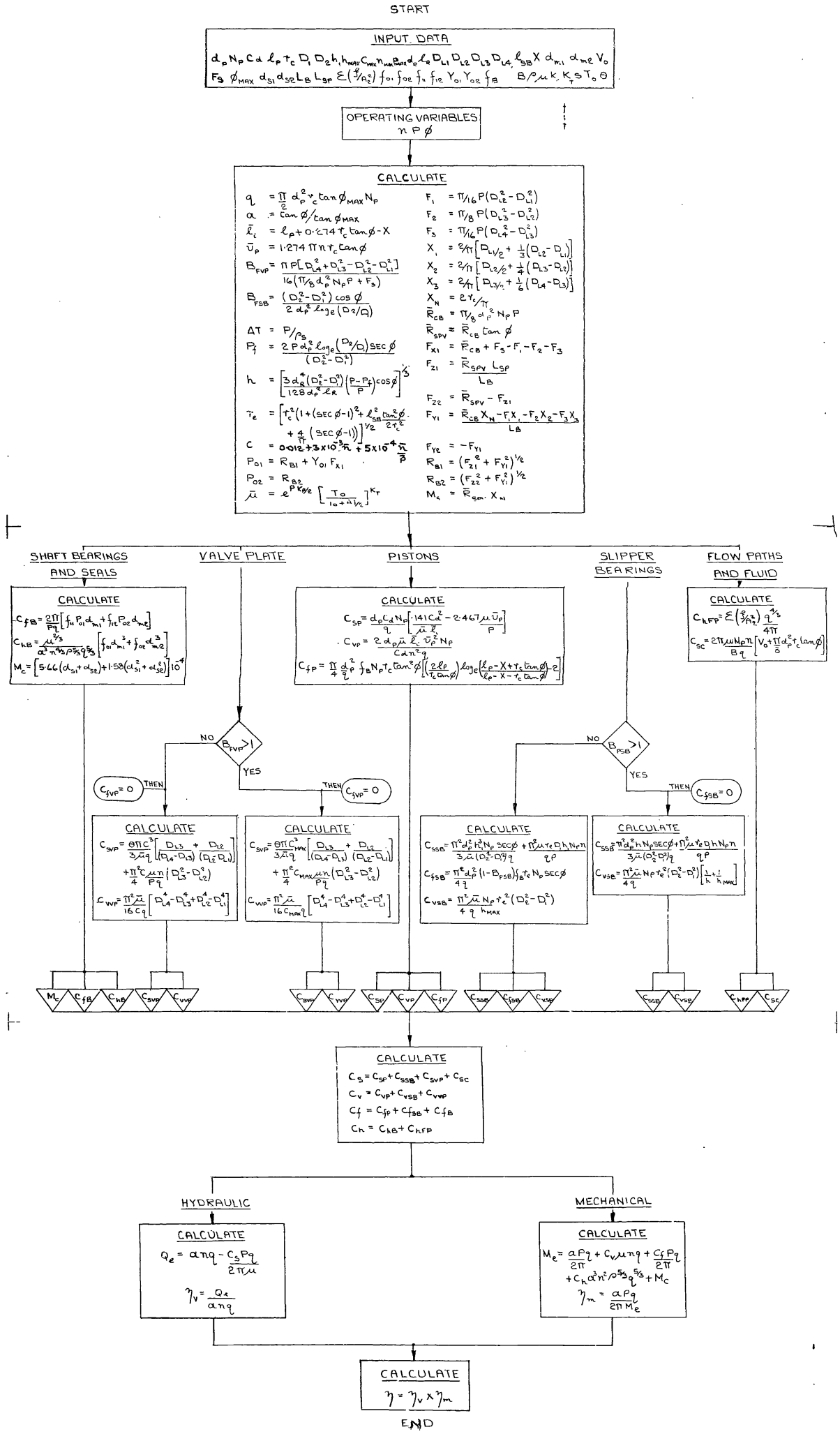

FIGURE 8.1. PERFORMANCE PREDICTION CHART FOR AXIAL PISTON PUMPS

8.2 Predicted Performance of Lucas HD900 Pump

To enable the performance prediction method to be applied to the HD900 pump the following data was obtained from the pump drawings, the bearing manufacturers' catalogues and the oil companys' data sheets.

Pump Data

Diameter of piston	d_p	=	23.619mm
Number of pistons	N_p	=	7
Piston diametral clearance	c_d	=	0.036mm
Length of piston	ℓ_p	=	61.300mm
Pitch circle radius of cylinder bores	r_c	=	41.275mm
Outside diameter of slipper bearing	D_2	=	30.724mm
Diameter of slipper bearing recess	D_1	=	17.221mm
Diameter of slipper bearing choke	d_R	=	0.838mm
Length of slipper bearing choke	ℓ_R	=	3.937mm
Maximum slipper bearing clearance	h_{MAX}	=	0.248mm
O.Dia. of outer valve plate load	D_{L4}	=	88.570mm
I.Dia. of outer valve plate land	D_{L3}	=	84.125mm
O.Dia. of inner valve plate land	D_{L2}	=	65.075mm
I.Dia. of inner valve plate land	D_{L1}	=	60.503mm
Maximum valve plate clearance	C_{MAX}	=	0.445mm
Length of slipper bearing	ℓ_{SB}	=	15.000mm
End of cylinder to tilt axis	X	=	14.554mm
Maximum swashplate angle	ϕ_{MAX}	=	15°
Diameter of seal	d_S	=	50.800mm
Cylinder spring force	F_S	=	1200 N
Mean diameter of bearing 1	d_{m1}	=	77.5mm
Mean diameter of bearing 2	d_{m2}	=	53.5mm

Distance from bearing 2 to swashplate face	L_{SP}	= 185mm
Distance between bearings	L_B	= 250mm
Trapped volume per piston	V_o	= 1.782×10^{-5} m^3
Angle subtended by valve plate port	θ	= 2.32 Radian
Total flow path characteristic	$\mathcal{E}\left(\mathcal{E}_3/A_2^2\right)$	= 14×10^6

Bearing Data

Bearing design and lubrication factor 1	f_{01}	= 1.226×10^{-8}
Bearing design and lubrication factor 2	f_{02}	= 1.226×10^{-8}
Bearing design and load factor 1	f_{11}	= 0.0004
Bearing design and load factor 2	f_{12}	= 0.0004
Bearing static load factor 1	Y_{01}	= 2.8
Bearing static load factor 2	Y_{02}	= 2.2

Hydraulic Fluid Data

Shell Tellus 27 Mineral Hydraulic Fluid

Dynamic viscosity at 50°C	μ	= 17.4×10^{-3} Ns/m^2
Density	ρ	= 850 kg/m^3
Pressure coefficient of viscosity	K_P	= 2.5×10^{-3} bar^{-1}
Temperature coefficient of viscosity	K_T	= 2.96
Specific heat	S	= 2.03 kJ/kg^oK
Bulk modulus	B	= 12 kbar

Coefficient of Friction

Bronze on hardened and ground steel with mixed lubrication	f_B	= 0.03

Pump Operating Range

Maximum pump speed	N_{MAX}	=	2900 rev/min
Maximum pump pressure	P_{MAX}	=	350 bar
Hydraulic fluid inlet temperature	T_o	=	$50^{o}C$

Derived Values at Maximum Displacement Setting

Volumetric displacement	q	=	$6.784 \times 10^{-5} m^3/rev$
Displacement setting	α	=	1
Mean length of piston immersion	$\bar{l}_i$	=	49.776mm
Mean piston velocity	$\bar{V}_p$	=	$44.265\ n \times 10^{-3} m/s$
Valve plate balance factor	B_{FVP}	=	$\frac{P}{1.112P+(8.7\times10^{5})}$
Slipper bearing balance factor	B_{FSB}	=	0.968
Temperature rise	ΔT	=	$5.795\ P \times 10^{-7}\ ^{o}K$
Pressure in slipper bearing recess	P_f	=	$0.449\ P$
Height of slipper bearing gap	h	=	0.0025mm
Effective radius for slipper bearings	r_e	=	42.300mm
Height of valve plate gap	C	=	$1.2\times10^{-3}+3\times10^{-3}\bar{n}+5\times10^{-4}\frac{\bar{n}}{\bar{P}}$
Valve plate balance force	F_1	=	$1.127\ P \times 10^{-4}\ N$
Valve plate balance force	F_2	=	$11.161\ P \times 10^{-4} N$
Valve plate balance force	F_3	=	$1.507\ P \times 10^{-4}\ N$
Valve plate centre of force	X_1	=	20.229mm
Valve plate centre of force	X_2	=	23.746mm
Valve plate centre of force	X_3	=	27.249mm
Resultant valve plate centre of force	X_N	=	26.276mm
Reaction of cylinder and valve plate	$\bar{R}_{CB}$	=	$1.533\ P \times 10^{-3}\ N$
Reaction of swashplate	$\bar{R}_{SPV}$	=	$4.108\ P \times 10^{-4}\ N$

Load on bearing 1 in 'x' direction	F_{X1}	$= (1.535 P \times 10^{-4}) + 1200$ N
Load on bearing 1 in 'y' direction	F_{Y1}	$= 2.957\ P \times 10^{-5}$ N
Load on bearing 1 in 'z' direction	F_{Z1}	$= 3.040\ P \times 10^{-4}$ N
Load on bearing 2 in 'y' direction	F_{Y2}	$= -2.957\ P \times 10^{-5}$ N
Load on bearing 2 in 'z' direction	F_{Z2}	$= 1.068\ P \times 10^{-4}$ N
Resultant load on bearing 1	R_{B1}	$= 3.054\ P \times 10^{-4}$ N
Resultant load on bearing 2	R_{B2}	$= 1.108\ P \times 10^{-4}$ N
Equivalent static load on bearing 1	P_{o1}	$= (7.352\ P \times 10^{-4}) + 3360$ N
Equivalent static load on bearing 2	P_{o2}	$= 1.108\ P \times 10^{-4}$ N

Values of $\bar{\mu}$

Pressure P (bar)	$\bar{\mu}$
50	.977
100	.959
150	.942
200	.928
250	.916
300	.905
350	.897

Valve Plate Gap Height C(mm)

P \ n	500	1000	1500	2000	2500	3000	rev/min
50	.0148	.0158	.0168	.0176	.0182	.0187	
100	.0140	.0148	.0154	.0159	.0164	.0167	
150	.0136	.0143	.0148	.0152	.0156	.0159	
200	.0134	.0140	.0144	.0147	.0150	.0153	
250	.0132	.0138	.0142	.0145	.0148	.0150	
300	.0131	.0136	.0140	.0143	.0145	.0147	
350 bar	.0130	.0135	.0138	.0141	.0143	.0145	

Pump Performance Coefficients

Slip Flow Coefficients

Pistons $C_{SP} = \frac{3.221}{\bar{\mu}} \times 10^{-10} - 1.667 \frac{n}{P} \times 10^{-4}$

Slipper Bearings $C_{SSB} = \frac{4.732}{\bar{\mu}} \times 10^{-12} + 3.227 \frac{n}{P} \times 10^{-5}$

Valve Plate $C_{SVP} = 1.189 \frac{C^3}{\bar{\mu}} \times 10^{-3} + 1.799\, C \frac{n}{P} \times 10^{-3}$

Fluid Compressibility $C_{SC} = 2.537\, n \times 10^{-10}$

Torque Loss Coefficients

Piston Viscous Drag $C_{VP} = 1.321 \bar{\mu} \times 10^{4}$

Slipper Bearing Viscous Drag $C_{VSB} = 1.189 \bar{\mu} \times 10^{3}$

Valve Plate Viscous Drag $C_{VVP} = 1.454 \frac{\bar{\mu}}{C} \times 10^{-1}$

Piston Friction $C_{fP} = 1.417 \times 10^{-2}$

Slipper Bearing Friction $C_{fSB} = 5.971 \times 10^{-3}$

Valve Plate Friction $C_{fVP} = 1.625 \times 10^{-1}(1 - B_{FVP})$

Pump Bearings Friction $C_{fB} = 2.330 \times 10^{-3} + \frac{9647}{P}$

Pump Bearings Hydrodynamic $C_{hB} = 5.92 \times 10^{-2} n^{3/4}$

Flow Path Hydrodynamic $C_{hFP} = 4.082$

Constant Torque Loss in Seals $M_c = 0.416$ Nm

Performance Equations

Effective Pump Flow Rate Qe (m^3/S)

$$nq - \frac{Pq}{2\pi\mu}\left[\frac{3.268 \times 10^{-10}}{\bar{\mu}} - 1.344\frac{n}{P} \times 10^{-4} + 1.188\frac{C^3}{\bar{\mu}} \times 10^{-3} + 1.799\, C\frac{n}{P} \times 10^{-3} + 2.537\, n \times 10^{-10}\right]$$

Effective Pump Torque Me (Nm)

$$\frac{Pq}{2\pi} + \mu n q\left[1.440\bar{\mu} \times 10^{4} + 1.454\frac{\bar{\mu}}{C} \times 10^{-1}\right] + \frac{Pq}{2\pi}\left[2.247 \times 10^{-2} + \frac{9647}{P} + 0.1625\left(1 - B_{FVP}\right)\right] + n^2 \rho q^{5/3}\left[\frac{5.92 \times 10^{-2}}{n^{4/3}} + 4.082\right] + 0.416$$

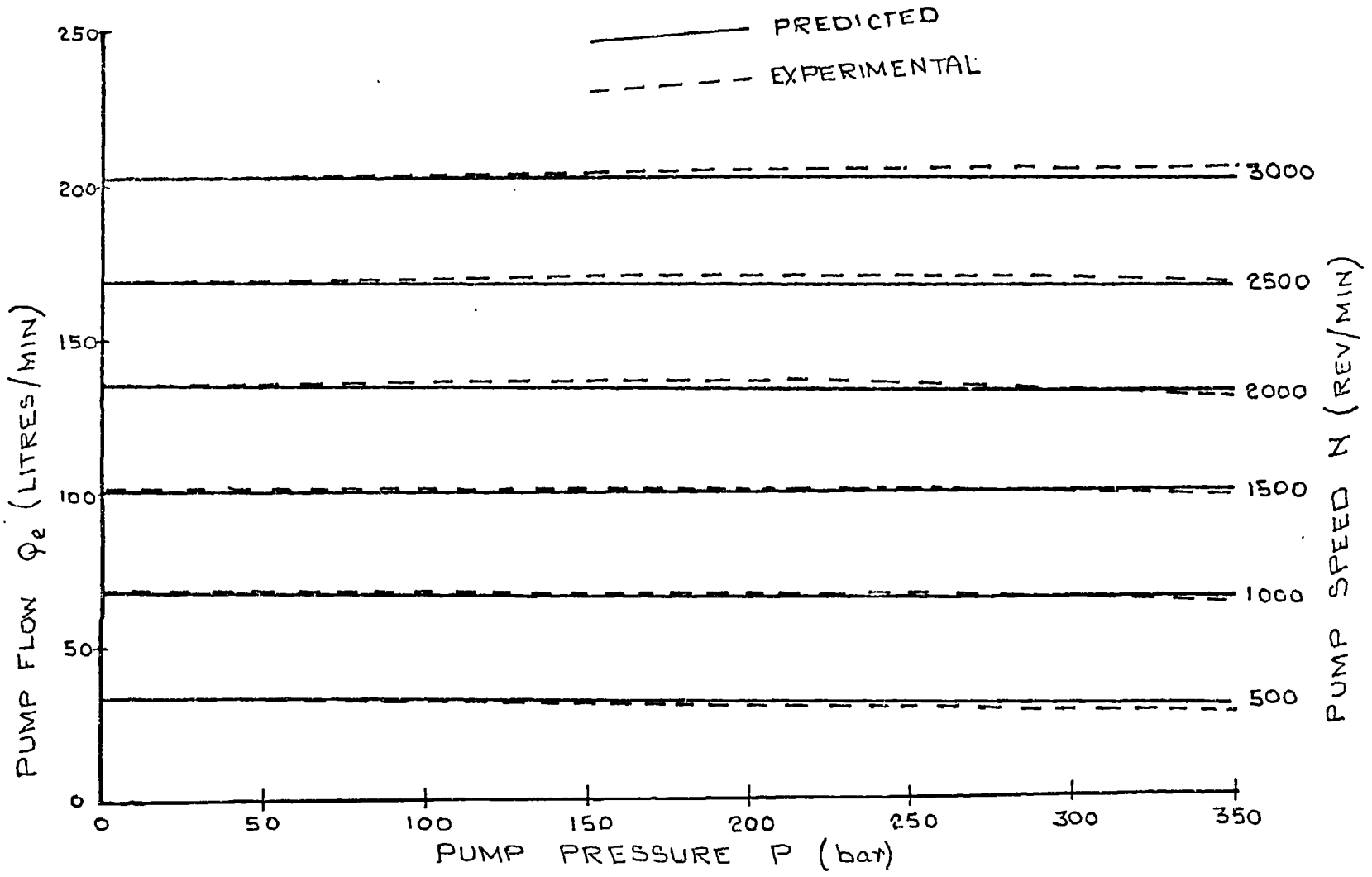

FIGURE 8.3. GRAPH OF PREDICTED AND EXPERIMENTAL PUMP FLOW AGAINST PUMP SPEED AND PUMP PRESSURE FOR HD900 PUMP.

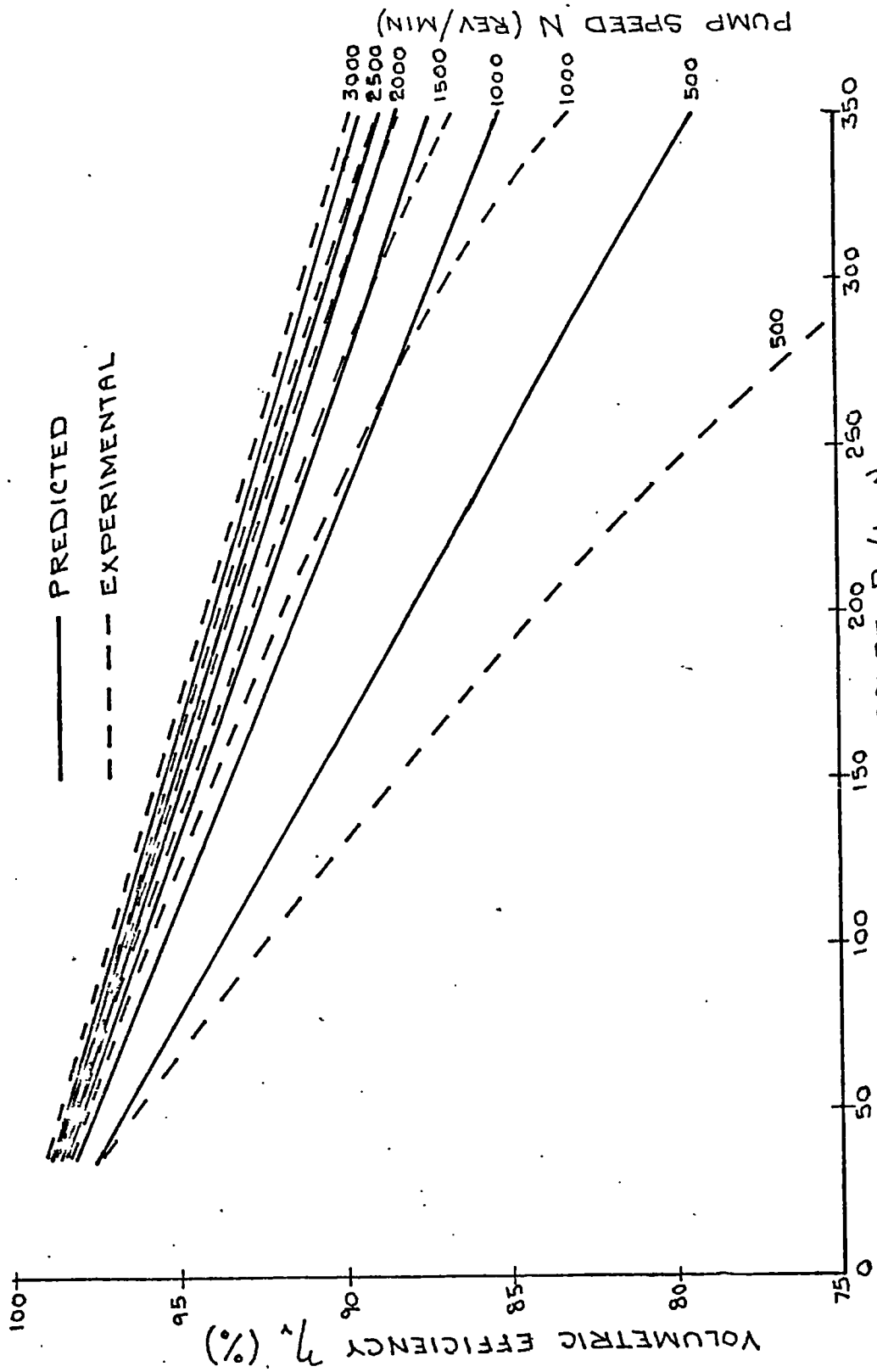

FIGURE 8.4. GRAPH OF PREDICTED AND EXPERIMENTAL VOLUMETRIC EFFICIENCY AGAINST PUMP SPEED AND PUMP PRESSURE FOR HD900 PUMP.

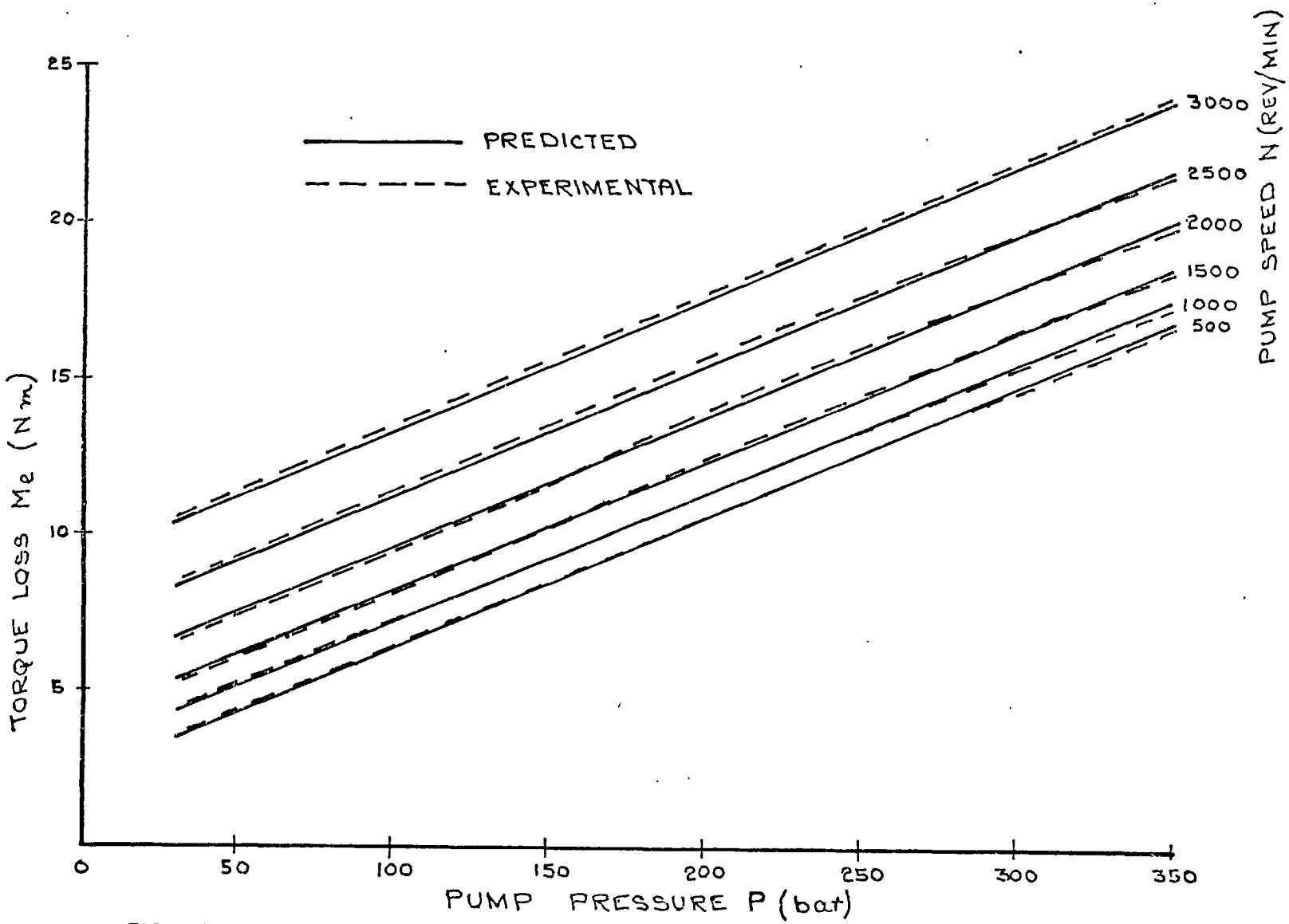

FIGURE 8.5. GRAPH OF PREDICTED AND EXPERIMENTAL TORQUE LOSS AGAINST PUMP SPEED AND PUMP PRESSURE FOR HD900 PUMP.

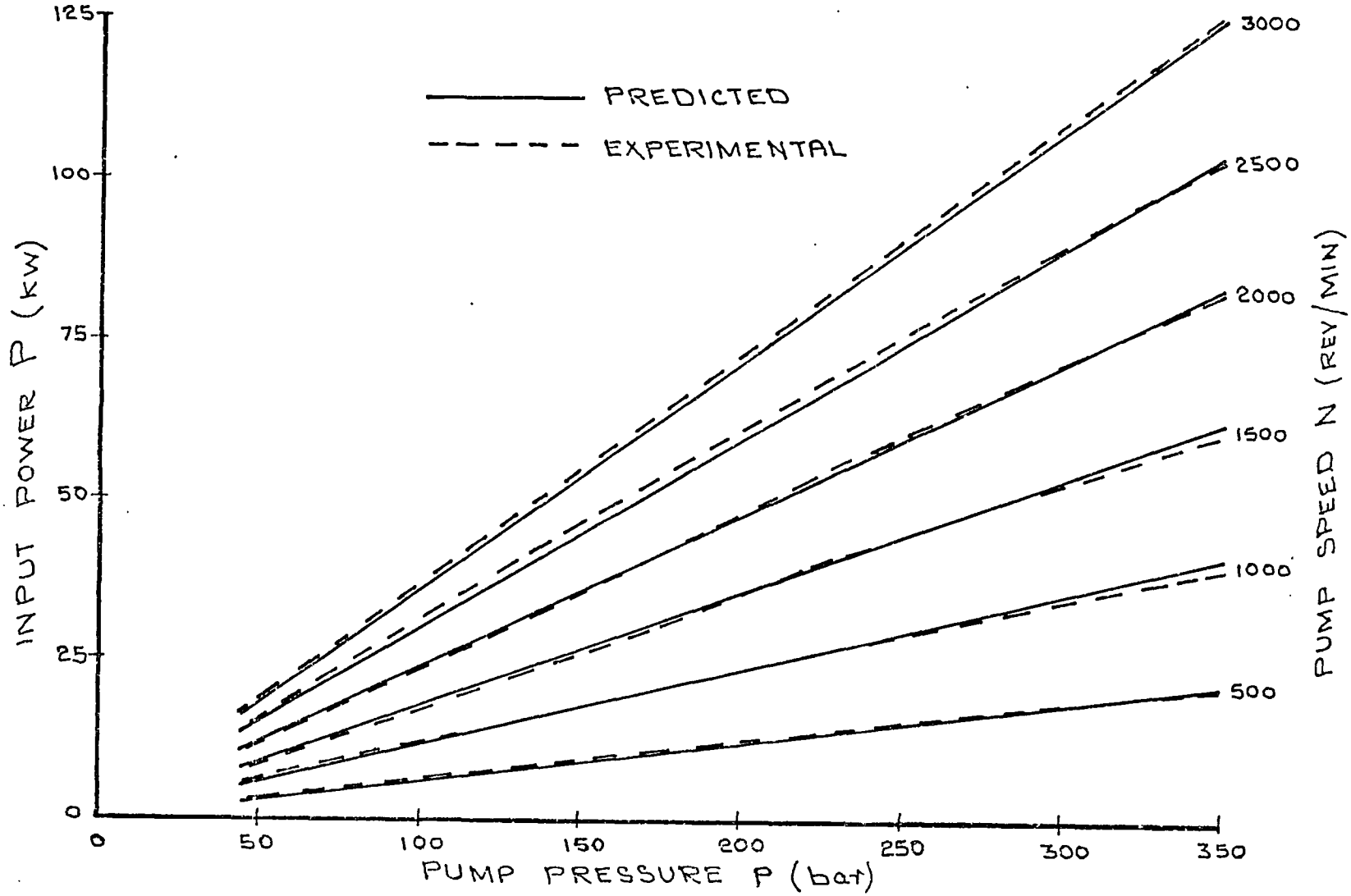

FIGURE 8.6. GRAPH OF PREDICTED AND EXPERIMENTAL INPUT POWER AGAINST PUMP SPEED AND PUMP PRESSURE FOR HD900 PUMP.

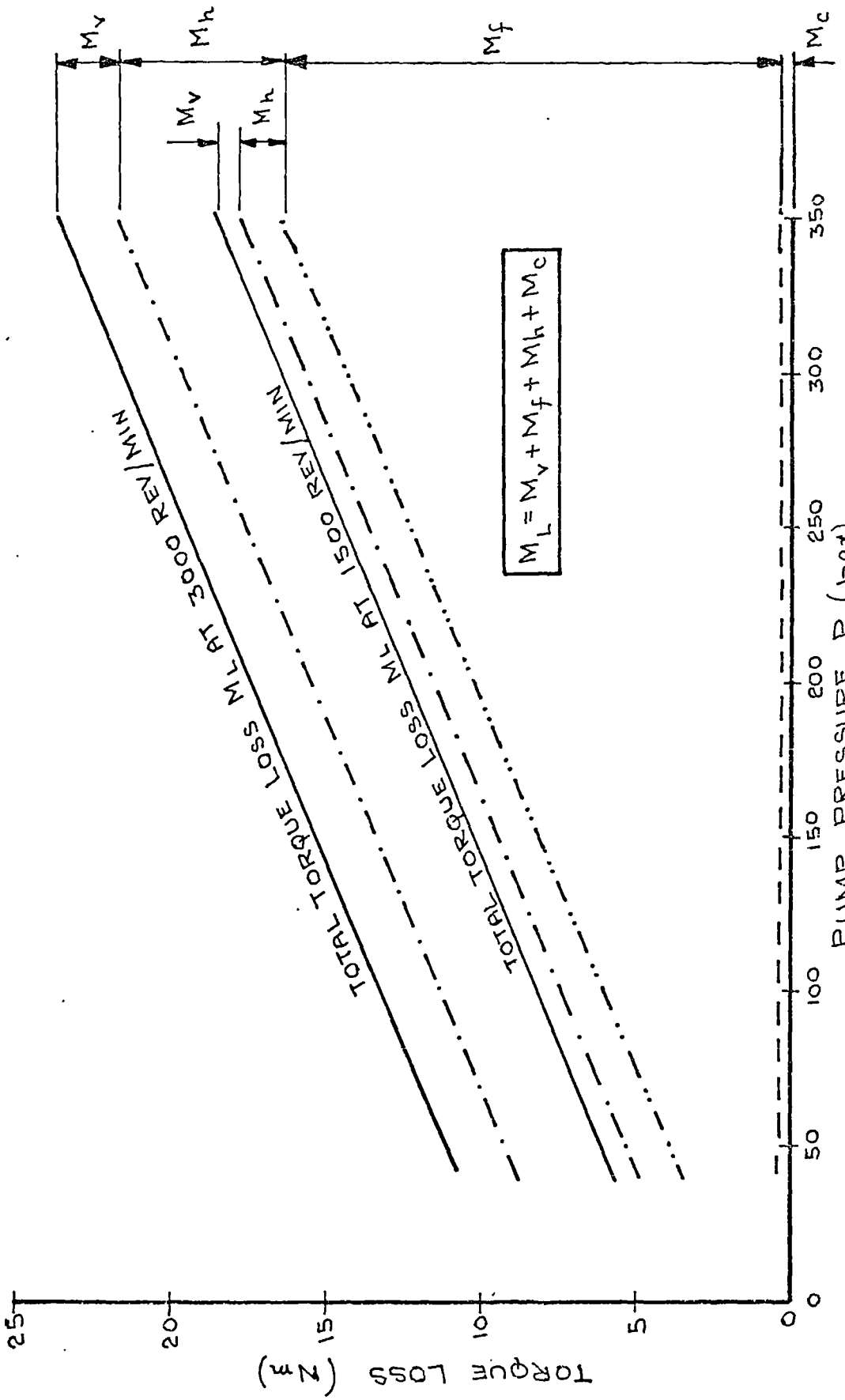

FIGURE 8.7 COMPONENT TORQUE LOSSES FOR HD900 PUMP AT 3000REV/MIN. AND 1500 REV/MIN.

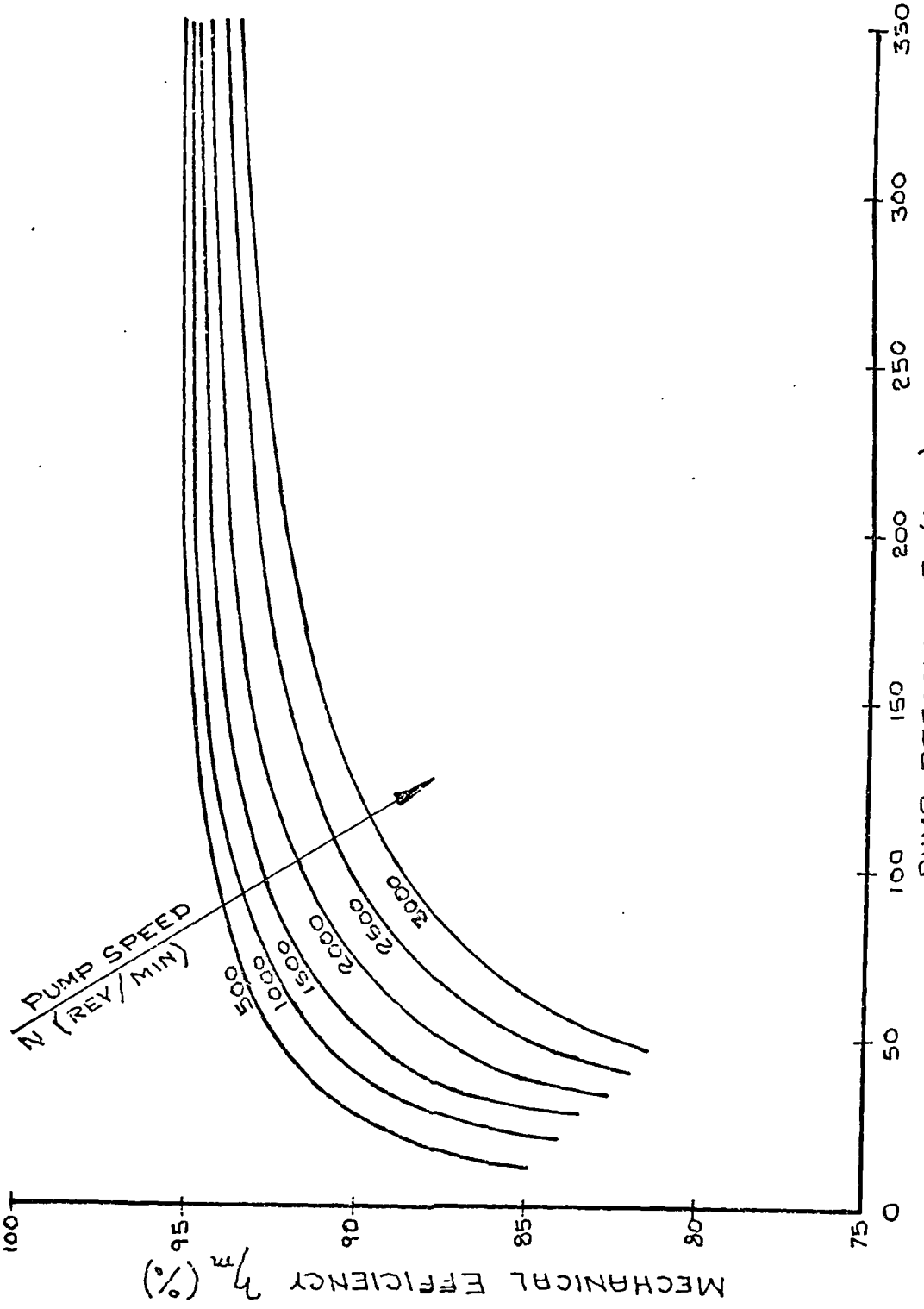

FIGURE 8.8. GRAPH OF PREDICTED MECHANICAL EFFICIENCY AGAINST PUMP SPEED AND PUMP PRESSURE FOR HD900 PUMP.

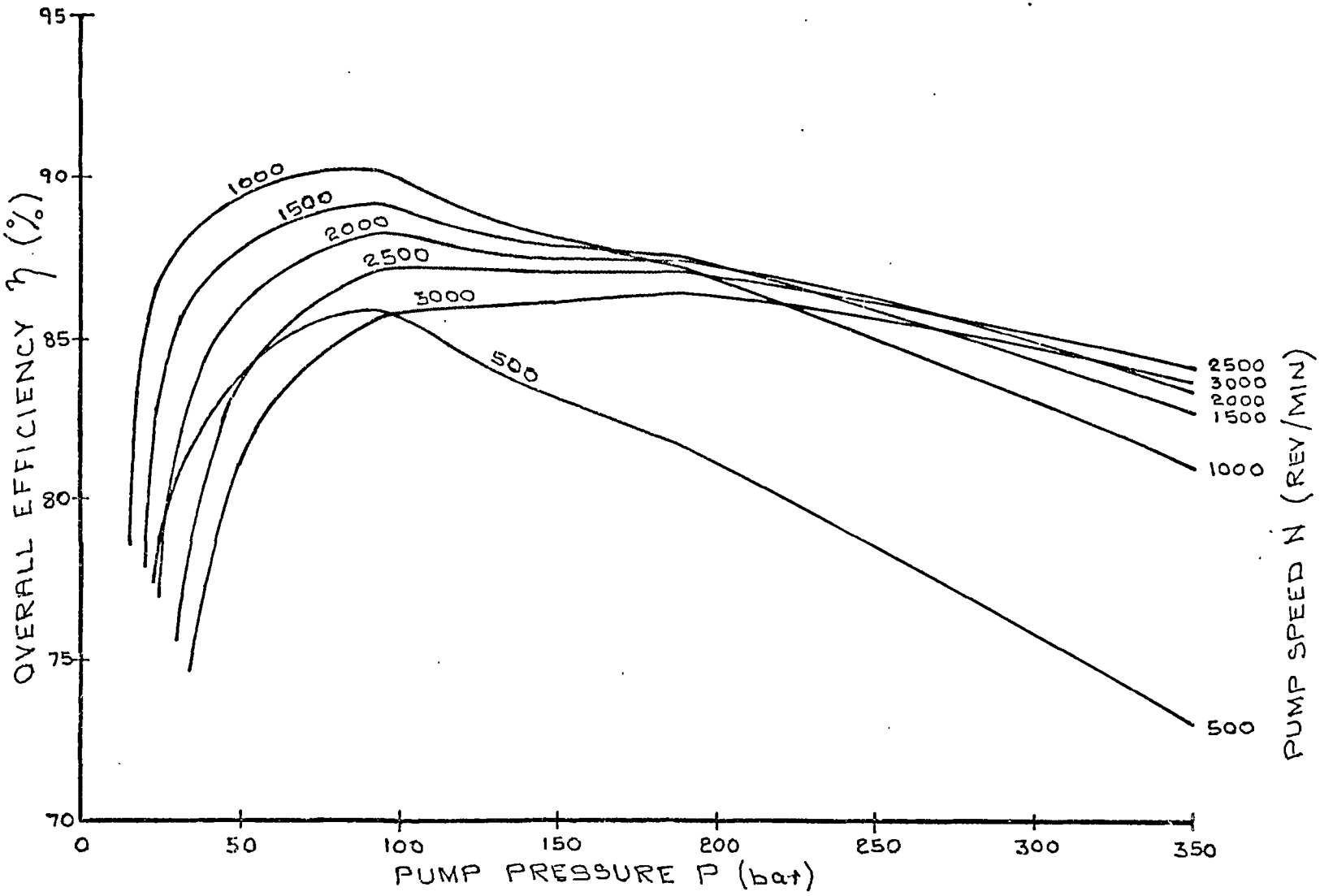

FIGURE 8.9. PREDICTED OVERALL EFFICIENCY OF HD900 PUMP.

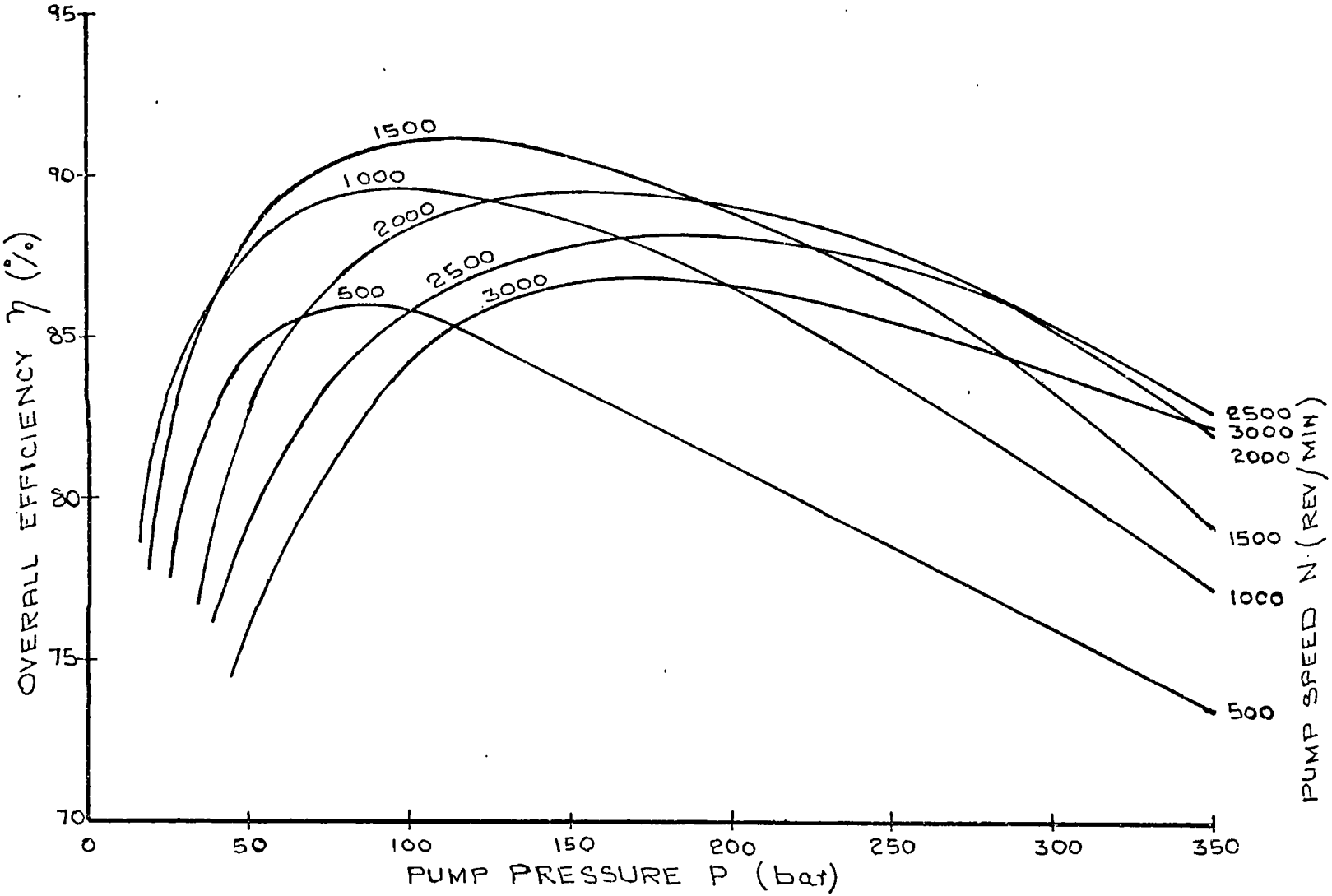

FIGURE 8.10. EXPERIMENTAL OVERALL EFFICIENCY OF HD900 PUMP.

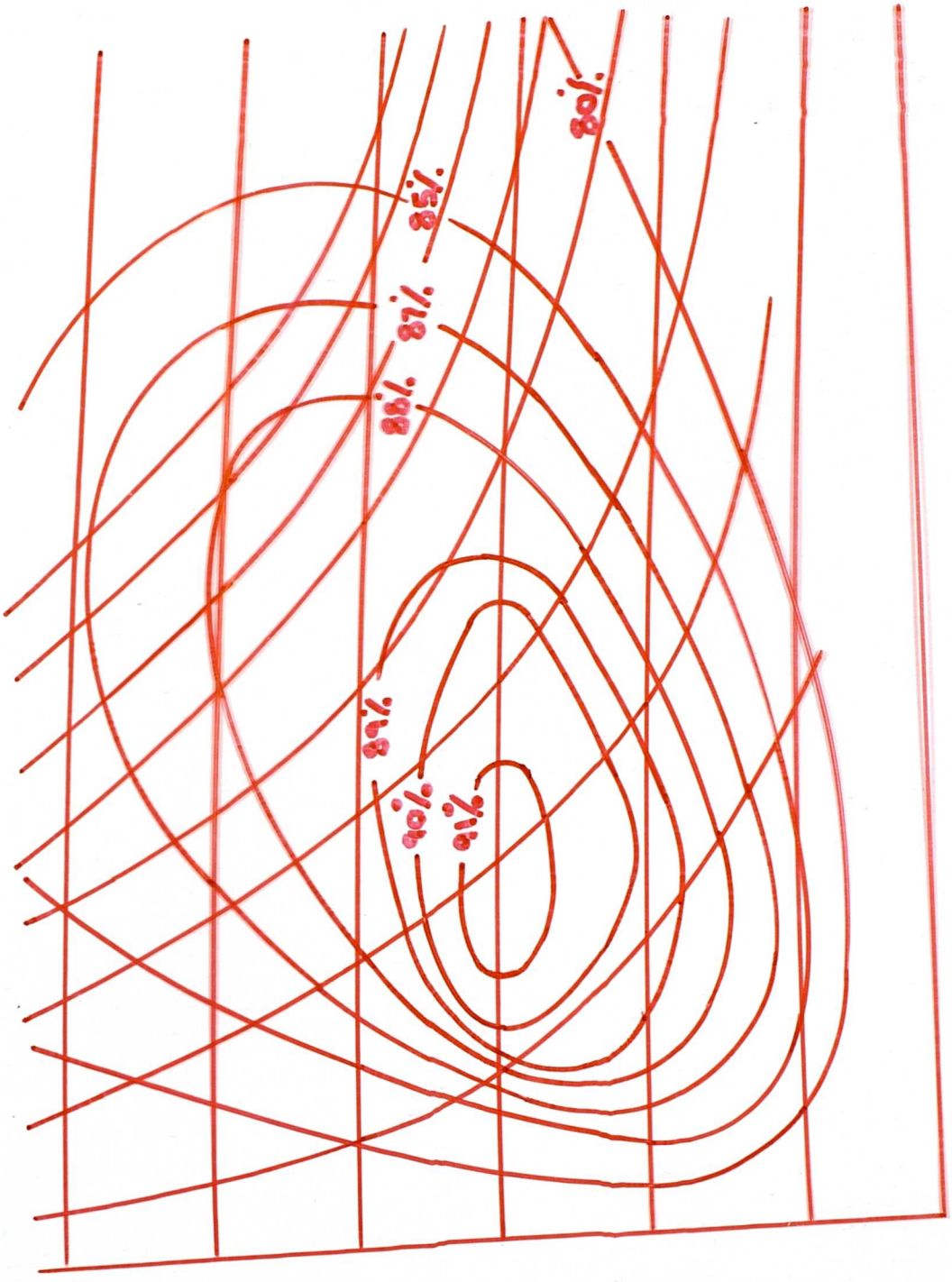
80%
85%
87%
86%
89%
90%
91%

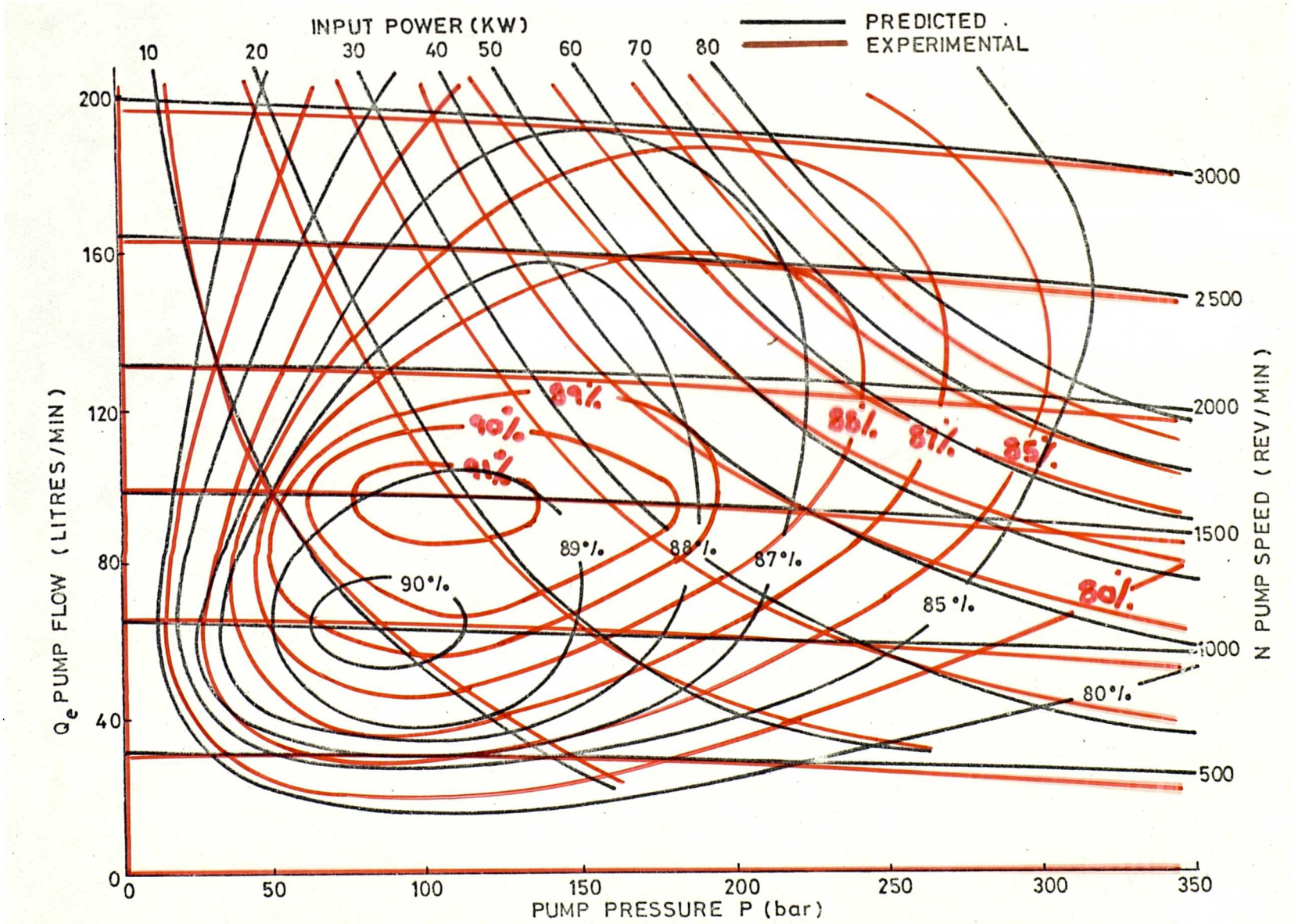

FIGURE 8.11 EXPERIMENTAL AND PREDICTED PERFORMANCE CHARACTERISTICS OF HD900 PUMP AT FULL DISPLACEMENT SETTING. WITH SHELL TELLUS 27 OIL AT 50°C INLET TEMPERATURE.

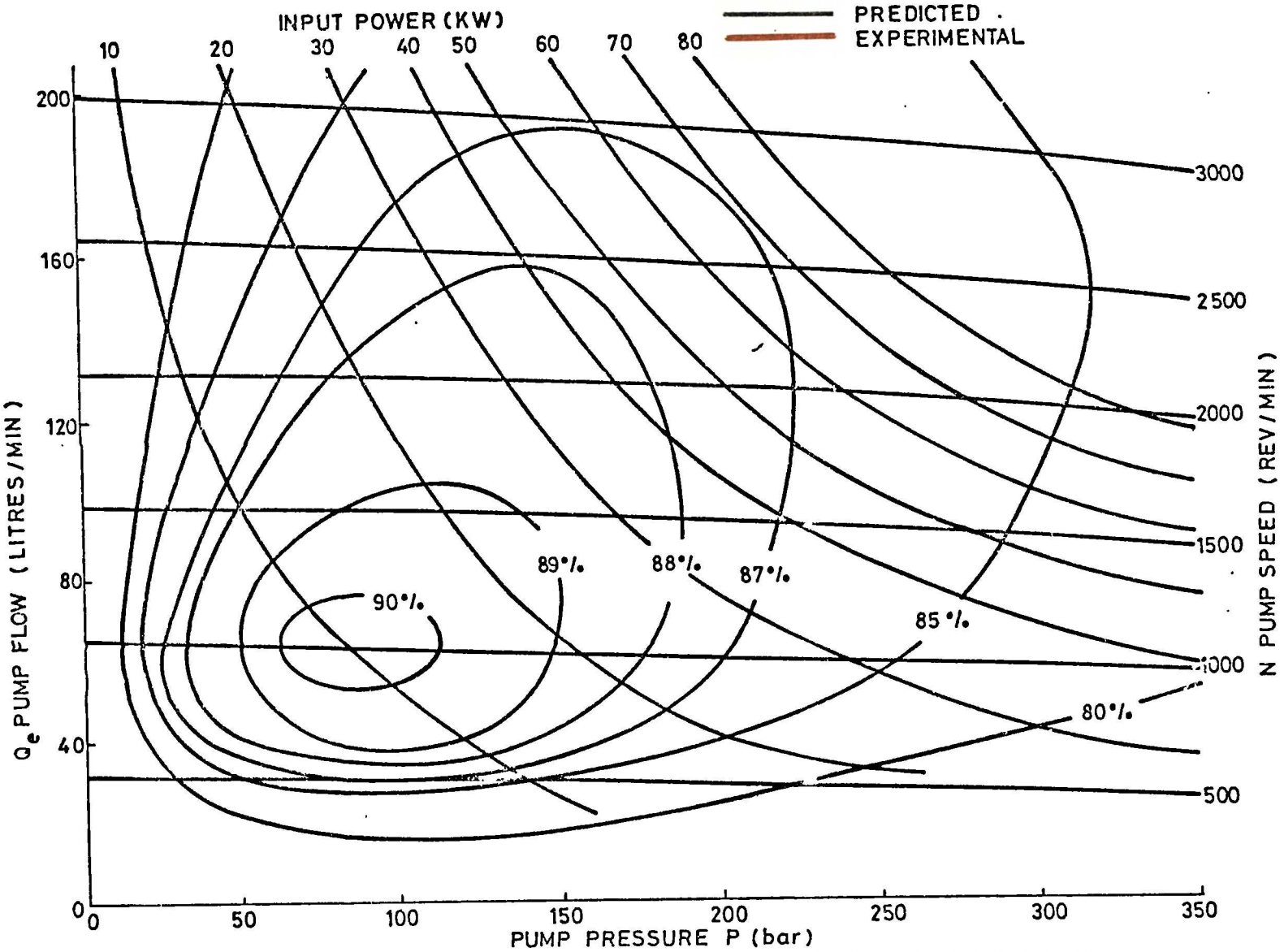

FIGURE 8.11 EXPERIMENTAL AND PREDICTED PERFORMANCE CHARACTERISTICS OF HD900 PUMP AT FULL DISPLACEMENT SETTING. WITH SHELL TELLUS 27 OIL AT 50°C INLET TEMPERATURE.

8.3 Predicted and Experimental Performance of Lucas Pump

Figs. 8.3 to 8.11, compare the experimental and predicted performance of the HD900 pump. It will be seen that in general the predicted effective flow rate Q_e varies little from the measured flow rates. However at low pump speeds the resulting difference in volumetric efficiency is marked and this shows up clearly in the variations in overall efficiency at low speeds.

On the other hand, there is very good agreement over the operating range of the pump for the input torque and the related mechanical efficiency and this together with close agreement of the volumetric efficiency gives very good agreement for the pump overall efficiency at moderate and high pump speeds.

It will be seen from Fig.8.11, that the peak overall efficiency is predicted as 90% and is 91% from experimental measurements. When considering that some fourteen losses were considered in this analysis, it is of some satisfaction that the difference was not greater than 1%. In any event due regard must be made to the likelihood of experimental errors.

A breakdown of the percentage losses are given in Table 8.1.

8.4 Predicted Performance on New Pump Design

The predicted performance of the JD900 pump was not obtained as it was felt that no useful purpose would be served at this stage in validifying the performance prediction method. Because of the similarity in design, it was anticipated that few difficulties could be expected in applying the method. As discussed earlier, it is anticipated that a small improvement in performance over that of the HD900 could be expected.

Pump Pressure (bar)	100			200			300		
Pump Speed (rev/min)	1000	2000	3000	1000	2000	3000	1000	2000	3000
Piston Slip Flow	0.03	-0.06	-0.09	0.23	0.04	0.03	0.43	0.14	0.04
Slipper Bearing S.Flow	0.03	0.03	0.03	0.04	0.03	0.03	0.04	0.03	0.03
Valve Plate Slip Flow	2.23	1.39	1.08	3.88	2.26	1.70	5.46	3.18	2.31
Compressibility S.Flow	2.32	2.32	2.32	4.64	4.64	4.64	6.96	6.96	6.96
Piston Viscous Drag	0.23	0.46	0.69	0.11	0.22	0.33	0.07	0.15	0.21
Slipper Bearing V.Drag	0.02	0.04	0.06	0.01	0.02	0.03	0.01	0.01	0.02
Valve Plate V.Drag	0.17	0.32	0.46	0.09	0.17	0.24	0.06	0.11	0.16
Piston Coulomb Friction	1.42	1.42	1.42	1.42	1.42	1.42	1.42	1.42	1.42
Slipper Bearing C.F.	0.60	0.60	0.60	0.60	0.60	0.60	0.60	0.60	0.60
Valve Plate C.Friction	2.70	2.70	2.70	2.20	2.20	2.20	2.02	2.02	2.02
Bearing Coulomb Friction	0.33	0.33	0.33	0.28	0.28	0.28	0.27	0.27	0.27
Bearing Hydrodynamic Loss	Negligible			i.e.	below	0.01			
Flow Path H. Loss	0.10	0.40	0.91	0.05	0.20	0.45	0.03	0.13	0.30
Seal Friction	0.39	0.39	0.39	0.19	0.19	0.19	0.13	0.13	0.13
Total % Loss	10.57	10.34	10.82	13.74	12.27	12.14	17.50	15.15	14.47

Table 8.1 Comparison of percentage loss of efficiency for HD900 Pump at various regions and for differing pump pressures and speed.

CHAPTER 9. CONCLUSIONS

9.1 Conclusions

At the commencement of this programme of research no known design method existed for adequately and logically outlining a procedure for the successful design of axial piston pumps. The same can be said for performance prediction methods where the only aids available were those heavily dependent upon obtaining coefficients by experimental means or those used 'in company' by adjusting curve matching equations to estimate the performance of pumps of similar design.

The desirability of a reliable design and performance prediction method which can be used throughout the design stage has been established and has been confirmed by the support of industry to this present work. It would therefore seem that the aims and objectives of this research project would, if achieved, fulfil a real need and make a significant contribution to knowledge in the field of fluid power design.

It is claimed that the aims and objectives have been achieved. The design method is an adequate design procedure which integrates known theory and technological data with the author's own contributions to form a logical aid to design. In addition the performance prediction method is novel in that although it is based on well established mathematical models it eliminates the need to obtain suitable coefficients by experimental methods and so is effective during all stages of the design process. The application of the method is also particularly straightforward and involves no complexities which would inhibit its use in an industrial situation.

Its effectiveness is increased by the facility to make detailed comparisons of the individual losses within the pump and to indicate what design parameters are contributing to these specific losses. This constitutes a major improvement on any previous method which uses 'lumped' coefficients.

It is therefore concluded that the project was successful and fully met the aims and objectives specified. The validity of the design method was demonstrated by the design of the JD900 pump and of the improvements incorporated. The close agreement between the experimental and predicted performance of the HD900 pump led to the conclusion that the prediction method is reliable and constitutes a powerful aid to improving design and reducing subsequent development time.

The contributions made by this work can be summarised as follows:-

1. The development of a logical design method which incorporates known work and augments it by the addition of an analytical approach to estimating the static and dynamic forces in a working pump.

2. The proposal of a working theory to estimate more accurately than hitherto the intensity of stress in the cylinder block bores.

3. The development of graphical optimisation methods which aid the choice of satisfactory clearances between the piston and cylinder bore and between the slipper bearing and the swashplate and which take into account losses during the suction stroke.

4. The concept of an effective viscosity at various stages of the pump which greatly facilitates the estimation of leakage and torque losses.

5. The development of design charts to facilitate decision making at the design stage.

6. The development of a prediction method based on known mathematical models but not dependent on empirical coefficients. Regions of leakage and torque losses are identified and equations derived for each condition. The various equations are used to derive further expressions for the loss coefficients and these facilitate the easy compilation of relative and actual loss comparisons and those of pump efficiency.

The prediction method enables all aspects of pump performance to be estimated at the drawing board stage.

9.2 Suggestions for Further Work

i) Because of the high cost involved it has not been possible to manufacture a pump to the JD900 design. Further study, mainly of an experimental nature would be appropriate, particularly if it is directed towards obtaining reliable data of losses in the region of the valve plate. A comparison of the measured and predicted values of the losses would enhance the value of this present work.

ii) The generation of noise in hydrostatic power transmissions remains a cause of concern. Investigations to date have been mainly centred on the rate of pressure rise within the pump but further work correlating all aspects of noise generation and emission in pumps and hydraulic motors would be very relevant.

REFERENCES

1. Guillon M
'Hydraulic servo systems analysis and design'
Butterworths, London. p.9. 1969.

2. Oniga
'Thesis calcul des tuyaux'
Matamine, Paris. 1949.

3. Massey B S
'Mechanics of fluids'
Van Nostrand Reinhold, London. Section 14.3.6. 1970.

4. Pearsall I S
'Cavitation'
Engineering, London. Tech. file 14.

5. Ernst W
'Oil hydraulic power and its industrial applications'
McGraw-Hill, New York. p.142. 1960.

6. Gerber H
'Rudiments of calculations for axially acting pistons and flat distributor volumetric machines'
Hydraulic Pneumatic Power, Part 2. August 1970.

7. Korn J
'Hydrostatic transmission systems'
Intertext Books, London. p.148. 1969.

8. Richmond T D
'Piston return springs for hydrostatic machinery'
Joint Conv. for Marine Applic. of Fluid Power,
Inst. of Mech. Engineers, London. Paper 10. 1967.

9. Wilson W E
'Positive displacement pumps and motors'
Pitman, London. p.146 et seq. 1950.

10. Schlosser W M J
'Measurements on displacement pumps'
Dissertation - Technical University of Delft, October 1959.

11. Thoma J
'Performance of hydrostatic units'
Hydraulic Power Transmission, August 1962 and January 1963.

12. Blackburn J, et al
'Fluid power control'
Wiley, New York.

13. Harpur N F
'Some design considerations of hydraulic servos of the jack type'
Proc. of Conf. of Hydraulic Servo Mechanisms,
Inst. of Mech. Engineers, Paper 4, London 1953.

14. Helgestad B O, et al
'Pressure transients in an axial piston hydraulic pump'
Proc. Inst. of Mech. Engineers, London 1974.

15. Ainsworth F W
'The effects of oil column acoustic resonance'
Trans. of A.S.M.E., Paper 78, p.773. 1956.

16. Streeter V L, and Wylie E B
'Hydraulic transients'
McGraw-Hill, New York. pp.101-115. 1967.

17. Merritt Herbert E
'Hydraulic control systems'
Wiley, New York. p.18. 1967.

18. Merritt H E, and Gavin J T
'Friction loads on hydraulic servos'
Proc.National Conf. on Industrial Hydraulics,
Paper 16, pp.174-184. 1962.

19. Davies R M, and Lambert T H
'Transient response of an hydraulic servomechanism
flexibly connected to an inertial load'
Journal of Mech. Engineering Science, Vol.6, p.32. 1964.

20. Zaborszky J, and Harrington H J
'Describing functions for electrohydraulic valves'
A.I.E.E. trans., Vol.76, Part 1 - May 1957, and
Part 2 - January 1958.

21. Cataldo R S
'Analysis of electrohydraulic valves and systems'
J.A.C.C. Boston, September 1960.

22. Thayer W J
'Transfer functions for Moog servo valves'
Moog Inc., U.S.A. January 1965.

23. Nikiforuk P N, and Westlund D R
'The large signal response of a loaded high-pressure
hydraulic servomechanism'
Inst. of Mech. Engineers, London. Vol.180, Part 1. 1966.

24. Edghill C M, and Rubery A M
'Hydraulic pumps and motors - development testing, its
relationship with field failure diagnosis'
First European Fluid Power Conf., N.E.L. Paper 33,
Scotland 1973.

25. Wilson W E
'Design of optimum clearances in positive displacement
pumps and motors'
Trans. of A.S.M.E., p.117-122. January 1956.

26. Exline Paul G
'Leakage in capillary seals of hydraulic valves and pumps'
Product Engineering, p.290 et seq. April 1946.

27. Shute Norman A, and Turnbull David E
'Minimum power loss conditions of the pistons and valve plate in axial-type pumps and motors'
A.S.M.E., Paper 63-WA-90, November 1963.

28. Sumner L
'The management of design for economic production'
B.S.I. Publication, PD647C, London, July 1973.

29. Shute N A and Turnbull D E
'Minimum power loss of hydrostatic slipper bearings for axial piston machines'
Hydraulic Pneumatic Power and Controls, November 1963.

30. Shute N A, and Turnbull D E
'The axial and tilting stiffness of hydrostatic slipper bearings'
B.H.R.A. Research Report 759, March 1963.

31. Fisher M J
'A theoretical determination of some characteristics of a tilting slipper bearing'
B.H.R.A. Research Report 728, April 1962.

32. Bennett T P
'The resistance to tilt of hydrostatic slipper pads'
B.H.R.A. Research Report 713, December 1961.

33. Peterson, R E
'Stress concentration design factors'
Wiley.

34. Anon
'Wrought steels in the form of blooms, billets, bars and forgings'
B.S.I. London, B.S. 970, Parts 1, 2 and 3. 1972.

35. Baumeister T, editor
'Marks' mechanical engineers' hand-book'
McGraw-Hill, New York. pp.8-60 et seq. 1975.

36. Hartog Den
'Mechanical vibrations'
McGraw-Hill, New York.

37. Shute N A, and Turnbull D E
'A review of some recent developments in the design of axial piston machines'
B.H.R.A. Tech. Notes 793, January 1964.

38. Saitchenko J S
'Force balance conditions of the valve plate and rotor of an axial piston pump'
Translated by B.H.R.A. Trans. 750, March 1963.

39. Franco N
'Pump design by force balance'
Hydraulics and Pneumatics, Vol.14, p.101. November 1961.

40. Mauroschat R
'Leakage losses of valve plates of axial pumps and motors'
Maschinenbautechnik, Vol.11, p.270. 1962.

41. Shute N A, et al
'The hydrostatic pressure distribution across the lands of a valve plate of an axial piston machine'
B.H.R.A. Research Reports 795, 796 and 810. 1964.

42. Thoma H
'High pressure hydraulic power transmission'
Proc.Inst. of Mech.Engineers, 172, p.29. London 1958.

43. Thoma J
'Sealing gaps'
Hydraulic and Pneumatic Power Control 9, 105, p.627.
September 1963.

44. Blok P
'Theoretical and experimental investigations in connection with a transmission mechanism'
Zurich F.T.U. Thesis 2116.

45. Prokopiev V N, editor
'Variable delivery axial piston pumps, motors and transmissions'
Machine Construction, Moscow 1969.

46. Palmer K, et al
'The hydrostatic balancing of valve plates'
A.S.M.E. Paper 64-WA/LUB-13. November-December 1964.

47. Mayer E
'Mechanical seals'
Iliffe, London. p.82 et seq., London 1969.

48. Nau B S
'Design, performance and testing of valve plates for axial piston pumps and motors'
Fluid Power International Conf., Paper 8, London 1972.

49. Vogelpohl G
as reported by Mayer E (47) Ref. 138.

50. Brangs E
'Axial piston pumps with angled swashplate'
Thesis - T.H. Aachen, Germany. 1965.

51. Shute N A, and Turnbull D E
'The thrust balancing of axial piston machines'
B.H.R.A. Research Reports 772 and 773. May 1963.

52. de Raucourt F
'Le graissage de surfaces planes par coin thermique'
Translated by B.H.R.A. T.794,. March 1964.

53. Dowson D, and Hudson J D
'Thermo-hydrodynamic analysis of the infinite slider bearing'
Part 2, Paper 5, Proc. Lub. and Wear Convention, Inst. of Mech. Engineers, May 1963.

54. Swift H W
'Contributions to "Fluid film lubrication of parallel thrust surfaces"'
Proc. Inst. of Mech. Engineers, Vol.155, p.49. 1946.

55. Neal P B
'Film lubrication of plane-faced thrust pads'
Paper 6, Proc. Lub. & Wear Conv., Mech. Engineers, May 1963.

56. Heinze E
as reported by Mayer E (47), Ref. 58.

57. Boon E F, et al
'Some notes on seals for rotating shafts'
Proc. World Petrol. Conf., Rome 1955.

58. Willenkens F A M
'Fluid borne noise in hydraulic systems'
1st European Fluid Power Conf., N.E.L. Scotland 1973.

59. Helgestad B O, et al
'Noise in an axial piston pump - its causes and control'
Proc. Inst. of Mech. Engineers, Vol.187, pp.51-62, London 1973.

60. Kronenbourg K
'Measure of the characteristics of a screw motor'
Thesis, Eindhoven 1966.

61. Ishihara T
'Oil Hydraulics'
Tokyo 1968.

BIBLIOGRAPHY

(1) Wilson, Warren E
'Positive Displacement Pumps and Fluid Motors'
Pitman, London 1950.

(2) Wilson, Warren E
'Design of Optimum Clearances in Positive Displacement Pumps and Motors'
A.S.M.E. Paper 55-5-4. 1955.

(3) Wilson, Warren E
'Clearance Design in Positive Displacement Hydraulic Pumps and Motors'
Machine Design, February 1973 and October 1974.

(4) Thoma, Jean U
'Modern Oil Hydraulic Engineering'
Trade and Technical Press, London 1970.

(5) Thoma, Jean U
'Hydrostatic Power Transmission'
Trade and Technical Press, London 1964.

(6) Thoma, Jean U
'Sealing Gaps'
Hydraulic and Pneumatic Power Control 9, 105, p.627.
September 1963.

(7) Thoma, Jean U
'Systematic Design of Axial Piston Hydraulic Machines'
Hydraulic Pneumatic Power, October 1971.

(8) Ernst Walter
'Oil Hydraulic Power and its Industrial Applications'
McGraw-Hill, New York. 1960.

(9) Turnbull D E
'Fluid Power Engineering'
Newnes-Butterworths, London 1976.

(10) Franco N
'Pump Design by Force Balance'
Hydraulics and Pneumatics, 14, p.101. November 1961.

(11) Saitchenko J S
'Force Balance Conditions of a Valve Plate and Rotor of an Axial Piston Pump'
Stankii Instrument 10, p.28, 1950.
Translated by B.H.R.A. T750. March 1963.

(12) Palmer, Kenneth P, et al
'The Hydrostatic Balancing of Valve Plates'
A.S.M.E. Paper No. 64-WA/LUB-13, November-December 1964.

(13) Shute, N A, et al
'The Hydrostatic Pressure Distribution across the lands of a Valve Plate of an Axial Piston Machine'
Parts 1, 11, 111. B.H.R.A. RR795, January 1964. RR796, March 1964, and RR810, January 1965.

(14) Shute, N A, and Turnbull, D E
'Minimum Power Loss Conditions of the Pistons and Valve Plate in Axial Type Pumps and Motors'
A.S.M.E. Paper No. 63-WA-90. November 1963.

(15) Shute, N A, and Turnbull, D E
'Minimum Power Loss of Hydrostatic Slipper Bearings for Axial Piston Machines'
Proc. Conf. Lub. and Wear,
I.Mech.E., Paper No.1, London, May 1963.

(16) Fisher M J
'A theoretical determination of some characteristics of a tilting hydrostatic slipper bearing'
B.H.R.A. RR728, April 1962.

(17) Shute N A, and Turnbull D E
'The Axial and Tilting Stiffnesses of Hydrostatic Slipper Bearings'
B.H.R.A. RR759, March 1963.

(18) Richmond, T D
'Piston Return Springs for Hydrostatic Machinery'
Joint Conv. Marine Applic. of Fluid Power, N.E.L., Paper 10, Scotland 1967.

(19) Gerber H
'Rudiments of Calculation for Axially Acting Piston and Flat Lapped Distributor Volumetric Machines'
Hydraulic Pneumatic Power, 15, 177. September 1969.

(20) McCallum J
'A Theoretical Analysis of the Valveplate B Bearing of a Hydrostatic Unit'
Thesis M.C.T., N.E.L. 1965.

(21) Nau B S
'Design, Performance and Testing of Valve Plates for Axial Piston Pumps and Motors'
Fluid Power Inter. Conf., Paper 8. 1972.

(22) Edghill C M, and Rubery A M
'Hydraulic Pumps and Motors - Development Testing, its Relationship with Field Failure Diagnosis'
First European Fluid Power Conf., N.E.L. Paper 33, Scotland 1973.

(23) Beasley S A
'Components and Development of Hydraulic Transmissions'
Proc. Danish Conf. on Hydrostatic Transmissions, Paper 8. 1969.

(24) Price, C K J
'Control of Rotary Power Transmission'
Oil Hydraulic Conf., Inst. of Mech. Engineers. 1961.

(25) Edghill C M
'Control Features for Hydrostatic Transmissions'
Fluid Power International Conf. Paper 1. 1970.

(26) Merritt H E
'Hydraulic Control Systems'
Wiley, New York. 1967.

(27) Watson C D
'Variable Hydraulic Pump Servos and a Method of Testing'
Conf. on Hydraulic Servos, Inst. of Mech. Engineers, 1953.

(28) Walters R
'Hydraulic and Electro-hydraulic Servos'
Iliffe, London. 1967.

(29) Guillon M
'Hydraulic Servo Systems Analysis and Design'
Butterworths, London 1969.

(30) Nikiforuk P N, and Westlund D R
'The Large Signal Response of a Loaded Hydraulic Servomechanism'
Proc. Inst. of Mech. Engineers, 180. 1965.

(31) Thayer W J
'Transfer Functions for Moog Servo Valves'
Moog Inc., U.S.A. 1965.

(32) Wilson W E
'Performance Criteria for Positive Displacement Pumps and Fluid Motors'
Trans. A.S.M.E., February 1949.

(33) Schlösser W M J
'Mathematical Model for Displacement Pumps and Motors'
Hydraulic Power Transmission, May 1961.

(34) Thoma Jean
'Performance of Hydrostatic Units'
Hydraulic Power Transmission, August 1962.

(35) Dozortsev A G
'Coefficient of Delivery and Volumetric Efficiency of a Piston'
Russian Engineering Journal, Vol.L. No.9.

(36) Schlösser W M J
'Testing Techniques for Positive Displacement Pumps'
Second European Fluid Power Conference, 1975.

(37) Smith D J M, and Williamson J
'Steady State Performance Assessment of Hydrostatic Pumps and Motors'
First European Fluid Power Conf., N.E.L. Scotland 1973.

(38) Elloy, Martin
'Computer Helps Speed Hydraulic Pump Design'
Design Engineering, September 1972.

(39) Helgestad B O, et al
'Noise in an Axial Piston Pump'
Inst. of Mech. Engineers, London. 1973.

(40) Helgestad B O, et al
'Pressure Transients in an Axial Piston Hydraulic Pump'
Inst. of Mech. Engineers, Vol.188. London 1974.

(41) Wilson P J
'Noise in Hydraulic Systems'
Inst. of Mech. Engineers, C.M.E. 1973.

(42) Currie J, and Kane J
'The Design of Low Noise Hydraulic Equipment'
First European Fluid Power Conf., N.E.L. Paper 29.
Scotland 1973.

(43) Willekens F A M
'Fluid Borne Noise in Hydraulic Systems'
First European Fluid Power Conf., N.E.L.
Scotland 1973.

APPENDIX 1. FORCE BALANCE IN AXIAL PISTON PUMP BY SAITCHENKO'S METHOD

In axial piston pumps the rotor is loaded by forces proportional to the oil pressure. If these forces are not balanced correctly the adjacent faces of the rotor and port plate may part and this results in pump failure. The force producing this parting is due to the pressure distributions across the valve plate port and lands.

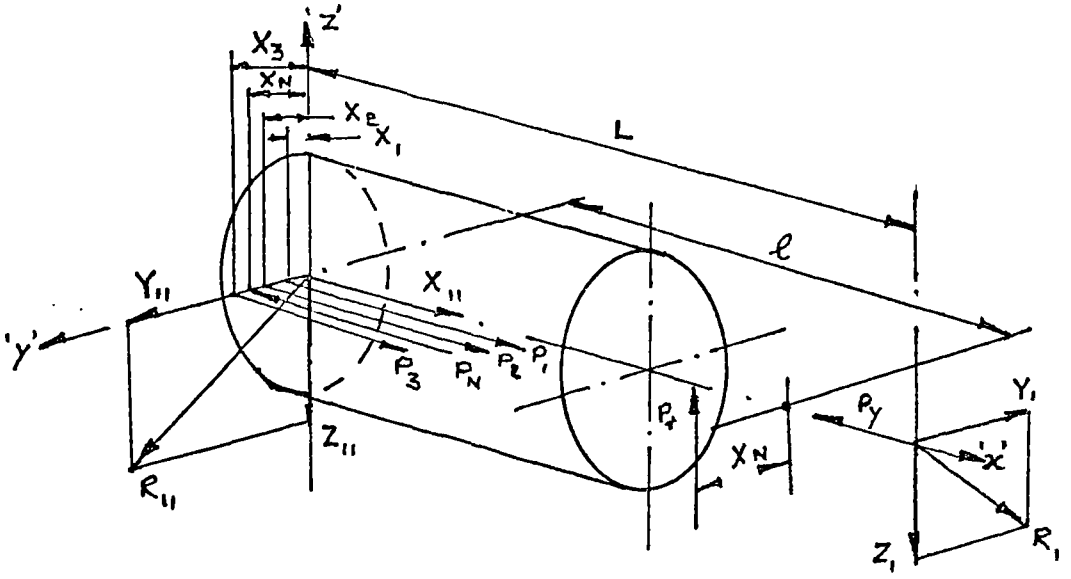

The resultant forces P_1, P_2 and P_3, arising from these pressure distributions are given by -

$$P_1 = \frac{\pi}{16} p \left(D_{L2}^2 - D_{L1}^2 \right) \quad (1)$$

$$P_2 = \frac{\pi}{8} p \left(D_{L3}^2 - D_{L2}^2 \right) \quad (2)$$

$$P_3 = \frac{\pi}{6} p \left(D_{L4}^2 - D_{L3}^2 \right) \quad (3)$$

where p is the operating pressure.

Along any radius the centres of pressure are given by -

$$X_1' = \frac{D_{L1}}{2} + \left(\frac{D_{L2} - D_{L1}}{3}\right)$$

$$X_2' = \frac{D_{L2}}{2} + \left(\frac{D_{L3} - D_{L2}}{4}\right)$$

$$X_3' = \frac{D_{L3}}{2} + \left(\frac{D_{L4} - D_{L3}}{6}\right)$$

The line of action of these forces will occur on the vertical axis of the section shown at radii of X_1, X_2 and X_3 given by -

$$X_1 = \frac{2}{\pi}\left\{\frac{D_{L1}}{2} + \left(\frac{D_{L2} - D_{L1}}{3}\right)\right\} \quad (4)$$

$$X_2 = \frac{2}{\pi}\left\{\frac{D_{L2}}{2} + \left(\frac{D_{L3} - D_{L2}}{4}\right)\right\} \quad (5)$$

$$X_3 = \frac{2}{\pi}\left\{\frac{D_{L3}}{2} + \left(\frac{D_{L4} - D_{L3}}{6}\right)\right\} \quad (6)$$

The force P_N produced by the operating pressure acting on the ends of the cylinders is given by -

$$P_N = \frac{A_p N_p P}{2} \quad (7)$$

In addition to the above force there is a perpendicular component P_r arising from the reactions at the swashplate given by -

$$P_r = \frac{A_p N_p P}{2} \tan\phi \quad (8)$$

where ϕ is the swashangle.

It should be noted that the effects of a finite suction pressure have been neglected since it is generally negligible compared with the operating pressure.

The position of the forces described above is shown in the diagram where the origin of the coordinates is assumed to lie at the centre of the valve plate end of the rotor. It is assumed that the rotor is connected to the shaft via two bearings, one being at the

origin and another at a distance L from it along the x axis. The reactions at these bearings are denoted by R_{11} and R_1 respectively and these may be resolved into components Y_{11}, Z_{11}, and Y_1, Z_1 along the y and z axes.

For equilibrium the six following equations apply -

$$P_1 + P_2 + P_3 + X_{11} - P_N - P_Y = 0 \qquad (9)$$

$$P_t - Z_1 - Z_{11} = 0 \qquad (10)$$

$$Y_{11} - Y_1 = 0 \qquad (11)$$

$$Z_1 L - P_Y \ell = 0 \qquad (12)$$

$$P_N X_N - P_1 X_1 - P_2 X_2 - P_3 X_3 - Y_1 L = 0 \qquad (13)$$

$$P_t X_N = M_{Kt} \qquad (14)$$

where X_{11} is the reaction of the port plate on the rotor in the x direction and this is assumed to be uniformly distributed over the contact area.

P_Y is the force of any spring system used to maintain contact between the rotor and valve plate.

ℓ is the distance to the swashplate axis of tilt.

M_{Kt} is the torque applied to the pump shaft.

Since in one revolution the work done is $p A_p N_p D \tan\phi$, where D is pitch circle diameter of piston we have -

$$M_{Kt} = \frac{p A_p N_p D \tan\phi}{2\pi}$$

so that equations (8) and (14) then give -

$$X_N = \frac{D}{\pi} \qquad (15)$$

In general, equations (9) and (13) are most useful for design purposes and to avoid failure of the machine it is essential that $X_{11} > 0$ and $Y_1.L > 0$.

We may write -

$$\frac{X_{11}}{P_N} = S_c \quad \text{and} \quad \frac{Y_1 L}{P_N X_N} = S_m$$

and experimental results indicate that it is desirable for -

$$S_c \geqslant 0.15 \quad \text{and} \quad S_m \geqslant 0.15$$

Summarising, the following method of design should be adopted:

1. From equations (1) to (7) and (15) calculate the values of P_1, P_2, P_3, X_1, X_2, X_3, P_N and X_N.

2. From equations (9) and (13) calculate the values of X_{11} and $Y_1.L$.

3. Calculate the values of S_c and S_m. If their values are less than 0.15 the design should be modified.

APPENDIX 2. LOAD DEPENDENT TORQUE LOSSES IN ROLLING BEARINGS

Load dependent torque losses are predominant at slow speed and result from the elastic deformation of the bearing components and the partial sliding which occurs at the loaded contact surfaces.

Estimations of these losses may be obtained from -

$$M_1 = f_1 g_1 P_o d_m$$

where

M_1	is the load dependent torque loss (Nm).
f_1	is a factor dependent on bearing design and bearing load
g_1	is a factor dependent on the direction of the bearing load
P_o	is the equivalent static bearing load (N).
d_m	is the mean diameter of the bearing (nm).

Bearing Type	f_1	$g_1 P_o$
Deep groove ball bearings	$9\times10^{-7}\left(\frac{Po}{Co}\right)^{0.55}$	$(2 \text{ to } 3)F_a - 0.1\ F_r$
Self Aligning ball bearings	$3\times10^{-7}\left(\frac{Po}{Co}\right)^{0.4}$	$1.4F_a - 0.1\ F_r$
Angular contact ball bearings	$1.3\times10^{-6}\left(\frac{Po}{Co}\right)^{0.33}$	$F_a - 0.1\ F_r$
Cylindrical roller and needle bearings	2.5×10^{-7} to 3×10^{-7}	F_r
Spherical roller bearings	4×10^{-7} to 5×10^{-7}	$1.2\ Y\ F_a$
Taper roller bearings	4×10^{-7} to 5×10^{-7}	$2\ Y\ F_a$

Bearing Type	f_1	$g_1 P_o$
Thrust ball bearings	$1.2 \times 10^{-6} \left(\frac{Po}{Co}\right)^{0.33}$	F_a
Cylindrical roller and needle thrust bearings	1.8×10^{-6}	F_a
Spherical roller thrust bearings	5×10^{-7} to 6×10^{-7}	F_a

where C_o = Basic static load rating (N).

F_a = Axial load (N)

F_r = Radial load (N)

Y = Axial load factor from bearing tables.

In general, the lower values quoted are for light series bearings, and the upper values for heavy series bearings.

APPENDIX 3. HYDRODYNAMIC TORQUE LOSSES IN ROLLING BEARINGS

Hydrodynamic torque losses are predominant at high speeds and result from the hydrodynamic losses in the lubricant. Most rolling bearing designs provide oil lubrication with relatively small quantities of oil within the bearing region. In the case of an axial piston pump with the bearings immersed in the hydraulic fluid, the hydrodynamic losses are similar to those of heavy series bearings with oil bath lubrication on a vertical shaft.

Estimations of these losses may be obtained from -

$$M_o = f_o \times 10^{-10} (\nu n)^{2/3} d_m^3$$

where M_o is the hydrodynamic torque loss (Nm).

f_o is a factor dependent on bearing design and lubrication

ν is the kinematic viscosity of the lubricant (mm^2/s)

n is the bearing speed (rev/min)

d_m is the mean diameter of the bearing (mm).

Bearing Type	f_o
Deep groove ball bearing self aligning ball bearing	4
Angular contact bearing	4
Cylindrical roller bearing	8
Needle roller bearing	20
Spherical roller bearing	10
Taper roller bearing	8
Thrust ball bearing	4
Cylindrical roller thrust bearing	4
Needle roller thrust bearing	5
Spherical roller thrust bearing	8